The Role of Cannabidiol in Sport: Mechanistic Insights, Ergogenic Potential, and Regulatory Implications

By

Scott Henry Gillham

A thesis submitted in partial fulfilment of the requirements of Liverpool John Moores University for the Degree of Doctor of Philosophy

Date: Friday 23rd January 2026

Authors Declaration

I declare that the work in this thesis was carried out in accordance with the regulations of Liverpool John Moores University. Apart from the help and advice acknowledged, the work within was solely completed and carried out by the author.

Any views expressed in this thesis are those of the author and in no way represent those of Liverpool John Moores University and the School of Sport and Exercise Science.

This thesis has not been presented to any other University for examination either in the United Kingdom or overseas. No portion of the work referred to in this research project has been submitted in support of an application for another degree or qualification of this or any other university or institute of learning.

Signed: 

Date: Tuesday 5th August 2025

Abstract

Cannabidiol (CBD), a non-intoxicating constituent of the *Cannabis Sativa* plant, has gained popularity amongst athletes for its purported therapeutic potential related to analgesia, inflammation and anxiety. In 2018, CBD was removed from the World Anti-Doping Agency's (WADA) list of prohibited substances, igniting widespread interest in its use in sport. However, scientific insight into its efficacy, mechanisms of action and safety – remain elusive. This thesis aimed to investigate CBD from three distinct, yet interrelated perspectives: (i) its mechanistic influence on skeletal muscle, (ii) its ergogenic effects, and (iii) its safety from an anti-doping perspective. Preliminary *in vitro* investigations revealed that acute CBD exposure might influence myogenesis at higher doses. These findings were extended through transcriptomic analyses offering insights into the molecular and biological pathways modulated by CBD. In parallel, a human investigation demonstrated that three-weeks of broad-spectrum CBD supplementation did not enhance performance in a 10-minute cycling time trial. Perhaps most importantly, a final study explored the implications of prolonged (10-week) supplementation. This study demonstrated that broad-spectrum CBD led to the appearance of prohibited cannabinoids in urine. Notably, moderate-intensity exercise appeared to amplify this risk in both males and females, highlighting a previously underappreciated interaction between exercise metabolism and contaminant exposure to cannabinoids. Taken together, these findings add important context to the emerging discourse on CBD in sport. While further work is required to elucidate its mechanisms of action, the anti-doping implications are unequivocal: off-the-shelf, broad-spectrum CBD supplements pose a significant risk to athletes. This thesis contributes novel evidence to inform athlete decision-making, guide regulatory policy, and support future education, whilst laying the foundation for further exploration into cannabinoids through the lens of sport and exercise.

Table of Contents

List of Tables

List of Figures

Acknowledgements

I would primarily like to thank my supervisory team, Professor Graeme Close, Dr Daniel Owens and Dr Neil Chester for giving me the opportunity to complete this PhD. Graeme, I am glad that you took a chance on me, and I hope I have confirmed my promise to you that you were making the right decision. Dan, thank you. Thank you for affording me not only your experience, knowledge and expertise – but also your friendship. Neil, your guidance, mentorship and experience have enabled me to mature beyond my years in academia and have changed my outlook on life – thank you. In addition to the academic stewardship offered by you all, I consider you all the closest of friends and I hope to retain these relationships for the rest of our careers and beyond.

I would like to thank our Director, Dr. Becky Murphy and Prof. Dave Low. Your support, especially in the last 12 months, has been transformative for my career. I would also like to thank the wider community at RISES and LJMU more broadly. LJMU was a dream for so long, and for that to become my reality makes me feel so proud. Stepping into TRB excites me today as much as it did on day one, and I thank you all for affording me the opportunity to be a part of this outstanding institution. I would specifically like to thank Dean Morrey, Mark Doyle, Dr Karl Gibbon and Dr Alan Simm who were all essential components of various aspects of this thesis. In addition, I would like to thank the participants and students who volunteered their time to participate in the studies herein. Your dedicated participation is one of the primary reasons this body of work could be completed. To my fellow PhD students and colleagues, Andy, Sam, Ross and Paige. The relationships we forged made coming to the laboratory fun, engaging and challenging – words I feel are fundamental in the growth of any postgraduate student. I am therefore excited to see the constituents of “Owens Lab” flourish in the coming years. Finally, outside of the institution, I would also like to thank colleagues at the Lambert Initiative for Cannabinoid Therapeutics, University of Sydney for their

assistance with this work. This body of work would not have been possible without your expertise.

To my family. Family is something we often take for granted, and while I might not voice my gratitude as often as I should – I thank you all for being there for me in the good times – and the bad. Life has been challenging for me in many respects over the last few years and each of you have stood by me, unequivocally. To my Mum, Dad and Fiona. Mum, I hope that completing this body of work fulfils your lifelong wish – for one of your children to become "Dr. Gillham" – I am just sorry I am a doctor of making people run – and not a General Practitioner (!). Jokes aside, thank you for everything you have done to support me. Dad, thank you for instilling in me a relentless work ethic, unrelenting drive to continue and unyielding stoicism – even when life deals you a tough hand. Fiona, thank you for always being there for me, your support means the world to me. To my auntie Carol and cousin David, thank you for your unwavering support – not only during the completion of this PhD, but throughout my life to date. Your commitment and care to me is something I hold forever dear. I thank you all for your support, and more than anything, I hope I make you all proud.

Finally, and most importantly, to Ivy. You came into our world in 2020, two-weeks before the world stopped due to a global pandemic, I had no clue how I was going to support you, all I knew is that I *would* support you. Being offered this PhD was the touch paper we needed. I am sorry I have not been as present as I should have in recent times, and I am sorry I have had to answer emails and phone calls at the weekend. Rest assured, providing for you is the reason I get out of bed every day. When you are a big girl and read this, I hope you understand that everything I do is for you. I love you more than anything, and I hope I make you proud.

Dedication I

Ernest Williams

&

Georgina Laidlaw Fraser Williams

Thank you for teaching me what matters.

Dedication II

In the final stages of completing this body of work, I lost my dad after a battle with illness. Dad, you got to call me “Dr. Gillham”– and although you did not get to see me graduate, I know you enjoyed being able to say it.

This thesis is dedicated to your memory, and I thank you for every sacrifice you made for me.

I hope I made you proud.

John Henry Gillham

19.04.1961 – 07.10.2025

Publications Arising from this Thesis

Burr, J.F., Cheung, C.P., Kasper, A.M., **Gillham, S.H**. and Close, G.L. Cannabis and athletic performance. Sports Medicine, 1-13.

Close, G.L., **Gillham, S.H**. and Kasper, A.M. (2021) Cannabidiol (CBD) and the athlete: Claims, Evidence, Prevalence and Safety Concerns.

Gillham, S.H., Starke, L., Welch, L., Mather, E., Whitelegg, T., Chester, N., Owens, D.J., Bampouras, T. and Close, G.L., 2024. Does a broad-spectrum cannabidiol supplement improve performance in a 10-min cycle ergometer performance-test? European Journal of Sport Science.

Gillham, S.H., Cole, P.L., Viggars, M.R., Nolan, A.H., Close, G.L. and Owens, D.J., 2024. Comparative transcriptomics of broad-spectrum and synthetic cannabidiol treated C_2C_{12} skeletal myotubes. *Physiological reports*, *12*, p.e70059.

Gillham, S.H., Cole, P.L., Owens, D.J., Chester, N., Bampouras, T.M., McCartney, D., Gordon, R., McGregor, I.S. and Close, G.L., 2026. Daily use of a broad-spectrum cannabidiol supplement produces detectable concentrations of cannabinoids in urine prohibited by the world anti-doping agency: an effect amplified by exercise. *Medicine & Science in Sports and Exercise, 58(1), 121-131*

Conference Attendances

Society for Redox Biology and Medicine: Orlando, FL. November 2022

International Sport & Exercise Nutrition Conference: Manchester, UK. December 2022

Healthy Muscle Ageing Conference: Liverpool, UK. September 2023

Conference Presentations

Gillham, S. H., Heaton, R. A., Kumiscia, J., Jackson, M. J., McArdle, A., Owens, D. J., and Close, G.L. (2022). The effects of cannabidiol on ROS signalling and cytokine/chemokine production in C2C12 myotubes (Poster).

Abbreviations

Δ^9-THC	Tetrahydrocannabinol
1-RM	1-Repetition maximum
11-COOH-THC	11-Carboxy-tetrahydrocannabinol
11-OH-THC	11-Hydroxy-tetrahydrocannabinol
2-AG	2-Arachidonoylglycerol
6-OH-CBD	6-Hydroxy-Cannabinol
7-COOH-CBD	7-Carboxy-Cannabinol
7-OH-CBD	7-Hydroxy-Cannabinol
AAF	Adverse Analytical Finding
ACh	Acetylcholine
AChR	Acetylcholine receptor
ADE	Adverse Drug Event
ADP	Adenosine diphosphate
ADRV	Anti-Doping Rule Violation
AEA	Anandamide
AMPk	AMP Kinase
ATP	Adenosine triphosphate
AU	Arbitrary Unit
BCAA	Branched Chain Amino Acid
BCP	Beta-Caryophyllene
BDDCS	Biopharmaceutics Drug Disposition Classification System
bHLH	Basic Helox Loop Helix
BLa	Blood Lactate
BrdU	Bromodeoxyuridine
Ca^{2+}	Calcium ion
CB_1	Cannabinoid receptor 1
CB_2	Cannabinoid receptor 2
CBD	Cannabidiol
CBDV	Cannabidivarin
CBDVA	Cannabidivarinic Acid
CBG	Cannabigerol
CBGA	Cannabigerolic Acid
CBN	Cannabinol
CBR	Cannabinoid receptor
CK	Creatine Kinase
CNS	Central Nervous System
CNS	Central Nervous System
CV	Coefficient of Variation
DDI	Drug-Drug Interaction
DEA	Docosatetraenylethanolamide
DEG	Differentially Expressed Gene
DEPC H_2O	Diethylpyrocarbonate water
dH_2O	Distilled water
DMD	Duchenne Muscular Dystrophy
DMEM	Dulbecco's Modified Eagles' Medium

DOMS	Delayed Onset Muscle Soreness
ECS	Endocannabinoid System
EdU	5-ethynyl-2´-deoxyuridine
EFSA	European Food Standards Agency
EIMD	Exercise induced muscle damage
FAAH	Fatty Acid Amide Hydrolase
FBS	Fetal bovine serum
FDA	Federal Drugs Administration
FSA	Food Standards Agency
FSC	Forward Scatter
GI	Gastrointestinal
GPCR	G Protein-Coupled Receptors
H_2O	Water
HDAC2	Histone Deacetylase 2
HEA	Homolimolenylethanolamide
Hmax1	Heme-oxygenase-1
HPLC	High-Performance Liquid Chromatography
HPLC	High-Performance Liquid Chromatography
HR	Heart Rate
HS	Horse serum
IGF-1	Insulin-like Growth Factor 1
IIMD	Impact induced muscle damage
IOC	International Olympic Committee
IOC	International Olympic Committee
LC-MS/MS	Liquid Chromatography Tandem-Mass Spectrometry
LN_2	Liquid Nitrogen
MCT	Medium-Chain Triglyceride
MF-20	Myosin Heavy Chain
MHRA	Medicines and Healthcare Products Regulatory Agency
MTT	Diphenyl Tetrazolium Bromide
MYO	Myoglobin
Myog	Myogenin
Na^+	Sodium ion
NAM	Negative Allosteric Modulation
NBCS	Newborn calf serum
NMJ	Neuromuscular junction
NSAID	Non-steroidal anti-inflammatory drugs
OEA	Oleoylethanolamide
OTC	Over-the-Counter
OTS	Off-the-Shelf
PAR-Q	Physical Activity Readiness Questionnaire
PBS	Phosphate buffered saline
PCA	Principal Component Analysis
PCSA	Physiological cross-sectional area
PD	Pharmacodynamic
PEA	Palmitoylethanolamide
PFA	Paraformaldehyde
Pi	Inorganic Phosphate
PI	Propidium Iodide

PK	Pharmacokinetic
PPARγ	Peroxisome Proliferator-Activated Receptor Gamma
QC	Quality Control
RCF	Relative centrifugal force
RFD	Rate of force development
RMR	Resting Metabolic Rate
RNA	Ribonucleic Acid
ROS	Reactive Oxygen Species
RPE	Rating of Perceived Exertion
RSI	Reactive Strength Index
sCBD	Synthetic Cannabidiol
SENr	Registered Sport Nutritionist
SLE	Supported Liquid Extraction
SR	Sarcoplasmic Reticulum
SSC	Side Scatter
SSRI	Selective Serotonin Reuptake Inhibitor
SST	Serum Separator Tube
St-T1b	Stormal Cell Line
TF	Transcription Factor
THC-COOH	11-nor-9-carboxy-tetrayhdocannabinol
THCA	Tetrahydrocannabinolic Acid
TRP	Transient Receptor Potential
UHPLC-MS/MS	Ultra-high performance liquid chromatography-tandem mass spectrometry
UPR	Unfolded Protein Response
USFDA	United States of America Food and Drug Administration
$\dot{V}O_{2max}$	Maximal Oxygen Consumption
$\dot{V}O_{2peak}$	Peak Oxygen Consumption
W	Watts
WADA	World Anti-Doping Agency

1 General Introduction

This chapter provides a broad introduction to cannabidiol and presents a rationale for investigating its potential utility in providing therapeutic effects in humans

1.1 General Introduction

The Cannabis plant has been used for centuries in various applications, from treating human ailments to textile production. In recent years, cannabidiol (CBD), a naturally occurring phytocannabinoid derived from the plant, has garnered significant attention from both athletes and the scientific community for its potential therapeutic benefits. For example, of the 13,241 PubMed articles with "CBD" in the title, 10,062 have been published since 2015. The purported benefits of CBD are vast and include relieving pain, reducing inflammation, and managing anxiety – though there are also many more cited in wider literature. CBD's popularity has grown across diverse groups, from individuals aiming to optimise their overall well-being to those managing specific health conditions. Among its most prominent users are recreational and elite athletes seeking natural alternatives to traditional medications in their quest for optimal performance and recovery. Due to this growth in interest, financial analysts predict that the global CBD market will reach $47 (£35) billion in sales by 2028.

CBD was originally prohibited for use by athletes by the World Anti-Doping Agency (WADA), the regulatory body responsible for promoting, coordinating, and monitoring efforts to ensure a doping-free sporting environment worldwide. However, in January 2018 CBD was removed from WADA's list of prohibited substances. While these changes were generally well-received by the athletic population, likely because of the growing media interest and anecdotal claims surrounding CBD, there were some caveats. Despite the shift in WADA legislation, there are still some countries across the globe which do not permit the use and/or sale of CBD products. For example, CBD commerce was recently prohibited in Hong Kong, with significant consequences for those ignoring this prohibition. As such, the trade and consumption of CBD remains a complex phenomenon but because of CBD's removal from WADA's prohibited list, the scientific community has begun to pay more interest in this compound from the perspective of optimising athletic performance.

Despite the increased popularity and anecdotal reports surrounding the benefits of CBD, there remains a paucity of high-quality empirical research to support the

compounds – from a general populous perspective, but especially so within athletes. Much of the current understanding of CBD's application from an exercise perspective is limited to pre-clinical, pilot, and underpowered research. Many of the studies to date in humans report equivocal findings and there has been no research that has been able to identify any clear mechanism of action in CBD target tissues relevant to the athlete, such as skeletal muscle. Taken together, there is currently a clear evidence gap of insufficient studies and data to support claims regarding the efficacy and safety of CBD use for the athlete.

1.2 Thesis Aims & Objectives

This thesis has four, interlinked aims. In the first instance, this thesis aims to explore how dosing can affect *in vitro* cell cultures. This first aim is in place to establish an optimal dose to conduct a non-bias exploration into the mechanisms by which broad-spectrum might exert its effects on skeletal muscle compared to those of synthetic, isolated CBD. Thereafter, the thesis aims to explore the potential utility of CBD when considering aerobic exercise. Finally, given the considerable ambiguity surrounding the supplementation of CBD in athletic populations, this thesis proposes to investigate the potential accumulation of CBD and other cannabinoids in blood and urine. These aims have been designated to provide athletes, practitioners and the broader scientific community with a sound body of evidence. It is hoped that the findings taken from this thesis can influence future applied practice and policy with regards to well-informed decision making by athletes and help to inform policy formulations across sporting clubs, organisations and even governing bodies.

2 Review of the Literature

Publications associated with this Chapter:

Burr, J.F., Cheung, C.P., Kasper, A.M., Gillham, S.H. and Close, G.L. (2021) Cannabis and athletic performance. Sports Medicine, 1-13.

2.1 The Cannabis Plant

2.1.1 Background and Historical Perspective

The cannabis plant is thought to be one of the earliest plants cultivated by humans, and the plant possesses a complex and diverse history. Evidence suggests that the plant may have been cultivated as early as 4000 BC to aid in the manufacture of textiles, rope, and paper (Crini et al., 2020; Sakal et al., 2021). In addition, cannabis has also been used for medicinal purposes, since the pre-biblical period with some reports of its use in anaesthesia during surgery preparation (Li, 1974). While much literature to date has linked early cannabis cultivation to East and Central Asia, the cultivar, commerce, and consumption of the plant spread West as rates of human resettlement increased (Clarke and Merlin, 2016). Notwithstanding its use throughout the ages, the plant has endured extensive periods of prohibition since the early 20th Century (Haney, 2020; Martin et al., 2020). Indeed, several sociological viewpoints may aid in the explanation for this. For example, following the influx of Mexican migrants into the USA in the early 20th Century there was a considerable increase in the use of the cannabis plant as a source of recreation, which was termed the "Marijuana Menace" (Chopra, 1969). In addition, since the League of Nations 1930 statement concluded that Cannabis had no medicinal significance, it was prohibited in many countries across the globe (Nutt, 2019). The legislative landscape regarding the cultivation and commerce of the plant has changed significantly during the 21st Century and remains to do so at the present day. These complications are likely because of the plant's promiscuous potential, and variety of applications - from medicinal to recreation (Bridgeman and Abazia, 2017).

2.1.2 Cannabis Legislation

The Cannabis plant is used not only for medicinal purposes but also for recreation. Cannabis has now been specified as one of the most widely used psychoactive substances across the globe, with 9.5% of American citizens reporting use at some stage over the last decade (Miller, Bonawitz and Ostrovsky, 2020). However, as per UK law, Cannabis is controlled as a Class B substance under the Misuse of Drugs Act 1971. Nevertheless, the UK Government both legalised and made Cannabis medication available under a Medicines and Healthcare Products Regulatory Agency (MHRA)

Specials Licence in November 2018 because of numerous campaign strategies for the application of cannabis in medicine (Gornall, 2020). That said, few conditions are currently treated with medicinal cannabis and even fewer patients have been prescribed cannabis as medicine via the National Health Service (Schlag, 2020), which may underscore that over one million people currently self-medicate with illegally sourced cannabis (Couch, 2020). This self-medication and sourcing from non-authorised traders might be considered as criminal activity when compared to the sourcing of medical cannabis (Shepard and Blackley, 2016). Meanwhile, in the United States of America, Federal law states that the possession, sale, or use of cannabis is illegal, and considered a Schedule 1 drug under the Controlled Substances Act of 1970. However, some States have exemptions to this from a medicinal, industrial, and recreational standpoint (Pertwee, 2014). For example, The State of California legalised the medicinal use of Cannabis in 1996 – which, with the benefit of hindsight, was the stimulus for widespread reform. This reform has led to (at the time of writing this thesis), 37 States, three Territories and the District of Columbia permitting the medicinal use of Cannabis. Moreover, the 2018 "Farm Bill" was signed into Federal law, which removed hemp (defined as Cannabis and derivatives of Cannabis < 0.3% Δ^9-THC) from the definition of marijuana in the Controlled Substances Act (Close, Gillham and Kasper, 2021).

2.1.3 Cannabis Botany

The Cannabis plant is typically referred to as an herbaceous annual plant. While botanical taxonomists continue to debate the number of cultivars at the present day, there are primarily three commonly accepted species: *Cannabis Sativa, Cannabis Indica,* and *Cannabis Ruderalis* (Piomelli and Russo, 2016; McPartland, 2017). It has been proposed that all of these species are derived from a single phenotype, but following cultivation across a ranging geographic locality, their properties have changed because of climate-based specifics such as temperature and humidity (McPartland, 2017). Genotype specification can typically be achieved through two methods, morphologically – which considers leaf shapes, with *Indica* leaves broader and wider, with *Sativa* narrower in nature (Jin et al., 2021) (Figure 2.1) and b) direct quantification of phytocannabinoid concentrations within the trichomes of female

flowers (Gülck and Møller, 2020). Regarding phytocannabinoid concentrations, it is generally agreed upon that the most important phytocannabinoid in this regard is Δ^9-THC (McPartland and Small, 2020). For example, while the *Cannabis Ruderalis* (native to areas of central and eastern Europe) has been defined as a low-concentration Δ^9-THC subspecies, *Cannabis Indica* which contains significantly higher Δ^9-THC concentrations has been proposed to originate from areas of Central Asia (McPartland, 2018). However, most notable for this body of work is the Cannabis Sativa L-Strain – (commonly referred to as Hemp), which contains many of the compounds found within other strains of the Cannabis plant including phytocannabinoids, flavonoids, terpenoids and alkaloids (Oomah et al., 2002). For a Cannabis plant to be defined as "Hemp" it must contain <0.3% Δ^9-THC, with any concentrations above that threshold being classified as *Cannabis Indica* (McPartland and Small, 2020).

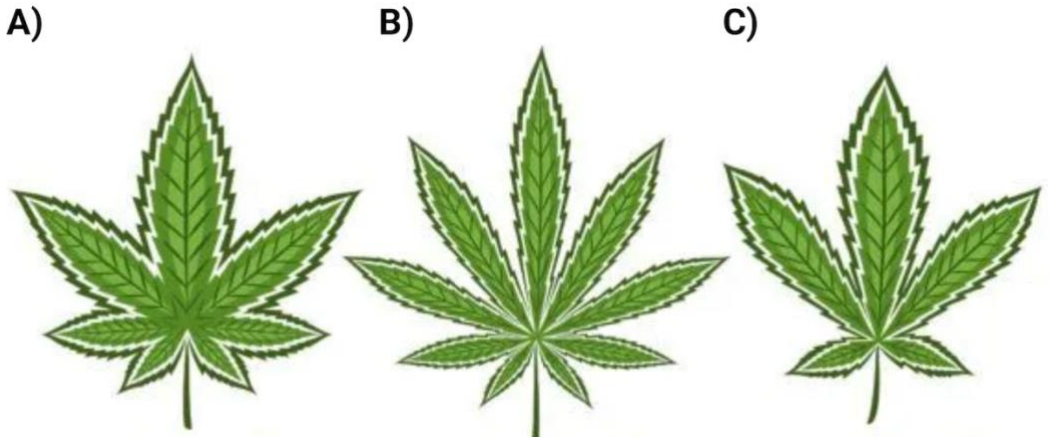

Figure 2.1. Cannabis subspecies morphology A) Cannabis Indica; B) Cannabis Sativa; C) Cannabis Ruderalis (Adapted from Jin et al. 2021).

2.2 Phytocannabinoids

2.2.1 Background

As mentioned previously, the Cannabis plant has been used for Millenia in various guises and the subspecies characterisation of the plant might be responsible for its diversity (Hanuš et al., 2016; ElSohly et al., 2017; Freeman et al., 2019). While it is accepted that Δ^9-THC content is vital for characterisation, it is important to remember that this is only one of many phytocannabinoids. While these have structural similarities (each containing 21 carbon atoms), their individual structures allow them

to function in a remarkably diverse fashion (Figure 2.1) (Lange and Zager, 2022). These phytocannabinoids are isolated from the resin produced by female plants, which then allows them to be categorised via an 11-point classification system (Table 2.1). To date, the most researched categories are Δ^8-THC, Δ^9-THC, CBD and Cannabigerol (CBG). The first individual phytocannabinoid to be elucidated was Cannabinol (CBN; Figure 2.2a) and was reportedly done so in the late 19th Century (Pertwee, 2006). Thereafter, the next phytocannabinoid isolated was CBD by (Adams, Hunt and Clark, 1940) then later in 1964, THC and CBG were isolated (Gaoni and Mechoulam, 1964). Finally, CBDV was isolated in 1969 (Vollner, Bieniek and Korte, 1969).

Table 2.1. Cannabinoid Classification. Adapted from (Filipiuc et al., 2021)

Compound Class	Number of Compounds Per Class
Δ^9-trans-tetrahydrocannabinol	25
Δ^8-trans-tetrahydrocannabinol	5
Cannabidiol	10
Cannabigerol	16
Cannabichromene	9
Cannabinol	11
Cannabinodiol	2
Cannabicyclol	3
Cannabielsoin	5
Cannabitriol	9
Other (Unspecified)	30

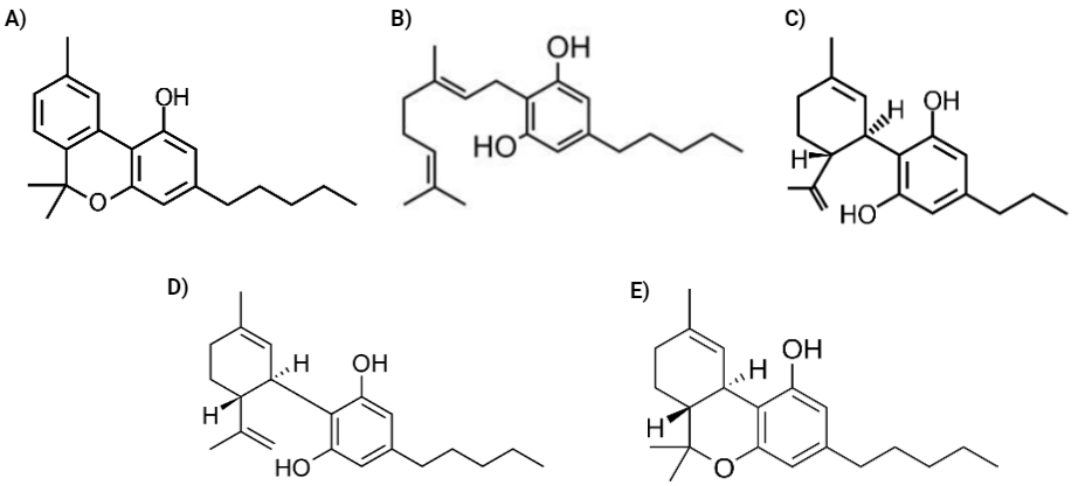

Figure 2.2. Chemical Structure of Phytocannabinoids A) CBN; B) CBDV; C) CBG; D) CBD; E) THC

2.2.2 Cannabigerol (CBG)

Cannabigerol (CBG), was first isolated in the 1960's by Gaoni and Mechoulam as a component of their foundational investigations on cannabinoid structures (Gaoni and Mechoulam, 1964). This "minor" cannabinoid (~1%) abundance in cannabis has, like CBD, been suggested to be "non-psychoactive" (Gugliandolo et al., 2018). Though an important consideration for this cannabinoid is that in its acidic form (CBGA) it has been termed the "mother cannabinoid" (Cuttler et al., 2024). This term has perhaps been coined because of its ability to act as a direct precursor to other cannabinoids, including CBD, CBC and Δ^9-THC (Jastrząb, Gęgotek and Skrzydlewska, 2019).

From a pharmacological perspective, CBG has been suggested to, much like various other cannabinoids – interact with a variety of molecular targets. Indeed, CBG has been evidenced to act as a partial agonist of both CB_1 and CB_2 receptors, though with a lower affinity at either CBD or Δ^9-THC (Cascio et al., 2010). In addition to CBG's interaction with cannabinoid specific targets, it has demonstrated an ability to interact α-2 adrenergic receptors and TRPM8 channels. These TRPM8 channels are non-selective cation channels which have been shown to be activated by multiple factors, including pain (Proudfoot et al., 2006) and thermoregulation (Reimúndez et al., 2018).

In addition, some investigations have evidenced that CBG may also act in an inhibitory manner on COX-1 and COX-2 enzymes (Borrelli et al., 2013), both of which are involved in inflammation and as such, it could be postulated that CBG may provide anti-inflammatory effects in several distinct instances. It is however important to appreciate that much of the mechanistic investigation into these mechanisms has been completed in pre-clinical models and therefore, these findings should be interpreted in context.

Like many other cannabinoids, there remains a paucity of literature relating to the therapeutic potential of CBG in comparison to its better-known counterparts such as CBD or Δ^9-THC. There remains minimal empirical evidence regarding work in humans specifically. However, as noted above, some pre-clinical models have been used to encourage scientific debate in this area. A specific area of interest from a perspective of health is that CBG might influence outcomes associated with neurodegenerative disorders, such as Huntington's disease. For example, a pre-clinical investigation of this suggested that several genes associated with the disease were downregulated following CBG treatment in mice (Valdeolivas et al., 2015). Interestingly, some of these genes were associated with inflammation – including Histone deacetylase 2 (HDAC2), Peroxisome proliferator-activated receptor-γ (PPARγ) and Insulin-like growth factor-1 (IGF-1), proposing a potential anti-inflammatory utility of CBG. Unsurprisingly, these proposed anti-inflammatory mechanisms have also given rise to research surrounding some inflammatory-induced conditions of the gut (Anderson et al., 2024). Despite the encouraging pre-clinical research into this minor cannabinoid, only a single study to-date has investigated the utility of CBG from the perspective of exercise in humans. A 2023 study recruited 40 "exercise-trained" participants, who were randomised into a double-blind, placebo-controlled, repeated-dose pilot investigation on upper-body DOMS. Importantly, the formulation used in this study (consumed twice/day) was not CBG-only, and contained CBD (35 mg), beta caryophyllene (BCP; 25 mg), Branched Chain Amino Acids (BCAA's; 3.8g), and magnesium citrate (420 mg) in addition to the 50 mg of CBG therein. Following use of the formulation, participants reported modest effects surrounding self-reported soreness 72-hours post-DOMS, which the authors attributed to the enhancement of "Functional indicators of well-being". However,

these assertions were made despite the study reporting no change in any objective physical measures related to recovery from DOMS (Peters et al., 2023).

2.2.3 Cannabidivarin (CBDV)

Similarly to CBG, Cannabidivarin (CBDV) has been cited for decades as a non-psychoactive phytocannabinoids derived from the cannabis plant. Following its isolation in 1969 (Vollner, Bieniek and Korte, 1969), CBDV has been cited to have a relatively low abundance in cannabis, and has therefore been referred to as non-psychoactive "minor" cannabinoid, sharing a similar structure to CBD (Figure 2.2B). While this chemical structure is similar, there are some differences and these result in several distinct pharmacological properties. The biosynthesis of this molecule follows the decarboxylation of cannabidivarinic acid (CBDVA) – which is often modulated by temperature, or time-mediated mechanisms (Olejar and Kinney, 2021). Like some other cannabinoids - such as CBD, CBDV does not bind strongly to CB_1 or CB_2, instead it has been suggested to modulate the ECS through alternate pathways, such as in transient receptor potential (TRP) channels, which will be discussed below.

Given that CBDV may not strongly modulate the traditional components of the ECS (via activation at CB_1 or CB_2, research has identified that it acts on TRP channels (Iannotti et al., 2014). Indeed, these TRP channels have been associated with nociception, thermic response and pain mediation (Rosenbaum, Morales-Lázaro and Islas, 2022). Specific channels which have been shown to modulated by CBDV include TRPV1, TRPV2 and TRPA1. In addition to the action at TRP channels, a further avenue of investigation regarding CBDV's action are its ability to act as an antagonist at GRP55 - a G-protein coupled reception which has been suggested to also play a role in pain modulation (Armin et al., 2021). Finally, it has also been suggested that CBDV can modulate intracellular calcium levels and inhibit the degradation of AEA by fatty acid amide hydrolase (FAAH) – which has subsequently resulted in indirect enhancement of "endocannabinoid tone' – which has been previously described as an individual's "baseline" endocannabinoid levels (Toczek and Malinowska, 2018).

In a similar fashion to other cannabinoids, human research regarding CBDV specifically is sparce (Izzo et al., 2009). Much of the available research surrounding this molecule has been developed in pre-clinical models though some more recent investigations have recruited human participants. Pre-clinical work has suggested that CBDV might play a role in neurodevelopmental and epilepsy-related conditions, though the exact mechanisms by which these effects occur remain elusive (Morano et al., 2020). For instance, some studies have identified CBDV to reduce both seizure severity and frequency in rodent models of epilepsy -though authors of this investigation noted that the mechanisms of this action remained unclear (Amada et al., 2013). Indeed, this pre-clinical work then gave rise to clinical investigations whereby this interest led to the development of pharmaceutical-grade formulations (GWP42006) of the compound, which are now being investigated from several neurological perspectives (Morales, Reggio and Jagerovic, 2017). Indeed, in addition to the potential utility of CBDV in epilepsy, it has shown promise in other neurological conditions. More specifically, CBDV (10 mg/kg/day) significantly reduced mean monthly seizure rates in 5 female children with Rett syndrome, a neurological condition which can result in frequent seizures by 79%. When this percentage is expressed in absolute seizure number, patients had a mean reduction from 32 to 7.2 seizures per month (Hurley et al., 2022).

However, research relating to CBDV and muscle is considerably less established. To date, only a single study as investigated this potential interaction. In a pre-clinical model of Duchenne Muscular Dystrophy (DMD), it was elucidated that CBDV (3 µM) promoted the differentiation of murine C_2C_{12} myoblasts into myotubes by increasing [Ca2+]i which was proposedly mediated by TRPV1 activation. Moreover, in human primary satellite cells and myoblasts isolated from healthy and/or DMD donors, CBDV promoted myotube formation via TRPA1 activation. Finally, in mice, CBDV (60 mg·kg-1) prevented the loss of locomotor activity, reduced inflammation and restored autophagy (Iannotti et al., 2019a). Importantly, there is seemingly a paucity of evidence relating to CBDV from the perspective of exercise, either *in vitro*, or *in vivo*. As such, the safety, application and utility of this molecule remain elusive within the context of exercise.

2.2.4 Δ^9-Tetraydracannabinol (Δ^9-THC)

Since its elucidation (Gaoni and Mechoulam, 1964; Pertwee, 2006), Δ^9-THC has since received considerable attention from scientists, physicians as well as various authorities and governments (Miller, Bonawitz and Ostrovsky, 2020). This phytocannabinoid is typically formed via the decarboxylation of Δ^1-Tetrahydrocannabinolic acid (THCA) during the drying step of cannabis preparation and after heating (typically via smoking, vaping or cooking (Pressman et al., 2024). Importantly, Δ^9-THC possesses considerable intoxicating potential, and is the most widely consumed psychoactive substance on earth. As such, these capabilities are the primary reason for its cultivation, use for recreational purposes and ongoing prohibitive nature (Gorelick et al., 2013; Freeman et al., 2019; Burr et al., 2021). It is however important to note that there are several utilities of Δ^9-THC beyond its use in recreation. For example, Δ^9-THC possesses antiemetic properties and consequently, the FDA has approved two drugs for the symptomatic relief of nausea experienced following chemotherapy, namely Dronabinol™ and Nabilone™ (Taylor, Mueller and Sauls, 2018). These promising clinical properties of Δ^9-THC are primarily achieved through partial agonism of both CB_1 and CB_2 receptors (Di Marzo and Piscitelli, 2015). In addition to the antiemetic capabilities of Δ^9-THC, it has also been proposed to be a potent Anti-inflammatory (Gaffal et al., 2013), Neuroprotector (Hampson et al., 1998), Anti-Cancer (Li et al., 2022) and analgesic agent (Linher-Melville et al., 2020). Notwithstanding these capabilities, the legislative nature surrounding Δ^9-THC mean that extensive human research is difficult to complete, as such – there is still considerable scope for research on this phytocannabinoid.

2.2.5 Cannabidiol (CBD)

First isolated in 1940 (Adams, Pease and Clark, 1940) and chemical structure elucidated 23 years later using nuclear magnetic resonance (Mechoulam and Shvo, 1963), CBD is considered the most abundant phytocannabinoid within Cannabis *Sativa* (Micalizzi et al., 2021). Following its discovery, an accelerated effort was made to research the mechanistic actions and utilities of the compound (Chan and Duncan, 2021). This research elucidated several potential bioactivities and health-related

functions (Peng et al., 2022). Indeed, these uses are closely linked to the activation of the body's endocannabinoid system [Reviewed in Section 2.3] (Lu and Mackie, 2020).

The biosynthesis of CBD within cannabis sativa occurs via the condensation of olivetolic acid (a biosynthetic precursor to cannabinoid production) and geranyl phosphate (Anderson et al., 2022), which forms Cannabidiolic acid (CBDA), which, like previously mentioned cannabinoids is then decarboxylated to CBD which is mediated by prolonged storage and/or temperature related mechanisms (Tahir et al., 2021). From a structural perspective, CBD follows a similar pattern to other cannabinoids but importantly is without the "psychoactive" tricyclic core of Δ^{9}-THC (Table 2.2). Indeed, this structural distinction contributes to the distinct pharmacological profile and actions of CBD. Regarding CBD's mechanism of action, it has been shown to have a low affinity to well-established cannabinoid receptors (CB_1, CB_2) and instead primarily modulates the endocannabinoid system through indirect mechanisms (de Almeida and Devi, 2020). That said, there are some investigations which have suggested that CBD binds to CB_1 and CB_2 allosterically – meaning that the molecule interacts with the receptor at an alternate site from the primary (orthosteric) binding site (Jakowiecki et al., 2021). These assertions were confirmed with evidence from an *in vitro* investigation suggesting CBD to be a non-competitive negative allosteric modulator (NAM) of CB_1 receptors (Laprairie et al., 2015). Subsequently, it has been suggested that CBD's NAM of CB_1 may reduce the potency of 2-AG and/or Δ^{9}-THC (Nguyen et al., 2017). In addition to these mechanisms, there are also non-CBR-related molecular targets of CBD, which are outlined in Table 2.2.

Table 2.2. Pharmacodynamic properties of CBD at related receptors (Adapted from (Peng et al., 2022).

Receptor	Affinity (nM)	Function
CB_1	Ki = 3.3 ~ 4.9mM	Inverse agonist/antagonist
	IC50 = 0.27 – 0.96 mM	Negative allosteric modulator
CB_2	Ki = 4.3 μm	Antagonist
	EC_{50} = 503 nM	Inverse agonist
	IC_{50} = 3nM	Negative allosteric modulator
GPR55	IC_{50} = 445nM	Antagonist
TPPA1	EC_{50} = 110 nM	Agonist
TRPV1	EC_{50} = 1000 nM	Agonist
TRPV2	EC_{50} = 1250 nM	Agonist
TRPV3	EC_{50} = 3700 nM	Agonist
TRPV4	EC_{50} = 800 nM	Agonist
TRPM8	IC_{50} = 160 nM	Antagonist
5-HT_{1A}	N. D	Indirect agonist
PPARγ	EC_{50} = 2010 nM	Agonist
FAAH	27.5 μM	Inhibitor
D2	Ki = 11 nM at $D2_{High}$	Partial agonist
	KI = 2800 nM AT $D2_{LOW}$	

Abbreviations: 5-HT1A, serotonin receptor 1A; CB_1, cannabinoid receptor 1; CB_2, cannabinoid receptor 2; D2, dopamine receptor 2; FAAH, fatty acid amide hydrolase; FLAT, FAAH-like anandamide transporter protein; GABAA, γ-aminobutyric acid type A (GABAA) receptors; GPR12, G-protein-coupled receptor 12; GPR3, G-protein-coupled receptor 3; GPR55, G-protein-coupled receptor 55; GPR6, G-protein-coupled receptor 6; PPARγ, peroxisome proliferator activated receptor gamma; TRPM8, transient receptor potential cation channel 8; TRPV1, transient receptor potential vanilloid type 1; TRPV2, transient receptor potential vanilloid type 2; TRPV3, transient receptor potential vanilloid type 3; TRPV4, transient receptor potential vanilloid type 4.

CBD has been suggested to have a diverse therapeutic potential across several domains of human health. This varied therapeutic potential which might be linked to its multifaceted pharmacology and range of related receptor sites, as discussed above. Interestingly, one of the most well-researched areas in this regard is the potential

utility of CBD in the treatment of neurological conditions (Singh et al., 2023). More specifically, several studies have evidenced that CBD might prove beneficial in treatment-resistant epilepsy, with regards to Dravet and Lennox-Gastaut syndromes (Chen, Borgelt and Blackmer, 2019). The strength of this research lead to the development of a pharmaceutical-grade CBD (Epidiolex®; (Sekar and Pack, 2019).

Beyond epilepsy, there have been proposals that CBD may prove to be anxiolytic – which might question the assertion that CBD is "non-psychoactive'. Indeed, the administration of CBD has been evidenced to reduce anxiety in both pre-clinical (Wright, Di Ciano and Brands, 2020) and human trials (Bhuller, Schlage and Hoeng, 2024). However, it should be acknowledged that the research in humans is less well-established than the pre-clinical research with Bhuller et al. (2024) concluding that much more research is required. While the research to date in humans is not confirmatory, the pre-clinical findings, coupled with the early evidence in humans may have played a role in the accelerated consumer interest in commercially-available CBD formulations in recent years (Wheeler et al., 2020; Choi and Hwang, 2023). A further potential utility of CBD from the perspective of brain health and/or function relates to the notion that CBD might prove to be neuroprotective. Given that CBD has been proposed to obtain anti-inflammatory properties, various investigations have studied the potential role of CBD in neurodegenerative diseases, such as Alzheimer's and Parkinson's diseases (Cassano et al., 2020). Aside from the utility of CBD surrounding conditions associated with the brain, research has begun to explore the role CBD might play in the modulation of pain, or chronic pain more specifically (Boyaji et al., 2020). While it must be acknowledged that the potency of potential analgesia provided by CBD might be considerably less than Δ^{9}-THC, it comes with less potential for abuse or use from a recreational perspective. Similarly to other cannabinoids, it has been suggested that this analgesic potential of CBD could be attributed to its anti-inflammatory properties associated with the activation of TRPV1 channels and PPARγ (Khosropoor et al., 2023). While a full appraisal of the conditions associated with CBD-mediated symptoms is beyond the scope of this thesis, it was important to acknowledge the varied potential applications of the molecule, with specific areas of interest to be explored later within this literature review.

CBD has low solubility in water (12.6 mg/l) and high lipophilicity, as indicated by a logP of 6.3 (Franco et al., 2020). As such, CBD is classified as class II by the Biopharmaceutics Drug Disposition Classification System (BDDCS), meaning that a compound has poor water solubility, in addition to low permeability (Muta et al., 2025). As such, the pharmacokinetics of CBD are considerably variable, depending on the route of administration, with reports of dynamic pharmacokinetics following intravenous administration, oromucosal spray, inhalation, and transdermal application (Franco and Perucca, 2019). However, this thesis is focused on sublingual-oral CBD administration, and the pharmacokinetics and metabolism of CBD will be discussed in this regard. It is important to note that there is a highly variable degree of metabolism in humans with high intra - and inter-individual variability common, which is often attributed to age, sex, adiposity, general health and nutrition (Ujváry and Hanuš, 2016). The notion of nutrition playing a role in CBD metabolism is an important consideration, given CBD's high lipophilicity, CBD may dissolve in the fat from the diet – meaning that the rate of absorption can be accelerated (Millar et al., 2018). However, there are currently no published studies on the absolute oral bioavailability of medical-grade CBD products, such as Epidiolex®. Instead, there have been reports of fasted oral administration of commercially available CBD, which resulted in ~6% bioavailability in healthy adults (Bialer et al., 2018; Perucca and Bialer, 2020). Importantly, following oral administration, CBD exerts a somewhat complex and variable pharmacokinetic journey. This complexity is characterised by the effects of food, tissue distribution and extensive metabolism. Despite this, the T_{max} of orally consumed CBD is suggested to be ~0-4 hours (Millar et al., 2018). This T_{max} is coupled with a half-life of up to five-days following chronic oral ingestion (Millar et al., 2018).

This lack of clarity surrounding CBD's pharmacokinetics is an important consideration for the consumer, given that many of the products available for purchase over-the-counter (OTC) are in oral form (Tran and Kavuluru, 2020), with individuals able to consume as much of their product as they desire (notwithstanding the UK Government's recent reduction in recommended intakes of 10 mg/day). These rates of metabolism are indeed important for an individual's dose-optimisation and the

avoidance of Drug-Drug-Interactions (Brown and Winterstein, 2019). More recently, varying doses have been administered to humans, with a single oral dose reported to be tolerable up to 6,000 mg (Taylor et al., 2018). However, this perception of CBD's relative safety is not without its caveats. Given that CBD is primarily metabolised in the liver by CYP450, CYP2C19 and CYP3A4 isoenzymes (Devinsky et al., 2018), it exhibits both pharmacodynamic (PD) and pharmacokinetic properties that could lead to adverse drug events (ADEs) and drug–drug interactions (DDIs). Specifically, these adverse events and interactions might occur because various popular prescription medications (including opiates, non-steroidal anti-inflammatory drugs [NSAIDs], and selective serotonin reuptake inhibitors (SSRIs]) are also metabolised by the same enzymes as CBD (Brown and Winterstein, 2019). It is therefore vital to remember that CBD (and other cannabinoids) within OTC formulations can both potentiate or negate the functionality of these medications.

Because of the purported effects of CBD, its commerce and consumption has increased significantly in recent times, though not without controversy (Close, Gillham and Kasper, 2021). While legal for trade in many countries across the globe, there have been dynamic changes in legislation over the last 5-years. For example, in the UK, CBD is currently legal to be sold as a food supplement providing that the final product contains < 1 mg of Δ^9-THC, and that no medical claims are made surrounding its utility. However, In January 2019, CBD was confirmed as a "novel food" by The European Food Standards Agency (EFSA). This novel food classification is defined as "A food that has not been consumed to a significant degree by humans in the EU before 15th May 1997" (Pisanello and Caruso, 2018). Following the UK's withdrawal from the European Union in January 2020, the UK Food Standards Agency (FSA) requirements for CBD extracts (using the EFSA guidance for novel food applications) apply in England, Wales, and Northern Ireland. Meanwhile, Novel Food regulations in Scotland are covered by Food Standards Scotland, but the same regulations apply as in the rest of the UK. The FSA is responsible for the regulation of CBD as a novel food, but importantly, this does not include cosmetics, vapes, prescription products or products containing controlled substances, such as Δ^9-THC. Where CBD extracts also contain detectable or higher amounts of Δ^9-THC (or other controlled cannabinoids)

they are prohibited under the Misuse of Drugs Act 1971. In early 2020, the FSA issued a deadline of 31st March 2021 for CBD companies to submit novel food authorisation applications. Following that date, only products owned by companies that had submitted a valid application were permitted to continue trading. The authorisation process was designed to ensure the novel food (in this case, CBD) met legal standards, with regards to safety and cannabinoid concentrations.

Meanwhile, In USA, the 2018 Farm Bill removed hemp (defined as Cannabis and derivatives of Cannabis with no more than 0.3% Δ^9-THC) from the definition of Marijuana under the Controlled Substances Act (Abernethy, 2019). The Farm Bill meant that the Hemp plant was a potential source of commerce for companies across the country. However, under the U.S. Food, Drug, and Cosmetics Act (FD&C Act), CBD and products containing CBD cannot be marketed or sold as dietary supplements or foods. This is because, under the FD&C Act, it is unlawful to introduce into interstate trade a product that contains a substance that is an active ingredient in an approved drug, (e.g., Epidiolex®). Moreover, this was also the case if a substance had been the target of considerable clinical investigation. While the Food and Drug Administration has enforcement authority under the FD&C Act, at the time of writing this thesis, only a single article has reported the findings. This article suggested that only 39 letters had been sent out in the USA, 97% were for violations made on company websites. Almost all letters (97%) cited violations of marketing CBD as an unapproved new drug. These illicit therapeutic claims were made for > 125 health problems, including cancer, diabetes, pain and inflammation and arthritis (Close, Gillham and Kasper, 2021; Wagoner et al., 2021). Finally, one of the most recent changes in global CBD legislation is the prohibition of CBD trading in Hong Kong. CBD is now defined it as a "potentially dangerous drug" because of the potential contamination of CBD products with psychoactive cannabinoids (Storozhuk, 2023). Indeed, CBD has been coined as being "non-psychoactive", yet given its potential applications in treating disorders of the mind including anxiety and depression it perhaps should not be considered non-psychoactive, instead non-intoxicating (Piomelli and Russo, 2016).

2.3 The Endocannabinoid System

2.3.1 Key Components of the Endocannabinoid Signalling Pathway

The increase in research into the cannabis plant in the mid-20th Century led to questions pertaining to how the body processes the phytocannabinoids within the plant (Maccarrone, 2020). Originally, it was assumed that phytocannabinoids acted upon the body in a non-specific membrane-associated mechanism, though this hypothesis was discredited in the late 1980's (Devane et al., 1988). Indeed, this group identified the existence of CB_1 in porcine brain using radioligand binding assays (Devane et al., 1988). Thereafter, a second receptor, defined CB_2 and found within the periphery was identified (Munro, Thomas and Abu-Shaar, 1993). Both CB_1 and CB_2 are G protein-coupled receptors (GPCR), with the discovery of these serving to aid researchers understand the potential medicinal and euphoric effects of the plant in humans (Kilaru and Chapman, 2020). This section will review the contemporary literature on endocannabinoid signalling.

2.3.2 Cannabinoid Receptor 1

CB_1, the first receptor to be elucidated is primarily enriched within the central nervous system (CNS) and was first discovered in the brain (Kumar et al., 2019). Later, using methods including autoradiography, in-situ hybridization and immunohistochemistry, CB_1 was recognised as the most widely-expressed GPCR protein in this region (Mackie, 2005). It is however important to note that CB_1 are not exclusive to the CNS, and are also present peripherally, such as in the liver, pancreas, and both adipose tissue and skeletal muscle (Figure 2.3) (Haddad, 2021a). As such, CB_1 activation has been associated with a myriad of biological processes, namely, in-utero brain development, motor learning and behaviour, appetite regulation and glucose metabolism, body temperature and inflammatory and analgesic capacities (Lu and Mackie, 2020). Interestingly, CB_1 stimulation has also been shown to decrease mitochondrial biogenesis in mice, which may explain the role of this receptor in glucose metabolism and/or obesity-related conditions (Tedesco et al., 2010).

2.3.3 Cannabinoid Receptor 2

Cannabinoid receptor 2 meanwhile, is primarily expressed in T cells of immune tissues and peripheral nerve endings (Kilaru and Chapman, 2020; Lu and Mackie, 2020). Originally, it was assumed that these receptors were only present in these immune system related cells however, receptors have now also been identified throughout the CNS (Navarro et al., 2016). Though these are present throughout the body (Figure 2.3), it is important to remember that these are at lower levels in the CNS than CB_1 receptors and microglial CB_2 receptor activation is generally considered anti-inflammatory, and a potential route of research is the role of this in psychotic disorders (Lu and Mackie, 2020) and sports-related concussions (Singh and Neary, 2020; Lins et al., 2023).

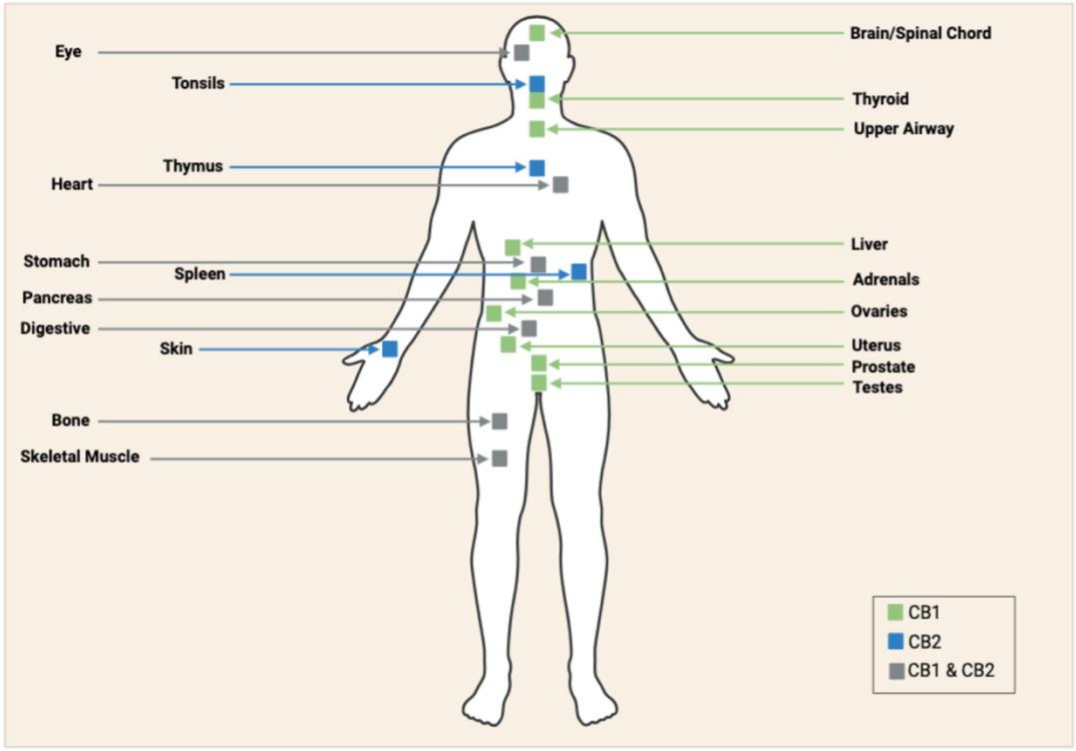

Figure 2.3. Location of CB_1 and CB_2 receptors in humans. Adapted from (Muralidhar Reddy, Maurya and Velmurugan, 2019).

2.3.4 Endocannabinoids

Soon after the discovery of CB_1, the endogenously produced N-arachidonoylethanolamine was discovered, which showed an ability to activate CB_1 (Devane et al., 1992). This "endocannabinoid" has since been termed Anandamide

(AEA), which is taken from the Sanskrit word “Ananda”- translating to words such as “joy, bliss and delight” (Klumpers and Thacker, 2019). Thereafter, 2-arachidonoylglycerol (2-AG) was also reported to be a cannabinoid receptor-activating endocannabinoid (Sugiura et al., 1995). While the first to be elucidated, at the time of writing this thesis, these compounds remain the best-studied arachidonic acid derivate endocannabinoids (Tsuboi et al., 2018).

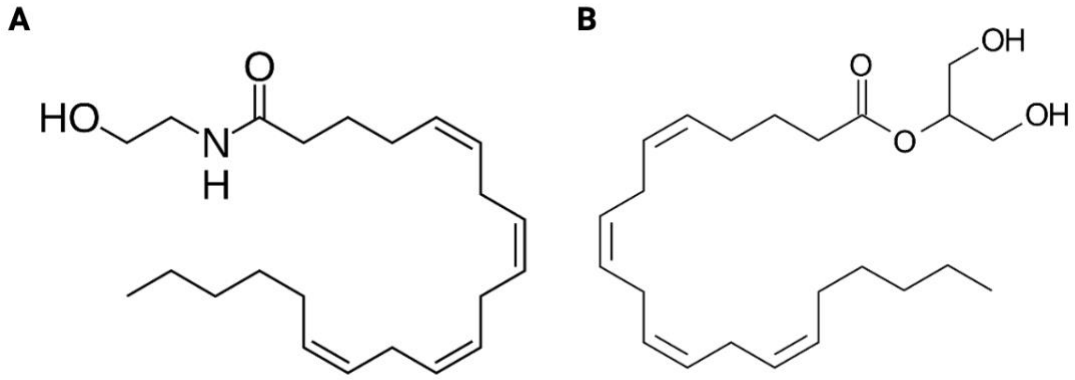

Figure 2.4. Chemical structures of A) Anandamide (AEA) and B) 2-arachidonoylglycerol (2-AG).

Following the discovery of AEA within porcine brain in 1992 (Devane et al., 1992), It was elucidated that this agonist could not fully reproduce the effects of Δ^9-THC, which then prompted research into the discovery of 2-AG. Interestingly, while both lipid-based molecules are similar in structure (Figure 2.4), each possess somewhat distinct properties and, as such play different physiological roles. Specifically, AEA is a high-affinity partial agonist of CB_1 and a weak partial agonist of CB_2. Meanwhile 2-AG acts as a full agonist towards both CB_1 and CB_2 with moderate to-low affinity (Hermann, Kaczocha and Deutsch, 2006). While AEA and 2-AG are the most well-known bioactive endocannabinoids (Figure 2.5), the family of these lipid mediators include other molecules such as: virodhamine, noladin ether, and N-arachidonoyldopamine (Rohlfs et al.), homo-linolenylethanolamide (HEA), docosatetraenylethanolamide (DEA), and others such as palmitoylethanolamide (PEA) and oleoylethanolamide (OEA) (Battista et al., 2012). Importantly, these compounds are often referred to as

"endocannabinoid-like", and instead of having a direct affinity for CB_1 or CB_2, can modulate endocannabinoid signalling indirectly (Cravatt et al., 1996).

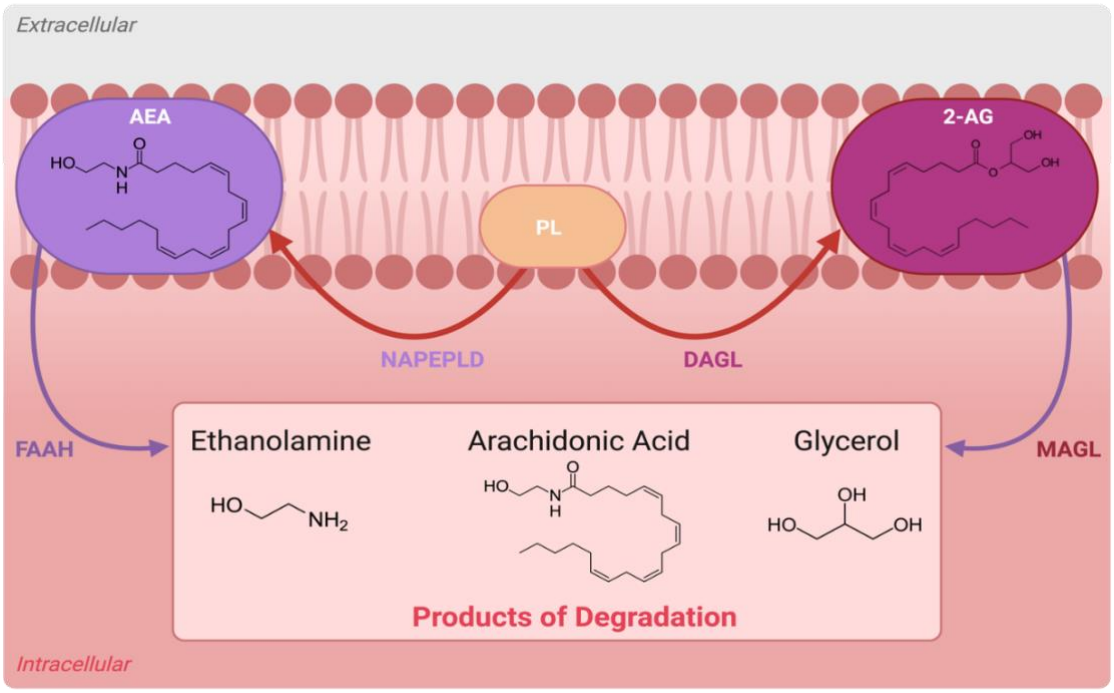

Figure 2.5. Endocannabinoid Synthesis. N-acylphosphatidylethanolamine-specific phospholipase D (NAPEPLD) and diacylglycerol lipase (DAGL) synthesize anandamide (AEA) and 2-arachidonoylglycerol (2-AG) from phospholipids (PL), respectively. AEA and 2-AG are degraded by fatty acid amide hydrolase (FAAH) and monoacylglycerol lipase (MAGL), respectively. (Adapted from Schönke, Martinez-Tellez and Rensen, 2020).

2.3.5 TRPV1

In addition to endocannabinoid activation of CB_1 and CB_2, there are suggestions that AEA and 2-AG interact with various other receptors. One of the most prominent is transient receptor potential vanilloid channel 1 (TRPV1). These channels are considered fundamental in the transduction of noxious stimuli such as heat and inflammation (Walder et al., 2012) and synaptic transmission (Di Marzo and De Petrocellis, 2012). Given that TRPV1 is also expressed in the sarcoplasmic reticulum of skeletal muscle cells where activation leads to increased cytoplasmic calcium concentrations, elevations have been linked to an upregulation in peroxisome proliferator-activated receptor-gamma coactivator-1α (PGC-1α) expression, thereby stimulating mitochondrial biogenesis (Wu et al., 2002).

2.4 Cannabinoid Signalling in Skeletal Muscle

2.4.1 Background

In humans, skeletal muscle is developed in-utero, accounts for ~40% of total adult body mass, 50-75% of total body proteins and plays a vital role in metabolic homeostasis because of its ~30% contribution to resting metabolic rate (RMR)(Sharples and Stewart, 2011; Frontera and Ochala, 2015; Periasamy, Herrera and Reis, 2017). Another vital role of skeletal muscle is its ability to store and provide substrates important for exercise regulation including various amino acids (Felig, 1975; Dyar et al., 2018) and carbohydrates (Saltin, 1973; Frontera and Ochala, 2015). However, the primary role of skeletal muscle is contraction and relaxation, therefore regulating posture and locomotion (McLeod et al., 2016). Skeletal muscle plays a vital role in health, well-being, and exercise performance and given this importance, the relative re-or degeneration of this tissue is imperative to our quality of life, as well as in sports performance (Gries et al., 2018). This can be from a range of perspectives, from functional capacity to metabolic process' such as substrate utilisation (Dalle et al., 2022). As such, the maintenance and/or increase in a muscle's functional capacity and overall quality has been at the forefront of research surrounding skeletal muscle over the last decade (Brady, Straight and Evans, 2014).

Human skeletal muscle is comprised of several layers and components. At the most superficial level, the epimysium, an outer connective tissue, wraps skeletal muscle in a sheath-like fashion. Below the epimysium is the perimysium, surrounding bundles of myofibres encased in connective tissue, termed the endomysium. The content of these myofibres are where essential components required for force production are located. These myofibres are surrounded by the sarcolemma, a thin elastic membrane which surrounds and protects myofibre cellular content (Frontera and Ochala, 2015). Surrounding each myofibril is the sarcoplasmic reticulum (SR) containing a highly concentrated store of calcium ions (Ca^{2+}) which are essential in the muscle contraction and relaxation process (Murakami et al., 2005). These myofibres are made up of a collection of myofibrils, with individual myofibrils containing numerous repeating

units in series, termed sarcomeres. Sarcomeres are found between two thin filament Z-lines, or spaces within the myofibril formed by the protein actin which are attached to the Z-line by α-actinin at the end of each sarcomere. At the centre of the sarcomere are thick filaments, located at the m-line, containing myosin (Mukund and Subramaniam, 2020). The interaction of these actin and myosin proteins within the sarcomere contribute to the mechanism of skeletal muscle contraction. A visual representation of skeletal muscle structure and organisation is available in (Figure 2.6).

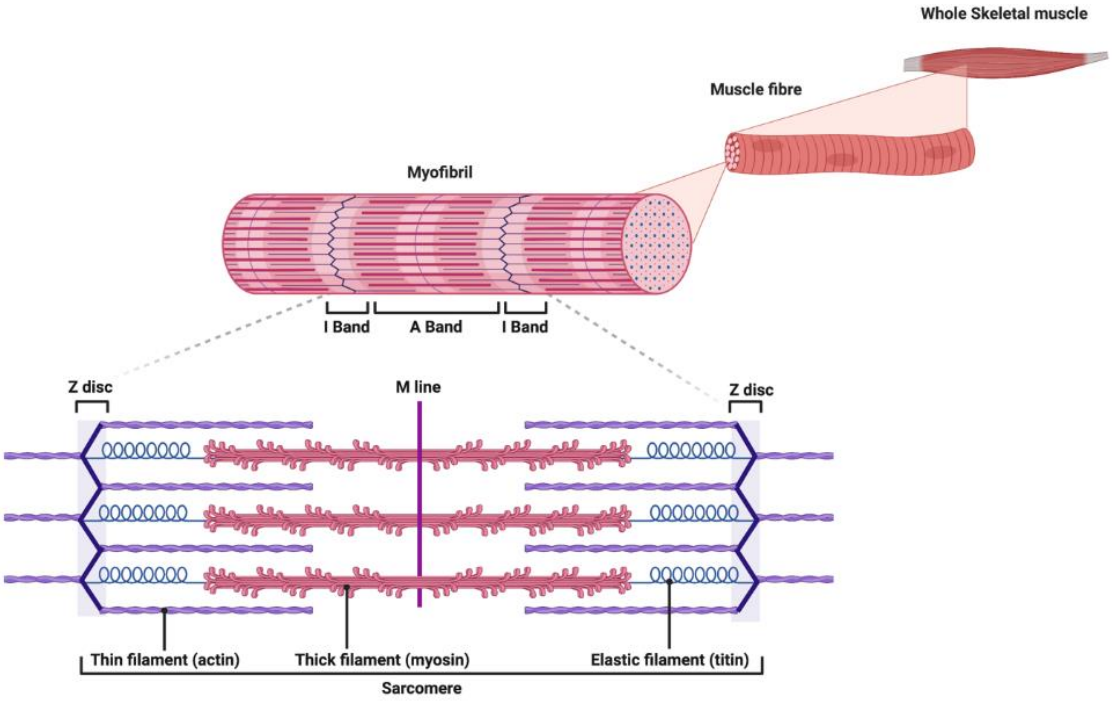

Figure 2.6. Schematic representation of the macro and microstructures found within whole skeletal muscle

2.4.2 Expression of the Endocannabinoid system in Skeletal Muscle Tissue

Despite the ECS being well characterised in several tissues (Section 2.3), less is known about this system in skeletal muscle (Kalkan et al., 2023b). While it is generally accepted that CB_1 receptors are primarily expressed within the CNS, there is some evidence to suggest the expression of CB_1 in mouse (Singlár et al., 2022), rat (Haddad, 2021a) and human (Cavuoto et al., 2007a) skeletal muscle. It should however be noted

that the findings in rodents have been limited to immunolabelling, while the findings in humans have been elucidated using RT-PCR and western blot. Meanwhile, the abundance of CB_2 in skeletal muscle has been observed in mice (Jiang et al., 2020) rats (Yu et al., 2010), and humans (Dalle and Koppo, 2021). It should however be acknowledged that there is a paucity of evidence via mass spectrometry to substantiate ECS machinery abundance in humans.

Notwithstanding the limitations in methodological characterisation, the observable ECS machinery means that the scientific interest in ECS modulation in muscle is unsurprising. More specifically, given that skeletal muscle is relevant to many physiological phenomena, including – but not limited to energy expenditure (Zurlo et al., 1990), metabolic regulation (Stump et al., 2006; Koves et al., 2008; Yang, 2014), protein turnover (Phillips, Glover and Rennie, 2009) and adaptation to exercise (Pillon et al., 2020). Indeed, these mechanisms make CBR abundance in skeletal muscle an interesting prospect for those interested in metabolic disease. From the perspective of performance and adaptation, the ECS might influence the regulation of skeletal muscle response to exercise (Schönke, Martinez-Tellez and Rensen, 2020) in addition to inflammatory signalling (Haddad, 2021a) – both of which an important considerations from health and performance perspectives. In addition to receptor abundance, circulating endocannabinoids are a further consideration. More specifically, AEA and 2-AG have been shown to fluctuate in response to changes in energy metabolism and/or diseased populations (Le Bacquer et al., 2022). Finally, and perhaps most pertinent to this thesis are the potential utilities of exogenous cannabinoid ingestion and their influence on skeletal muscle during and/or following exercise via ECS modulation. Taken together, it is largely unsurprising that the ECS broadly is of interest to the scientific community and individuals seeking health or performance benefits from the perspective of muscle.

2.5 The Use of CBD in Sport and Exercise

2.5.1 Background

Given the increased level of performance in elite sport, coupled with the associated high training load, athletes and associated personnel have explored various avenues

to improve performance and accelerate recovery for many years (Le Meur and Torres-Ronda, 2019; Naderi et al., 2025). In addition to the increased physical and psychological demands associated with performance, more recent advancements in technology mean that athletes can gain a better understanding of their physical and psychological well-being via wearable technologies, including (but not limited to) Whoop™, Oura™, and Garmin™ devices (Seçkin, Ateş and Seçkin, 2023). Given the commercial availability of these devices, it may be postulated that the data offered has encouraged athletes to explore new and more varied methods to optimise their well-being (Migliaccio, Padulo and Russo, 2024). While many of these phenomena might be best described as "trends" in sports performance, it is important to accept that athletes may use these even if the literature to support them is not without debate. The methods cited for optimising recovery are broad and include but are not limited to environmental manipulation – via the strategic implementation of temperature manipulation (Chaillou et al., 2022). Others may comprise physical and/or technological strategies including; compression garments (Brown et al., 2017), foam rollers (Wiewelhove et al., 2019) or percussive devices (Sams et al., 2023). However, the most traditional means of optimising recovery, fuelling performance and driving adaptation have been achieved through the consideration of the athletes' nutritional intake.

To achieve this, some of the most popular methodologies include the strategic use of functional foods or sports supplements (Naderi et al., 2025). These "functional foods" have been defined as such if they *"satisfactorily demonstrated to affect beneficially one or more target functions in the body, beyond adequate nutritional effects, in a way that is relevant to either an improved state of health and well-being and/or reduction of risk of disease"* (Henry, 2010). Meanwhile a "sports supplement" have previously been described as "*Products that are used to provide a practical form of energy and nutrients when it is impractical to consume everyday foods*" (Maughan et al., 2018). Indeed, both definitions may, therefore, seem desirable to athletes who wish for accelerated recovery in a convenient manner. As such, the global market for sports supplements has increased significantly in recent years (Arenas-Jal et al., 2020). In

addition to the commercial and athletic interest in sports supplements, the scientific community have adopted these products as an avenue for considerable research. For several decades, various nutritional strategies have been explored to modulate the physical symptoms associated with exercise-induced muscle damage and/or recovery, though an in-depth appraisal of each of these strategies is beyond the scope of this thesis, please see (Owens et al., 2019) for review.

2.5.2 Pharmacological or Medicinal Approaches to Support Recovery

At times, the magnitude of discomfort or pain associated with exercise might also encourage athletes to use analgesic or anti-inflammatory agents (King, 2014; Matava, 2018). Common phenomena associated with some modes of exercise are exercise, and/or impact induced muscle damage (EIMD;IIMD), Indeed, following damage of both kinds, there is evidence to confirm that athletes will often turn to various pharmacological analgesic agents (Naughton, Miller and Slater, 2018). Of these, some of the most widely consumed are non-steroidal anti-inflammatory drugs (NSAIDs), namely - ibuprofen and naproxen (Tsitsimpikou et al., 2009; Schoenfeld, 2012). Furthermore, following traumatic injury, other agents, including opiates such as tramadol have been used historically – a compound prohibited by WADA since January 2024 (Vernec, Pipe and Slack, 2017; Thevis, Kuuranne and Geyer, 2024).

While these agents may provide the analgesic and anti-inflammatory properties promised, they are not without their shortcomings. For example, the chronic use of NSAIDs has been associated with various side effects including, kidney failure, bleeding ulcers and gastrointestinal injuries more broadly (Goldstein and Cryer, 2015; Holgado et al., 2018a). Moreover, of particular concern to athletes competing in collision sports, who are at risk of IIMD as well as EIMD, is the suggestion that chronic NSAID use may inhibit platelet function (Driver, Marks and van der Wal, 2020). It is also important to consider that the efficacy and ethical considerations of accepting the use of these compounds might be questionable. There are data to suggest that agents such as these might have a detrimental effect on muscle protein synthesis (Trappe et al., 2002; Krentz et al., 2008). In addition, given their purported analgesic

effects, these agents can “blunt” pain (Emerson et al., 2021), this might facilitate premature return-to-play and therefore an increased re-injury likelihood (Lundberg and Howatson, 2018).

2.5.3 The Application of CBD in Sport and Exercise

As highlighted in Section 2.2 there have been various purported utilities of cannabinoids (including CBD) in several distinct instances. Notwithstanding the paucity of mechanistic insight into ECS machinery in muscle, the interest from key stakeholders involved in elite sport is growing significantly. This, coupled with the detrimental effects associated with pharmaceutical interventions, has meant that cannabinoids have more recently been seen as an alternate method to traditional medications in the quest for pain relief. Concernedly, a large 2020 systematic review reported that 23% of > 46,000 athletes admitted to having used some form of cannabis in the previous year (Docter et al., 2020). However, CBD has been seen as a “safer” alternative to whole-cannabis products. For example, Kasper and colleagues (2020) completed a survey to understand the prevalence of CBD use in elite rugby union and league players, across the 25 clubs surveyed, 517 players responded and reported interesting results. More specifically, the survey found that 26% of players had previously or were currently using CBD supplements. Moreover, many of the respondents (80%), cited improved recovery and pain management as their primary motives for supplementation. However, only 14% of players perceived improvement in recovery or pain management (Kasper et al., 2020b). This prevalence in use now means that understanding the utility and implementation of CBD are key considerations for athletes and practitioners.

The purported anti-inflammatory and analgesic qualities of CBD has meant that research investigating the compounds supplementation following exercise has become more prominent in the literature. One of the earliest studies investigating the efficacy of CBD recruited trained participants to an exercise bout comprising 4 sets of 10 back squats at 80% of participants’ respective one-repetition maximum (1RM) to induce EIMD. When participants completed their exercise session, they were

randomly assigned to either a CBD group (16.67 mg in MCT oil) or a visually identical MCT-only placebo. Promisingly, The CBD group reported reduced soreness 24 h post-exercise compared with immediately postexercise and 72 h postexercise compared with 48 h postexercise (Hatchett et al., 2020). These results however must be interpreted with caution as the baseline strength measures of the groups were considerably different (CBD = 102.8 ± 45.2 kg; PLA = 82.4 ± 34.4; null = 65.9 ± 16.2 kg). Given that EIMD is typically associated with unaccustomed exercise, these large differences in participant characteristics might explain the elucidated results. In a later study, Isenmann and colleagues recruited 21 trained participants to investigate muscle recovery following 3 sets of 12 back squats at 70% 1RM and 3 sets of 15 drop jumps. These authors noted that CBD restored the loss in back squat performance to a greater level than a visually identical and taste-matched placebo. In addition, CBD diminished plasma increases in creatine kinase (CK) and myoglobin. That said, these results were only observable at 72-h post-exercise (Isenmann, Veit and Diel, 2020). Furthermore, Cochrane-Snyman and colleagues recruited untrained males to complete an eccentric elbow flexor muscle-damage protocol and were supplemented with 150 mg CBD or placebo 2, 24, and 48 h following exercise. Though this dose was considerably higher than the previous studies' mentioned, however the authors were unable to detect any effect of their 150 mg dose of CBD on perceived soreness, arm circumference, hanging joint angle, or peak torque following exercise (Cochrane-Snyman et al., 2021). Though, it should be noted that this exercise modality might not have been appropriate to induce "damage", and furthermore, the dosing regime was limited to 4-days.

In female athletes, 5 $mg \cdot kg^{-1}$ CBD provided in the 10-hours following muscle-damaging exercise had no influence on concentrations of plasma inflammatory cytokines including IL-1b, IL-10 or IL-6 at any time-point (4-48h). In addition, these authors also reported no changes in subjective measures of fatigue and they noted there to be no accelerated return to baseline of performance in the CBD group compared to placebo (Crossland et al., 2022). In addition, a 2023 pilot study recruited four participants to complete an eccentric exercise protocol comprising 6 sets of 10 eccentric-only bicep curls. After the exercise stimulus, participants were provided with a placebo, low-dose

(2 $mg \cdot kg^{-1}$) or high-dose (10 $mg \cdot kg^{-1}$) CBD product. Consistent with the findings of Crossland and colleagues (2022), this study failed to evidence any reduction in the inflammatory marker IL-6. Like many of the other studies to date, these results should be interpreted with caution because of the low sample size and the variable exercise programme design.

A 2023 study investigated the effects of a CBD-CBG based recovery powder (containing 35 mg CBD; 50 mg CBG; 25 mg beta-caryophyllene [BCP]; 3.8 g BCAAs and 420 mg Magnesium Citrate) on recovery from DOMS. The damaging protocol in this study comprised 5 sets of 15 repetitions of eccentric bicep curls at 60% of the participants' pre-determined 1RM. Following damage, participants consumed their respective supplement on the evening of the first study visit, and then at 08:00 h and 20:00 h (± 1 hour) every day until their final (72-hours post-exercise) visit. The last dose occurred 60-minutes before the 72-hour post-DOMS visit. Given this was a pilot study, a traditional statistical approach was not conducted, instead the authors opted for an inference-based method. It was concluded that the supplement used in the study might prove beneficial for accelerated recovery from DOMS and may also decrease the subjective measures of soreness/discomfort associated with DOMS. Once more, these findings from a CBD perspective should be interpreted with caution as CBD was not the lone compound within the formulation, and as such, basing a suggestion that CBD was the molecule responsible for any observations in this would not be appropriate (Peters et al., 2023).

In a study on topical CBD treatment, (Alpy et al., 2023) recruited 21 participants to complete a muscle damaging protocol comprising 3 sets of 3-second eccentric, unilateral bicep curls until failure. Thereafter, participants were provided with either a placebo or a 1g of a 1000 mg concentration (~20mg CBD/dose) CBD-balm daily for 72-hours. The authors suggested there to be no influence of CBD on any of their associated markers of performance and attributed this lack of effect to the "moderate-to-high" dose that was used within their study and then suggested maximising the recommended daily dose in future investigations. Isenmann et al (2024) continued their research into CBD and recovering muscle and aimed to

investigate the influence of short-term chronic CBD application on muscle damage, inflammation and performance in competitive athletes following an “intense” training week. Participants (n = 17) were provided with 60 mg CBD (sublingual oil) each day of a 6-day “shock” exercise microcycle, which evidenced equivocal findings within their study cohort. More specifically, the authors noted that CBD moderately reduced myoglobin (MYO) concentrations in “advanced” athletes, but less-so in “highly-advanced” individuals (defined based upon the participants’ relative strength levels. However, researchers reported no change in their associated performance outcomes (Isenmann et al., 2024).

While much of the research surrounding CBD and performance pertain to recovery from exercise, there is some emerging evidence that CBD may also play a role in aerobic performance. These investigations began with (Sahinovic et al., 2022), who completed a pilot study which aimed to understand the physiological and bioenergetic implications of CBD supplementation in endurance-trained males. Following supplementation of 300 mg oral CBD 1.5 h before incremental exercise to exhaustion, CBD appeared to increase $\dot{V}O_2$, blood lactate ($mmol \cdot l^{-1}$) and subjective ratings of pleasure (AU) compared to control. In addition, it was suggested that CBD might have also increased $\dot{V}O_{2max.}$ Importantly however, this study used only acute doses of CBD prior to exercise. Various studies have now suggested that given CBD’s low bioavailability (Vučković et al., 2018), a longer supplementation period may have elucidated strong results. Thereafter, a further study recruited 42 regular cannabis users to take part in a treadmill run following the *ad libitum* consumption of either a high-THC or high-CBD strain of cannabis. This study suggested that participants’ enjoyment of exercise was greatest in the high-CBD group (Gibson et al., 2024). The authors suggested this result was surprising because CBD is not “psychoactive”, yet this is a somewhat unsubstantiated assertion as CBD has also been proposed to play a role in several conditions related to anxiety (Skelley et al., 2020). Furthermore, (Cheung et al., 2024) recruited 14 habitual cannabis users to complete a sub-and maximal exercise time-trial on a cycle ergometer after inhaling THC-dominant, CBD-dominant or control vapour. The authors’ findings suggest that CBD predominant cannabis had no effect on the physiological response to exercise or performance.

Noteworthy, however was that the CBD-dominant product contained only 100 mg of CBD and was administered acutely. As mentioned previously, these short-term, low-dose dosing protocols may not be appropriate to provide any ergogenic effect to exercise. In a similar fashion to the previously mentioned studies, surrounding the pleasure associated with exercise, a 2024 randomised control trial recruited 51 healthy participants who ingested 150 mg CBD or placebo 90-mins before a 10 km run. Once more, *during* exercise, the 150 mg of CBD failed to attenuate any of the negative feelings or emotions associated with high-intensity exercise (McCartney et al., 2024). Finally, a more recent investigation provided participants with 298 mg CBD ~ 60 mins before exercise in the heat and the authors suggested no affect of supplementation on thermorgulation, but interestingly an immunosuppressive response was noted following reductions in CD14 and IL-6 responses (Johnson et al., 2025). Indeed, the lack of affect may once more be attributed to the acute nature of supplement ingestion. Taken together, while some notable work has been carried out in this regard, many of the studies have methodological inconsistencies and/or shortcomings. Many of the studies mentioned have a wide range of participant characteristics, dosing strategies and exercise protocols. In addition, the common and overriding theme with many of the investigations discussed herein have adopted acute treatment strategies, and future work may seek to investigate how longer-term CBD treatment might influence health and performance outcomes.

2.5.4 Anti-Doping Concerns Surrounding Cannabinoids

The World Anti-Doping Agency (WADA) was established in response to the historical doping scandals including, but not limited to the 1998 Tour De France and the questions of integrity surrounding the International Olympic Committee (IOC) (Waddington and Møller, 2019). As per the WADA mission statement *"WADA's mission is to lead a collaborative worldwide movement for doping-free sport by developing, harmonizing, coordinating and monitoring anti-doping rules and policies across all sports and countries"* (WADA, 2025). WADA exists to encourage clean sport and mitigate the risks of athletes consuming prohibited substances. While these key functions of WADA are vital to protect sport, it might be argued that athletes also need protection. More specifically, given that nutritional supplements are incredibly

popular with elite sport(Garthe and Ramsbottom, 2020), coupled with the risk associated with contaminated substances (Close et al., 2022), a level of support is required. Indeed, to give athletes confidence in sport nutrition supplements, many companies now offer a batch-testing service, which tests products for prohibited substances and dangerous materials (Judkins and Prock, 2012). However, it must be stressed that this does not guarantee supplement safety, rather it reduces risk (Close et al., 2022). As per the World Anti-Doping Code strict liability in the context of anti-doping rules is the principle that athletes are solely responsible for any prohibited substance found in their bodies, regardless of intent or negligence. This means that if a prohibited substance or its metabolites are detected in an athlete's sample, it might lead to an adverse-analytical finding – or even an Anti-Doping Rule Violation (Ten Haaf et al.), regardless of how the substance entered their body or whether there was intent to "cheat". (Aagaard et al., 2002)

In 2018, CBD was removed from WADA's list of prohibited substances (Gamelin et al., 2020). Importantly however, all other cannabinoids remain prohibited (Figure 2.7). It is important to note that Δ^9-THC is considered a "threshold" substance by WADA, meaning that an AAF would only be reported if urinary concentrations of Δ^9-THC, or it's metabolites (11-OH-THC, 11-COOH-THC) breach the 150 ng/ml threshold. Concernedly, cannabinoids other than Δ^9-THC may pose an even greater risk because they are not threshold compounds, meaning that any detectable concentration in urine could result in an AAF (Mareck et al., 2021). It should be noted however, that Section 8 of the World Anti-Doping Prohibited List (2025; Figure 2.8), does not state any information regarding thresholds.

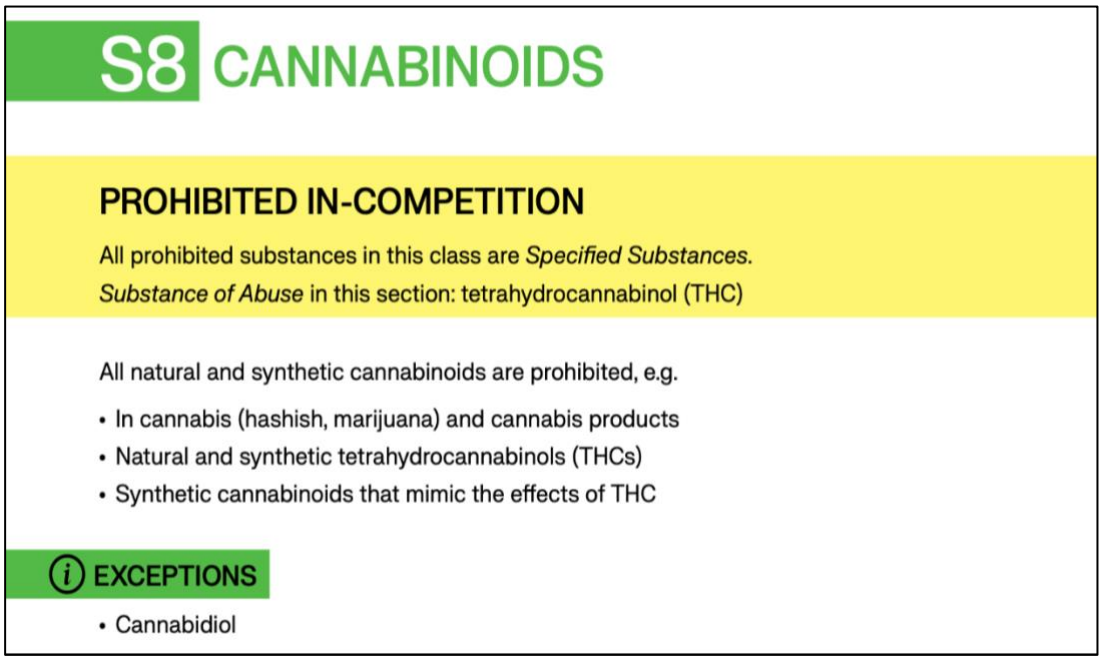

Figure 2.7 Section 8 of the 2025 World Anti-Doping Prohibited List (WADA, 2025).

While many CBD products claim to be Δ^9-THC-free, it is crucial to re-emphasize that all other cannabinoids remain prohibited, regardless of concentration. As such, athletes must ensure that CBD products are not only free of Δ^9-THC but also devoid of all other cannabinoids. This issue is further complicated as there are also differing formulations of CBD available, either off-the-shelf or via the internet. This means that differing CBD formulations are available to the consumer – regardless of their knowledge surrounding the complexities surrounding CBD or their requirement to consume batch-tested supplements (Table 2.3) (Bhamra et al., 2021). Moreover, it is also concerning that in the survey completed by Kasper and colleagues (2020), 52% of CBD users were not concerned about committing an ADRV, with 79% of respondents under the impression that the product they were using was batch-tested for prohibited substances. Indeed, despite many professional rugby teams having qualified nutritionists in-situ, athletes are more likely to gain their knowledge on CBD from alternate sources – including the internet (Kasper et al., 2020b).

Table 2.3: Phytocannabinoid content of off-the-shelf CBD formulations. * Denotes the likely inclusion of CBD in addition to other cannabinoids, but not Δ^9-THC. ** Denotes the likely inclusion of CBD in addition to other cannabinoids, including Δ^9-THC.

Product	Δ^9-THC	Other Phytocannabinoids
CBD Isolate	☒	☒
Broad-Spectrum CBD*	☒	☑
Full-Spectrum CBD**	☑	☑

A concern for athletes and associated personnel, however, is that there are often disparities between the advertised and actual content of many CBD products. Various research groups from across the globe have confirmed these assertions in several recent publications. For example, using gas chromatography - flame ionization detection it was concluded that of 25 tested CBD oils, only 88% contained measurable quantities of CBD, meaning 12% of tested products contained no phytocannabinoids whatsoever (Gurley et al., 2020). Similarly, in the State of Kentucky, Liquid Chromatography – Tandem Mass Spectrometry (LC-MS/MS) elucidated yet more confirmation that there are considerable discrepancies between the label claims of CBD oils, compared to their actual contents. This investigation demonstrated that of 80 products tested, 31% were under labelled and 15% were over labelled, meaning only 54% of sampled had accurate concentrations of CBD within them (Johnson, Kilgore and Babalonis, 2022). While these collective findings might be significantly underwhelming for the general consumer, more concerning were the findings of Gurley and colleagues (2018) who also reported concentrations of cannabinoids that were not reported on the CBD bottles. More specifically, three products (12%) contained concentrations of Δ^9-THC which breached the 0.3% legal limit, with one product containing 45% Δ^9-THC. Moreover, it was reported that 16% of products were contaminated with synthetic cannabinoids, which are indeed prohibited (Gurley et al., 2020). Additionally, Liebling and colleagues (2020) completed a blinded analysis of 29 commercially available CBD oils from off-the-shelf in the United Kingdom. Their research evidenced that there was an average variability of actual content versus label claims of 76% - with a range of 0-155%. In addition, over 50% of the products tested

contained controlled substances, such as Δ^9-THC. Overall, only 38% of products were within a 10% range of the advertised content of CBD and 34% of products had 50% or less than their advertised CBD content (Liebling et al., 2020). Because of the prevalence of CBD being sold in various forms beyond oil only, Johnson and colleagues (2023) assessed the CBD concentrations of 63 products from 40 brands, comprising 13 aqueous tinctures, 29 oils, 10 e-liquids and 11 drinks. Their investigation highlighted that only 8% of tested products contained within 10% of their advertised concentrations. While this study does not necessarily highlight anti-doping considerations per sé, it emphasises that the content versus claim issues surrounding CBD commerce is a real problem for the consumer.

These ongoing and more recent content versus claim issues are not exclusive to the United Kingdom and Europe. A 2022 US investigation aimed to analyse commercially available CBD products of varying formulations and concentrations (Miller et al., 2022). Once more using High Performance Liquid Chromatography (HPLC), the authors once more demonstrated that the advertised concentrations of CBD were not consistent with their actual content in oils (63.64%), aqueous products (92.86%) "other" products (66.7%) (defined as chocolates, polymer blends, coconut oils, soft-gels, honey or Epsom salts). However, perhaps more concernedly was that of the products tested, Δ^9-THC was observed in 54.55% of oils, 23.81% of aqueous products and 71.43% of those defined as "other". While we must accept that from the perspective of consumers, the CBD content is important, the real concern is the concentration of prohibited cannabinoids. This study highlights the potential for considerable Δ^9-THC concentrations and as such, might have implications not only on athletes, but the general population who might undergo routine drug testing in the workplace. Indeed, it has been highlighted that 4-weeks supplementation of CBD (containing < 1 mg Δ^9-THC) can result in the appearance of THC-COOH in urine in 50% (n = 7) of participants (Dahlgren et al., 2021). As such, this variability in cannabinoid concentrations in commercial products presents a significant challenge for athletes and nutritionists, raising the risk of unintentional AAFs. Additional to these factors are the consideration that given the lipophilic nature of cannabinoids, some research has evidenced cannabinoid concentrations can be influenced by nutrition. More

specifically, rats who received 10 $mg \cdot kg^{-1}$ Δ^9-THC for 10 days evidenced signs of elevates blood cannabinoid levels following a food deprivation protocol (Gunasekaran et al., 2009). Furthermore, a 2013 study recruited 14 regular cannabis users to complete 35-minutes of moderate intensity exercise which resulted in a significant increase in plasma-THC levels (Wong et al., 2013). It is however unclear whether trace cannabinoids can be accumulated in adipose tissue and then released following longer-term supplementation protocols.

One possible alternative to mitigate these risks is the use of synthetic CBD, which eliminates concerns about contamination with other cannabinoids. However, research on synthetic CBD is limited, and the potential loss of the "entourage effect" requires studies to evaluate its safety, efficacy, and optimal dosing before it can be recommended for athletes. More specifically, there have been suggestions that the utility of cannabinoids might be increased with the synergistic application of cannabinoids, beyond solely CBD (André et al., 2024). Taken together, it has become clear that there is considerable work to be done regarding the understanding of CBD supplementation from an anti-doping perspective. Given that there is seemingly a large disparity in the actual versus advertised content of many CBD supplements, from containing no CBD, through to containing concentrations of prohibited cannabinoids, it is paramount that research is completed to provide athletes and the general population alike with rigorous data to confirm if these concerns are translated to biological matrices which could be interrogated by WADA.

2.6 Perspective

Based on the review of literature presented, it is evident that research into phytocannabinoids - particularly CBD has intensified in recent years (Figure 2.8). Nevertheless, several important knowledge gaps remain. While several investigations have examined the utility of CBD as a recovery modality, little to no research has explored the role that CBD might serve as an ergogenic aid during exercise itself. Furthermore, while some mechanistic work has aimed to elucidate the underlying pathways of CBD's action, there remains limited understanding of its specific actions

on skeletal muscle. In parallel, there is now a growing body of evidence to suggest that commonly available CBD products often fail to contain the cannabinoids advertised. However, there is little data on the practical implications of these discrepancies for end-users, particularly those competing in sports under the jurisdiction of WADA. Consequently, this thesis adopts an integrative and translational approach to address these key unresolved questions. This thesis aims to generate a robust and systematic series of investigations to advance the understanding of the scientific community, while also informing safer, more effective use of CBD by athletes and practitioners. In doing so, the findings may also contribute to the evidence base required to inform regulatory frameworks, quality standards, and anti-doping policies relating to phytocannabinoids in sport. The aims and objectives of this thesis are available in section 1.2.

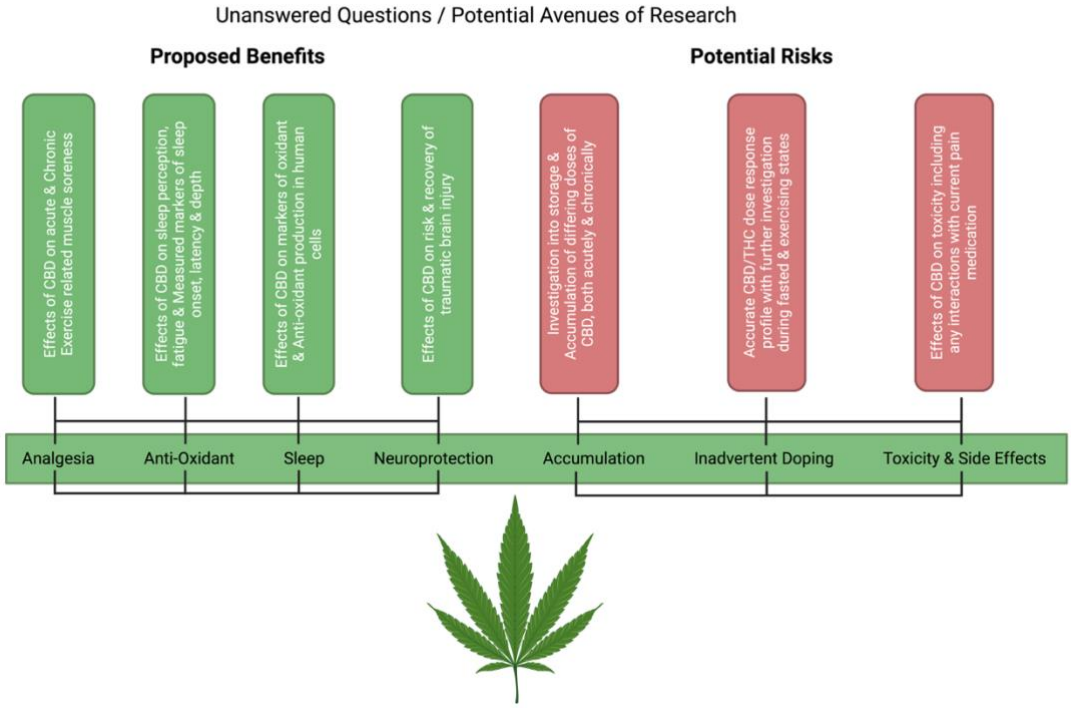

Figure 2.8. Proposed broad themes of research surrounding the CBD supplementation in humans. Adapted from Close et al., (2021).

3 General Methods

This chapter describes and explains the theory and implementation of the methodologies pertinent to the investigation within this thesis.

3.1 Cell Culture

All cell culture experiments were performed in a sterile laminar flow Kojair Biowizard Silverline class II hood (Kojair. Vippula, Finland). Cells were incubated at 37°C and 5% CO_2 in a Binder incubator (Binder, NY, USA). All liquids, waste media and supernatants were removed via an extraction pump (Charles Austen Pumps Ltd. Surrey, UK).

3.2 Plasticware

Cell populations were cultured on T75 cm^2 culture flasks (Corning, NY, USA), with experiments conducted on 6 and 12-well plates (Corning, NY, USA). Experimental Eppendorf tubes were purchased from (Eppendorf, Hamburg, Germany) and cryogenic vials from Simport Scientific (Saint Mathieu-de-Beloeil, Canada).

3.3 Reagents

Porcine (0.2%) gelatin solution was prepared by mixing 1 g of powdered porcine gelatin (Sigma-Aldrich Company Ltd, Dorset, UK) into 500 mL of dH_2O. This solution was applied to both T75 cm^2 culture flasks and well plates to encourage cell adhesion. Phosphate buffered Saline (PBS) used to wash cell monolayers was prepared by placing 5 PBS tablets (Sigma-Aldrich, Sigma Life Sciences, St Louis, MO, USA) into 500 ml of dH_2O. Each of these solutions were autoclaved before use in any cell culture experiments. Dulbecco's modified eagles' medium (DMEM) with ultraglutamine and high (4×10^4 $mg \cdot L^{-1}$) glucose was purchased from Lonza (Verviers, Belgium). Growth Media (GM) for C_2C_{12} cells comprised DMEM, 10% Fetal Bovine Serum (FBS), 10% Newborn Calf Serum (NBCS; Gibco Life Technologies, California, US) and 1% syringe-filtered penicillin-streptomycin solution. C_2C_{12} differentiation media (DM) comprised DMEM, 2% Horse Serum (HS) and 1% syringe-filtered penicillin-streptomycin solution, with all sera purchased from Gibco (Life Technologies, California, US). Broad-spectrum cannabidiol (CBD; 314.47 $g \cdot mol^{-1}$) was provided by Naturecan Ltd. Stockport, UK in powdered form and reconstituted in DMSO. Solutions containing H_2O were prepared using dH_2O from a MilliQ water purification system (Merck KGaA. Darmstadt, Germany).

3.4 Propagation of Myoblasts

Cryovials containing 1 x 10^6 C_2C_{12} myoblasts were stored and resuscitated from liquid nitrogen (LN_2) to commence all experimental procedures. Myoblasts were seeded on pre-gelatinised culture flasks containing 14 mL of GM. These culture plates were then incubated (37°C, 5% CO_2) until 80% confluency was reached (Figure 3.1).

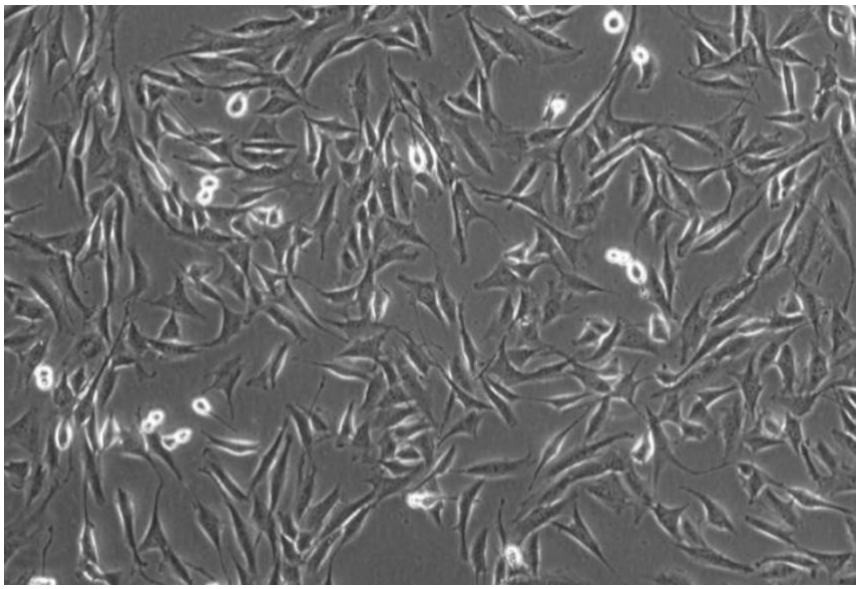

Figure 3.1. C_2C_{12} myoblasts at ~80% confluence.

3.5 Passaging Cells

Once ~80% confluence was reached, T75s were passaged by trypsinisation. Briefly, existing medium was removed, and monolayers were washed twice with 5 mL pre-warmed 1 x PBS. Thereafter, 1 mL of trypsin EDTA was added to the culture flask, which was incubated for 5-minutes (37°C, 5% CO_2). Following incubation, 4 mL of GM was added to the flask to neutralise trypsin. This solution was then gently homogenised by pipetting the cell suspension and added to a 50 ml falcon tube containing 25 ml of fresh GM. This solution was again homogenised before the suspension was split 50:50 onto 2 x T75 culture flasks.

3.6 Cell Counting and Seeding by Trypan Blue Exclusion

When cells reached 80% confluence, existing medium was removed, and monolayers were washed twice with 5 ml pre-warmed PBS. Thereafter, 1 mL of trypsin EDTA was added to the culture flask, which was incubated for 5-minutes (37°C, 5% CO_2). Following incubation, 4 mL of GM was added to the flask to neutralise trypsin. Following homogenisation, 20 µL 0.4% trypan blue (Sigma-Aldrich, Sigma Life Sciences, St Louis, MO, USA) and 20 µL cell/GM solution were added to a 1 mL Eppendorf and cells were counted using a Neubauer haemocytometer. Cells in the four corner grids were counted under a microscope (Olympus CKX31 Microscope) at x10 magnification. Viable cells were recognized as small, round, and clearly visible, while non-viable cells were misshapen, slightly larger and had lost their membrane integrity, hence were trypan blue positive. The resultant mean of 4 grids was calculated, which represented average cell numbers occupied 0.1 mm^3. This value was then multiplied by 2 to account for the dilution factor of 1:1. A further multiplication by 10^4 was undertaken to extrapolate the number of cells in 0.1 mm^3 to 1 cm^3 (equivalent to 1 mL of cell suspension). The total number of cells contained in the cell suspension could be calculated by multiplying by the total volume of cell suspension (mL). Following the cell count, seeding was completed as per the below equation:

$$Required\ cell\ suspension\ (ml) = \frac{Required\ seed}{cell\ count} * Required\ Total\ Media$$

3.7 Microscopy

Cell imagining was performed using a Leica DMI 6000B live Imaging Microscope (Leica Biosystems, Wetzlar, Germany). Images of cell monolayers were captured using the 10x objective and 0.5 magnification. Image inspection and processing were completed using Leica Application Suite for Windows, Biosystems, Wetzlar, Germany and ImageJ (version 1.53a, National Institutes of Health, USA).

3.8 EdU Assay

Measuring a cell's ability to proliferate is a fundamental method for assessing cell health, determining genotoxicity, and evaluating anti-cancer drugs. The most accurate

method of doing this is by directly measuring DNA synthesis. Older methods achieved this by incorporating radioactive nucleosides (for example, H-thymidine). This method was replaced by antibody-based detection of the nucleoside analogue bromo-deoxyuridine (BrdU). The ClickiT® EdU Assay from Invitrogen is a novel alternative to the BrdU assay. EdU (5-ethynyl-2´-deoxyuridine) provided in the kit is a nucleoside analogue of thymidine and is incorporated into DNA during active DNA synthesis.1 Detection is based on a click reaction,2-5 a copper-catalyzed covalent reaction between an azide and an alkyne. In this application, the EdU contains the alkyne and the Alexa Fluor® dye contains the azide. The advantages of the ClickiT® EdU labelling are readily evident while performing the assay. The small size of the dye azide allows for efficient detection of the incorporated EdU using mild conditions. Standard aldehyde-based fixation and detergent permeabilization are sufficient for the ClickiT® detection reagent to gain access to the DNA. This contrasts with BrdU assays that require DNA denaturation (typically using HCl or heat or digestion with DNase) to expose the BrdU so that it may be detected with an anti-BrdU antibody. The denaturation step in the BrdU protocol can disrupt dsDNA integrity, which can affect nuclear counterstaining, and can also destroy cell morphology and antigen recognition sites. In contrast, the EdU assay kit is not only easy to use, but is fully compatible with DNA staining, including dyes for cell cycle analysis. The EdU assay kit can also be multiplexed with surface and intracellular marker detection using antibodies. Finally, unlike the BrdU assay, which relies upon antibodies which can exhibit nonspecific binding, the Click-iT® EdU assay uses bioorthogonal (biologically unique) moieties, producing low backgrounds and high detection sensitivities. The kit contains all the components needed to label and detect the incorporated EdU as well as perform cell cycle analysis on samples from adherent cells. For cell cycle analysis, the kit is supplied with Hoechst 33342 dye.

3.9 MTT Cell Viability Assay

The MTT (diphenyl tetrazolium bromide) assay is a colorimetric assay used to measure cell metabolic activity. It is based on the ability of nicotinamide adenine dinucleotide phosphate (NADPH)-dependent cellular oxidoreductase enzymes to reduce the tetrazolium dye (MTT) to its insoluble formazan, which has a purple colour. The absorbance of this coloured solution can be quantified by measuring at a particular wavelength (570 nm). This assay, therefore, measures cell viability in terms of reductive activity as enzymatic conversion of the tetrazolium compound to water-insoluble formazan crystals by dehydrogenases occurring in the mitochondria of living cells.

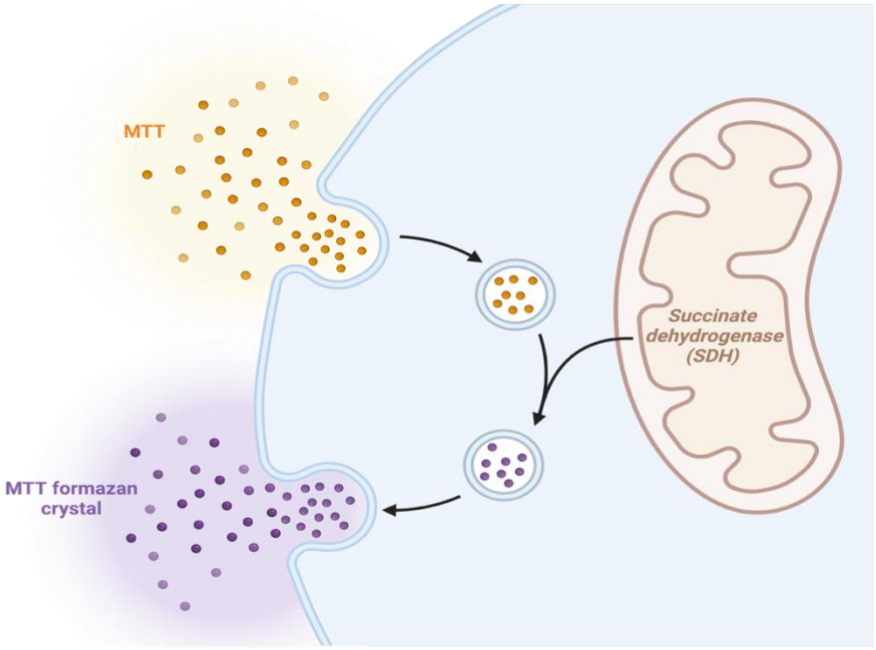

Figure 3.2. Schematic representation of the mechanism by which metabolic activity can be calculated via the MTT assay.

3.10 Flow Cytometry

3.10.1 General Principle:

Flow cytometry is typically used because of its ability to quantify the optical and fluorescent characteristics of single cells, microorganisms, nuclei, and chromosome preparations (McKinnon, 2018) (Figure 3.3). The quantification of single-cell

characteristics is possible via a liquid passing through a (or multiple) light streams. Flow cytometry can quantify the granularity and fluorescent aspects of cells (Adan et al., 2017). The quantification of various aspects of a molecule can be assessed as a given molecule will scatter and/or emit light as it moves through a known light source. This can then be measured by various detectors. For the flow cytometer to accurately calculate the properties of individual cells within a population, the suspension must first pass through a stream of sheath fluid, which subsequently hydrodynamically focuses the cells into single file as they pass through the laser. Before any fluorescent probe analysis can be completed, the cytometer must first measure two dynamics of light, forward scatter (FSC) and side scatter (SSC; Figure 3.4). The FSC detector sits in line with the beam of light from the laser and as the cell moves through the laser beam it deflects the light creating a shadow on the detector behind. This procedure then allows the cytometer to calculate the size of a cell (as a larger shadow is associated with a larger cell). With regards to the SSC, this sits perpendicular to the laser beam. When light hits the cell, it is scattered by the cell's internal cellular components, and the more light that is scattered, the more granulated, or complex the cell is. These two components (FSC and SSC) are plotted on a dot plot, where populations of similarly sized cells will group together, as with cells of a similar complexity. This population grouping allows the researcher to differentiate between "healthy" cells which are grouped together, while cells which are going through apoptosis usually shrink in size and increase in complexity (resulting in movement from the grouped population on the graph (Myoblasts: Figure 3.4a and Myotubes Figure 3.4b).The flow cytometer is also able to quantify cellular fluorescence, which can be used to accurately measure any changes in emission from fluorescent probes which can be added to a cell population to detect a specific aspect of cellular homeostasis. The BD Accuri™ C6 Plus Flow Cytometer (BD biosciences, Berkshire, UK) which was used throughout this thesis had four channels to measure fluorescence intensity (FL-1, FL-2, FL-3, and FL-4).

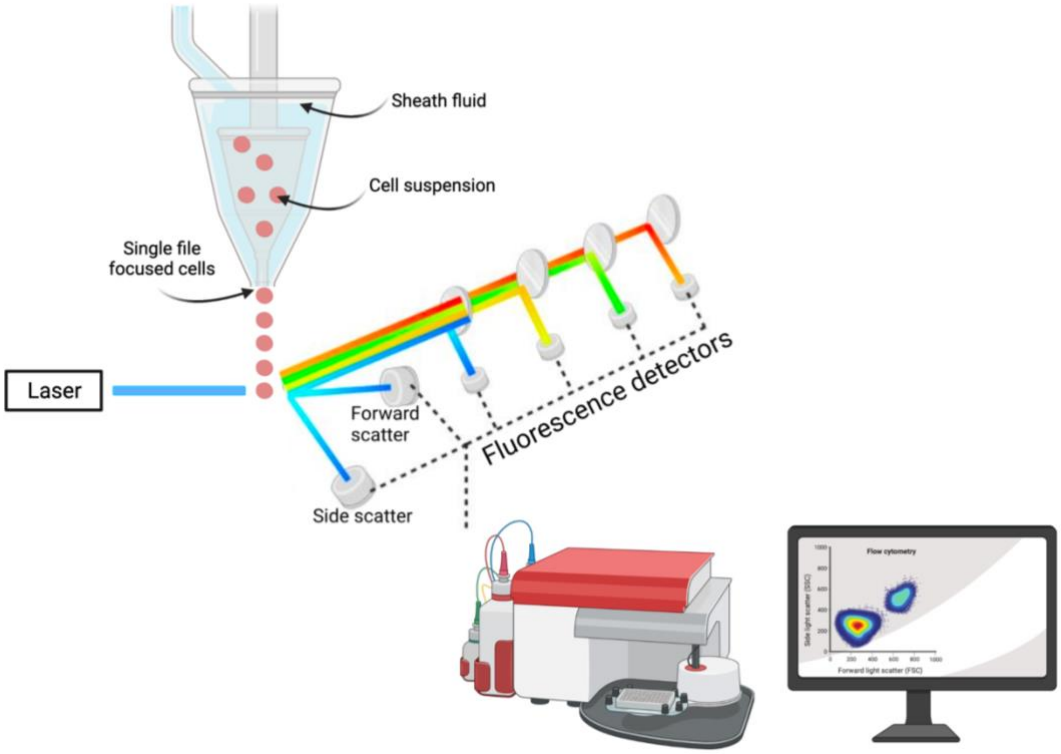

Figure 3.3. Basic workflow using the BD AccuriTM C6 Flow Cytometer. Cells in suspension flow in single file through an illuminated volume where they scatter light and emit fluorescence. This is then detected by the detectors which pick up a combination of scattered and fluorescent light. This data is then analysed using BD Accuri software.

3.10.2 General Protocol

Before any experimental procedure could be completed, a control group of cells was run through the flow cytometer which gated the FSC and SSC and quantified the background fluorescence. To complete this, 200 µl of a cellular suspension was put into the flow cytometer and the population was gaited. Cell gaiting was completed whereby the densest area of the population was gated and considered a viable population according to (Figure 3.4 A, B). Once these parameters were set, they remained consistent in each experiment using the same cell type.

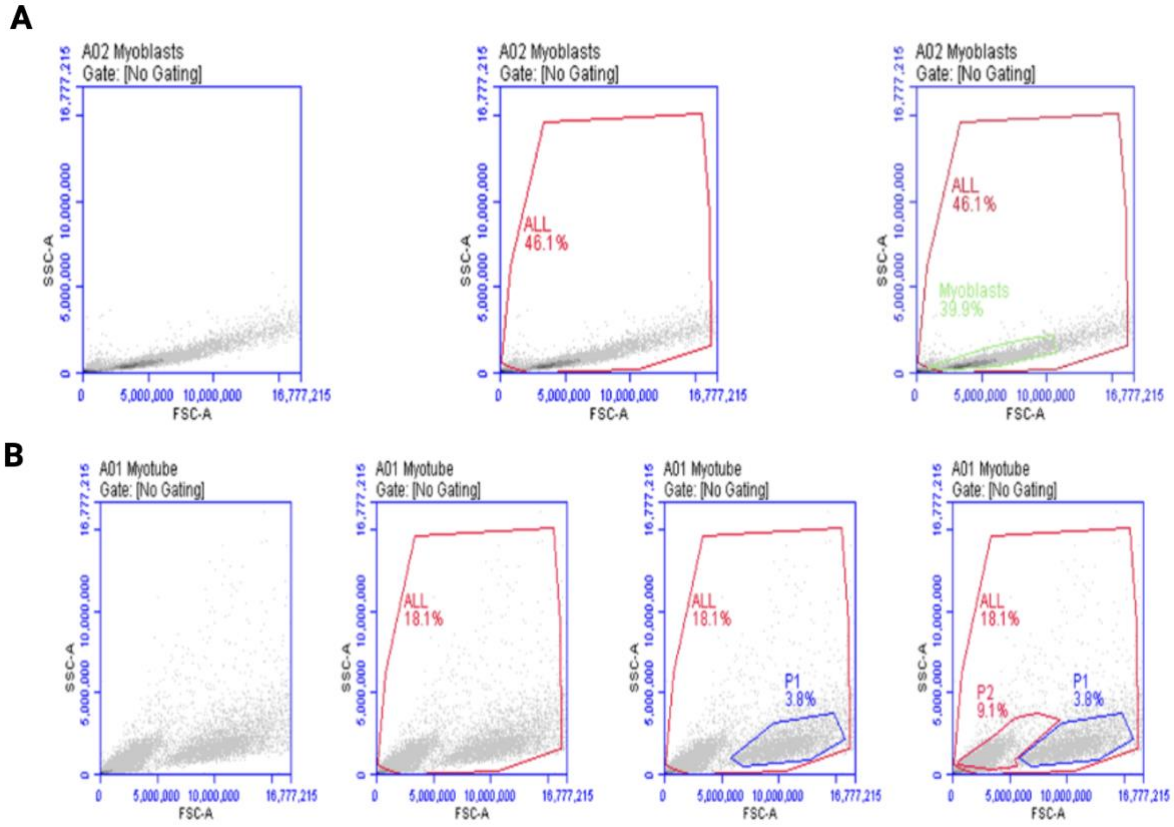

Figure 3.4. A) Gating strategy of C2C12 myoblasts on the BD Accuri C6 flow cytometer. Cells were gated around to include all events on the scatterplot. Debris located in the bottom left of the scatterplot was excluded. A second gate was included to better visualise myoblast population. B) Gating strategy of C_2C_{12} myotubes on the BD Accuri C6 flow cytometer. Gating strategy was like myoblasts with two separate gates used to visualise the myotube populations.

3.11 Propidium Iodide Assay

3.11.1 General Principle:

Using the principle of flow cytometry, the propidium iodide (PI; Sigma-Aldrich, Sigma Life Sciences, St Louis, MO, USA) assay is used because of its ability to bind to double-stranded DNA through intercalating between the bases, with little to no sequence preference (Lecoeur, 2002). The flow cytometer is able to quantify cell death as PI is excluded from cells which have an intact plasma membrane, meaning that dead cells have a significantly increased fluorescence intensity compared to that of live cells (Stiefel et al., 2015; Crowley et al., 2016) (Figure 3.5).

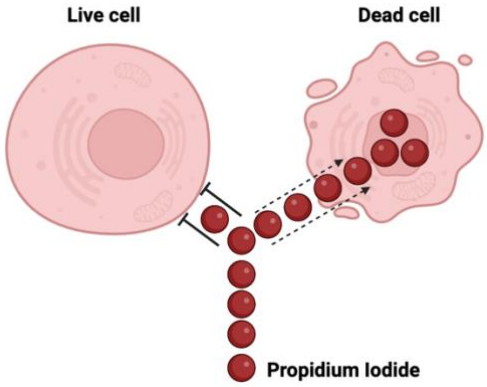

Figure 3.5. Propidium iodide (Red spheres) can only penetrate cells without an intact membrane, meaning that dead cells have a significantly increased fluorescence intensity compared to that of live cells.

3.11.2 General Protocol:

Existing media from each treatment was removed from the corresponding well and aliquoted into 1.5 mL Eppendorf tubes. Media-free monolayers were then washed twice with PBS. Thereafter, 200 µL trypsin was added to each well and plates were incubated for 5-minutes (37°C degrees, 5% CO^2). The previously removed media was then placed back onto its corresponding well to neutralise trypsin. This solution was then aliquoted into a 1.5 mL Eppendorf and centrifuged for 5-minutes at 3000 rcf. Following centrifuge, the existing media was aspirated from each Eppendorf, leaving a small pellet of cells. Fresh DM (200 µL) was then added to each Eppendorf, where pellets were fully homogenised, creating a solution of cells and DM. Propidium Iodide (PI; 5mg·mL^{-1} in dH_2O; Sigma-Aldrich, Sigma Life Sciences, St Louis, MO, USA) was then added to each Eppendorf at a concentration of 1:100 immediately before the sample

was processed by the flow cytometer. PI was added immediately before as it has a known toxicity, which could impact the consistency of results if it were left on a cell population for too long. The population and PI solution were then vortexed a final time before analysis using the flow cytometer.

3.12 Immunocytochemistry (ICC)

3.12.1 General Principle

ICC is a technique used for the visualisation of a specific antigen using an antibody (Ab). An Ab can be defined as a protein complex produced by B cells of the immune system. These units comprise four polypeptide chains, two identical heavy chains and two identical light (V_L) chains. These structures are "Y-shaped", with each arm of the "Y" partitioned into two antigen-binding fragments (Fab), with each of these arms containing a single V_L, V_H, C_L and C_H1 each. In addition to the single crystallisable fragment (Fc), which forms the trunk of the "Y" shape (Figure 3.6A). The "arm" portion of these structures are variable and can be termed the antigen-binding site. Meanwhile, the trunk region facilitates antigen detection through a single fluorophore-labelled antibody or indirect detection through the binding of a fluorophore-labelled secondary Ab raised against the Fc domain of an unlabelled primary Ab. Upon exposure to specific light wavelengths, the secondary Ab containing a fluorochrome will emit fluorescence. Fluorescence is a form of luminescence and is a process in which susceptible molecules emit light upon the creation of an excited electronic singlet state, which is caused by the absorption of light and other electromagnetic radiation (Figure 3.6c). To investigate Ab detection, fluorescence microscopy techniques are implemented. This detection is possible when a wavelength of light is focused on the Ab-labelled specimen to excite the electrons of the fluorochrome molecules to a higher energy state (excitation), termed "Stokes shift". Subsequently, the excited electron relaxes to a lower energy level and emits light in the form of a lower-energy photon in the visible light region. The fluorescence light is then filtered through a dichroic mirror and visualised through a microscope (Figure 3.6D).

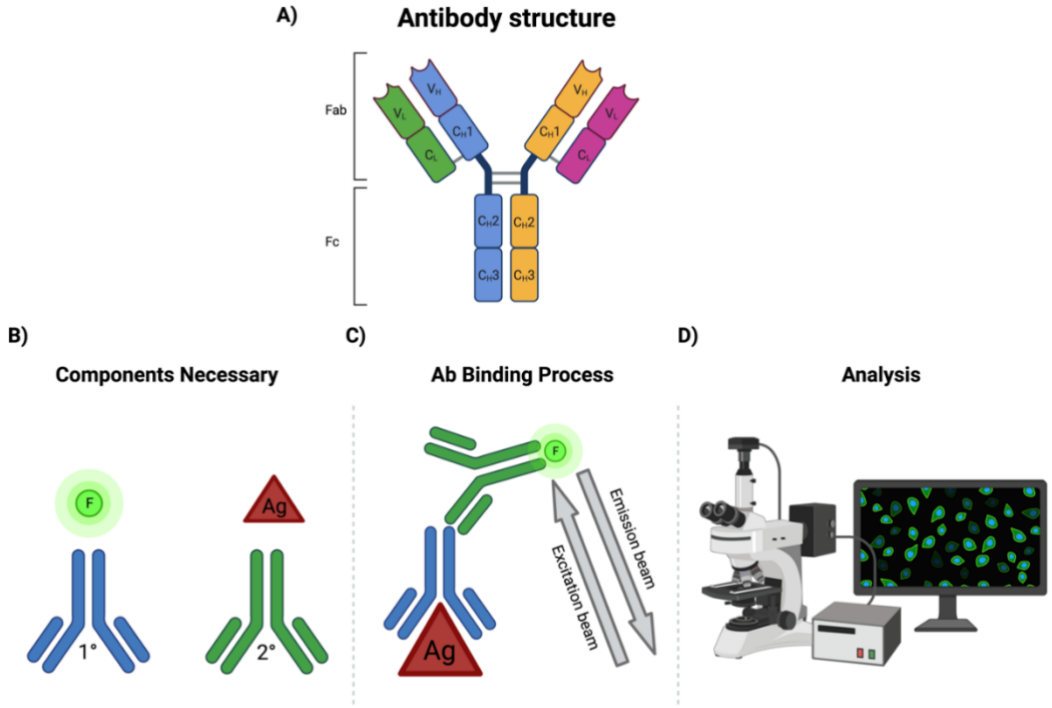

Figure 3.6. A) General structure of an antibody. B) Components required for immunolabelling, comprising the primary (1°) and secondary (2°) Ab, fluorochrome molecule (F) and antigen (Ag). Calibri Light (Headings)C) Outline of the Ab binding process, whereby 1° binds to Ag which together bind to 2°. Thereafter, the fluorochrome molecule binds to the 2°, which is excited by specific light wavelengths. D) Analysis process of cell imaging monolayers.

3.12.2 General Protocol:

Existing medium was removed from monolayers and washed 3-times using PBS. Thereafter, monolayers were fixed using paraformaldehyde (PFA 4%) and incubated at room temperature for 10-minutes. Fixation agent was then removed, and monolayers were washed 3 times with PBS. Monolayers were then permeabilized (Triton X-100, 0.1% in PBS) at room temperature for 15-minutes. Permeabilization buffer was then removed, and monolayers were washed 3 times with PBS before a blocking buffer was added (10% goat serum in PBS) and incubated for 30-minutes at room temperature. Monolayers were then provided with 1 PBS wash and the primary antibody (Myosin heavy chain [MF-20] 1:300, 1% bovine serum albumin [BSA]) was applied. Monolayers were then refrigerated (5˚C) overnight. Following overnight

refrigeration, the primary antibody was removed. Following three 5-minute PBS washes, the secondary antibody (Alexa Fluor 388; 1:500) was applied and incubated at room temperature for 60-minutes. Following secondary antibody removal, monolayers were washed with PBS. Finally, 4′, 6-diamidino-2-phenylindole (DAPI; 1:100 dH_2O) was applied to monolayers for 15-minutes. DAPI was then removed, and monolayers were stored in PBS for immunofluorescence imaging using microscopy procedures as detailed in section 3.4.

3.13 Ethics Approval

Ethical approval for Chapter 6 and 7, respectively was granted by the Liverpool John Moores University Research Ethics and Governance Committee. Study three (M22_SPS_2273) was approved on Tuesday 29th March 2022 and study four (21/SPS/062) was approved on Wednesday 29th September 2021. All samples and data were collected and stored according to the Declaration of Helsinki.

3.14 Health Screening & Inclusion Criteria

Participants who volunteered to take part in the human investigations within this thesis were required to provide written informed consent prior to any experimental procedures. In the first instance, participants were provided with a participant information sheet which outlined the study's procedures and thereafter they completed a physical activity readiness questionnaire (PAR-Q). Given the nature of the studies in this thesis, there were several exclusion criteria, which were:

- Participation in WADA-sanctioned sporting events or are requirement to complete drug testing for cannabis (e.g., court-ordered, workplace testing).
- Uncontrolled physical or mental health problems.
- A history of allergic reaction (e.g., rhinitis, urticaria, contact dermatitis, anaphylaxis) or significant adverse response to cannabis, cannabis products or cannabinoids.
- Inability to refrain from using cannabis, cannabis products or cannabinoids while participating in this project.

- Use of medications with the potential to influence CBD metabolism (e.g., inducers or inhibitors of the CYP450 enzyme system).
- Use of medications handled by transporter proteins or CYP enzymes that may be inhibited by CBD.
- Pregnant or lactating; females of childbearing potential and males with a female partner must agree to use a reliable form of contraception during and 1 month following participation in this project.

4 Optimisation of *in vitro* experimental CBD doses on C_2C_{12} health and differentiation

Publications associated with this Chapter:

Gillham, S.H., Cole, P.L., Viggars, M.R., Nolan, A.H., Close, G.L. and Owens, D.J., 2024. Comparative transcriptomics of broad-spectrum and synthetic cannabidiol treated C_2C_{12} skeletal myotubes. Physiological reports, 12, p.e70059.

Chapter 4 Prologue

There remains a paucity of evidence regarding the mechanisms by which CBD may exert its effect in skeletal muscle. To this end, this chapter broadly aims to establish the experimental conditions to examine the skeletal muscle cellular response to CBD *in vitro*, with a view to study the transcriptional response to CBD exposure in chapter 5. Specifically, dose-dependent effects of CBD on C_2C_{12} cytotoxicity and myogenesis will be established.

4.1 Abstract

Background: There is little research on the effect of CBD in skeletal muscle cells despite its use in athletic contexts for muscle recovery. Several mechanistic investigations have been conducted in different cell lines, but none in skeletal muscle cells. **Objective(s):** The purpose of this chapter was to validate the *in vitro* conditions to study the effect of CBD on C_2C_{12} myoblasts and myotubes for downstream mechanistic studies to be performed. Specifically, the aims were to investigate CBD treatments of 1, 2.5, 5, 10, 20 and 50 µM on muscle cell health and differentiation to establish the highest tolerable dose for further investigation. **Methods**: C_2C_{12} myoblast proliferation following acute CBD exposure was quantified using the EdU incorporation assay (DNA synthesis [%]), metabolic activity following acute exposure of CBD to C_2C_{12} myoblasts and myotubes was measured using the MTT assay, with cell viability following acute CBD exposure to myoblasts and myotubes quantified using the propidium iodide assay via flow cytometry. **Results**: There was no significant difference in rates of DNA synthesis (%) in any CBD dose compared to control ($P > 0.05$). Metabolic activity (%) was significantly reduced in myoblasts following 24-h exposure with 50 µM CBD ($P = 0.002$), which was consistent with myotubes ($P < 0.0001$). A non-significant but potentially meaningful decrease in metabolic activity was also observed at 20 µM CBD in myotubes. Myoblast viability (%) was also significantly increased following 24-h exposure to 50 µM CBD ($P < 0.0001$). **Conclusion:** This optimisation experiment established that C_2C_{12} myoblasts and myotubes can tolerate CBD *in vitro*, and that the highest tolerable dose without any signs of detriment was 10 µM CBD.

4.2 Introduction

Understanding the cellular and molecular processes underpinning skeletal muscle development and adaptation is essential for progressing both basic and translational muscle research. While in vivo models offer physiological relevance, they are often limited by ethical considerations, invasive sampling procedures, and constraints on precise manipulation of experimental variables such as drug dosing or specific time points. To overcome these challenges, in vitro models of myogenesis provide a valuable and controlled environment for studying muscle cell proliferation, differentiation, and response to stimuli. These models typically involve the culture of myogenic precursor cells, such as C_2C_{12} murine myoblasts or primary human myoblasts, which can be induced to differentiate into myotubes by altering serum growth factor concentrations in the culture medium (Chal and Pourquié, 2017; Denes et al., 2019).

There is a paucity of evidence to confirm claims surrounding the efficacy of CBD as an aid to muscle recovery, particularly from a mechanistic perspective. Therefore, this chapter aims to develop the muscle, with a focus on dose tolerability at two different stages of myogenesis; during proliferation in high serum media and in terminally differentiated myotubes after several days of serum withdrawal. To ascertain an appropriate dose that would maximise the signal but minimise cytotoxicity to the terminally differentiated C_2C_{12} myotubes used in this study, we relied on previous literature to develop our own dose tolerance experiments. For general cell culture studies, across multiple cell lines a systematic review reported that CBD negatively affects cell viability at doses >2 µM, inducing apoptosis at doses >10 µM (Pagano et al., 2020). In muscle specific studies (Langer, Avey and Baar, 2021) 5 µM has been used as the upper limit in dose–response experiments on skeletal muscle myotubes, however a subset of experiments with 10 µM also reported no negative effects. Taken together, we used these previous data as a reference and investigated 1, 2.5, 5 and 10 µM of CBD and sCBD. We utilised a metabolic activity assay and propidium iodide exclusion assay to determine cytotoxicity of the CBD.

4.3 Methods

Cell Culture

General cell culture experiments were conducted in accordance with the general procedures in Chapter 3.1. Additionally, plasticware and reagents were as per Chapter 3.2 and 3.3, respectively – unless stated otherwise.

4.3.1 Experiment 1 Procedures – EdU Assay

The Edu Assay Priniciple (Chapter 3.8.1) was used herein. Low passage C_2C_{12} myoblasts were seeded at $2x10^4$ on pre-gelatinised 12-well plates at 17:00 h on day-1 of the experiment. Cells were then incubated overnight at 37°C degrees, 5% CO_2. The following morning, (09:00 h) existing media was removed from cell monolayers. Thereafter solutions of GM+Vehicle (DMSO) and GM + CBD at concentrations of 1-50 µM were added to cell monolayers. This was spread across plates, with each dose in triplicate. The EdU probe was then added to each solution and cells were then incubated for 60-minutes (37°C degrees, 5% CO_2). Existing media was then removed, and monolayers were washed once with PBS before fixing which was completed following a 15-minute treatment of 4% PFA. The fixative was then removed, and monolayers were washed twice with 3% BSA in PBS. Monolayers were then permeabilized with 0.5% Triton and incubated for 30-minutes at room temperature. Monolayers were again washed twice with 3% BSA in PBS before preparing the Click-iT™ reaction buffer (Table 4.1). Monolayers were then treated with the reaction buffer immediately after preparation and received a 30-minute, light-protected incubation. The reaction buffer was then removed from monolayers which were then washed once with 3% BSA in PBS, and then once with PBS. To complete nuclear counter-staining, Hoechst was prepared in PBS (1:2000) and added to monolayers before a 30-minute, light-protected incubation at room temperature. Finally, the Hoechst solution was removed and 1000 µl PBS was added to monolayers for imaging.

Table 4.1. Click-iT reaction buffer recipe, which was multiplied as appropriate to meet the needs of each well to be treated.

Step	Reaction Component	Volumes
1	Reaction Buffer	430µL
2	$CuSO_4$	20µL
3	Alexa Fluor	1.2µL
4	Reaction Buffer Additive	50µL

4.3.2 Experiment 2 Procedures – MTT Assay

This assay was completed following the principles outlined in Chapter 3.9. For part A (Figure 4.1A) of this experiment C_2C_{12} myoblasts were seeded at 3 x 10^4 cells·ml^{-1} in pre-gelatinised 12-well plates in GM. Plates were first incubated for 24-hours to attach and recover. Thereafter, existing media was removed, and monolayers were treated with GM only (CON) or at various concentrations of a CBD ranging from 1-50 µM. Upon cessation of the experiment metabolic activity (%) was assessed using methods already described (Chapter 3.8) Briefly, this comprised monolayers -being treated with MTT (10% of total well volume) and incubated for 180-minutes. Thereafter, existing media was removed from monolayers before another, short incubation period (6 minutes), which was completed with plate lids off. DMSO (500 µL) was then added to each well, and plates were agitated on a plate rocker for 2-minutes to ensure all cells were lifted off the plate. Plates were then analysed in a microplate reader. For part B (Figure 4.2A) of the experiment, C_2C_{12} myoblasts were seeded at 4 x 10^4 cells·mL^{-1} in pre-gelatinised 12-well plates in GM (Figure 4.3). Plates were incubated for 24-hours and once ~80% cell confluence was reached GM was removed and cell monolayers were washed twice with PBS. Monolayers were then treated with DM which was incubated for a further 48-hours. Existing media was then removed, and monolayers were washed once with PBS, and fresh DM was introduced to monolayers. Thereafter, monolayers were topped up every 48-hours with fresh DM corresponding to 10% of well concentration (100 µL) for 4-days. On the 8^{th} day, DM was removed from monolayers, which were treated with either differentiation media (DM; 20% serum;

CON) or at various concentration of CBD (1-50 µM). Metabolic activity was assessed using the same methods as part A of this experiment.

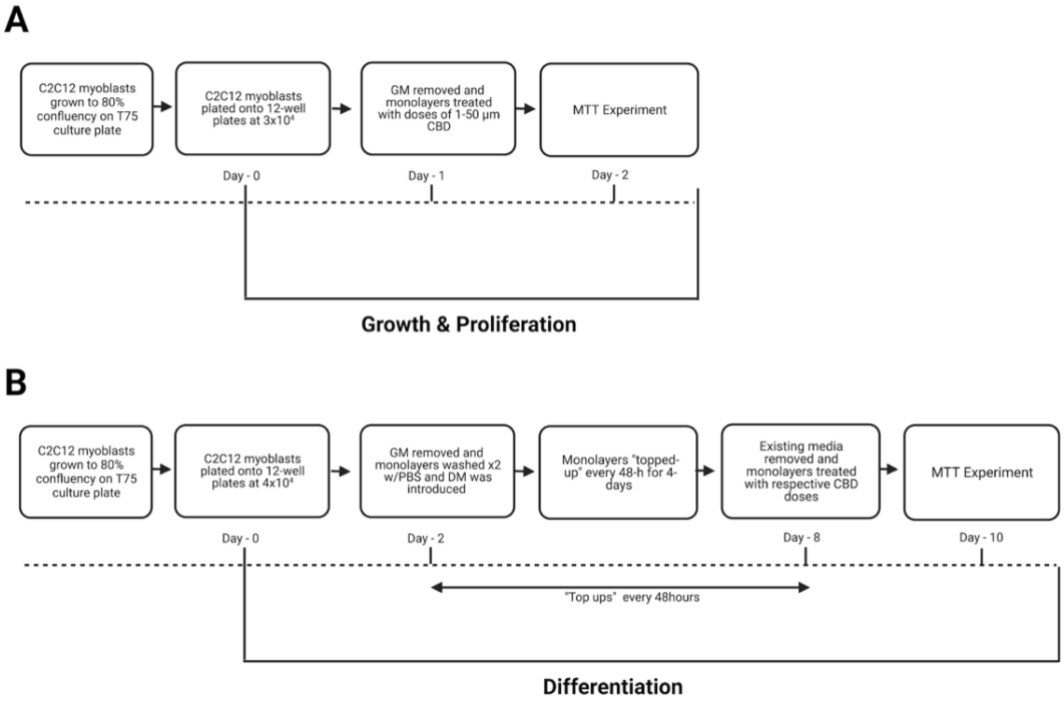

Figure 4.1. Schematic representation of a) experimental design for assays completed on C_2C_{12} myoblasts and b) experimental design for assays completed on C_2C_{12} myotubes.

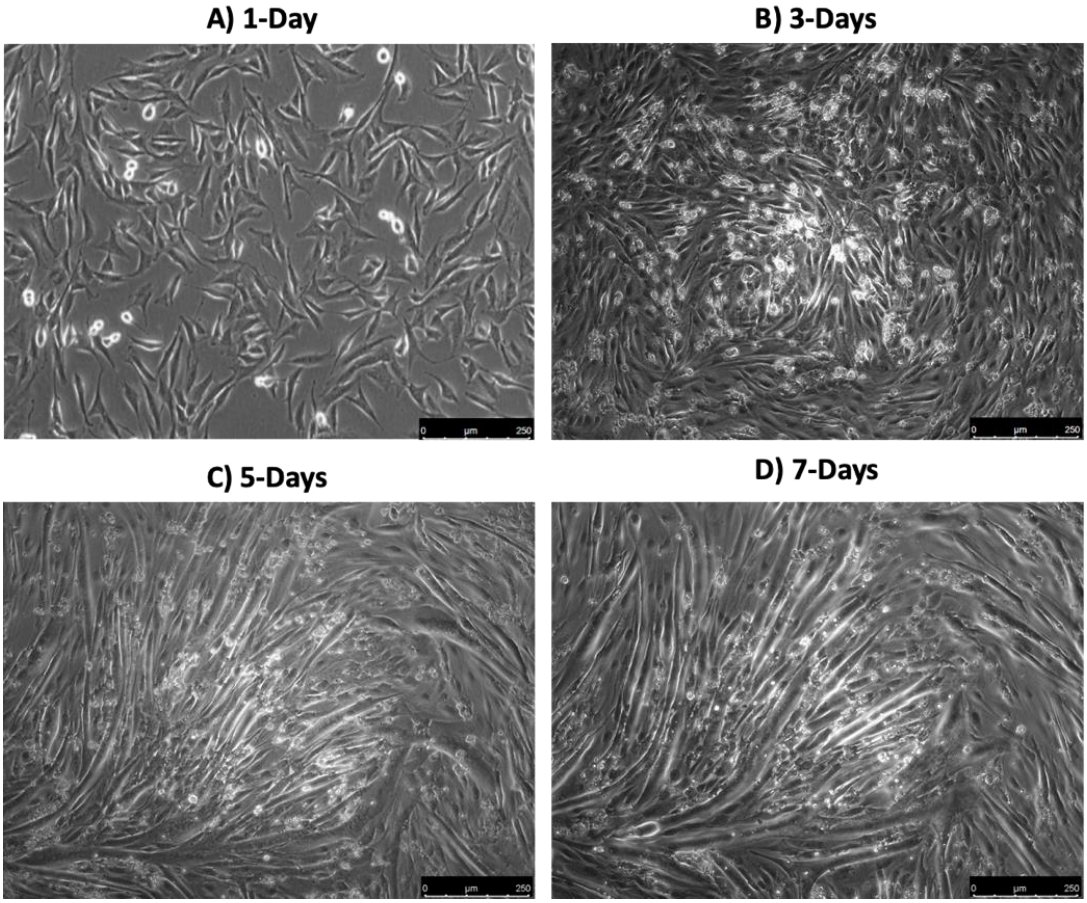

Figure 4.2. Low Passage (~5-10) C2C12 populations following induction of differentiation by serum starvation from 1-7 days post serum withdrawal. At 7-days a high proportion of cells have fused into multinucleated myotubes.

4.3.3 Experiment 3 Procedures – Propidium Iodide (PI) Assay

This experiment was included, given the principles outlines in Chapter 3.10.1. Before the investigation could be completed, a gating procedure had to be conducted (Chapter 3.10.2). Thereafter, part A of this investigation began with C_2C_{12} myoblasts were seeded at $3x10^4$ on pre-gelatinised 12-well plates in GM. Plates were incubated for 24-hours (37°C degrees, 5% CO_2). Existing GM was then removed, and monolayers were washed twice with PBS. Thereafter, monolayers were treated with a GM+CBD solution at doses ranging 1-50 µM. Cells were then incubated for a further 24-hours (37°C degrees, 5% CO_2). Following 24-h treatment, existing media was pipetted into 1.5 mL Eppendorf tubes and monolayers were washed twice with PBS. Thereafter, 200

µL trypsin was added to each well and plates were incubated for 5-minutes (37°C degrees, 5% CO_2). The removed media was then placed back onto its corresponding well to neutralise trypsin. This solution was then pipetted into a 1.5 mL Eppendorf and centrifuged for 5-minutes at 3000 rcf. Following centrifugation, the existing media was aspirated from each Eppendorf, leaving a small pellet of cells. Fresh DM (200 µL) was then added to each Eppendorf, where pellets were fully homogenised, creating a solution of cells and DM. Propidium Iodide (5 $mg{\cdot}mL^{-1}$) in dH_2O; (Sigma-Aldrich, St Louis, USA) was then added to each Eppendorf at a concentration of 1:100. Solutions were vortexed a final time and placed on a BD Accuri™ C6 Plus Flow Cytometer, (BD biosciences, Berkshire, UK) for analysis.

4.3.4 Statistical Analysis

All statistical analysis and figures regarding dose tolerability experiments were conducted using GraphPad Prism™ for Macintosh (Version 9.3.1). All data were normally distributed, and as such were assessed with a one-way ANOVA. Significance was assumed if α reached ≤ 0.05. All data are presented as mean (95% confidence intervals [CIs]), ± standard deviation (SD).

4.4 *Experiment 1 – Effects of CBD on Cell Myoblast Proliferation*

Aim & Hypothesis

Experiment 1 sought to investigate the effect of CBD on myoblast proliferation when treated with increasing doses of 1-50 µM of CBD. Based on available literature suggesting that cell health may be affected at doses above 10 µM, it was hypothesised that CBD would negatively impact rates of cell proliferation in doses > 10 µM.

Results

There was no significant difference between control or any doses ranging 1-50 µM ($P > 0.05$; Figure 4.3).

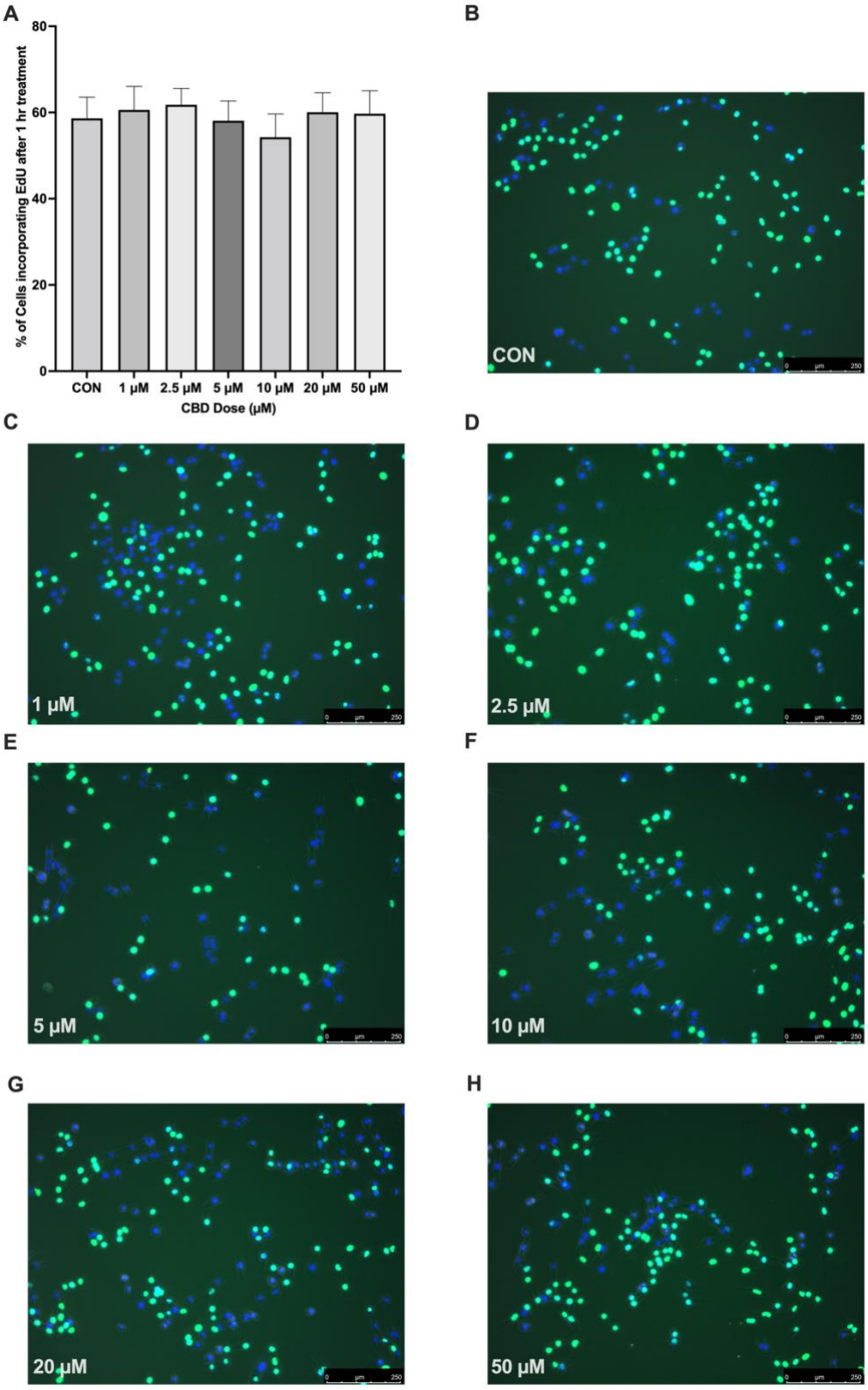

Figure 4.3. A) Percentage of cells incorporating EdU after 1 -hour of treatment with a GM+CBD solution in doses ranging from 1-50 µM. B-H) Representative microscope images of monolayers labelled with EdU (green) and DAPI as nuclear counterstain (blue). Scale bar = 250 µM.

4.5 *Experiment 2 – Effects of CBD on Metabolic Activity*

Aim & Hypothesis

To date, metabolic activity in C_2C_{12} myoblasts and myotubes following CBD treatment remains unknown. Therefore, experiment 2 aimed to determine metabolic activity in C_2C_{12} myoblasts and myotubes in the presence of a range of CBD via the use of the MTT assay (Section 3.8). As previously stated, the literature surrounding CBD treatment on the C_2C_{12} cell line is sparse and given that no significant change was observed in experiment 1, doses of 1-50 µM CBD were used. Given the previously mentioned available literature, it was hypothesised that metabolic activity (%) would be significantly reduced in doses > 10µM CBD in both myoblasts and myotubes.

Results

When myoblasts were treated with CBD for 24-h there was a significant reduction in metabolic activity (%) at only a single dose (50 µM; P = 0.002; Figure 4.4A). This result was consistent when myotubes were treated with CBD, where a dose of 50 µM significantly reduced metabolic activity (P < 0.0001; Figure 4.4B).

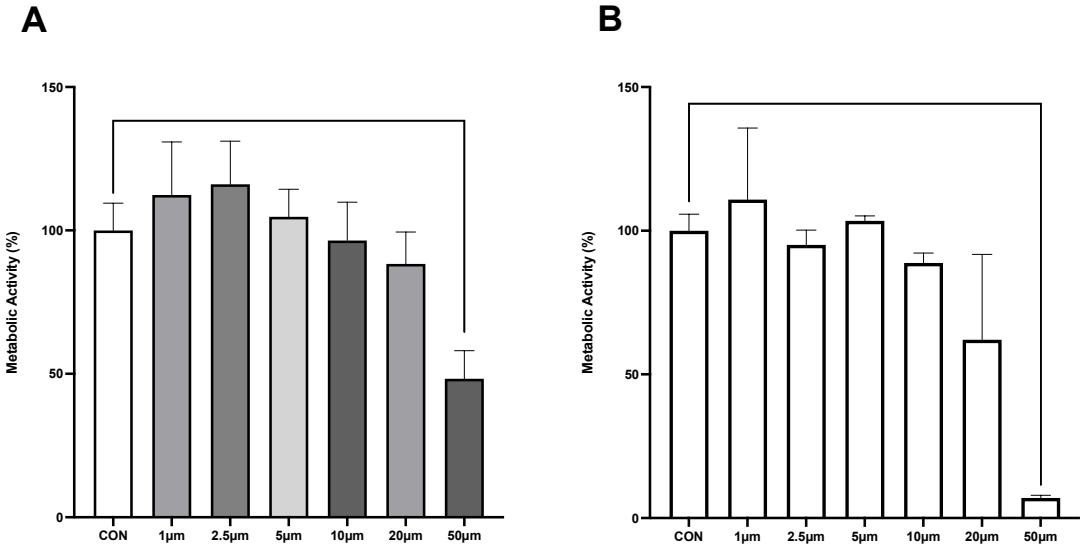

Figure 4.4. A) Metabolic activity (%) when myoblasts were exposed to GM only, or GM+CBD solutions 1-50 µM for 24-hours and b) Metabolic activity (%) when myotubes were treated with DM only or DM+CBD solutions 1-50 µM for 24-hours. **** Denotes a significant difference (P 0.0001) from control.

4.6 *Experiment 3 –Effects of CBD on Cell Cytotoxicity*

Aim & Hypothesis

Given there is conjecture surrounding the sole use of the MTT assay as a measure of cell viability (%), experiment 3 aimed to investigate cell death (%) using the principles of flow cytometry (Section 3.10) and the Propidium Iodide (PI; Section 3.11) assay, specifically. The primary aim of this study was to investigate if any concentrations (1-50 µM CBD) proved cytotoxic to myoblasts and myotubes. Based on the findings of experiment 2, it was hypothesised that cell death (%) would be increased in both myoblasts and myotubes which were treated with 50 µm CBD.

Results

Following 24-hours in a GM-CBD solution, cell death in myoblasts was significantly increased at 50 µM compared to control ($P < 0.0001$; Figure 4.5A). This was not consistent in myotubes, where no significant difference was observed at any dose of CBD compared to control ($P > 0.05$; Figure 4.5B).

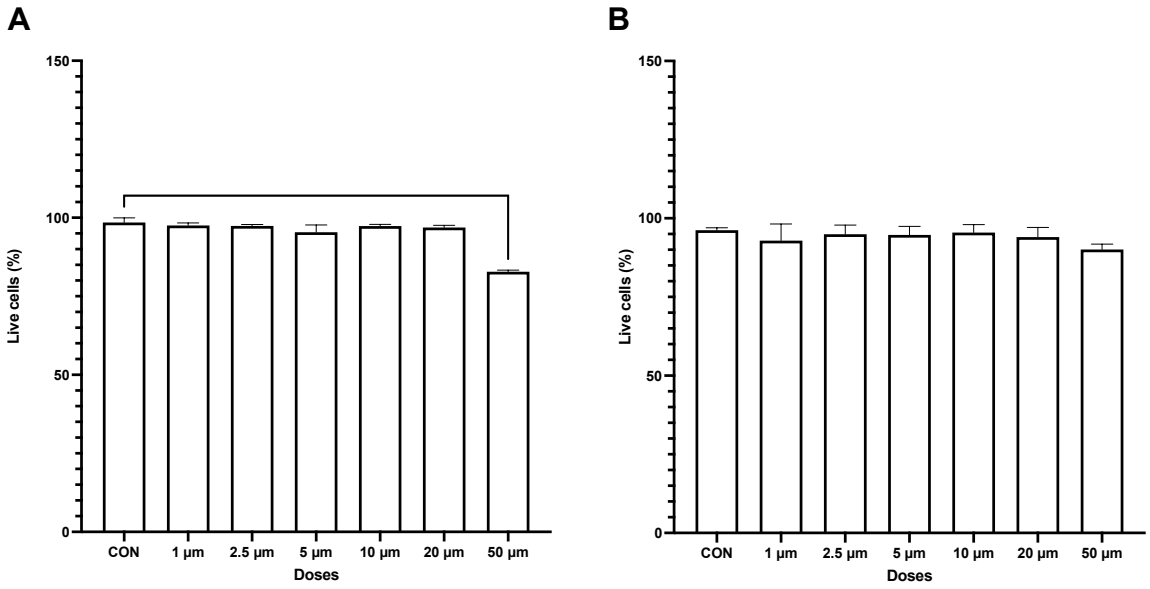

Figure 4.5. A) Live cells (%) when myoblasts were exposed to GM only, or GM+CBD solutions 1-50 µm for 24-hours and b) live cells (%) when myotubes were treated with DM only or DM+CBD solutions 1-50 µM for 24-hours. **** Denotes a significant difference ($P < 0.0001$) from control.

4.7 Discussion

The primary aim of these pilot studies was to establish appropriate in vitro conditions for investigating the effects of CBD on skeletal muscle cells, thereby supporting the design of subsequent mechanistic experiments. Short-term (60-minute) exposure to CBD at concentrations up to 50 µM did not affect DNA synthesis in C2C12 myoblasts, suggesting no acute impact on proliferative capacity. However, following 24-hour exposure, 50 µM CBD significantly reduced metabolic activity and increased cell death in myoblasts, indicating cytotoxicity at this concentration. In differentiated myotubes, metabolic activity was also significantly reduced at 50 µM, and a non-significant but notable reduction was observed at 20 µM, suggesting a possible threshold effect. Unlike myoblasts, however, myotube viability was not significantly affected at any dose. These findings indicate that while lower concentrations of CBD are tolerated, doses above 10 µM may begin to compromise cellular health, particularly in proliferative muscle cells.

Given the importance of quantifying rates of proliferation to determine cell health (Luo et al., 2014), it was surprising to see only a single study to date has investigated the effects of CBD on proliferation *in vitro*. Moreover, this study was completed using HT-29 cells, and therefore it was vital to complete this experiment on the C_2C_{12} cell line (Sainz-Cort, Müller-Sánchez and Espel, 2020). Inconsistent with previous findings (Sainz-Cort, Müller-Sánchez and Espel, 2020), this pilot study evidenced no change ($P > 0.05$) in proliferation rates at any dose of CBD compared to control. It is worth noting however that the probe used to investigate DNA synthesis was only applied to cell monolayers for 60-minutes, considerably less than in (Sainz-Cort, Müller-Sánchez and Espel, 2020) who assessed synthesis rates over 48-hours. Nevertheless, the results reported here clearly show strong signal for EdU indicating that cell doublings had occurred over 24h and permitting us to make assumptions about the effect of CBD on cell proliferation. As such, we propose that CBD doses up to 50 µM do not influence cell proliferation rates in C_2C_{12} myoblasts.

Metabolic activity was next assessed in response to CBD treatment in both a) myoblasts and b) myotubes. A significant reduction in metabolic activity (%) was

observed following 24-hour exposure to 50 µM CBD in myoblasts ($P = 0.002$), with a similar effect in myotubes ($P < 0.001$). These findings align with previous reports showing no change in metabolic activity across 0.01–10 µM CBD in Caco-2 or HCT116 cell lines (Aviello et al., 2012) and in SZ95 epithelial cells (Oláh et al., 2014). , further supporting the tolerance of lower CBD concentrations across various cell types. However, it is important to note that the MTT assay reflects mitochondrial metabolic activity rather than viability per se. Cells in the early stages of death may still reduce MTT and maintain membrane integrity, making it an imperfect proxy for cell survival (Ghasemi et al., 2023).

Given the limitations of MTT as a sole indicator of cell viability, the propidium iodide (PI) assay was used to further assess the cytotoxic effects of CBD on C2C12 cultures. In myoblasts, 24-hour treatment with 50 µM CBD resulted in a significant reduction in the proportion of live cells ($P < 0.0001$), corroborating the metabolic impairment observed in the MTT assay. However, this effect was not observed in myotubes, where no CBD dose significantly increased cell death relative to control ($P > 0.05$). These findings suggest that proliferating myoblasts may be more vulnerable to CBD-induced cytotoxicity than terminally differentiated myotubes.

Limitations

While this chapter provides an important foundation for subsequent mechanistic studies and contributes novel data to the literature, several limitations should be acknowledged. First, *in vitro* models are simplifications of biological systems and cannot fully replicate the complexity of skeletal muscle in vivo. As such, any dose-response findings presented here should not be directly extrapolated to animal or human models. Second, the CBD formulation used was broad-spectrum, meaning that other cannabinoids may have contributed to the observed effects. Future studies may benefit from comparing broad-spectrum preparations with isolated or synthetic CBD to isolate compound-specific effects. Additionally, it should be noted that CBD is never present without it's associated metabolites, and as such – these may be a consideration for investigation in future studies.

Furthermore, each physiological parameter; proliferation, metabolic activity, and viability, was assessed using a single assay. While these assays are widely accepted, future studies should consider incorporating complementary methods to strengthen conclusions. Finally, this work did not investigate time-dependent effects of CBD exposure. Although clear responses were observed following 24-hour treatment, the possibility of transient or cumulative effects across myogenic progression remains unexplored.

Conclusion

This chapter presents a series of optimisation experiments that establish a foundational in vitro framework for investigating the cellular effects of CBD in skeletal muscle. The results indicate that 50 µM CBD is detrimental to C_2C_{12} myoblasts and myotubes, reducing metabolic activity and increasing cell death in proliferative cells. Moreover, a non-significant but notable decline in myotube metabolic activity at 20 µM suggests a potential threshold of tolerance. Based on these findings, 10 µM has been selected as the maximum CBD concentration for use in subsequent transcriptional studies described in Chapter 5.

5 Comparative Transcriptomics of Broad-Spectrum and Synthetic Cannabinoids Treated C_2C_{12} Skeletal Myotubes

Publications and data sets associated with this Chapter:

Gillham, S.H., Cole, P.L., Viggars, M.R., Nolan, A.H., Close, G.L. and Owens, D.J., 2024. Comparative transcriptomics of broad-spectrum and synthetic cannabidiol treated C_2C_{12} skeletal myotubes. Physiological reports, 12, p.e70059.

The RNAseq data set are publicly available at:

https://www.ncbi.nlm.nih.gov/geo/query/acc.cgi

Chapter 5 Prologue

In Chapter 4, the effects of CBD dose *in vitro* were explored using a range of techniques. It became clear that higher (50 µM) doses of broad-spectrum CBD could prove cytotoxic to cell cultures. A further important observation within Chapter 4 was that metabolic activity of myotubes was evidencing signs of reduction following doses greater that 10 µM. As such, in combination with the findings of Chapter 4, alongside the findings of other research groups it was elected that a dose of 10 µM should be used in future experiments to a) maximize signal and b) minimize cytotoxicity in cell cultures. As mentioned previously, there is a paucity of mechanistic insight into the mechanisms by which CBD interacts with skeletal muscle. Given this lack of evidence in this tissue of interest, it was important to conduct this investigation in a non-bias manner. In addition, there has been discussion in the scientific community of the notion of an "entourage effect" of phytocannabinoids. This entourage effect alludes to the synergistic application of phytocannabinoids to potentially amplify their utility in humans. As such, this chapter aims to explore the global transcriptional response when skeletal muscle myotubes are treated with either a broad-spectrum CBD compound, containing phytocannabinoids other than CBD or with a CBD-only, synthetic compound.

5.1 Abstract

Background: Cannabidiol (CBD) is widely used in sports for recovery, pain management, and sleep improvement, yet its effects on muscle are not well understood. **Objective(s):** This study aimed to determine the transcriptional response of murine skeletal muscle myotubes to broad-spectrum CBD and synthetic CBD (sCBD). **Methods**: Differentiated C_2C_{12} myotubes were treated with 10 µM CBD, sCBD, or vehicle control (DMSO) for 24 hours before RNA extraction. Poly-A tail enriched mRNA libraries were constructed and sequenced using 2x50 bp paired-end sequencing. **Results**: CBD and sCBD treatment induced 4489 and 1979 differentially expressed genes (DEGs; $p < 0.001$, FDR step-up <0.05), respectively, with common upregulation of 857 genes and common downregulation of 648 genes. Common upregulated DEGs were associated with “response to unfolded protein”, “cell redox homeostasis”, “endoplasmic reticulum stress”, “oxidative stress,” and “cellular response to hypoxia”. Common downregulated DEGs were linked to “sarcomere organization”, “skeletal muscle tissue development”, “regulation of muscle contraction”, and “muscle contraction”. CBD treatment induced unique DEGs compared to sCBD. **Conclusions:** The data indicate CBD may induce mild cellular stress, activating pathways associated with altered redox balance, unfolded protein response, and endoplasmic reticulum stress. It may be hypothesized therefore that CBD interacts with muscle and may elicit a 'mitohormetic' effect that warrants further investigation.

.

5.2 Introduction

CBD is one of many cannabinoids derived from the *cannabis sativa* plant, which produces cannabinoids in addition to more than 550 other compounds (Puntel et al., 2016; Capano, Weaver and Burkman, 2020). Regarding cannabinoids, there have been >140 elucidated (Ujváry and Hanuš, 2016), with two of the most well-known being Δ^9-tetrahydrocannabinol (Δ^9-THC) and cannabidiol (CBD) (Gaoni and Mechoulam, 1964; Brunt and Bossong, 2020). The former is best known for its intoxicating properties, whilst CBD has shown little intoxicating or abuse potential (Sekar and Pack, 2019). These exogenous phytocannabinoids have been suggested to exert their action via their ability to bind to components of the body's endocannabinoid system (ECS). The ECS, primarily comprises CB_1, and CB_2 and endogenous cannabinoids AEA and 2-AG (Lu and Mackie, 2020).

Cannabidiol (CBD) use has recently been prevalent in professional sports and has reportedly been used for improving recovery, managing perceived pain and improving sleep, with 68% of players reporting a perceived benefit (Kasper et al., 2020a). Others have reported similar findings for the use of cannabis, with one large meta-analysis reporting that in a sample of >46,000 athletes,~23% admitted to having used some form of cannabis in the past year (Docter et al., 2020). Despite the use of CBD by athletes as an alternative to opioids (Vernec, Pipe and Slack, 2017) and non-steroidal anti-inflammatory drugs (NSAIDs) (Schoenfeld, 2012), there is a scarcity of evidence for any interaction between CBD and muscle. There is evidence that the cannabinoid receptors CB_1 and CB_2 gene (Cavuoto et al., 2007b; Haddad, 2021b) and protein are expressed in human, mouse and rat skeletal muscle (Crespillo et al., 2011; Mendizabal-Zubiaga et al., 2016; Dalle and Koppo, 2021; Kalkan et al., 2023a), however the latter is limited to immunolabelling studies. Antibody specificity and absolute quantification of the receptors by mass spectrometry have not yet been performed to confirm abundance in human skeletal muscle.

In vitro studies on skeletal myoblasts demonstrate no effect of a hemp-derived CBD isolate (99.8% purity) on anabolic signalling through mTORC1 or inflammatory signalling through nuclear factor kappa B, as well as no CB_1 receptor expression

(Langer, Avey and Baar, 2022). However, others provide evidence that synthetic CBD may be pro-myogenic, an effect attributed to increasing [Ca^{2+}], mostly via TRPV1 activation (Iannotti et al., 2019b). Similar observations have been made in primary satellite cells and myoblasts isolated from healthy and/or Duchenne muscular dystrophy (DMD) donors. *In vivo*, synthetic CBD administration confers anti-inflammatory properties and protects skeletal muscle against degeneration in *mdx* mice (Iannotti et al., 2019b). In a separate study on healthy rats undergoing eccentric loading of the tibialis anterior, administration of hemp derived CBD isolate decreased pro-inflammatory signalling without blunting the anabolic response to exercise in rats (Langer et al., 2021). As such, the limited available evidence points toward a pro-myogenic and anti-inflammatory effect on skeletal muscle.

Whilst CBD is thought to exert its effects via the ECS, it cannot be dismissed that the many other compounds found in the cannabis plant could contribute towards the effects of broad-spectrum CBD. Indeed, untargeted and targeted metabolomics of cannabis cultivars identified a total of 377 analytes after controlling for pesticides (Wishart et al., 2024). The most abundant analytes included lipids and lipid-like molecules and organic acids and their derivatives. Notably, the cultivars all contained high amounts of polyphenols including catechin and several other quantifiable cannabinoids. Given that polyphenols for example, have been extensively studied in the context of exercise-induced muscle damage, inflammation and repair, with many studies reporting positive effects (Rickards et al., 2021), it is important to dissect where muscle specific effects of CBD exposure might be derived.

Taken together, this investigation aimed to determine the global transcriptional response of C_2C_{12} skeletal muscle myotubes following exposure to broad-spectrum CBD and synthetic CBD. The primary aims were to ascertain if 1) skeletal muscle is responsive to broad-spectrum CBD and synthetic CBD and 2) whether these effects are attributable solely to CBD or the vast array of other compounds in commercially available broad-spectrum CBD. It was hypothesised that both commercially available broad-spectrum CBD and synthetic CBD would induce significant transcriptional changes in skeletal muscle myotubes related to metabolism, myogenesis and

inflammatory signalling based on the findings of others. Furthermore, it was also hypothesised that there would be a significant number of differentially expressed genes that are unique to broad-spectrum CBD treatment when compared with synthetic CBD.

5.3 Methods

5.3.1 Chemicals, Reagents and Plasticware

THC-free, broad spectrum, hemp-derived CBD was provided by Naturecan. Ltd (Stockport, UK) as crystalline CBD. The CBD was dissolved in DMSO as a stock concentration of 36 mg/ml. Pure synthetic CBD (sCBD) powder was provided by Pureis CBD. Ltd (Hungerford, UK). The sCBD was reconstituted in DMSO as a stock concentration at 36 $mg \cdot ml^{-1}$. Reconstituted CBD and sCBD were stored at -20^{o}C and used within 3 weeks of reconstitution. When required, CBD and sCBD stock solutions were diluted further in culture media for the experiments outlined herein.

Dulbecco's modified eagle medium (DMEM. Cat. ID. 11965092), fetal bovine serum (FBS. Cat. ID. A5256801), new-born calf serum (NBCS. Cat. ID. 16010159), penicillin-streptomycin (pen-strep. Cat. ID. 15070063), and horse serum (HS. Cat. ID. 16050122) were purchased from Thermo Fisher Scientific (Oxford, UK). Phosphate buffered saline tablets (PBS. Cat. ID. 524650), DMSO (Cat. ID. D2438-50ML), trypsin-EDTA (Cat. ID. T4049), MTT (Cat. ID. 475989), propidium iodide (Cat. ID. 537059) and gelatin from porcine skin (Cat. ID. G1890) were purchased from Sigma Aldrich (Gillingham, UK). T75 culture flasks and 6 well culture plates were purchased from Nunc (Thermo Fisher Scientific. Oxford, UK).

C_2C_{12} myoblasts were purchased from ATCC (Cat. ID. CRL-1772. LGC Standards, Middlesex, UK). All experiments detailed in this chapter were performed on C_2C_{12} myotubes between passage 5 and 10. For the isolation of high-quality RNA, RNeasy isolation kits (Cat. ID. 74104) were purchased from Qiagen (Qiagen Ltd. Manchester, UK).

5.3.2 Cell Culture

Cell Culture experiments were conducted in accordance with chapter 3.1. C_2C_{12} murine myoblasts were cultured on gelatin (0.2%) coated 6-well culture plates in humidified 5% CO_2 at 37°C in growth media comprising DMEM, 10% FBS, 10% NBCS and 1% of a pen-strep solution. Upon reaching ~80% confluence, monolayers were washed twice with pre-warmed PBS and switched to low serum differentiation media (DM), DMEM, 2% HS and 1% pen-strep. Every 48h thereafter, DM was removed from monolayers via aspiration and was replaced with fresh media. Cells were terminally differentiated by day-8 of low serum DM exposure.

5.3.4 Next Generation RNA Sequencing

Cell Treatments

After determining the tolerability of C_2C_{12} myotubes to varying doses of CBD and sCBD, chapter 4 evidenced that 10 µM was the upper limit tolerated by both treatments in MTT and PI experiments (see Chapter 4). To determine the transcriptional response to 10 µM CBD and sCBD, C_2C_{12} myotubes were terminally differentiated as described above. On day 8 of differentiation, the differentiation medium (DM) was removed and replaced with DM containing either vehicle (DMSO), CBD (10 µM), or sCBD (10 µM). Myotubes were then cultured in the respective treatments for 24 hours before being harvested for RNA extraction. Duplicate wells (technical replicates) were used for each treatment, and the experiment was repeated three times (experimental replicates), generating (n = 6) samples per treatment.

RNA Isolation

Following a 24-hour treatment with CBD/sCBD/vehicle control, terminally differentiated C_2C_{12}monolayers were lysed with buffer RLT from the Qiagen RNeasy kit (Qiagen Ltd). RNA was then extracted from cell lysates using the RNeasy kit with proteinase K digestion, as per the manufacturer's guidelines. Eluted RNA was stored at -80^{o}C until required for determination of total RNA and library processing.

Determination of RNA Quantity and Quality

Total RNA was quantified using a Nanodrop 8000 and RNA quality was assessed using an Agilent® Bioanalyser (average RIN score = 7, 260/280 = 2.1, 260/230 = 1.6). RNA samples were then diluted to 20 ng·µL^{-1} using RNase-free water.

RNA Library Preparation and Sequencing

Libraries were constructed from 100 ng of total RNA with Poly-A tail enrichment of mRNA using NEBNext® Ultra™ II RNA Library Prep Kit for Illumina® (Cat. ID. E7770L. New England Biolabs UK. Hitchin, Herts) with Agencourt AMPureXP Sample Purification Beads (Cat. ID. A63880. Beckman Coulter. Wycombe, UK) as per manufacturers guidelines, by Bart's and the London Genome Centre at Queen Mary, University of London. The resultant-barcoded libraries were sequenced on an Illumina NextSeq 2000 using 2x50 bp paired-end sequencing. An average of 22 million paired-end reads was achieved per sample (details in Supplementary Table 1).

5.3.5 Statistical Analysis

RNA sequencing

FastQ files were imported to Partek® Flow® Genomic Analysis Software Partek Inc. (Missouri, USA) for pipeline processing. Pre-alignment QA/QC was performed on all reads prior to read trimming. STAR alignment 4.4.1d was used to align trimmed reads to the Mus musculus genome. Aligned reads were then quantified to the Ensemble transcriptome annotation model associated with Mus musculus mm39 genome. Post alignment QC reports are provided in Supplementary Table 1 (Appendix 1). Filtered raw counts were used for normalisation and differential analysis with DESeq2 (Love, Huber and Anders, 2014) through Partek® Flow®. Gene transcripts were considered significantly different between groups when the FDR < 0.05 and fold change > 1. Volcano plots and annotation charts were generated in R studio (version 2023.06.1+524), Principal Component Analysis (PCA) plots were generated in Partek® Flow® and bar charts were constructed in GraphPad Prism version 10.0.0 for Windows (GraphPad Software, Boston, Massachusetts USA).

Bioinformatics

Hypergeometric Optimization of Motif EnRichment - HOMER (v4.11) motif analysis was performed on DEGs commonly up/downregulated by treatment with CBD or sCBD, to identify the enrichment of known motifs (6–12 bp long) in the gene body and up to 2 kb upstream of the transcription start site (Heinz et al., 2010). The sequence logos in Table 5.1 are produced by the HOMER v4.11 tool. Venn Diagram Analysis was performed using the VIB/UGent Venn online tool http://bioinformatics.psb.ugent.be/webtools/Venn/.

To visualise gene interactions and clusters of proteins that they encode with known physical interactions, STRING (Version 12. string.db.org) was deployed on commonly up regulated and down regulated DEGs. Only physical interactions are shown with the highest degree of confidence (0.900). K-means clustering was used to visualise clusters of genes based on their centroids. Experimental workflows are presented schematically in Figure 5.1.

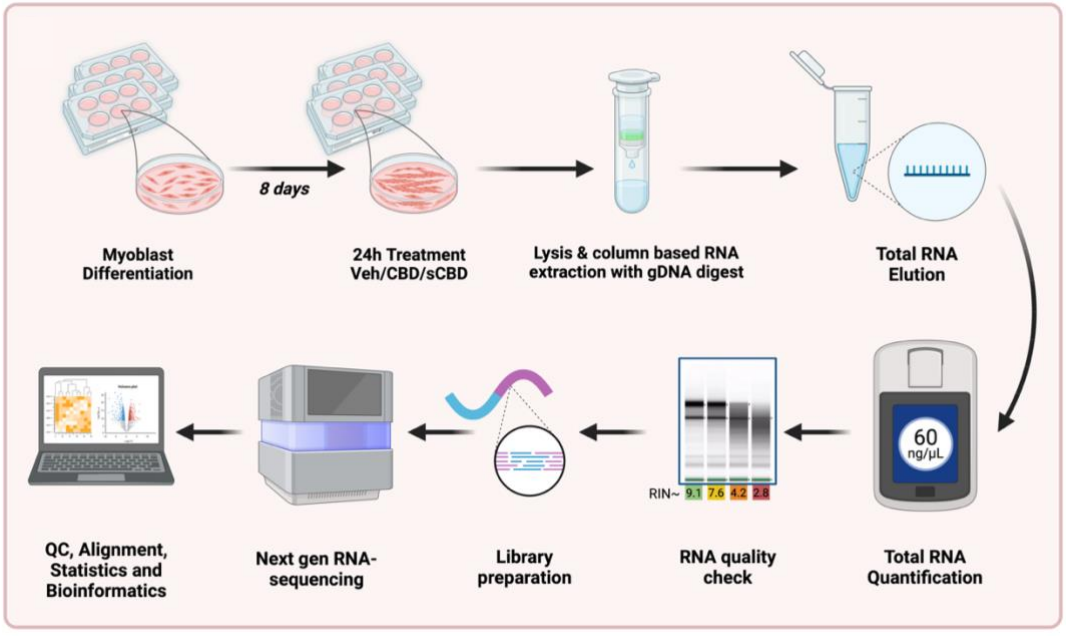

Figure 5.1. Experimental workflow: Differentiated myotubes were exposed to 10 µM CBD, sCBD and vehicle control for 24h before being lysed for column-based RNA extraction. Total RNA quantity and quality were determined prior to library preparation and next generation sequencing. Pre-alignment QC was performed prior to trimming and STAR alignment, followed by quantification to annotation model, counts were then normalised by median ratio, prior to DSeq2 statistical analysis. Image created using Biorender.

5.4 Results

Transcriptional responses of terminally differentiated C_2C_{12} *Myotubes to CBD and sCBD treatment*

The PCA plot (Figure 5.2) visualizes the multidimensional relationships amongst the gene expression profiles of CON, CBD, and sCBD-treated cells. The plot reveals distinct clusters of gene expression profiles for each treatment, but less separation between CBD and sCBD clusters versus CON, indicative of underlying patterns within the data. Using an 0.05 FDR cut off, 4480 genes were differentially expressed in CBD versus CON. Of these genes, 2051 were significantly upregulated and 2429 were significantly downregulated. In the sCBD treatment, 1979 genes were differentially expressed compared to CON. Of these genes, 899 were significantly upregulated and 1080 were significantly downregulated (Figure 5.2). Interestingly, of the 5 most up and downregulated genes in CBD and sCBD treated cells, 3 of the most downregulated genes (Osteoglycin; *Ogn*, Leucine-rich repeat-containing protein 17; *Lrrc17* and Cadherin-related family member 1; *Cdhr1*) and 3 of the most upregulated genes (Metallothionein 1 and 2; *Mt1*, *Mt2*, and solute carrier family 3 member 2; *Slc3a2*) were conserved across treatments (Figure 5.3).

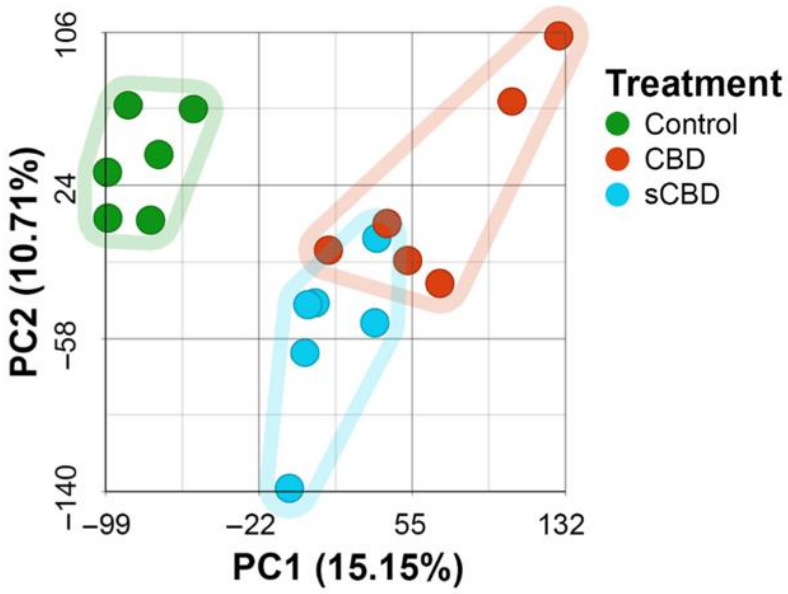

	# of DEGs	Up vs. Con	Down vs. Con
CBD	4480	2051	2429
sCBD	1979	899	1080

Figure 5.2. Principal component analysis plot and summary of differentially expressed genes (P < 0.001, FDR step-up P < 0.05) by condition.

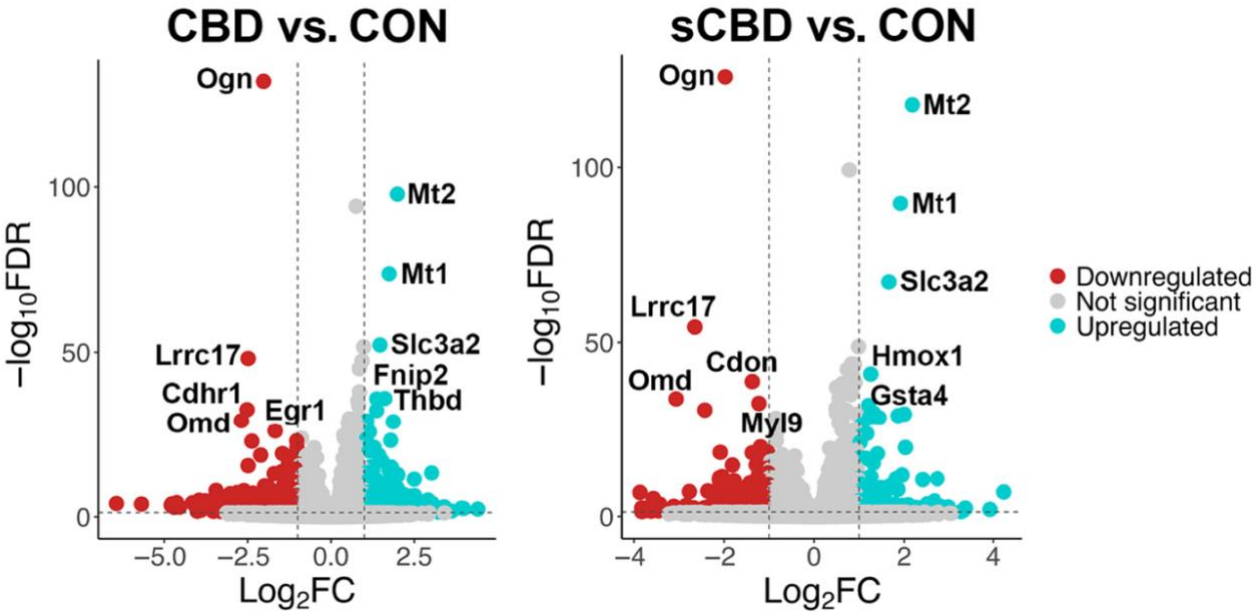

Figure 5.3. Volcano plot illustrating the relationship between $-\log_{10}$ FDR step-up and $\log_2$ fold-change for DEGs. Gray data points represent genes that are not statistically significant ($-\log_{10}$FDR step up (<0.05) and $\log_2$FC > −1.1), whilst blue data points are

significantly up regulated and red data points are significantly downregulated. Top 5 up and downregulated DEGs are labelled for comparison.

Common upregulated transcriptional responses in CBD and sCBD treated Myotubes

To identify similarities in the transcriptional responses and gain deeper insight into the genes that may be directly influenced by CBD alone, Venn diagram analysis was performed on significantly up and downregulated DEGs. Of all DEGs, 857 were commonly upregulated by both CBD and sCBD treatments versus CON (Figure 5.4a) and 648 commonly downregulated by both CBD and sCBD versus CON (Figure 5.5a).

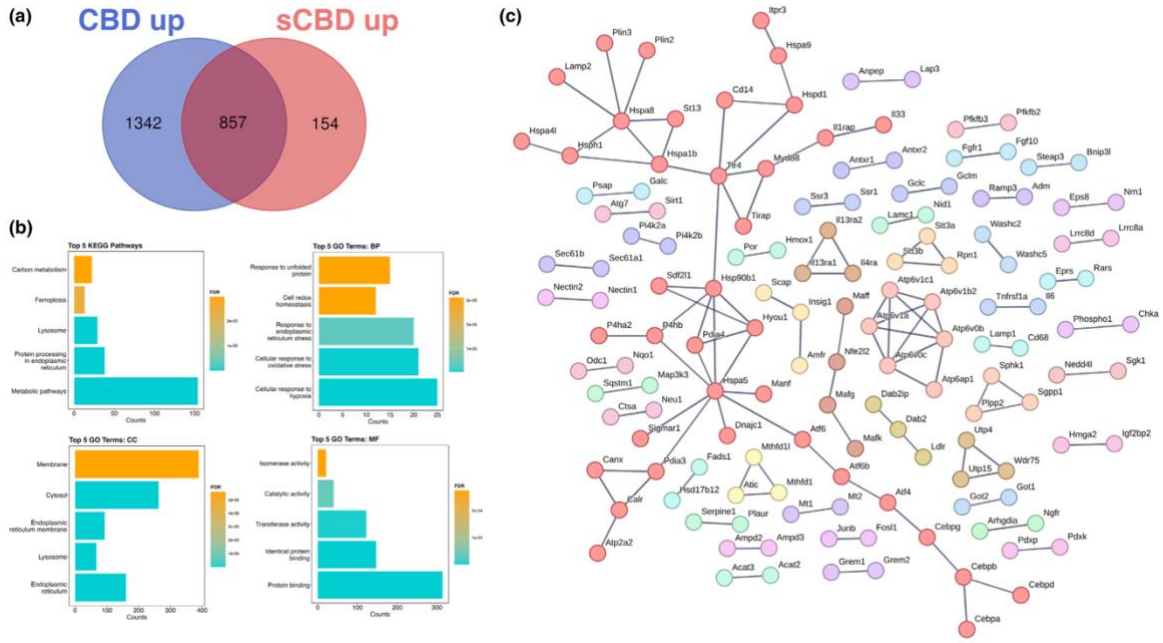

Figure 5.4. Common upregulated genes: (a) Venn diagram illustrating DEGs uniquely upregulated by CBD and sCBD and common upregulated genes in the overlapping region. (b) The top 5 Enriched KEGG pathways and GO terms for common upregulated genes. BP, biological process; CC, cellular compartment; MF, molecular function. (c) Common up-regulated genes and their known protein–protein interactions, single nodes are not shown, highest confidence (0.9), clusters are coloured individually using *K*-means clustering.

To ascertain biological context to these data, network analysis of known protein–protein interactions for proteins encoded by the DEGs in the data set was performed

using STRING analysis. By visualizing the data in this way, it made it easier to determine which proteins and their associated networks might be the most influential to the dataset, and specifically to CBD – since these networks were commonly regulated in both CBD and sCBD treatments. Figure 5.4c reveals several networks enriched in the data set for commonly upregulated DEGs. The largest network of protein interactions contains several connected chaperones (Heat shock proteins; *Hspa8*, *Hspa1b*, *Hsph1*, *Hspa4l*, *Hsp90b1*, *Hspa5*, *Hspa9*, *Hspd1*) and components of the unfolded protein responses/endoplasmic reticulum (UPR/ER) stress response (Activating transcription factors; *Atf6*, *Atf6b*, *Atf4*) and lysosomal associated membrane protein 2 (*Lamp2*). These results are congruent with the gene ontology analysis of commonly upregulated DEGs, whereby KEGG pathways and GO biological processes show significant enrichment of oxidative stress, UPR/ER stress, and lysosomal pathways (Figure 5.4b)

Commonly Downregulated transcriptional responses in CBD and sCBD treated Myotubes

Bioinformatics analyses on the 648 commonly downregulated DEGs was then performed. The largest network in the STRING analysis (Figure 5.5c) consists of motor genes encoding motor proteins, including alpha actin (*Actc1*, *Acta1*, *Actn1*, *Actn4*), myosin light and heavy chains (*Myl1*, *Mylpf*, *Myh4*) and tropomyosin (*Tpm1*, *Tpm2*) as well as cell–cell contact proteins Vinculin (*Vcl*) and Vasodilator stimulated phosphoprotein (*Vasp*). Other clusters also contain motor proteins including troponins (*Tnni2*, *Tnnc2*, *Tnnc1*, *Tnnt2*) and structural collagen proteins (*Col5a1*, *Col1a2*, *Col5a3*, *Col3a1*). Gene ontology analysis of commonly downregulated DEGs revealed pathways associated to muscle contraction, skeletal muscle tissue development, motor proteins, sarcomere organization, and actin binding - amongst others (Figure 5.5b).

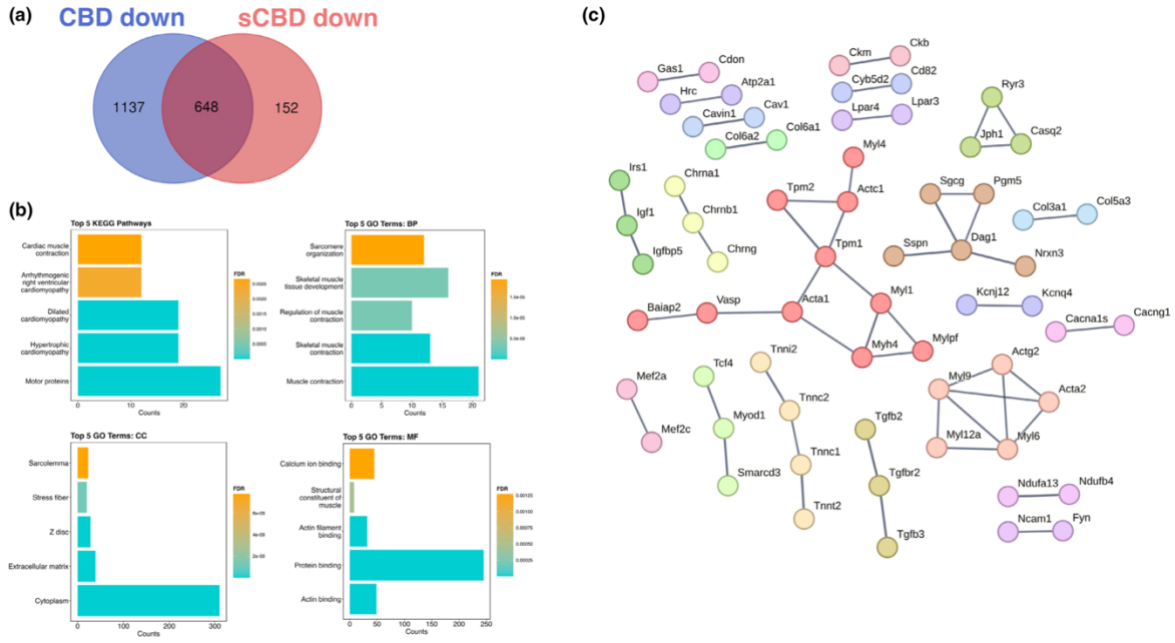

Figure 5.5. Common downregulated genes: (a) Venn diagram illustrating DEGs uniquely downregulated by CBD and sCBD and common downregulated genes in the overlapping region. (b) The top 5 Enriched KEGG pathways and GO terms for common downregulated genes. BP, biological process; CC, cellular compartment; MF, molecular function. (c) Common downregulated genes and their known protein–protein interactions, single nodes are not shown, highest confidence (0.9), clusters are coloured individually using *K*-means clustering.

Conserved putative upstream regulators of CBD and sCBD transcriptional responses

Finally, to gain an understanding of the transcription factors regulating the common transcriptional responses between treatments, hypergeometric optimization of motif enrichment (HOMER) analysis was performed to identify enriched transcription factor DNA binding motifs in the gene body and up to 2kb upstream of the transcription start site within DEGs. HOMER analysis of commonly upregulated DEGs identified four basic Helix Loop Helix (bHLH) and one zinc finger transcription factor (TF) in the top 5 TF's (Table 5.1), with transcriptional activity related to stress responses such as hypoxia and oxidative stress. These features fall in line with the pathway analysis of conserved upregulated genes evidenced in Figure 5.4. Enrichment of the circadian clock TF bHLHE40, a ubiquitously expressed TF with strong expression in skeletal muscle was identified herein. Interestingly, bHLHE40 can be induced by various cellular stressors including hypoxia (Miyazaki et al., 2002) and has been identified to protect skeletal

muscle from ROS-induced damage by activating the expression of heme-oxygenase-1 (*Hmox1*) (Vercherat et al., 2009), a gene that appears in the top 20 upregulated DEGs for both CBD (2.1-fold change) and sCBD (2.4-fold change) in this data set. Similarly, the bHLH TF Myc was enriched and has been linked to cellular responses to stress including oxidative stress and hypoxia (Le et al., 2021). Both treatments also increased expression of *Myc* (~1.4 fold), suggesting a common mechanism of action. Downstream targets of MYC such as MYC downstream regulated gene 1 (*Ndrg1*), also a common upregulated DEG in our dataset, are known to regulate the cellular adaptive response to hypoxia (Park et al., 2022). Moreover it was noticed that USF1 and the zinc finger TF SP1 in this HOMER analysis and they too have been shown to regulate the expression of downstream targets in response to hypoxic conditions (Turkoglu and Kockar, 2016). USF1 is thought to mediate transcriptional activity to AMPK activation, driven by an increase in AMP:ATP ratio (Irrcher et al., 2008). Moreover, overexpression of USF1 in skeletal muscle cells leads to increased PGC-1α promoter activation and similar increases at the mRNA level (Irrcher et al., 2008) indicating the importance of this TF in transcriptional responses to energetic stress.

Table 5.1. Top 5 conserved putative upstream regulators of CBD and sCBD transcriptional responses.

	% of targets	Log *p*-value	TF (family)
Motif (upregulated genes)			
	36.60	−1.93E+01	USF1 (bHLH)
	26.52	−1.38E+01	bHLHE40 (bHLH)
	39.36	−1.28E+01	CLOCK (bHLH)
	49.17	−1.25E+01	Sp1 (Zf)
	44.34	−1.22E+01	n-Myc (bHLH)
Motif (downregulated genes)			
	46.21	−1.12E+01	Myf5 (bHLH)
	94.95	−1.01E+01	Nkx2.1 (Homeobox)
	46.99	−9.08E+00	MyoD (bHLH)
	49.51	−8.24E+00	Otx2 (Homeobox)
	62.14	−7.33E+00	Ap4 (bHLH)

DNA binding motifs enriched in the present downregulated DEGs included myogenic regulatory factors MYF5 and MYOD1 which have extensive roles in myogenesis and the latter, homeostasis of terminally differentiated muscle and the sarcomere. *Myod1* was found to be downregulated in both treatment groups (~1.6-fold), again suggesting a common mechanism of action. Indeed, it might be suggested that this may be responsible for the downregulation of many sarcomeric proteins, as evidenced in Figure 5.5c. Collectively, these TF's lend support to the pathway analysis presented in Figure 5.5b, suggestive of a cellular stress response induced by CBD and sCBD exposure, which may be partially responsible for downregulation of Myod1 and a number of genes encoding sarcomeric/contractile components.

5.5 Discussion

The main findings of this investigation evidence that CBD treatment leads to the transcriptional activation and repression of several hundred genes and this is at least partly due to CBD itself rather than the many other compounds found in hemp-derived, broad-spectrum CBD. Upon further examination of the DEGs commonly up and downregulated by CBD and sCBD, many of the upregulated genes are indicative of a "stress" response, and commonly downregulated genes allude to muscle remodelling of motor and structural proteins. In line with this study's hypothesis, these findings suggest that broad-spectrum CBD treatment induced 1342 unique upregulated DEGs and 1137 unique downregulated DEGs, compared to 154 and 152 unique up- and downregulated DEGs in sCBD presumably due to the array of additional compounds present compared to sCBD.

This is the first investigation to report transcriptome responses to CBD and sCBD in skeletal muscle, a tissue in which relatively few data exist characterizing the effects of cannabinoids. Mechanistic studies by Langer and colleagues found that CBD exerted no effect on anabolic signalling through mTORC1 or inflammatory signalling through nuclear factor kappa B with CBD doses of 1–5 μM in C_2C_{12} myotubes (Langer, Avey and Baar, 2022). Using a different experimental design, Iannotti and colleagues established that 1 μM CBD enhanced myogenesis, but 3 μM had an inhibitory effect on myogenin (*Myog*) mRNA expression (Iannotti et al., 2019a). *In vivo* studies provide further complexity. Intraperitoneal injection of 60 $mg \cdot kg^{-1}$ CBD prevented loss of locomotor activity, reduced inflammation, and restored autophagy in mdx mice (Iannotti et al., 2019a). In a separate study on healthy rats undergoing eccentric loading of the tibialis anterior, administration of 100 $mg \cdot kg^{-1}$ hemp-derived CBD decreased pro-inflammatory signalling without blunting the anabolic response to exercise in rats (Langer, Avey and Baar, 2022). These studies provide valuable targeted insights, but not a clear systems-level picture of the effects of CBD on skeletal muscle.

With regards to dissecting this study's findings, insights may be found by examining the reported anti-cancer properties of cannabinoids in various other cell types. One of the mechanisms by which CBD may act to reduce cancer cell proliferation is through

apoptosis, with some studies highlighting increased ROS production as a central mechanism. For example, CBD can trigger *Noxa* (*Pmaip1*) mediated apoptosis in colorectal cancer cells in a dose dependent manner (0-8μM) by generating ROS and inducing excessive endoplasmic reticulum (ER) stress, mainly driven by mitochondrial superoxide anion (Jeong et al., 2019). Notably, the induction of ER stress-mediated apoptosis was under the action of the activating transcription factors *Atf3* and *Atf4*. This dataset demonstrates transcriptional activation of *Atf4* and *Atf6*, as well as several molecular chaperones (*Hspa8, Hspa1b, Hsph1, Hspa4l, Hsp90b1, Hspa5, Hspa9, Hspd1*) integral to the ER stress response.

Oxidative stress and ER stress are interconnected cellular processes that can activate the Unfolded Protein Response (UPR). ROS generated during oxidative stress can modulate the activity of UPR signalling pathways by directly oxidizing critical cysteine residues within UPR proteins or by activating redox-sensitive transcription factors (Malhotra and Kaufman, 2007). Studies on other phytonutrients such as the green tea catechins highlight this link in a physiological setting and provide further insights to the observations presented herein. Once considered to be antioxidants, contrary evidence suggests that catechins may in fact act as pro-oxidants to mediate a mitohormetic responses. For example, (Tian et al., 2021) explored the effects of epigallocatechin- 3-gallate (ECGC) and epicatechin-3-gallate (ECG) on *Caenorhabditis elegans.* The authors show that 2.5 μM of green tea catechins significantly blocks mitochondrial complex I activity and mitochondrial respiration rate leading to a transient rise in ROS production and a drop in ATP production. Further, the authors show that lifespan was extended in *C.elegans* by catechin treatment and posit that this could be mediated through a subsequent upregulation in antioxidant defence enzymes including catalase (*Cat*) and superoxide dismutase (*Sod*) and the energy sensors AMP kinase (*Ampk*) and sirtuin 1 (*Sirt1*). Interestingly, this experiment evidenced *Sirt1* and *Sod2 to be* DEGs significantly upregulated by CBD and sCBD. Consistent with these observations and in support of a mitohormetic effect of CBD, ROS-mediated UPR activation can enhance cellular antioxidant defences by upregulating the expression of antioxidant enzymes. In the present study, the antioxidants hemeoxygenase-1 (*Hmox1*), NAD(P)H dehydrogenase quinone 1 (*Nqo1*),

glutathione reductase (*Gsr*), peroxiredoxins 5 and 6 (*Prx5*, *Prx6*), thioredoxin reductase 1 (*Txnrd1*) and superoxide dismutase 2 (*Sod2*) are all DEGs commonly upregulated by CBD and sCBD. Moreover, nuclear receptor subfamily 4, group A, member 2 (*Nr4a2*) was also commonly upregulated by CBD and sCBD and serves as a key regulator of antioxidant gene expression (Li et al., 2004; Motohashi and Yamamoto, 2004), via binding of antioxidant response elements and integrating cell signalling pathways to co-ordinate the expression of antioxidant genes and maintain cellular homeostasis.

During conditions of ER stress, the UPR is activated to restore ER homeostasis by attenuating protein synthesis, enhancing protein folding capacity, and promoting protein degradation through the ubiquitin-proteasome system and autophagy. Notably, autophagy is required to maintain muscle mass (Masiero et al., 2009) and in a murine model of muscular dystrophy, intraperitoneal injection of CBD restored autophagy as evidenced by an increase in the ratio of LC3-II to LC3-I (Iannotti et al., 2019a) often used as a marker of autophagic activity (Terman, Gustafsson and Brunk, 2007), as well as restoring mRNA transcript levels of the autophagy genes beclin-1, Atg4, Atg12 and Ulk1. In support of this argument, this dataset evidenced that "Lysosome" is in the top 5 enriched KEGG terms and GO cellular compartment terms. The lysosome and autophagy are linked in a degradation pathway, where autophagic cargo is delivered to lysosomes for breakdown and recycling (Mizushima et al., 1998), maintaining cellular health and function. Moreover, the downregulation of contractile and motor proteins shown in Figure 5.5 could be interpretated as a feedback response to reduced protein translation. Whilst others have shown no attenuation of muscle anabolic signalling in response to CBD (Langer, Avey and Baar, 2021; Langer, Avey and Baar, 2022), the findings of this study suggest that investigation of individual peptide synthesis rates via deuterium labelling in muscle following CBD exposure may provide better resolution than bulk synthesis rates and anabolic signalling. This in turn, could uncover the possible cellular remodelling of the proteome by CBD.

Calcium mediated ER stress is also an emergent theme within this dataset with significant up regulation of Calnexin (*Canx*) and Calreticulin (*Calr*) as part of a larger

cluster of genes including chaperones and autophagy genes (Figure 5.2). Others have demonstrated that treatment of C_2C_{12} and human derived myoblasts with CBD increases $[Ca^{2+}]_i$ via TRPV1 activation (Iannotti et al., 2019a), an observation replicated in several other cell types and central to many of the established roles of CBD in pain mediation (Louis-Gray, Tupal and Premkumar, 2022). TRPV1 activation also promotes ER stress through modulation of endoplasmic reticulum calcium, $[Ca^{2+}]_{ER}$, leading to the downstream activation of nuclear targets *Atf4, Atf6* and *Xbp1 (Thomas et al., 2007)*. Increases in $[Ca^{2+}]_i$ may be a cause of mitochondrial ROS production, since elevated $[Ca^{2+}]_i$, due to TRPV1 channel opening, causes an initial increase in $[Ca^{2+}]_m$ and successive downstream effects, which can be attenuated by TRPV1 antagonists (Zhai et al., 2020). Future studies could explore treatment of myotubes with CBD in the presence or absence of TRPV1 antagonists to decipher the role of calcium in the signalling responses to CBD.

Limitations

A significant issue with cell culture experimentation is the translatability of findings *in vivo*, particularly with relevance to the concentration of compound under investigation. Deiana and colleagues report peak plasma CBD concentration of 14 $\mu g \cdot mL^{-1}$ at 120 min after injection of CBD at 120 $mg \cdot kg^{-1}$ body mass in rats, equivalent to about 45 µM (Deiana et al., 2012). Whilst plasma concentration and what the muscle is exposed to in the extracellular fluid may be very different, it is important to recognize that this investigation used a considerably lower concentration of CBD and sCBD (10 µM). Finally, it must be accepted that oral ingestion of CBD is associated with a diverse and complicated route of metabolism, and therefore this is highly likely to influence any of the discussed phenomena within this chapter.

A further limitation is that, whilst C_2C_{12} cells are regarded as a useful model to study basic muscle biology (Sharples and Stewart, 2011), findings must be replicated in human cells. The C_2C_{12} cell line, derived from murine skeletal muscle myoblasts, is an immortalized cell line widely used in muscle research due to its ease of culture and ability to differentiate into myotubes. However, its use introduces species-specific

differences in cell behaviour potentially limiting the translatability of findings to humans(Yaffe and Saxel, 1977; Blau, Chiu and Webster, 1983; Hernández-Hernández et al., 2017). Future work could replicate these findings using primary myoblasts obtained from human donors to provide a more translatable dataset. Moreover, it is difficult to achieve 100% differentiation of C_2C_{12} myoblasts into myotubes and thus there are always undifferentiated myoblasts in the cell population studied. Therefore, the signal detected in our RNAseq experiments is derived from a mix of myoblasts and myotubes. This could be overcome in future experimentation using bioengineered muscle constructs that typically allow for longer culture times and promote highly aligned and differentiated myotubes.

Messenger RNA is an important molecular readout of the response to homeostatic perturbations and precedes protein synthesis. It is, however, unclear whether mRNA transcript abundance directly correlates with changes in peptide synthesis (Vogel and Marcotte, 2012) and it cannot be ruled out that a first exposure effect, whereby the initial challenge to cellular homeostasis may be insufficient to repeatedly lead to the changes in the transcriptome described here. To resolve the preliminary insights described here, cellular remodelling following chronic exposure to CBD should be interrogated. Dynamic proteome profiling of muscle exposed to CBD could offer the required resolution to determine whether CBD leads to longer term cell remodelling (Hesketh et al., 2020).

Importantly, only one form of broad spectrum of CBD was used in this experiment. Whilst many metabolites of the cannabis plant are shared amongst several cultivars (Wishart et al., 2024), there are metabolites that are not shared across strains and therefore care should be taken in extrapolating these findings to other CBD products.

Finally, this study sought to identify the commonalities between broad-spectrum and sCBD and therefore focussed on unravelling the biological context of commonly up- and downregulated genes. It is accepted that there were many genes not commonly regulated by the treatments (i.e., DEGs unique to CBD or sCBD treatment), which were not examined in the current chapter as this was not the specific aim of the experiment. This study found that 1342 and 154 DEGs were upregulated by CBD and sCBD,

respectively. Whereas 1137 v 152 DEGs were downregulated by CBD and sCBD, respectively. As described earlier, broad-spectrum CBD contains hundreds of other compounds (Wishart et al., 2024) and whilst composition of the broad-spectrum treatment was not measured, this could explain the relatively large number of DEGs up and downregulated in CBD treatment compared with sCBD. Importantly, this data is publicly available, which provides a further avenue of investigation for future research.

Conclusion

The transcriptional data presented here provide evidence that CBD may induce a mild cellular stress that activates several pathways associated with altered redox balance, calcium homeostasis, unfolded protein response, and ER stress. Based on this work and previous work of others, it might be suggested that CBD can indeed interact with muscle to improve indices of cellular health. Future work should assess mitochondrial complex activity, mitochondrial metabolite production including ATP production, and ROS production following treatment with CBD to test the hypothesis that cannabinoids may act as mitohormetic compounds capable of improving cellular health. To summarise, this experiment was the first of its kind to contribute a publicly available transcriptomic profiling dataset on CBD and skeletal muscle. This should now prove to be a valuable contribution to the field, and it is hoped that this data might serve as the foundation for future progressions into better understanding the interaction of cannabinoids and skeletal muscle.

6 Does a Broad-Spectrum Cannabidiol (CBD) Supplement Improve Performance in a 10-minute Cycle Ergometer Performance Test?

Publications Arising from this Chapter:

Gillham, S. H., Starke, L., Welsh, L., Mather, E., Whitelegg, T., Chester, N., Owens, D., Bampouras, T., Close, G. L. (2024). Does a Broad-Spectrum Cannabidiol (CBD) Supplement Improve Performance in a 10-minute Cycle Ergometer Performance-Test? European Journal of Sport Science, 24, pp. 870-877.

Chapter 6 Prologue

Chapters 4 and 5 of this thesis aimed to a) understand if there was a dose-response relationship between the treatment of CBD and skeletal muscle health and b) the transcriptional response of this tissue following exposure to broad-spectrum CBD and synthetic CBD. However, given that this thesis proposed to follow a translational approach to adding to the body of literature relating to CBD and humans, the following chapter aims to begin this translation from *in vitro* to *in vivo* research. As mentioned earlier, in recent years there has been a considerable uptake in the general use of CBD supplements, in addition to interest from the scientific community. This interest has largely revolved around the potential utility of CBD as an aid to accelerated recovery and/or wellbeing following exercise or muscle damage. However, there have also been postulations that CBD might offer an analgesic effect to individuals with longitudinal health concerns, such as chronic pain and fibromyalgia. These assertions formed the early thought process behind the potential utility of CBD as an ergogenic aid to exercise performance. Moreover, previous research has attempted to understand the use of opioid-based analgesic products, such as tramadol in increasing exercise performance. As such, this chapter aimed to explore the utility of CBD to reduce the sensations of pain/discomfort associated with exercise via a potential decrease in perceived exertion.

6.1 Abstract

Background: Cannabidiol (CBD) is a non-intoxicating phytocannabinoid which has been proposed to possess anti-inflammatory and analgesic properties. It has been suggested that perceptions of pain have the capability to limit exercise performance, with athletes now turning to alternative to traditional means of analgesia. **Objective(s):** This study aimed to investigate if 3-weeks of daily CBD supplementation (150 $mg \cdot day^{-1}$) improved performance in a 10-minute performance-trial on a cycle ergometer. **Methods:** In a randomized, double-blind, placebo-controlled study, 22 healthy participants (n=11 male, n=11 female) completed two 10-minute performance-trials on a WattBike™ cycle ergometer interspersed with a 3-week supplementation period. Supplementation involved either 150$mg \cdot day^{-1}$ oral CBD, or 150$mg \cdot day^{-1}$ of a visually identical placebo. During trials, ratings of perceived exertion (RPE [6-20](Borg, Ljunggren and Ceci, 1985), heart rate (HR), and blood lactate (BLa) were collected every 2-minutes. Mean power (W) was also taken throughout the exercise at each timepoint. All data were analysed using two-way ANOVAs. **Results:** There were no significant differences ($P > 0.05$) between CBD or PLA groups for mean power (W) during the 10-minute performance-trial. There were also no significant differences ($P > 0.05$) in any of the physiological or perceptual parameters (HR, BLa, RPE) between conditions. **Conclusion:** Three weeks supplementation of a broad-spectrum CBD supplement did not improve performance via any change in RPE during a 10-minute time trial on a cycle ergometer, and as such this evidence does not support the claim that broad-spectrum CBD supplements could be performance enhancing in this exercise modality.

6.2 Introduction

As highlighted earlier in this thesis, the cannabis plant contains a diverse profile of chemical compounds including various phytocannabinoids. Indeed, there are suggestions that there may be ~144 constituent phytocannabinoids within this annual herbaceous plant (ElSohly et al., 2017). Of these phytocannabinoids, the most well-known are Δ^9-tetrahydracannabinol (Δ^9-THC) and cannabidiol (CBD), with the former best known for its psychotropic and intoxicating effects (Burr et al., 2021). Conversely, CBD has no known intoxicating effects or potential for abuse from a psychoactive standpoint (Iffland and Grotenhermen, 2017). Since the removal of CBD from the World Anti-Doping Agency (WADA) list of prohibited substances in 2018, the use of cannabis-related supplements has increased significantly (Docter et al., 2020). For example, it has been reported that 26% of professional rugby players have consumed CBD, with 80% of consumers citing enhanced recovery as their primary motive for consumption (Kasper et al., 2020b). Additionally, given that there are suggestions that CBD may be anxiolytic (García-Gutiérrez et al., 2020), can reduce inflammation (Burstein, 2015), and in some instances reduce sensations of pain (Urits et al., 2020) it is unsurprising that this compound is becoming increasingly desirable to many athletes. In a response to the athlete and practitioner interest in CBD supplements, the scientific community have also begun to explore the utility of CBD. Previous investigations (reviewed in Chapter 2) have attempted to provide insight into how CBD might influence recovery and/or adaptation following exercise. However, to date, there is a paucity of literature which discusses the potential utility of CBD before specific modes of exercise.

According to WADA, all cannabinoids (except for CBD) are prohibited in competition. Interestingly, Δ^9-THC is reported as an adverse analytical finding when levels of its metabolites exceed a urinary threshold of ≥ 150 ng·ml^{-1}, whereas in the case of other cannabinoids, no such thresholds exist. Many CBD supplements (particularly broad-spectrum products) available for purchase off-the-shelf have been reported to contain quantities of some of these other prohibited cannabinoids, posing a significant issue from an anti-doping perspective (Gurley et al., 2020; Liebling et al., 2020; Johnson, Kilgore and Babalonis, 2022). Indeed, it is important to consider the entourage effect

of cannabinoids. Specifically, it has been suggested that a wider profile of cannabinoids (termed the “entourage effect”) may be required for a supplement to elicit any of the proposed beneficial effects of cannabinoids (Russo, 2019). To date, there are limited data on the effects of broad-spectrum CBD products on athletic performance and as such it is difficult to fully establish if these multi-cannabinoid containing supplements have the potential to enhance performance.

One of the primary motives cited for CBD supplementation in athletic populations are the purported analgesic properties of the compound (Kasper et al., 2020b). These properties have not been established in sport specifically, but have been addressed in other fields (Urits et al., 2020). That said, while not a direct study on analgesia *per sé*, a recent pilot study investigated the effects of an acute dose (300 mg) of synthetic CBD on incremental running to exhaustion, and concluded there to be no changes in perceived exertion, but some measurable changes in subjective ratings of pleasure during exercise (Sahinovic et al., 2022). However, no study to date has investigated the effects of CBD on prolonged high-intensity exercise. There are well-defined links between pain and perceived exertion during exercise, which may somewhat explain the downregulation of pacing schema athletes employ during bouts of intense exercise (Waldron and Highton, 2014). Given that CBD has demonstrated potential to provide analgesia in humans (Argueta et al., 2020), and increase enjoyment during exercise (attributed to a proposed analgesic affect) (Sahinovic et al., 2022), CBD may provide an ergogenic effect during exercise which is associated with exercise-induced pain as seen during high-intensity exercise.

Therefore, the primary aim of the present study was to investigate if 3-weeks of daily CBD supplementation (150 $mg \cdot day^{-1}$) had the potential to enhance performance compared to placebo during a 10-minute power test on a cycle ergometer. It was hypothesised that following CBD supplementation, average power would be increased, and rating of perceived exertion would be reduced compared to placebo.

6.3 Methods

6.3.1 Participants and Study Design

With institutional Ethics approval (M22_SPS_2273) 24 (male n=12; female n=12) healthy, recreationally active participants (age: 27 ± 6.3 years; stature: 170.4 ± 10.1 cm; body mass: 69.4 ± 13.5 kg) were recruited in a randomised, placebo-controlled independent groups design. To be eligible for participation in this study, participants had to maintain their normal exercise regime, report no use of prescription medication and were instructed to avoid consuming any cannabis-related products for 4-weeks prior to, and throughout the experimental period. In addition, no participants were involved in any sports that were signatories to the World Anti-Doping Code at the time of testing. Finally, all participants agreed to using a reliable form of contraception during, and 3-months following participation in the study. Upon providing written informed consent, participants completed a health-screening, and readiness to exercise questionnaire and then participants were invited to the laboratory on a minimum of 4 (and maximum of 7) occasions. Visit 1 comprised collection of anthropometric variables and familiarisation with the Wattbike^{TM} cycle ergometer and exercise protocol. On this initial visit, participants also completed their first complete familiarisation 10-minute performance trial. This trial was then repeated on subsequent visits (separated by ~48h) until participants were able to achieve a coefficient of variation (CV) < 5% for average power (W), and distance covered (m) during each exercise protocol. When this was achieved participants were then eligible to begin the experimental period. Participants completed their pre-supplementation performance-trial 48h following their final familiarisation visit (Figure 6.1).

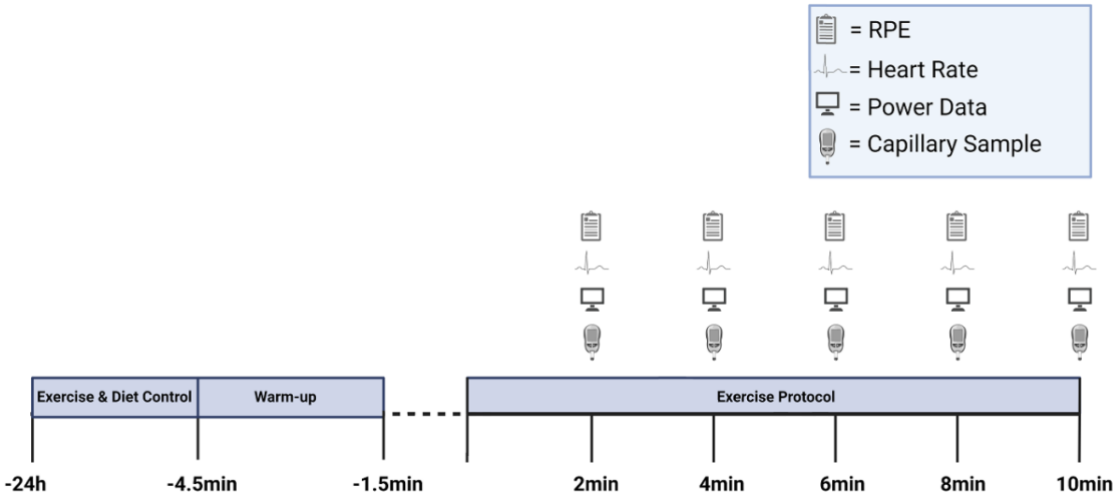

Figure 6.1. Schematic representation of study procedures.

6.3.2 Procedures

10-min time trial

Participants arrived at the laboratory at the same time of day (±1 h) for each visit so to avoid any diurnal variation. All performance-trials were completed on a Wattbike™ "Trainer" cycle ergometer (Nottingham, Nottinghamshire, UK). The ergometer flywheel and magnet were set at 5 and 1 for females and 5 and 5 for males, respectively. Before the performance trial, participants were fitted with a Polar H10 heart rate monitor (Polar Electro, Kempele, Finland) and completed a 3-minute active warm-up on the ergometer at a self-elected intensity. Thereafter, participants were provided with a 90-s passive recovery before the 10-minute performance-trial began. All exercise was completed with no verbal encouragement or visual feedback from the ergometer. Every two-minutes, power (W), and distance covered (m) were taken directly from the ergometer. Heart rate (beats·min^{-1}) was taken from the Polar app for iPhone (which was connected via Bluetooth), and perceived exertion was monitored as per the rating of Borg (6-20; (Borg, Ljunggren and Ceci, 1985)). Blood lactate was assessed via a capillary sample from a fingertip on the non-dominant hand and then analysed using the Biosen C-Line Glucose and Lactate analyser (EKF Diagnostics, Cardiff, UK).

Treatments, randomization, and blinding

The products (CBD/PLA) used in this study (Naturecan Ltd. Stockport, UK) were both 100% vegan certified, and third-party laboratory tested for cannabinoids, residual solvents, pesticides, heavy metals and microbials (Spring Creek Labs, Utah, USA). Participants in the experimental group received a 10 ml tincture of a 40% concentration broad-spectrum OTS oral formulation of CBD (395.13 mg·g), CBG (8.83 mg·g), and other cannabinoids in trace concentrations, including Δ^9-THC (< 0.0025 % [with 0.00025% the limit of detection]) in medium-chain triglyceride (MCT) oil. The placebo group were provided with a 10 mL, visually identical MCT-only oil tincture. Participants were familiarised with supplement ingestion, which comprised self-administrating 9-drops (~150 mg) of their treatment sublingually, waiting 30-seconds and then swallowing. Participants were instructed to consume their respective supplement at the same time of day (~ 08:00 am) +/- 1h daily, for 3-weeks, and instructed to store their respective supplements in a cool, dry place out of the reach of children. In addition, participants were instructed to consume their supplement without food so to avoid any nutrition-related variability in CBD metabolism as calorie dense meals have been reported to increase absorption rates in humans (Perucca and Bialer, 2020). Participants were instructed to inform the lead researcher if they failed to consume a dose, and that they must not "double dose" the next day, instead, informing the lead researcher. The final dose of participants' respective treatments was consumed 60-mins before arrival at the laboratory on the final day of testing.

Nutrition

As per recommended guidelines for carbohydrate (CHO) intake in the day before high-intensity exercise (Mata et al., 2019), participants were required to consume ~6g·kg^{-1} body mass CHO on the day before both the pre- and post-intervention performance-trials. Participants were also encouraged to replicate their nutritional intake from their pre-supplementation visit in their final visit. To verify participants consumed the desired CHO, the "snap-n-send" method, as described to be valid and reliable in recreational athletes (Costello et al., 2017). All data were analysed by a registered sports nutritionist (SENr) using Nutritics^{TM} software for Macintosh (Nutritics, Swords,

Ireland). In the morning of each performance trial, participants were required to have abstained from caffeine in the 12 h before their visit, with the "snap-n-send" method as previously described implemented for the participants' pre-exercise breakfast. Finally, participants were instructed to avoid alcohol consumption and any strenuous exercise in the 24 h before each visit to the laboratory.

Blinding

Following familiarisation, participants were block randomized into two groups, experimental (CBD) or control (PLA). Specifically, participants were matched for peak power (W) output achieved in their first familiarisation visit. Thereafter, the pair were then assigned to either the CBD or PLA condition, randomisation was completed using a commercially available random number generator by a staff member who was independent of the study.

6.3.3 Statistical Analysis

Statistical analysis was conducted in The Statistical Package for Social Sciences (SPSS; Version 27, IBM, Chicago, IL, USA). Collation and creation of figures was completed using GraphPad Prism™ for Macintosh (Version 9.3.1). All data were analysed using two-way ANOVA, with η^2p calculated to express magnitude of effects. Significance was assumed if α reached ≤ 0.05. All data are presented as mean ± standard deviation (SD).

6.4 Results

Two participants were removed from this study. The first was removed due to illness unrelated to the research intervention on the final day of testing and the second because of self-reported non-compliance (failure to adhere to the supplementation protocol) with the study procedures. Both participants were in the experimental group (CBD), as such analysis was completed on CBD (n = 10) and PLA (n = 12). The final characteristics of the participants included in all analysis were male = 11; female = 11; age: 26.18 ± 6.2 years; stature: 170.25 ± 10.27 cm; body mass: 69.32 ± 13.56 kg.

Blinding

Upon completion of the study participants were asked which group (CBD/PLA) they believed they had consumed. Twelve of the 22 (54%) of participants correctly guessed that they were consuming their respective treatment.

There was no significant effect of time (P = 0.341; partial Eta^2 = 0.046) or group (P = 0.701; η^2p = 0.008) in total distance (km) covered pre-post supplementation in either the PLA (5.68 ± 0.54 vs. 5.74 ± 0.59 km) or CBD (5.93 ± 0.56 vs. 5.95 ± 0.52 km) groups (Figure 6.2). In addition, there was no significant effect of time (P = 0.313; η^2p = 0.051) or group (P = 0.423; η^2p = 0.032) in average power (W) covered in the 10-mins of the performance trial pre-post supplementation in either the PLA (163.5 ± 43.37 vs. 169.5 ± 48.36 W) or CBD (185.9 ± 48.76 vs. 186.6 ± 46.5 W) groups (Figure 6.3).

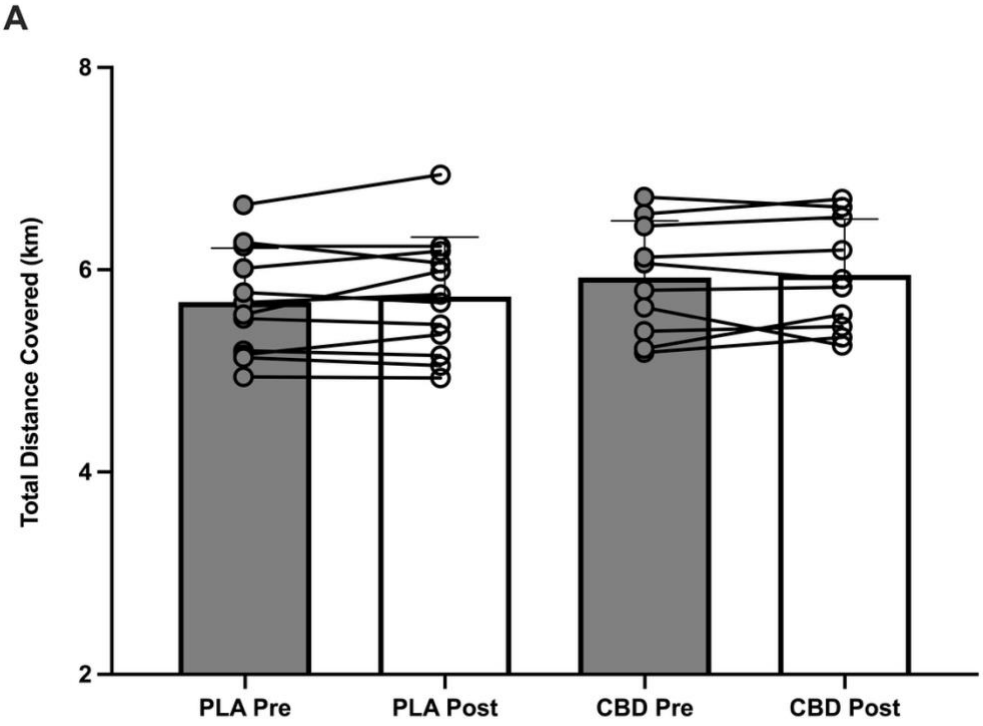

Figure 6.2. Average and individual (A) total distance covered (km) pre–post supplementation in the placebo and cannabidiol groups, respectively.

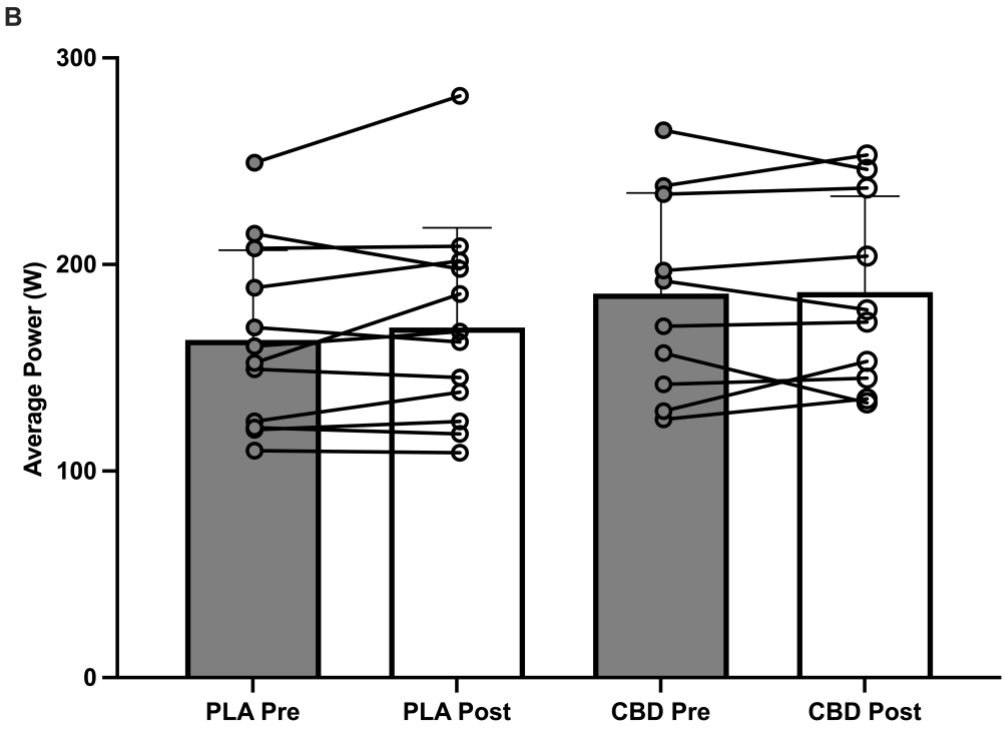

Figure 6.3. Average and individual 10-min power (W) pre-post supplementation in the PLA and CBD groups, respectively.

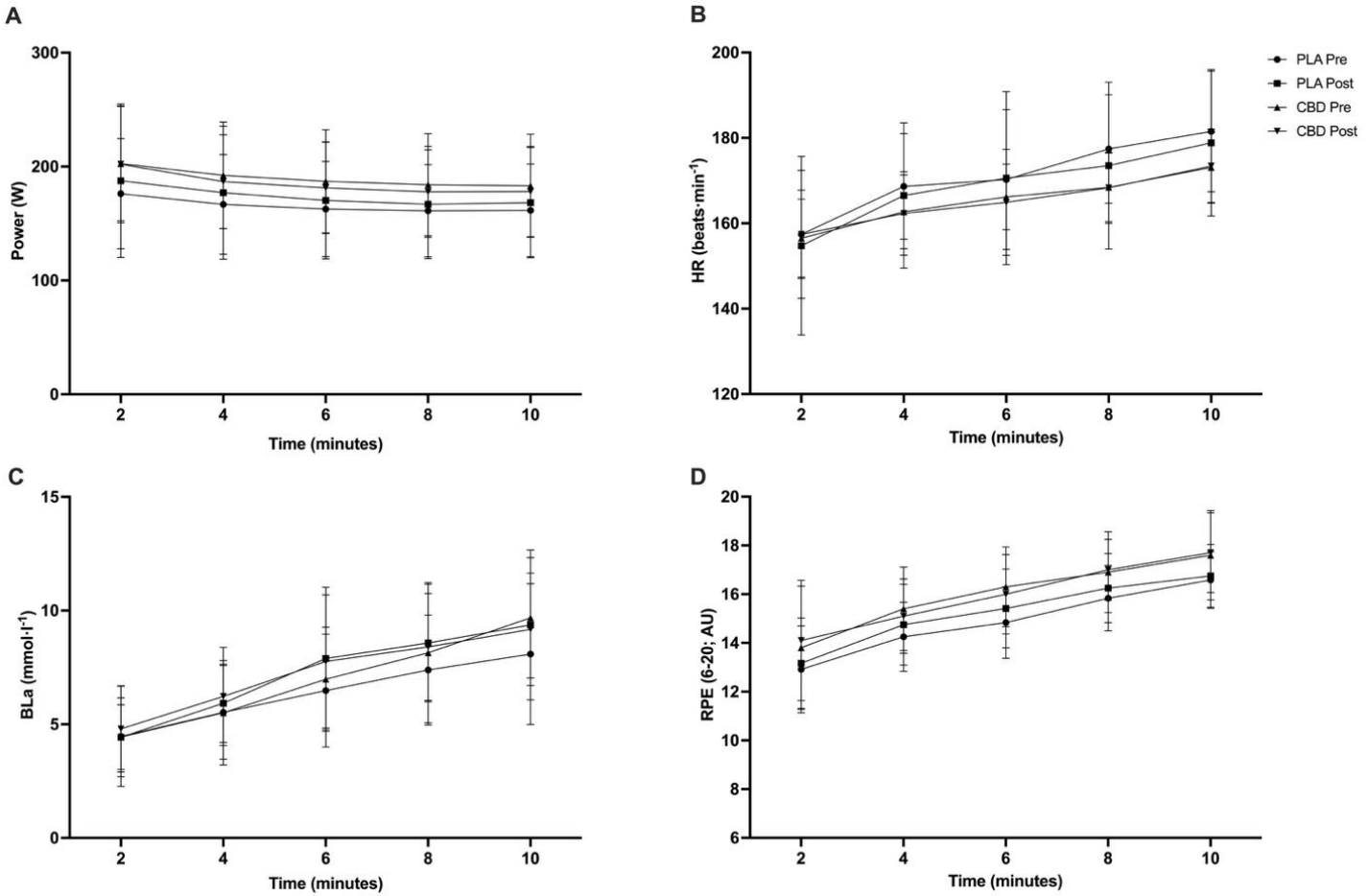

Figure 6.3. Pre–post supplementation changes in mean power (W) for PLA (A) and CBD (B). Pre–post supplementation changes in mean heart rate (b·min^{-1}) for PLA (C) and CBD (D). Pre–post supplementation changes in blood lactate (mmol·L^{-1}) for PLA (E) and CBD (F). Pre–post supplementation changes in RPE (AU; Borg 6–20) for PLA (G) and CBD (H). CBD, cannabidiol; PLA, placebo.

Average power (W) was not significantly changed pre-post supplementation (P = 0.77; η^2p = 0.004), with no time*group effect pre-post supplementation (P = 0.32; η^2p = 0.049). However, as expected there was a significant effect of timepoint (P < 0.001; η^2p = 0.72), with no difference between groups at each time point (P = 0.494; η^2p = 0.17; Figure 6.3a). There was no significant effect of time for average heart rate (beats·min^{-1}) pre-post supplementation (P = 0.528; η^2p = 0.02), time*group pre-post supplementation (P = 0.571; η^2p = 0.016). There was, however, a significant effect of time (P < 0.001; η^2p = 0.9), but this was not different between groups (P = 0.349; η^2p = 0.22; Figure 6.3b). There were no observed changes in BLa (mmol·l^{-1}) significant effect of time for pre-post supplementation (P = 0.151; η^2p = 0.1) or time*group pre-post supplementation (P = 0.472; η^2p = 0.026). Again, as expected, there was a significant effect of timepoint (P < 0.001; η^2p = 0.92), but this was not different between groups (P = 0.972; η^2p; Figure 6.3c). There was no significant effect of time for perceived exertion (RPE; 6-20) pre-post supplementation (P = 0.23; η^2p = 0.071), with no time*group pre-post supplementation effect present either (P = 0.19; η^2p = 0.086). Once more, there was a significant effect of timepoint (P < 0.001; η^2p = 0.82), but this was not different between groups (P = 0.823; η^2p = 0.081; Figure 6.3d).

6.5 Discussion

The aim of the present study was to assess if 3-weeks of daily CBD supplementation could improve performance during a 10-minute cycling performance-trial. Despite the growing popularity of CBD products, and contrary to the original hypothesis, the primary finding of this study was that chronic supplementation (150 mg·day^{-1}) of a broad-spectrum CBD product did not reduce perceived exertion or improve cycling performance in a 10-minute performance-trial when compared to placebo.

This study was formulated from the suggestion that CBD may provide an analgesic effect in humans (Urits et al., 2020; De Vita et al., 2021). The mechanistic basis for the proposed analgesic effect of CBD is that it is a non-competitive antagonist of both

cannabinoid receptors, type 1 (CB_1) and type 2 (CB_2). While CB_2 receptors are predominantly found in the periphery and cells of immune origin (Wiley and Martin, 2002; Zou and Kumar, 2018), it is important to remember that CB_1 are abundant within the central nervous system (CNS). Indeed, CB_1 receptors have been cited to be particular abundant in the midbrain and spinal cord, both of which are, in part, responsible for pain perception (Manzanares, Julian and Carrascosa, 2006). A further potential mechanism of analgesia is that CBD has been proposed to play a significant role in G protein-coupled receptor 3 (GPR3) activity which is expressed within the CNS and may play a role in both pain perception and emotional regulation (Laun et al., 2019). Moreover, improved subjective exercise enjoyment has been linked to a potentially analgesic effect (Sahinovic et al., 2022). This enhanced enjoyment of exercise could perhaps be attributed to CBD's interaction with 5-HT_{1A} receptors, which have been shown to play a role in cognition, and specifically mood regulation (Albert, 2012; Sahinovic et al., 2022). Despite these potential mechanisms of pain reduction, in this exercise modality, this study reports no improvements in either exercise performance or ratings of perceived effort. This is unlike other "pain killing" compounds, such as tramadol (a medication prohibited by WADA from 2024) which has somewhat conflicting results on exercise, with some reports of no effect (Zandonai et al., 2021), and others of improved performance (Holgado et al., 2018b; Mauger et al., 2023). That said, there is seemingly some contention surrounding an appropriate dose and route of administration of CBD. For example, it has been reported that CBD may provide analgesia post-surgery with a dose as little as 25 mg (Hurley et al., 2023). Conversely, a single dose of 800 mg had no reported effect on pain (Schneider et al., 2022). In exercise models specifically, a dose of 60 mg was reported to be beneficial in recovery from muscle damage (Isenmann, Veit and Diel, 2020), while 150 mg exhibited no effect on non-invasive markers of muscle damage (Cochrane-Snyman et al., 2021). Taken together, the dose used in the present study adds further questions relating to the "optimal" dose of orally consumed CBD.

Given the broad-spectrum product consumed in the present study did not enhance performance in this exercise modality, these observations should encourage further work in this field. It is perhaps advisable that now larger studies investigating various

exercise modalities are required to encourage the consideration of anti-doping reform. As discussed previously, all cannabinoids (except CBD) are classified as prohibited substances. The CBD used in this study was "broad-spectrum", containing compounds which would in principle result in an AAF by WADA. Indeed, the certificate of analysis provided by the manufacturer reported the presence of other cannabinoids including CBG, cannabichromeme (CBC) and cannabigerolic (CBGA). Whilst it is unclear if anti-doping laboratories actively test for all cannabinoids (rather than just the intoxicating cannabinoid Δ^9-THC), it is crucial to remember that only one of the 11 ADRV's involves an AAF. These considerations are vital as some of the therapeutic benefits associated with CBD have been suggested to be related to the "entourage effect", meaning that cannabinoids may be considerably more potent when they are co-ingested, particularly in the case of CBD and Δ^9-THC (Russo, 2019). Indeed, while isolating CBD is at present the only "safe" way for an athlete to take CBD from an anti-doping perspective, this may not be the most effective method to achieve any of the purported benefits of CBD-related products. Future research must now fully explore this entourage effect in athletic situations as well as provide more evidence for WADA to make an informed decision on the prohibited status of other cannabinoids, investigating their relative safety, effect on performance and if their use retracts from the spirit of sport.

Limitations

While important for the growing body of literature in CBD research, this study is not without its limitations. The sample size used, although in line with other similar studies (e.g. Sahinovic et al. 2022), was limited by logistical and practical considerations, such as financial cost and time constraints; both aspects generally accepted to impact on subject recruitment (Lakens, 2022). In addition, given that the present study did not have a large enough sample size to complete a sub-group sex analysis, it is not clear whether CBD supplementation affects the physiological response to exercise in the same way for both sexes and therefore, it is difficult to postulate whether the results could have been affected by the inclusion of both sexes. Future studies should examine sex differences in CBD supplementation responses in such parameters.

Nonetheless, the study provides useful information to further research into the area of broad-spectrum CBD supplementation in exercising individuals.

Practical Applications

This study provides athletes and associated personnel with novel data on the potential utility of broad-spectrum CBD supplements in reducing perceived exertion during aerobic exercise. These findings demonstrate that the commercially available CBD supplement used in this study does not enhance performance during a 10-minute cycle-ergometer performance trial. Given that there are anti-doping risks associated with CBD supplementation, coupled with the lack of any clear benefit to performance, it is advisable for athletes to maintain abstinence from CBD supplementation - especially if their motive for supplementation coesists with a desire to influence aerobic perfomrnace.

Conclusion

These data suggest that a broad-spectrum CBD supplement (containing < 0.0025% Δ^9-THC but including traces of other cannabinoids including CBG, CBC, and CBGA) did not enhance performance during a 10-minute cycle ergometer performance-trial. Given the concerning data outlining the disparity between advertised and actual cannabinoid content claims of OTS CBD products, coupled with only one cannabinoid being considered as a threshold substance, athletes should maintain abstinence of OTS CBD supplements. Research should now be performed to investigate if a range of other cannabinoids have the potential to influence performance in a variety of exercise modalities.

7 Daily Use of a Broad-Spectrum Cannabidiol Supplement Produces Detectable Concentrations of Cannabinoids in Urine Prohibited by the World Anti-Doping Agency: An Effect Amplified by Exercise

Publications Arising from this Chapter:

Gillham, S.H., Cole, P.L., Owens, D.J., Chester, N., Bampouras, T.M., McCartney, D., Gordon, R., McGregor, I.S. and Close, G.L., 2026. Daily use of a broad-spectrum cannabidiol supplement produces detectable concentrations of cannabinoids in urine prohibited by the world anti-doping agency: an effect amplified by exercise. Medicine & Science in Sports and Exercise, 58(1), 121-131.

Chapter 7 Prologue

Continuing the translational approach in this thesis, Chapter 7 aims to explore one of the most contentious contemporary debates in sport nutrition. Chapter 6 concluded with some closing remarks which highlighted the importance of the anti-doping considerations which surround CBD supplementation in elite sport. While many of the research studies which have both been reviewed (Chapter 2) or mentioned throughout this thesis have sought to explore the potential utility of CBD, there is currently no consensus statement on how athletes might safely use CBD as part of their regime. Indeed, while Chapter 6 reported no benefits of CBD during aerobic exercise, it was acknowledged that the predominant motive for athletes to use CBD was in their recovery from exercise. Given that the use of CBD in elite sport has grown considerably in recent years, it has been highlighted that there is a considerable misunderstanding from athletes surrounding the "safe" use of CBD (Kasper et al., 2020b). In addition to the evidence of athlete understanding, several studies from across the globe have highlighted the disparity which surrounds the actual contents of many commercially available CBD products and their actual content. Taken together, these issues leave athletes and associated personal in a difficult position. This chapter, therefore aimed to provide athletes, practitioners and governing bodies with rigorous data to help inform them of the potential risks associated with CBD supplementation from the perspective of anti-doping legislation.

7.1 Abstract

Background: Cannabidiol (CBD), a non-intoxicating phytocannabinoid, is used by athletes to enhance recovery and manage other conditions (e.g., poor sleep, anxiety). Although CBD is not prohibited by the World Anti-Doping Agency (WADA), other cannabinoids found in "broad-spectrum" CBD products (e.g., cannabigerol (CBG), cannabidivarin (CBDV)), remain prohibited. **Objective(s):** This study aimed to determine whether 10-weeks' use of a broad-spectrum CBD product (150 $mg \cdot day^{-1}$ [containing trace concentrations of CBG]) could lead to detectable concentrations of prohibited cannabinoids in urine and plasma. The influence of moderate-intensity exercise was also assessed. **Methods:** Thirty-six healthy individuals (47% male) self-administered either a broad-spectrum CBD product (n = 31; CBD) or a visually identical placebo (n=5; PLA) for 10-weeks. After 10-weeks, participants completed a fasted, 90-minute bout of moderate-intensity exercise (55% VO_{2peak}). Blood and urine samples were collected at baseline (pre-supplementation) and pre- and post-exercise. **Results:** No cannabinoids or metabolites were detected at baseline in either the PLA or CBD group. Following 10-weeks of supplementation, urinary concentrations of CBD and its metabolites (6-OH-CBD, 7-COOH-CBD, 7-OH-CBD) were present. CBG and CBDV were also detected in 42% and 68% of pre-exercise samples, respectively. Urinary concentrations of 6-OH-CBD (P=0.006), 7-OH-CBD (P=0.009), CBD (P=0.043), CBG (P=0.0023) and CBDV (P=0.033) also increased from pre- to post-exercise. CBG and CBDV were detected in 74% and 84% of post-exercise samples, respectively. Concentrations of Δ^9-THC or its metabolites (11-OH-THC, 11-COOH-THC) were not present at any timepoint. **Conclusion:** Daily use of a broad-spectrum CBD supplement resulted in detectable urinary concentrations of WADA-prohibited cannabinoids in urine. Exercise appeared to increase concentrations of these cannabinoids. Therefore, athletes should avoid consuming broad-spectrum CBD products, given the potential associated anti-doping risks.

7.2 Introduction

Cannabis sativa L. is an annual herbaceous plant that has been used for millennia for a variety of purposes from industrial, to medical, to ceremonial (Clarke et al., 2016). The cannabis plant possesses many bioactive molecules, most notably >140 terpenophenolic compounds known as phytocannabinoids. The best-studied of these is Δ^9-tetrahydrocannabinol (Δ^9-THC), the main intoxicating component of cannabis, while cannabidiol (CBD), cannabigerol (CBG) and cannabidivarin (CBDV) are non-intoxicating cannabinoids with emerging therapeutic potentials (ElSohly et al., 2017; Nachnani, Raup-Konsavage and Vrana, 2021). That said, there have been conflicting reports regarding the utility of cannabinoids, specifically CBD in supporting sports performance and recovery

Cannabis plants exhibit a wide range of different chemotypes: Δ^9-THC-dominant chemotypes are typically used to manufacture recreational cannabis products while CBD-dominant chemotypes are associated with industrial hemp production and used to manufacture CBD products or 'nutraceuticals' (Salehi et al., 2022). CBD products have become widely available over-the-counter and online where they are sold directly to consumers, with an exponential increase in commerce over the last decade (McGregor et al., 2020; Li et al., 2021). Product types include oils, aqueous creams, e-liquids, confectionery, drinks and topical gels/creams (Johnson et al., 2023). These formulations can either be "isolate" products, where CBD is the only cannabinoid present, "full spectrum" prducts, where CBD, Δ^9-THC and other phytocannabinoids (e.g. CBG, CBDV) are present, or "broad-spectrum" products, where CBD, other phytocannabinoids, but not Δ^9-THC, are present (Marinotti and Sarill, 2020).

In recent years, interest and supplementation with CBD appears to have become prevalent in professional sport. For example, 26% of professional rugby players surveyed (and 39% of those aged >28 years) reported either currently using or having previously used CBD (Kasper et al., 2020b). The most common reasons for use were to enhance recovery (80%), improve sleep (78%), reduce anxiety (32%), and treat 'other' medical conditions (e.g., concussion). Most (67%) of respondents also reported

a perceived benefit from supplementation (Kasper et al., 2020b). Indeed, some early-stage evidence suggests that CBD has anti-inflammatory, neuroprotective, analgesic and anxiolytic effects (McCartney et al., 2020).

An important consideration, however, surrounding athlete use of CBD are the anti-doping regulations pertaining to cannabinoids (Close, Gillham and Kasper, 2021). The World Anti-Doping Agency (WADA) Code prohibits all cannabinoids other than CBD in any concentration, except for Δ^9-THC, where urinary concentrations of Δ^9-THC metabolites (11-hydroxy-tetrahydrocannabinol [11-OH-THC] and 11-carboxy-tetrahydrocannabinol [11-COOH-THC]) should remain below a 150 ng/mL threshold (McCartney et al., 2020; Close, Gillham and Kasper, 2021). The trace concentrations of 'other' phytocannabinoids (e.g., CBG, CBDV) present in many full-spectrum and broad-spectrum CBD products, therefore, constitute a significant concern given that any concentration is theoretically an anti-doping violation.

An additional concern is that the cannabinoid concentrations within commercially available products often differ substantially from those stated on the labels. For example, in Mississippi, only 12% of products tested contained cannabinoids that were within 20% of the label claims (Gurley et al., 2020). Moreover, some studies have also identified the presence of Δ^9-THC in "Δ^9-THC-free" formulations (Johnson et al., 2022). Similar findings have also been elucidated in the United Kingdom, with one study reporting only 38% of products tested were within 10% of the advertised CBD content (Liebling et al., 2020). Another recent investigation observed that only 8% of products tested had quantifiable concentrations of CBD within 10% of those advertised (Johnson et al., 2023). Subsequently, the general message from sport nutritionists is that athletes should a) remain cautious when supplementing with CBD, or b) avoid CBD supplements. However, athletes often consume these products without the advice or knowledge of qualified personnel (Kasper et al., 2020b).

Finally, it is important to recognise that the pharmacokinetics of CBD, Δ^9-THC and other phytocannabinoids are notoriously erratic and appear to be influenced by several factors (e.g., genetics, drug interactions) in addition to diet and exercise (Lim,

Sharan and Woo, 2020). For example, some evidence suggests that the highly lipophilic nature of cannabinoids means they can be sequestered in adipose tissue and may be released back into systemic circulation under lipolytic conditions (e.g., fasting or exercise) (Kreuz and Axelrod, 1973; Johansson et al., 1989). Previous studies have shown that exercise and food deprivation can increase blood Δ^9-THC and 11-COOH-THC concentrations in rats pre-treated with THC (Gunasekaran et al., 2009; Wong et al., 2014). Thirty-five minutes of cycling at 50% aerobic capacity (VO_{2max}) was also found to increase blood Δ^9-THC concentrations in 'regular' (i.e., ≥5 days/week) cannabis users (Wong et al., 2013). The likelihood of detecting prohibited phytocannabinoids might, therefore, be increased under certain conditions (e.g., following fasted exercise). This is significant as the WADA Code stipulates that anti-doping samples can be taken at any time – including post-competition/exercise.

The aim of the present study was therefore to investigate if supplementing with 150 $mg{\cdot}day^{-1}$ of an orally consumed broad-spectrum CBD supplement for 10-weeks increased cannabinoid concentrations of CBD, Δ^9-THC and CBG in plasma and urine. In addition, we aimed to explore the influence that exercise might have in increasing metabolite concentrations following the 10-week intervention. It was hypothesised that 10-weeks of broad-spectrum supplement use would result in measurable concentrations of WADA-prohibited cannabinoids in plasma and urine biological matrices and the introduction of fasted, moderate-intensity exercise would further increase these concentrations.

7.3 Methods

7.3.1 Participants and Study Design

A randomised, double-blind, placebo-controlled parallel group trial was conducted at Liverpool John Moores University with institutional Ethics approval (21/SPS/062). Randomisation of participant group allocation was completed using an online number generator. In accordance with the funding allocation of this study, groups were distributed in an unbalanced fashion. To be eligible for participation, participants had to report no use of prescription medication and were instructed to avoid consuming any cannabis-related products for 3-months before, and throughout the experimental

period. In addition, no participants were competing in any sports that were signatories to the WADA Code at the time of testing. Finally, all participants confirmed they were not taking part in any other study and agreed to use a reliable form of contraception during and 3-months following participation to mitigate the risk of fetal cannabinoid exposure (Wu, 2011). Participants were instructed to continue their typical exercise regime throughout the experimental period and instructed to report any changes or injuries to the lead researcher. Participants were invited to provide written informed consent and thereafter completed health screening and readiness to exercise questionnaires, and if deemed fit to participate, participants were included in the study.

7.3.2 Protocol

Participants arrived at ~8:00am for visit 1 (Figure 7.1) following an overnight fast. Here, they received an information sheet and completed the Physical Activity Readiness Questionnaire (PAR-Q) form and a health screening questionnaire. Thereafter, stature was measured using a free-standing portable stadiometer (Seca, Hamburg, Germany), and body mass (kg) was assessed using (Seca mBCA 515; Seca, Hamburg, Germany). Thereafter, participants provided samples of venous blood and urine. Peak oxygen consumption was then assessed via a cycle ergometer-based incremental step test.

Finally, participants were familiarised with supplement ingestion and given one 15 mL bottle of their assigned treatment (containing a total of 5350 mg CBD or placebo) (detailed within the treatments section below) to take home. During visit 2 (following 5 weeks of supplementation), participants were given a second 15 mL bottle of their assigned treatment. The treatments were supplied in two separate batches as a safety measure given that the highest acute dose of CBD to have demonstrated tolerability is 6000 mg (Taylor et al., 2018).

Following 10-weeks of supplementation, participants attended the laboratory at ~8:00 am in a fasted state but were encouraged to arrive well-hydrated and having taken their supplement 60-mins before arrival. This visit began with participants providing measures of body mass (kg) in addition to blood and urine samples. Individuals then performed a 90-minute bout of moderate-intensity exercise followed by a 5-min active recovery. Following the recovery, participants provided additional blood and urine samples.

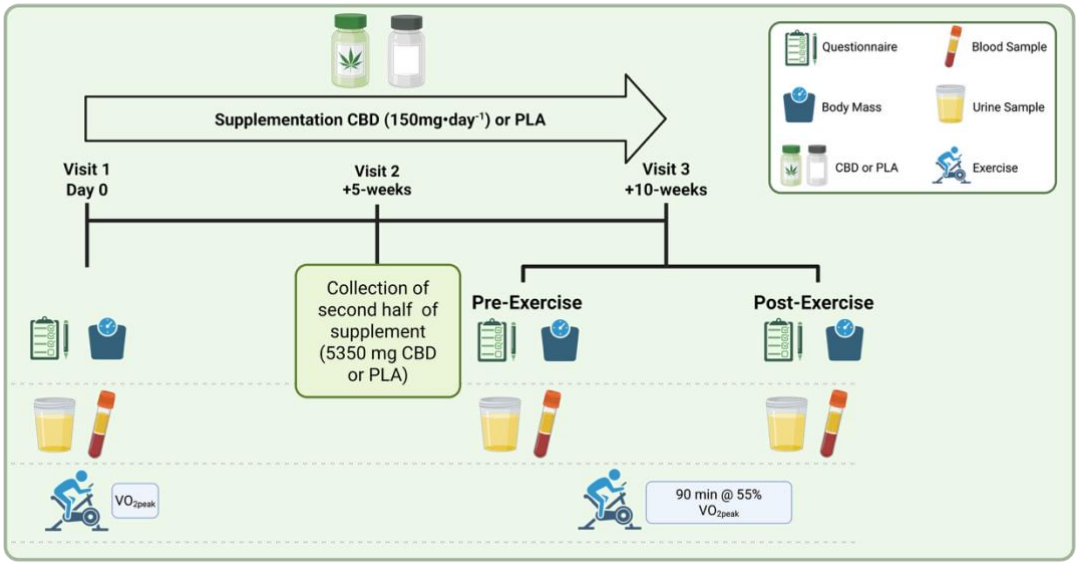

Figure 7.1. Schematic Representation of study procedures. Participants visited the laboratory on three occasions over a 10-week supplementation period. Blood and urinary cannabinoid concentrations were measured at visit 1 (baseline) and visit 3 (pre- and post-exercise).

7.3.3 Blood and urine sampling

Blood was collected into 10 mL pre-treated ethylenediaminetetraacetic acid (EDTA) and serum separator tube (SST) vacutainers (BD Biosciences, NJ, USA). Following collection, samples were inverted 10-times before centrifugation (Eppendorf 5810 R Centrifuge, Eppendorf, Hamburg, Germany) for 15-minutes at 2500 RCF and 4°C. Aliquots (1 mL) of supernatant were then stored at -80°C. Participants collected mid-flow urine samples into pre-labelled, sterile cups. Urine samples were rendered

acellular via 15-min centrifugation at 2500 RCF and ~16°C. Thereafter, 1 mL aliquots were stored at -80°C.

7.3.4 Assessment of Peak Oxygen Consumption ($\dot{V}O_{2peak}$)

VO_{2peak} was assessed using a graded exercise test. All exercise was performed on a cycle ergometer (Lode Corival, Groningen, The Netherlands). Before exercise began, participants were fitted with a chest-strap heart rate monitor (Polar H10; Polar, Kempele, Finland) and an appropriately fitting Hans-Rudolph 7450 facemask (Cortex Medical, Leipzig, Germany), which was connected to a pre-calibrated Cortex 3B metalyzer (Cortex Medical, Leipzig, Germany) for breath-by-breath gas analysis throughout the exercise protocol. Following a submaximal 5-minute warm-up (25 Watts [W] for females; 60 W for males) participants began the step protocol which increased in intensity by 35 W every 3 minutes until participants reached task-failure. In the final 30-seconds of each "step" researchers asked participants to provide a rating of perceived exertion (RPE; 6-20 Borg scale (Borg, Ljunggren and Ceci, 1985)). At the same time as RPE rating, a finger prick capillary blood sample was taken, which was analysed using a Biosen C-line Glucose and Lactate analyser (EKF Diagnostics, Cardiff, UK) for blood lactate concentration assessment.

7.3.5 Treatments

The active and placebo products used in this study were both 100% vegan certified and third-party (Spring Creek Labs, Utah, USA) laboratory tested for cannabinoids, residual solvents, pesticides, heavy metals and microbials. The product was a commercially available, off-the-shelf, oral formulation of CBD. The product came in two dropper bottles containing 15 mL of oil. Independent testing (Supplemental Content) evidenced a CBD concentration of 395.13 mg/g (43.184%), CBG at 8.83 mg/g (0.5955%), CBDV (not reported), with low Δ^9-THC (< 0.00025 % with 0.00025% the limit of detection). The placebo group received a 2 x 15 mL, visually identical dropper bottles of MCT oil. Participants were familiarised with supplement ingestion, which comprised self-administrating 9-drops (16.67 mg·CBD/drop) of their treatment sublingually, waiting for 30-seconds and then swallowing. This dose was elected as it

was like that used in other studies involving CBD and exercise (Cochrane-Snyman et al., 2021; McCartney et al., 2024), in addition to it being considerably below the maximum reported safe dose (Taylor et al., 2018).

Participants were instructed to consume their supplements at the same time (~08:00 am +/- 1 hour) each day for 10 weeks, and to store their supplements in a cool, dry place out of the reach of children. Participants were instructed to consume their supplement without food so to avoid any nutrition-related variability in CBD absorption. In addition, participants were required to inform the lead researcher if they failed to consume a dose and were told explicitly not to double dose the next day. There were no reported missed or double doses of participants who were within the final sample. The final dose of the participants' respective supplement was consumed 60-mins before arrival at the laboratory on the final day of testing.

7.3.6 Blinding

Participants were randomised into two groups, experimental (CBD) or control (PLA). Randomisation was completed using a commercially available random number generator by a staff member who was independent of the study.

7.3.7 Moderate Intensity Exercise Protocol

Before exercise commenced, participants' body mass was assessed as per visit 1. Thereafter, a blood draw was taken via venepuncture of the antecubital vein. Following which, participants provided a mid-stream urine sample. Exercise commenced with a 5-minute warm-up (as per visit 1). Participants then completed a 90-minute bout of moderate-intensity exercise at ~55% of the final wattage achieved during the initial $\dot{V}O_{2peak}$ protocol. Breath-by-breath indirect calorimetry was performed throughout; with average heart rate (beats·min$^{-1)}$, and respiratory exchange ratio (RER) calculated over 10-minute periods throughout exercise. Perceived exertion (RPE [Borg Scale; 6-20]) and blood lactate (BLa) concentrations (mmol·L^{1}) were also collected in the final 30-seconds of each 10-minute period during exercise. Upon completion of the exercise protocol participants repeated the pre-

exercise measures (body mass, urine sample and blood draws), which were all completed within 30-minutes of exercise cessation.

7.3.8 Biological Samples

Plasma Cannabinoids

Plasma cannabinoid concentrations were measured using ultra-high performance liquid chromatography-tandem mass spectrometry (UHPLC-MS/MS) and previously validated methods (Kevin et al., 2021). Briefly, samples underwent protein precipitation followed by supported liquid extraction. Gradient mode LC-MS/MS was then used to separate and quantify the target analytes. All samples were analysed in triplicate, with those derived from the same participant analysed on the same plate.

Urinary Cannabinoids

Reagents

Cannabinoid standards and deuterated internal standards: THC, THC-d3, CBD, CBD-d3, CBD, CBDV, 11-OH-THC, 11-OH-THC-d3, THC-COOH, THC-COOH-d9, THC-COOH-Glucuronide, and THC-COOH-Glucuronide-d3 were obtained from Cerilliant (Round Rock, TX, USA). 6-OH-CBD, 7-OH-CBD, 7-COOH-CBD, 6-OH-CBD-d9, 7-OH-CBD-d10, 7COOH-CBD-d10 were obtained from BDG Synthesis (Wellington, New Zealand). LCMS grade methanol, acetonitrile, n-hexane, aqueous ammonia, anhydrous sodium acetate, glacial acetic acid and formic acid were acquired from Fisher Scientific (Melbourne, VIC, Australia); and Kura Biotech, BG100 red abalone b-glucuronidase from PM Separations (Capalaba, QLD, Australia). All chemicals and solvents were at least HPLC or LCMS grade, respectively.

Sample Preparation

Urine samples were first thawed and 50 µL from each collected sample was transferred into a glass-lined 96-well plate. Thereafter, the calibrator and quality control (QC) samples were prepared by spiking the cannabinoid-free “blank”, to reach a maximum volume of 5 µL. All samples were then spiked with internal standard solutions and 5 µL MeOH was added to all study samples.

Hydrolysis

The sample pH was first adjusted to 4.5-5.0 by adding 200 µL of 0.1M acetate buffer (pH 4.4), and this was briefly vortexed. Thereafter 50 µL of β-glucuronidase (5000U; BG100, Kura Biotech) was added and vortexed for 2 minutes. This solution was then incubated at 65°C for 30 min. The sample pH was finally adjusted to 2.5-3.0 via the addition of 10 µL formic acid, and briefly vortexed.

Supported Liquid Extraction (SLE)

Samples were immediately transferred onto a 400 µL SLE 96-well- plate (Biotage ISOLUTE® SLE+). A brief nitrogen push was then performed, and the solution was then left to equilibrate for 5-min at room temperature. Analytes were then transferred into a fresh glass-lines 96-well-plate via a two-step method. First, 700 µL/sample Dichloromethane was added and allowed to flow under gravity for 5 min followed by a nitrogen gas push of 0.5 bar for 30 seconds. Methyl tert-butyl ether (900 µL/sample) was then added and again allowed to flow under gravity for 5 min followed by a nitrogen gas push of 0.5 bar for 120 seconds. A final push of 5 bars of nitrogen was then applied for 120 seconds. This eluate was then evaporated under a gentle stream of nitrogen for 45 mins. Samples were then reconstituted in their initial LCMS-MS mobile phase condition of 60% Mobile phase B (MeOH) and 40% Mobile phase A (0.1% Forminc Acid [FA] water) in two-steps, to a total volume of 100 µL, as follows: To a blank well containing internal standard only, 60 µL of MeOH containing 11-COOH-THC-Glucuronide and 11-COOH-THC-Glucuronide-d3 and 40 µL of 0.1% Formic Acid in water was added to reach 500 $ng{\cdot}ml^{-1}$of 11-COOH-THC-Glucuronide and 50 $ng{\cdot}ml^{-1}$ final concentration. To all proceeding wells 60µl MeOH was added, followed by 40 µL 0.1% FA water, and vortexed for 5 minutes, before the plate was sealed for immediate analysis.

7.3.9 Statistical Analysis

The plasma and urine cannabinoid concentrations of the intervention (i.e., CBD) group were analysed using One-way repeated measures ANOVA that included time

(baseline, pre-exercise, post-exercise). The PLA groups plasma and urine data were not formally statistically analysed as these were only ever intended to verify abstinence from external cannabis/CBD use. Statistical significance was defined as $p < 0.05$. Data are presented as means ± SD with 95% confidence intervals (CI). Statistical analysis was performed in IBM SPSS Statistics for Windows (Version 30.0.0.0; Armonk, New York, USA) and figures were prepared in GraphPad Prism V.9 for Macintosh (GraphPad Software, San Diego, California, USA).

Sample Size

For a moderate effect size ($f = 0.25$), for one group and three measurements, and for an alpha level of 0.05 and power of 0.8, a sample size of 28 participants was calculated (Faul et al., 2007). To account for dropout, 31 participants were recruited in the CBD group, with 5 participants in the PLA group. The unbalanced design was chosen to maximise the analysis of cannabinoids and their metabolites following supplementation and exercise. This is common when assessing the presence, distribution, metabolism or excretion of a compound, including its metabolites because only those exposed to the active compound will exhibit the measurable analytes making it both ethically and scientifically justifiable.

7.4 Results

Thirty-six healthy and physically active males (n = 17) and females (n = 19) (mean ± SD: age: 27 ± 6 years; stature: 171.9 ± 10.4 cm; body mass: 75.69 ± 16.82 kg; body fat: 25.00 ± 6.88 %; VO_{2peak}: 39.2 ± 8 ml/kg/min) were recruited between 12.10.2021 and 04.11.2023. Participants were recreationally active and were advised to continue their typical regime for the entirety of the experimental period. All 36 participants were randomised, completed the 10-week supplementation period and were included in the final analytical sample. The final analytical sample included the CBD group only (n = 31; 15 males, 16 females).

Blinding

Upon completion of the study, participants were asked which group (CBD/PLA) they believed they were in. Twelve of the 36 (33%) participants correctly identified their assigned treatment condition.

Cannabinoid Responses to Supplementation

No phytocannabinoids were present in either urine or plasma at baseline in either the CBD or PLA groups. Therefore, statistical analyses reported herein are comparisons of cannabinoid metabolites following 10-weeks of supplementation (pre-exercise) and post-exercise. In addition, 6-OH-CBD was not detectable in any plasma sample. Δ^9-THC, 11-OH-THC and 11-COOH-THC were not detected in any urine or plasma samples (i.e., from either group) at any time during the study. All other cannabinoids and their metabolites were observed in plasma or urine in the CBD group, as described in the following sections.

Table 7.1. Participants (n = 36) physical responses to moderate intensity exercise bout

Variable	Group	CBD (n = 31)	PLA (n = 5)
HR ($b \cdot min^{-1}$)	Male	132 ± 18 (95% CI, 129.48-135.32)	125 ± 21 (95% CI, 114.96 – 134.54)
	Female	136 ± 24 (95% CI, 132.40-1439.77)	125 ± 21 (95% CI, 126.88 – 143.95)
BLa ($mmol \cdot l^{-1}$)	Male	3.20 ± 1.87 (95% CI, 2.77 – 3.63)	3.88 ± 2.80 (95% CI, 1.88 – 5.88)
	Female	2.30 ± 1.25 (95% CI, 2.03 – 2.57)	2.81 ± 0.35 (95% CI, 2.61 – 3.02)
RER	Male	0.92 ± 0.05 (95% CI, 0.91 -0.93)	0.90 ± 0.05 (95% CI, 0.88 - 0.92)
	Female	0.91 ± 0.05 (95% CI, 0.90-0.91)	0.92 ± 0.05 (95% CI, 0.90-0.94)
VO2 ($L.min^{-1}$)	Male	2.06 ± 0.52 (95% CI, 1.97 – 2.14)	2.36 ± 0.47 95% CI, 2.14 – 2.58)
	Female	1.38 ± 0.35 95% CI, 1.32 – 1.43)	1.12 ± 0.21 (95% CI, 1.01-1.20)
RPE (AU; 6-20)	Male	12.26 ± 2.52 (95% CI, 11.86 – 12.67)	11.85 ± 2.50 (95% CI, 10.68 – 13.02)
	Female	11.93 ± 2.39 (95% CI, 11.55 – 12.30)	15.53 ± 2.91 (95% CI, 12.45 – 1.62)
Pre Exercise Body Mass (kg)	Male	87.66 ± 16.10 (95% CI, 78.12 – 97.19)	86.1 ± 13.55 (95% CI, -86.07-258.27)
	Female	65.06 ± 6.84 (95% CI, 61.14 – 68.98)	67.82 ± 6.29 (95% CI, 48.69 – 86.94)
Post Exercise Body Mass (kg)	Male	86.37 ± 16.82 (95% CI, 78.12 – 97.19)	85.63 ± 16.63 (95% CI, -87.5 – 258.75)
	Female	64.64 ± 6.87 (95% CI, 60.70 – 68.58)	67.35 ± 6.15 (95% CI, 48.64 – 86.06)

Plasma Cannabinoids

There was a significant effect of time on CBD ($F_{4.501}$, P = 0.043) indicating both groups showed a significant increase in this metabolite following exercise (Figure 2A). There was no significant effect of sex ($F_{.000}$, P = 0.983). There was a significant effect of time on 7-OH-CBD ($F_{11.919}$, P = 0.002) indicating both groups showed a significant increase in this metabolite following exercise (Figure 2B). There was no significant effect of sex ($F_{.314}$, P = 0.579). There was a significant effect of time on 7-OH-CBD ($F_{4.542}$, P = 0.042) indicating both groups showed a significant increase in this metabolite following exercise (Figure 2C). There was no significant effect of sex ($F_{.244}$, P = 0.625).

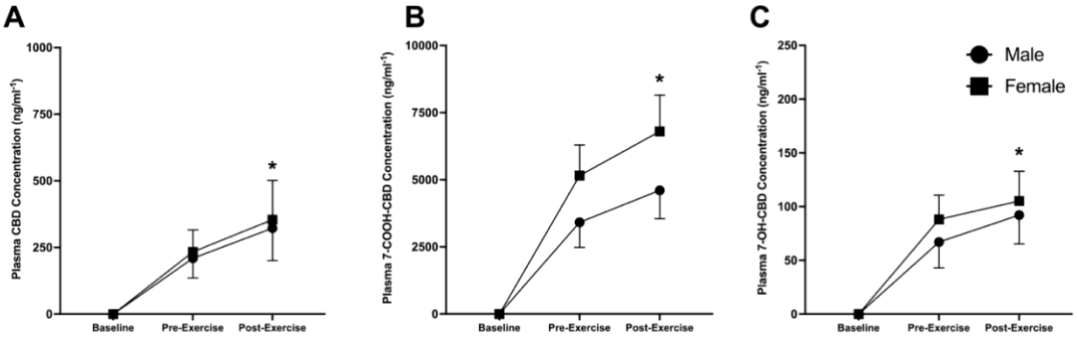

Figure 7.2. Plasma concentrations of A) CBD; B) 7-COOH-CBD; C) 7-OH-CBD at baseline, pre- exercise (10-weeks) and post-exercise (10-weeks) in the CBD group for males and females (n = 31). * Denotes a significant difference between pre - and post-exercise (P < 0.05). Values are expressed as mean ± SD.

Table 7.2. Plasma concentrations of cannabinoids and relevant metabolites CBD group (n = 31) and PLA group (n = 5) across each timepoint.

Metabolite	Condition	Male			Female		
		Baseline	Pre-Exercise	Post-Exercise	Baseline	Pre-Exercise	Post-Exercise
7-COOH-CBD	CBD	0.00 ± 0.00	3415.84 ± 3624.99 (95% CI, 1408.39 – 5423.29)	4604.46 ± 4100.90 (95% CI, 2333.45 – 6875.46)	0.00 ± 0.00	5154.71 ± 4555.66 (95% CI, 2727.18 – 7582.25)	6804.23 ± 5399.08 (95% CI, 3927.26 – 9681.20)
	PLA	0.00 ± 0.00	0.00 ± 0.00	0.00 ± 0.00	0.00 ± 0.00	0.00 ± 0.00	0.00 ± 0.00
7-OH-CBD	CBD	0.00 ± 0.00	66.98 ± 93.10 (95% CI, 15.42 – 118.53)	92.14 ± 103.85 (95% CI, 34.63 – 149.66)	0.00 ± 0.00	88.06 ± 90.68 (95% CI, 39.73 – 136.38)	105.19 ± 110.54 (95% CI, 46.29 – 164.09)
	PLA	0.00 ± 0.00	0.00 ± 0.00	0.00 ± 0.00	0.00 ± 0.00	0.00 ± 0.00	0.00 ± 0.00
CBD	CBD	0.00 ± 0.00	209.56 ± 2285.63 (95% CI, 51.38 – 118.53)	322.28 ± 470.10 (95% CI, 61.95 – 582.62)	0.00 ± 0.00	233.39 ± 331.88 (95% CI, 56.54 - 410.23)	354.50 ± 588.90 (95% CI, 40.70 – 668.30)
	PLA	0.00 ± 0.00	0.00 ± 0.00	0.00 ± 0.00	0.00 ± 0.00	0.00 ± 0.00	0.00 ± 0.00

Urinary Cannabinoids

There was a significant effect of time on CBD ($F_{4.501}$, P = 0.043) indicating both groups showed a significant increase in this metabolite following exercise (Figure 3A). There was no significant effect of sex ($F_{.000}$, P = 0.983). There was a significant effect of time on CBDV ($F_{5.008}$, P = 0.033) indicating both groups showed a significant increase in this metabolite following exercise (Figure 3B). There was no significant effect of sex ($F_{.198}$, P = 0.659). There was a significant effect of time on CBG ($F_{5.754}$, P = 0.023) indicating both groups showed a significant increase in this metabolite following exercise (Figure 3C). There was no significant effect of sex ($F_{.339}$, P = 0.565). There was a significant effect of time on 6-OH-CBD ($F_{8.626}$, P = 0.006) indicating both groups showed a significant increase in this metabolite following exercise (Figure 3D). There was no significant effect of sex ($F_{.002}$, P = 0.966). There was no significant effect of time on 7-COOH-CBD ($F_{2.458}$, P = 0.128) indicating neither group showed a significant increase in this metabolite following exercise (Figure 3E). There was no significant effect of sex ($F_{.154}$, P = 0.698). There was however a significant effect of time on 7-OH-CBD ($F_{7.510}$, P = 0.010) indicating both groups showed a significant increase in this metabolite following exercise (Figure 3F). There was no significant effect of sex ($F_{.239}$, P = 0.629).

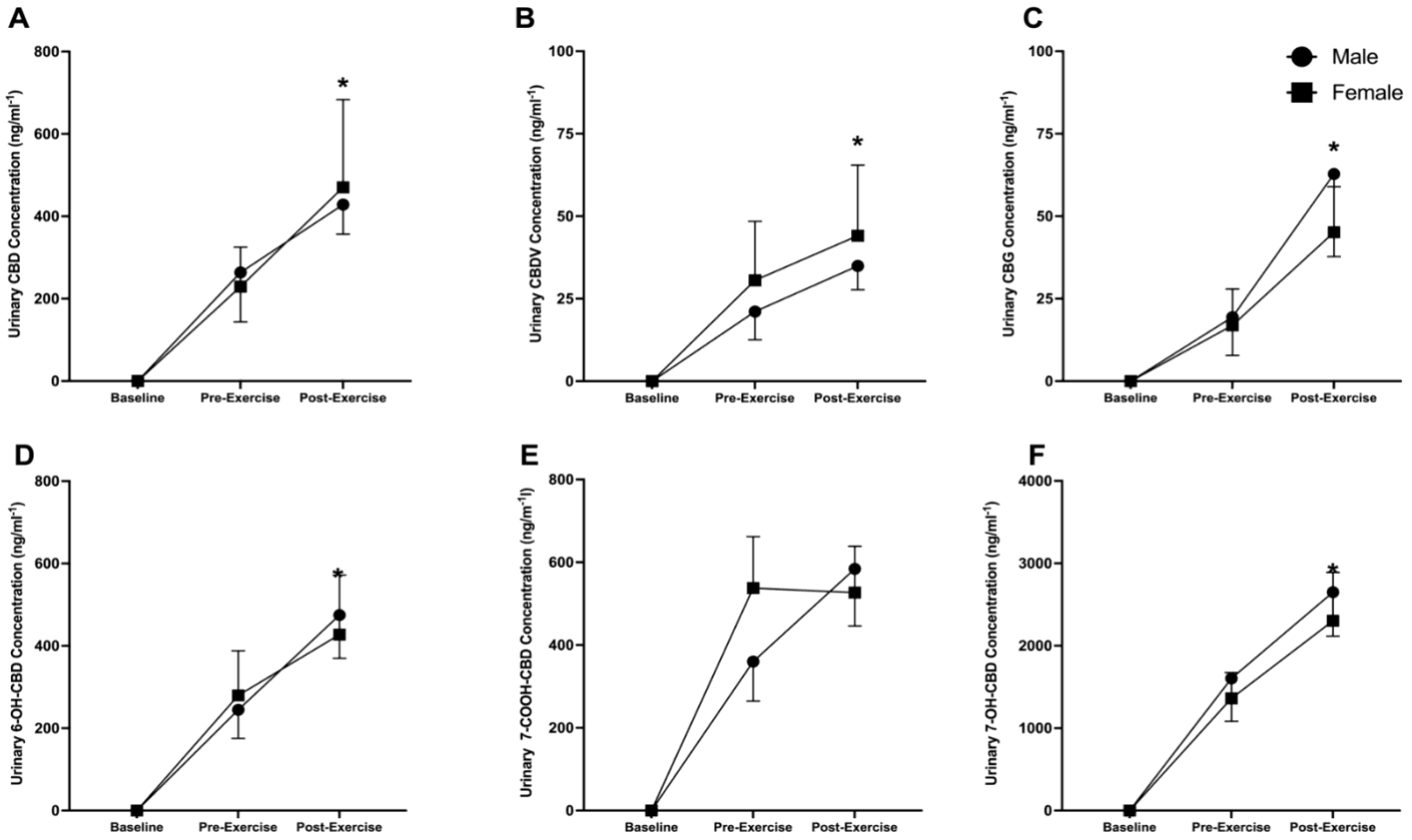

Figure 7.3. Urinary concentrations of A) CBD; B) CBDV; C) CBDG; D) 6-OH-CBD; E) 7-COOH-CBD; F) 7-OH-CBD at baseline, pre-exercise (10-weeks) and post-exercise (10-weeks) for males and females in the CBD group (n = 31). * Denotes a significant difference between pre - and post-exercise ($P < 0.05$). Values are expressed as mean ± SD.

Table 7.3. Urinary concentrations of cannabinoids and relevant metabolites CBD group (n = 31) and PLA group (n = 5) across each timepoint

Metabolite	Condition	Male			Female		
		Baseline	Pre-Exercise	Post-Exercise	Baseline	Pre-Exercise	Post-Exercise
6-OH-CBD	CBD	0.00 ± 0.00	244.87 ± 269 (95% CI, 95.9 – 393.83)	474.76 ± 407.05 (95% CI, 249.35 – 700.18)	0.00 ± 0.00	279.64 ± 433.67 (95% CI, 48.55 – 510.72)	427.44 ± 578.02 (95% CI, 119.44 – 735.45)
	PLA	0.00 ± 0.00	0.00 ± 0.00	0.00 ± 0.00	0.00 ± 0.00	0.00 ± 0.00	0.00 ± 0.00
7-COOH-CBD	CBD	0.00 ± 0.00	359.99 ± 370.11 (95% CI, 155.03 – 564.95)	583.94 ± 546.03 (95% CI, 287.10 – 880.78)	0.00 ± 0.00	537.66 ± 497.62 (95% CI, 272.49 – 802.82)	526.83 ± 447.90 (95% CI, 288.16 – 765.49)
	PLA	0.00 ± 0.00	0.00 ± 0.00	0.00 ± 0.00	0.00 ± 0.00	0.00 ± 0.00	0.00 ± 0.00
7-OH-CBD	CBD	0.00 ± 0.00	603.36 ± 2009.42 (95% CI, 490.58 – 2716.14)	2650.34 ± 2073.74 (95% CI, 1501.94 - 3798.74)	0.00 ± 0.00	1360.56 ± 1258.79 (95% CI, 6893.80 – 2031.32)	2302.39 ± 2344.68 (95% CI, 1053.00 - 3551.78)
	PLA	0.00 ± 0.00	0.00 ± 0.00	0.00 ± 0.00	0.00 ± 0.00	0.00 ± 0.00	0.00 ± 0.00
CBD	CBD	0.00 ± 0.00	263.88 ± 465.55 (95% CI, 6.07 – 521.69)	428.48 ± 278.35 (95% CI, 274.33 – 582.62)	0.00 ± 0.00	229.41 ± 383.95 (95% CI, 24.82 – 434.00)	470.26 ± 853.20 (95% CI, 15.62 - 924.90)
	PLA	0.00 ± 0.00	0.00 ± 0.00	0.00 ± 0.00	0.00 ± 0.00	0.00 ± 0.00	0.00 ± 0.00
CBG	CBD	0.00 ± 0.00	19.42 ± 45.01 (95% CI, -5.5 - 44.35)	62.80 ± 96.92 (95% CI, 9.13 – 116.48)	0.00 ± 0.00	16.91 ± 44.16 (95% CI, -6.62 – 40.44)	45.14 ± 55.24 (95% CI, 15.7 – 74.57)
	PLA	0.00 ± 0.00	0.00 ± 0.00	0.00 ± 0.00	0.00 ± 0.00	0.00 ± 0.00	0.00 ± 0.00
CBDV	CBD	0.00 ± 0.00	21.09 ± 33.07 (95% CI, 2.78 – 39.41)	34.95 ± 27.88 (95% CI, 19.51 – 50.39)	0.00 ± 0.00	30.58 ± 71.38 (95% CI, -7.46 – 68.61)	44.08 ± 85.71 (95% CI, -1.6 – 89.75)
	PLA	0.00 ± 0.00	0.00 ± 0.00	0.00 ± 0.00	0.00 ± 0.00	0.00 ± 0.00	0.00 ± 0.00

7.5 Discussion

This study measured plasma and urinary concentrations of three cannabinoids and three of their metabolites following 10-weeks of supplementation with 150 mg per day of a broad-spectrum CBD product. The secondary aim of this investigation was to identify whether cannabinoid concentrations might be magnified by a combination of fasting and moderate-intensity exercise on the assumption that cannabinoids may accumulate in adipose tissue and be liberated by the lipolytic stimulus of fasted exercise. This study demonstrates that 10-weeks of daily supplementation with 150 mg per day of an orally consumed broad-spectrum CBD product significantly increased various cannabinoid metabolite concentrations in plasma and urine, except for those associated with Δ^9-THC. The present study also explains that fasted, moderate-intensity exercise significantly increases urinary concentrations of WADA prohibited cannabinoids including CBG and CBDV. Further data presented herein is that there is seemingly no effect of biological sex on any of the cannabinoids or their metabolites measured in this study.

This is the first study to illustrate the significant anti-doping risks for athletes supplementing with an off-the-shelf CBD product. These data indicate conclusively that if an athlete were to consume a broad-spectrum CBD supplement, they are at risk of an adverse analytical finding (Ten Haaf et al., 2020). Importantly, the risk is not due to Δ^9-THC (at least, in the context of this broad-spectrum CBD product) but instead attributed to “minor” cannabinoids such as CBG and CBDV. This risk is elevated significantly by exercise as there are clear increases in urinary concentrations of these prohibited minor cannabinoids. Collectively, these data highlight the potential anti-doping risks for athletes using broad spectrum CBD products and a need for clarity and education from athlete and WADA perspectives, respectively.

The pharmacokinetics and sequestration of cannabinoids have been a topic of debate for some time (Grotenhermen, 2003; Odell et al., 2015), yet few studies have characterised the accumulation of cannabinoids over an extended period in healthy

individuals. Upon ingestion, CBD undergoes phase I metabolism, which primarily occurs via hydroxylation and subsequent carboxylation by liver cytochrome P450 enzymes (Jiang et al., 2011). These processes give rise to several metabolites, namely, 6-OH-CBD, 7-OH-CBD, 7-COOH-CBD (Austin et al., 2024). The dataset presented herein is consistent with the work of others, who show that 7-COOH-CBD can be observed in significantly greater concentrations than CBD, 6-OH-CBD and 7-OH-CBD, which might make this metabolite a more appropriate method of monitoring peak cannabinoid concentrations (Kevin et al., 2017).

Regarding sequestration, little is known regarding the effects of exercise and/or fasting on cannabinoid concentrations. In rats, lipolysis has been suggested to stimulate the release of cannabinoids from adipose tissue. The authors speculated that the animals in their study could re-intoxicate with Δ^9-THC (Gunasekaran et al., 2009). In humans, it has been reported that exercise increased plasma concentrations of Δ^9-THC following 35-minutes of aerobic exercise in some non-fasted regular cannabis users. However, fasting for 12-hours (independent of moderate-intensity exercise) did not significantly increase plasma Δ^9-THC or THC-COOH (Wong et al., 2013). It might be postulated that the lipolytic effect of moderate-intensity exercise can significantly affect cannabinoid release from adipose tissue. These data support the conclusions of these studies and indicate that participants in the experimental group had significantly greater post-exercise urinary concentrations of various cannabinoids and their metabolites compared to those evidenced before exercise commenced.

A further consideration within this study was the potential impact of sex. Previous work has illustrated that female participants may show a different response to supplementation due to generally higher body fat percentage and likelihood of sequestration, coupled with sex differences in CYP enzyme activity. CBD is metabolized primarily by CYP3A4, CYP2C19, and CYP2C9 (Zendulka et al., 2016; Ujváry & Hanuš, 2016). CYP3A4 activity is typically higher in females (Wolbold et al., 2003), which may lead to faster metabolism and increased production of certain CBD metabolites. Other enzymes like CYP2C19 and CYP2C9 may exhibit more variable or

male-biased activity, contributing to sex-specific differences in metabolite profiles (Anderson, 2005; Zanger & Schwab, 2013). However, this study failed to observe any sex differences in any of the detectable cannabinoids or their metabolites in the present study.

Perhaps most notable in this investigation were the findings associated with minor cannabinoids, which are considered non-threshold substances by WADA. Despite their relatively low concentrations within the formulation, CBG (8.83 $mg \cdot g^{-1}$; 0.5955%) and CBDV (not-reported on CoA) compared to CBD (395.13 $mg \cdot g^{-1}$; 43.1840%), both were present in detectable concentrations in urine. Specifically, urinary concentrations of CBG were present in 42% of pre-exercise samples (18 ± 44 $ng.ml^{-1}$) and 74% of post-exercise samples (54 ± 77 $ng \cdot ml^{-1}$). Similarly, urinary concentrations of CBDV were present in 68% of pre-exercise samples (26 ± 55 $ng \cdot ml^{-1}$) and 84% of post-exercise samples (10 ± 63 $ng \cdot ml^{-1}$).

It is also important to consider the half-lives of orally consumed cannabinoids. For example, recent reports have suggested that the half-life of CBD in humans might be >134 hours (Kolli and Hoeng, 2025). Similarly, it has been reported that Δ^9-THC has a dynamic pharmacokinetic profile, with a terminal half-life of ~72-96 hours (Huestis, 2007). However, this data indicates that given Δ^9-THC within the supplement used was <0.00025%, neither Δ^9-THC nor its metabolites were detectable. There is however a paucity of data on the pharmacokinetics of CBG and/or CBDV in humans. Despite the detection of these cannabinoids within this dataset half-life was not directly assessed and therefore future studies could seek to address this.

Limitations

While this study might be considered strong and impactful, it is not without its limitations. Firstly, it should be acknowledged that the observed pre- to post-exercise increases in cannabinoid metabolites may not be attributable to exercise alone, as participants administered CBD on the morning of testing and, given inter-individual variability in metabolism, this contribution cannot be discounted. In addition, the CBD

supplement provided was self-administered. Though participants were familiarised with correct supplement ingestion, adherence was not monitored - although the data indicate that all participants in the CBD group had increased CBD concentrations following 10-weeks of supplementation. Nevertheless, this dataset details substantial between-subject metabolite concentration variability in line with previous reports (Williams et al., 2021). While the participants of this study were instructed to consume their respective supplements 60 mins before presenting at the laboratory, there is marked variability in pre-exercise cannabinoid concentrations. In addition, despite the relatively poor oral bioavailability of cannabinoids, which are as low as 6% in some instances (Perucca and Bialer, 2020; Bar-Hai, Domb and Hoffman, 2022) – this study signals fair detection in all of those examined. However, other variables known to influence cannabinoid pharmacokinetics include the co-administration of food. For example, previous studies have evidenced that high-fat meals can influence CBD pharmacokinetics (Abbotts et al., 2022). As such, it should be acknowledged that overnight fasting may have limited peak plasma concentrations in this study, however this design was necessary to maximise lipolysis during exercise (Vieira et al., 2016). While the number of participants is greater than some other investigations of this kind, a larger pool of participants would be beneficial in future studies. It is also hypothesised that the increase in cannabinoids in plasma and urine following fasted exercise may be due to liberation of these metabolites from adipose tissue. However, it must be acknowledged that this cannot be confirmed absolutely from the current study design. It could be argued that changes in plasma volume following exercise explain the increase concentration of cannabinoids in plasma. However, males in this study had an average loss of body mass of 1.2 kg pre-to post-exercise, whereas females experienced a 260 g loss following exercise, yet there were no sex-differences at baseline or following exercise in any cannabinoid or associated metabolite. Moreover, the magnitude of change in the cannabinoids detected herein following exercise are beyond what would reasonably occur due to such changes in plasma volume. To test this hypothesis, future studies could utilise inhibitors of adipose tissue lipolysis, such as nicotinic acid, to confirm whether the same exercise-induced increases in plasma and urinary cannabinoids and associated metabolites still occur when lipolysis is significantly blunted. Finally, this study used only a single brand of

broad-spectrum CBD. Therefore, results should be treated with caution and independent analysis of other CBD products is advisable.

Conclusion

The data presented herein are the first to demonstrate that consuming a broad-spectrum CBD supplement containing trace amounts of WADA-prohibited cannabinoids results in detectable increases in their presence in urine. In addition, this data provides a novel insight that cannabinoid concentrations are increased following acute moderate-intensity exercise. Neither the presence of cannabinoids in these biological matrices or the response to exercise was affected by biological sex herein. These data add further support to previous recommendations (Chapter 6) that athletes should abstain from the use of CBD supplements until there is either **a**) batch-tested CBD -isolate available confirming the complete absence of all minor cannabinoids or **b**) WADA policy regarding cannabinoids is changed and minor cannabinoids are considered threshold substances like Δ^9-THC, or specific cannabinoids are named as prohibited rather than naming the CBD as the only cannabinoid not prohibited.

8 Thesis Synthesis

This Chapter provides an appraisal of the thesis aims and if they have been realised during the completion of this body of work. Thereafter, the limitations of each chapter are discussed and finally, recommendations for future research avenues are explored.

8.1 Realisation of Aims

This thesis set out to address four interlinked aims, each contributing to a broader understanding of the potential effects and applications of CBD in the context of skeletal muscle and sport. The first aim was to determine the impact of dosing on in vitro skeletal muscle, with the goal of identifying a tolerable and mechanistically relevant concentration of broad-spectrum CBD. This foundational work informed the second aim: to explore, in the cellular mechanisms by which broad-spectrum CBD and synthetic, isolated CBD may exert distinct effects on muscle tissue. Building on these mechanistic insights, the third aim investigated the potential utility of CBD in modulating physiological responses to aerobic exercise. Finally, the fourth aim addressed regulatory and practical concerns by examining the potential accumulation of CBD and related cannabinoids in blood and urine, holding relevance for anti-doping policies and athlete safety.

Rather than reiterating each empirical chapter in isolation, this synthesis integrates findings across the four studies to address a central question: what is the likely balance of benefit and risk associated with CBD use in sport when considering mechanistic plausibility, human performance outcomes, and anti-doping implications? Across this body of work, three general conclusions have emerged: (i) CBD's interaction with skeletal muscle appears to be exposure- and formulation-dependent; (ii) under the conditions tested, these mechanistic signals did not translate into a meaningful ergogenic effect; and (iii) the dominant issue within sport is currently safety and regulation, driven by product composition variability and the potential appearance of non-declared cannabinoids in biological matrices.

8.2 Research Theme 1: CBD and its Effects During Skeletal Muscle Exposure

A key contribution of this thesis is that CBD-related responses in skeletal muscle models appear to be shaped by two interacting determinants: dosing and formulation composition. This matters because the applied discourse around CBD in sport often treats "CBD" as a single, simple entity, despite substantial variability in product

composition and consumer pharmacokinetics. Across the in vitro investigations presented herein, acute exposure to broad-spectrum CBD indicated a practical boundary for tolerability. More specifically, lower concentrations did not alter myoblast proliferation, whereas higher doses produced reductions in metabolic activity and stage-specific cytotoxicity, with increased cell death observed in myoblasts. These data support the concept of a threshold effect, in which cellular stress responses might dominate beyond a given exposure range, and additionally suggest stage-dependent sensitivity during myogenesis.

The transcriptomic investigation revealed that broad-spectrum CBD elicited a broader gene expression signature than synthetic CBD. The considerably different observations within the broad-spectrum formulation supports the notion of formulation-specific biological activity. Importantly, the resulting publicly available dataset (GEO accession GSE272113) provides a platform for hypothesis generation and cross-study comparison and represents a resource enabling future discovery in a field currently limited by mechanistic data in muscle-relevant systems.

Taken together, Chapters 4 and 5 indicate that CBD's effects on skeletal muscle cannot be interpreted solely through the lens of "CBD dose" or "CBD presence", but instead through both exposure and formulation. The dose-response data define a boundary for tolerability within a model of myogenesis, while the transcriptomic data evidence that product composition may alter biological signalling. The mechanistic findings do not support a simple, generalisable recommendation that CBD is uniformly beneficial for skeletal muscle. Instead, they indicate that (i) claims of muscle-related benefits should be interpreted cautiously without evidence of physiologically relevant exposure, and (ii) practitioners should treat CBD products as distinct supplements across formulations rather than in an interchangeable manner. This therefore suggests a message of caution to athletes and support personnel, in which any education should be founded on formulation variability and limited translational evidence for muscle-specific claims. Taken together, it is important to consider that mechanistic modulation *in vitro* does not necessarily predict functional outcomes at the whole-body level. Therefore, the next step was to examine whether these

formulation and exposure-dependent signals translated into measurable changes in aerobic exercise performance in humans.

8.3 Research Theme 2: Mechanistic plausibility did not translate into an ergogenic effect under the tested conditions

Despite mechanistic rationale and claims that CBD can influence exercise experience (e.g., pain perception and enjoyment), the present human study provided limited evidence for any ergogenic effect. This finding is important because the general narrative surrounding CBD in sport has frequently implied performance benefits that have not yet been robustly demonstrated. Within the translational progression, Chapter 5 investigated whether three-weeks of broad-spectrum CBD supplementation could influence perceived exertion and subsequently improve aerobic performance. Under the conditions tested, no clear performance-enhancing effects were observed.

When considered alongside the mechanistic programme, the simplest explanation is not that CBD has no biological activity, but that any muscle-relevant signalling observed in vitro does not straightforwardly translate into measurable aerobic performance changes within the exercise-modality tested. This highlights the translational gap between cellular signals and whole-body outcomes, reinforcing the importance of bioavailability and various other factors including participant training status, exercise modality, dose and product composition) when interpreting applied claims. Given that this chapter did not demonstrate an ergogenic benefit, the justification for CBD use in performance environments is reduced, particularly when considering the regulatory considerations identified later in this thesis. Accordingly, practitioner education should emphasise that current evidence does not support CBD as an ergogenic supplement, and that athletes should be cautious when engaging with any anecdotal reports. Given the absence of an ergogenic signal under the tested conditions, the applied rationale for CBD use in WADA-governed sport becomes primarily a question of safety and regulatory risk, which was addressed in the final empirical study of this thesis.

8.4 Research Theme 3: The dominant applied issue in sport is safety and regulation, rather than performance

The most immediate applied contribution of this thesis concerns athlete safety and anti-doping risk. Chapter 7 investigated whether chronic broad-spectrum CBD supplementation could lead to detectable cannabinoids in biological matrices. This addresses a critical gap - while label discrepancies are generally well-established, the implication for athletes subject to doping control has been previously not been characterised.

Across ten weeks, Δ^9-THC and its metabolites were not detected, despite trace Δ9-THC being present in the product. However, CBD, CBG, and CBDV were detected in urine, which was especially concerning in the case of CBDV as this cannabinoid was not declared in the product CoA. This provides empirical support for a key applied concern: broad-spectrum CBD products may contain undeclared cannabinoids that accumulate sufficiently to be detectable, creating a plausible anti-doping and professional risk even when Δ^9-THC is not detected.

When synthesised with the earlier mechanistic and performance findings, the applied risk-benefit balance begins to become clearer. This thesis provides limited support for performance enhancement, while simultaneously demonstrating that broad-spectrum products can yield detectable non-declared cannabinoids in biological matrices. In WADA-governed environments, where cannabinoids other than CBD remain prohibited, this shifts the applied discourse away from efficacy and towards risk management, product verification, and education.

Applied implications for sport practice. The findings support three practical implications that should be central to athlete support systems:

- Athletes should abstain from using broad-spectrum CBD supplements, particularly when subject to doping control, due to the potential appearance of non-declared cannabinoids in biological matrices.

- Practitioners should prioritise education on supplement risk, cannabinoid regulation, and the limitations of current efficacy evidence.
- Education strategies should explicitly address the legal, pharmacological, and regulatory complexities of CBD products, including formulation variability and the distinction between CBD and other cannabinoids.

8.5 Future research priorities

Across the three themes of research, there are some recommendations for future work. These should consider each theme in a clear and systematic manner. To begin, further mechanistic work should prioritise: (i) quantification of tissue-specific CBD concentrations in vivo to inform physiologically relevant in vitro dosing; (ii) primary human and 3D muscle models; (iii) targeted validation of key pathways using pharmacological or genetic manipulation; (iv) integrated multiomic approaches; and (v) systematic comparison of full-spectrum, broad-spectrum, isolated and synthetic products to establish formulation-dependent effects. Regarding applied investigations considering exercise, future work should consider including larger cohorts, incorporate a broader battery of exercise modalities and intensities, and quantify psychophysiological factors such as affect and perceived pain in addition to performance, with concurrent verification of exposure via biological sampling. Finally, with regards to regulation and safety, future work might seek to investigate multi-brand and multi-batch testing cannabinoid testing. In addition, dose-response and time course kinetics under fed and fasted conditions (including post-exercise) might provide a more holistic view on this topic. Furthermore, the creation of clear guidelines for athletes and practitioners focused on risk communication and decision support should be considered.

8.6 Implications for Anti-Doping Regulation and Applied Decision Making

This thesis set out to inform practice regarding supplement safety and development in sport. In doing so, it provides evidence that the practical implications of CBD use in elite sport are best framed through a risk-benefit lens. Despite the removal of CBD

from WADA's prohibited list, all other cannabinoids remain prohibited. The findings presented herein demonstrate that broad-spectrum CBD supplements can result in detectable concentrations of prohibited cannabinoids in biological matrices, including compounds not declared on product CoA's. Therefore, even when Δ^9-THC risk appears minimal within specific products and conditions, the potential detection of other cannabinoids magnifies concerns relating to product transparency, athlete safety, and regulatory oversight.

A final synthesis of this body of work, indicates that broad-spectrum CBD supplementation is unlikely to enhance aerobic performance under the conditions tested, while posing a credible anti-doping and professional risk due to formulation variability and cannabinoid accumulation. Consequently, the most defensible applied position for WADA-governed sport is a precautionary approach underpinned by education, risk communication, and product verification strategies.

9 References

Aagaard, P., Simonsen, E.B., Andersen, J.L., Magnusson, P. and Dyhre-Poulsen, P. (2002) Increased rate of force development and neural drive of human skeletal muscle following resistance training. *Journal of Applied Physiology*, 93 (4), 1318-1326.

Abbotts, K.S.S., Ewell, T.R., Butterklee, H.M., Bomar, M.C., Akagi, N., Dooley, G.P. and Bell, C. (2022) Cannabidiol and cannabidiol metabolites: pharmacokinetics, interaction with food, and influence on liver function. *Nutrients*, 14 (10), 2152.

Abernethy, A. (2019) Hemp production and the 2018 farm bill. *US Food and Drug Administration*.

Adams, R., Hunt, M. and Clark, J. (1940) Structure of cannabidiol, a product isolated from the marihuana extract of Minnesota wild hemp. I. *Journal of the American Chemical Society*, 62 (1), 196-200.

Adams, R., Pease, D. and Clark, J. (1940) Isolation of cannabinol, cannabidiol and quebrachitol from red oil of Minnesota wild hemp. *Journal of the American Chemical Society*, 62 (8), 2194-2196.

Adan, A., Alizada, G., Kiraz, Y., Baran, Y. and Nalbant, A. (2017) Flow cytometry: basic principles and applications. *Critical reviews in biotechnology*, 37 (2), 163-176.

Albert, P.R. (2012) Transcriptional regulation of the 5-HT1A receptor: implications for mental illness. *Philosophical Transactions of the Royal Society B: Biological Sciences*, 367 (1601), 2402-2415.

Alpy, A., Yusuff, G., Simpson, T. and WYGAND, J. (2023) Topical Cannabidiol and the Progression Rate of Delayed Onset Muscle Soreness. *International Journal of Exercise Science*, 16 (3), 1426.

Amada, N., Yamasaki, Y., Williams, C.M. and Whalley, B.J. (2013) Cannabidivarin (CBDV) suppresses pentylenetetrazole (PTZ)-induced increases in epilepsy-related gene expression. *PeerJ*, 1, e214.

Anderson, B.D., Sepulveda, D.E., Nachnani, R., Cortez-Resendiz, A., Coates, M.D., Beckett, A., Bisanz, J.E., Kellogg, J.J. and Raup-Konsavage, W.M. (2024) High cannabigerol hemp extract moderates colitis and modulates the microbiome in an inflammatory bowel disease model. *The Journal of pharmacology and experimental therapeutics*, 390 (3), 331-341.

Anderson, L.L., Udoh, M., Everett-Morgan, D., Heblinski, M., McGregor, I.S., Banister, S.D. and Arnold, J.C. (2022) Olivetolic acid, a cannabinoid precursor in Cannabis sativa, but not CBGA methyl ester exhibits a modest anticonvulsant effect in a mouse model of Dravet syndrome. *Journal of Cannabis Research*, 4, 1-9.

André, R., Gomes, A.P., Pereira-Leite, C., Marques-da-Costa, A., Monteiro Rodrigues, L., Sassano, M., Rijo, P. and Costa, M.d.C. (2024) The entourage effect in cannabis medicinal products: A comprehensive review. *Pharmaceuticals*, 17 (11), 1543.

Arenas-Jal, M., Suñé-Negre, J., Pérez-Lozano, P. and García-Montoya, E. (2020) Trends in the food and sports nutrition industry: A review. *Critical reviews in food science and nutrition*, 60 (14), 2405-2421.

Argueta, D.A., Ventura, C.M., Kiven, S., Sagi, V. and Gupta, K. (2020) A balanced approach for cannabidiol use in chronic pain. *Frontiers in pharmacology*, 11, 561.

Armin, S., Muenster, S., Abood, M. and Benamar, K. (2021) GPR55 in the brain and chronic neuropathic pain. *Behavioural Brain Research*, 406, 113248.

Austin, M., Cairns, P., Conboy, D., Wang, G.X., Moody, T.S., Smyth, M., Wharry, S., Golding, B.T., Henderson, A.P. and Butler, P. (2024) Development and Scale-Up of 7-COOH CBD Synthesis, a Key Cannabinoid Metabolite. *Organic Process Research & Development*.

Aviello, G., Romano, B., Borrelli, F., Capasso, R., Gallo, L., Piscitelli, F., Di Marzo, V. and Izzo, A.A. (2012) Chemopreventive effect of the non-psychotropic phytocannabinoid cannabidiol on experimental colon cancer. *Journal of molecular medicine*, 90, 925-934.

Bar-Hai, A., Domb, A.J. and Hoffman, A. (2022) Strategies for enhancing the oral bioavailability of cannabinoids. *Expert Opinion on Drug Metabolism & Toxicology*, 18 (5), 313-322.

Battista, N., Di Tommaso, M., Bari, M. and Maccarrone, M. (2012) The endocannabinoid system: an overview. *Frontiers in behavioral neuroscience*, 9.

Bhamra, S.K., Desai, A., Imani-Berendjestanki, P. and Horgan, M. (2021) The emerging role of cannabidiol (CBD) products; a survey exploring the public's use and perceptions of CBD. *Phytotherapy Research*, 35 (10), 5734-5740.

Bhuller, R., Schlage, W.K. and Hoeng, J. (2024) Review of the current ongoing clinical trials exploring the possible anti-anxiety effects of cannabidiol. *Journal of Cannabis Research*, 6 (1), 40.

Bialer, M., Johannessen, S.I., Koepp, M.J., Levy, R.H., Perucca, E., Tomson, T. and White, H.S. (2018) Progress report on new antiepileptic drugs: A summary of the Fourteenth Eilat Conference on New Antiepileptic Drugs and Devices (EILAT XIV). I. Drugs in preclinical and early clinical development. *Epilepsia*, 59 (10), 1811-1841.

Blau, H.M., Chiu, C.-P. and Webster, C. (1983) Cytoplasmic activation of human nuclear genes in stable heterocaryons. *Cell*, 32 (4), 1171-1180.

Borg, G., Ljunggren, G. and Ceci, R. (1985) The increase of perceived exertion, aches and pain in the legs, heart rate and blood lactate during exercise on a bicycle ergometer. *European journal of applied physiology and occupational physiology*, 54 (4), 343-349.

Borrelli, F., Fasolino, I., Romano, B., Capasso, R., Maiello, F., Coppola, D., Orlando, P., Battista, G., Pagano, E. and Di Marzo, V. (2013) Beneficial effect of the non-psychotropic plant cannabinoid cannabigerol on experimental inflammatory bowel disease. *Biochemical pharmacology*, 85 (9), 1306-1316.

Boyaji, S., Merkow, J., Elman, R.N.M., Kaye, A.D., Yong, R.J. and Urman, R.D. (2020) The role of cannabidiol (CBD) in chronic pain management: an assessment of current evidence. *Current pain and headache reports*, 24, 1-6.

Brady, A.O., Straight, C.R. and Evans, E.M. (2014) Body composition, muscle capacity, and physical function in older adults: an integrated conceptual model. *Journal of aging and physical activity*, 22 (3), 441-452.

Bridgeman, M.B. and Abazia, D.T. (2017) Medicinal cannabis: history, pharmacology, and implications for the acute care setting. *Pharmacy and therapeutics*, 42 (3), 180.

Brown, F., Gissane, C., Howatson, G., Van Someren, K., Pedlar, C. and Hill, J. (2017) Compression garments and recovery from exercise: a meta-analysis. *Sports Medicine*, 47, 2245-2267.

Brown, J.D. and Winterstein, A.G. (2019) Potential adverse drug events and drug–drug interactions with medical and consumer cannabidiol (CBD) use. *Journal of clinical medicine*, 8 (7), 989.

Brunt, T.M. and Bossong, M.G. (2020) The neuropharmacology of cannabinoid receptor ligands in central signaling pathways. *European Journal of Neuroscience*.

Burr, J.F., Cheung, C.P., Kasper, A.M., Gillham, S.H. and Close, G.L. (2021) Cannabis and athletic performance. *Sports Medicine*, 1-13.

Burstein, S. (2015) Cannabidiol (CBD) and its analogs: a review of their effects on inflammation. *Bioorganic & medicinal chemistry*, 23 (7), 1377-1385.

Capano, A., Weaver, R. and Burkman, E. (2020) Evaluation of the effects of CBD hemp extract on opioid use and quality of life indicators in chronic pain patients: a prospective cohort study. *Postgraduate medicine*, 132 (1), 56-61.

Cascio, M.G., Gauson, L.A., Stevenson, L.A., Ross, R.A. and Pertwee, R.G. (2010) Evidence that the plant cannabinoid cannabigerol is a highly potent α2-adrenoceptor agonist and moderately potent 5HT1A receptor antagonist. *British journal of pharmacology*, 159 (1), 129-141.

Cassano, T., Villani, R., Pace, L., Carbone, A., Bukke, V.N., Orkisz, S., Avolio, C. and Serviddio, G. (2020) From Cannabis sativa to cannabidiol: Promising therapeutic candidate for the treatment of neurodegenerative diseases. *Frontiers in pharmacology*, 11, 124.

Cavuoto, P., McAinch, A.J., Hatzinikolas, G., Janovská, A., Game, P. and Wittert, G.A. (2007a) The expression of receptors for endocannabinoids in human and rodent skeletal muscle. *Biochemical and biophysical research communications*, 364 (1), 105-110.

Cavuoto, P., McAinch, A.J., Hatzinikolas, G., Janovská, A., Game, P. and Wittert, G.A. (2007b) The expression of receptors for endocannabinoids in human and rodent skeletal muscle. *Biochem Biophys Res Commun*, 364 (1), 105-110.

Chaillou, T., Treigyte, V., Mosely, S., Brazaitis, M., Venckunas, T. and Cheng, A.J. (2022) Functional impact of post-exercise cooling and heating on recovery and training adaptations: application to resistance, endurance, and sprint exercise. *Sports Medicine-Open*, 8 (1), 37.

Chal, J. and Pourquié, O. (2017) Making muscle: skeletal myogenesis in vivo and in vitro. *Development*, 144 (12), 2104-2122.

Chan, J.Z. and Duncan, R.E. (2021) Regulatory Effects of Cannabidiol on Mitochondrial Functions: A Review. *Cells*, 10 (5), 1251.

Chen, J.W., Borgelt, L.M. and Blackmer, A.B. (2019) Cannabidiol: a new hope for patients with Dravet or Lennox-Gastaut syndromes. *Annals of Pharmacotherapy*, 53 (6), 603-611.

Cheung, C.P., Baker, R.E., Coates, A.M. and Burr, J.F. (2024) Cannabis containing THC impairs 20-min cycling time trial performance irrespective of the method of inhalation. *Journal of applied physiology*, 136 (3), 583-591.

Choi, L. and Hwang, J. (2023) What drives consumer perceptions and adoption of cannabidiol (CBD) products? *Journal of Marketing Management*, 39 (15-16), 1417-1450.

Chopra, G.S. (1969) Man and marijuana. *International journal of the addictions*, 4 (2), 215-247.

Clarke, R.C. and Merlin, M.D. (2016) Cannabis domestication, breeding history, present-day genetic diversity, and future prospects. *Critical reviews in plant sciences*, 35 (5-6), 293-327.

Close, G.L., Gillham, S.H. and Kasper, A.M. (2021) Cannabidiol (CBD) and the athlete: Claims, Evidence, Prevalence and Safety Concerns.

Close, G.L., Kasper, A.M., Walsh, N.P. and Maughan, R.J. (2022) "Food first but not always food only": recommendations for using dietary supplements in sport. *International journal of sport nutrition and exercise metabolism*, 32 (5), 371-386.

Cochrane-Snyman, K.C., Cruz, C., Morales, J. and Coles, M. (2021) The Effects of Cannabidiol Oil on Noninvasive Measures of Muscle Damage in Men. *Medicine and science in sports and exercise*.

Costello, N., McKenna, J., Deighton, K. and Jones, B. (2017) Commentary: Snap-N-send: A valid and reliable method for assessing the energy intake of elite adolescent athletes. *Frontiers in Nutrition*, 4, 47.

Couch, D. (2020) Left behind: The scale of illegal cannabis use for medicinal intent in the UK. [online]
Available at:

Cravatt, B.F., Giang, D.K., Mayfield, S.P., Boger, D.L., Lerner, R.A. and Gilula, N.B. (1996) Molecular characterization of an enzyme that degrades neuromodulatory fatty-acid amides. *Nature*, 384 (6604), 83-87.

Crespillo, A., Suárez, J., Bermúdez-Silva, F.J., Rivera, P., Vida, M., Alonso, M., Palomino, A., Lucena, M.A., Serrano, A., Pérez-Martín, M., Macias, M., Fernández-Llébrez, P. and Rodríguez de Fonseca, F. (2011) Expression of the cannabinoid system in muscle: effects of a high-fat diet and CB1 receptor blockade. *Biochem J*, 433 (1), 175-185.

Crini, G., Lichtfouse, E., Chanet, G. and Morin-Crini, N. (2020) Applications of hemp in textiles, paper industry, insulation and building materials, horticulture, animal nutrition, food and beverages, nutraceuticals, cosmetics and hygiene, medicine, agrochemistry, energy production and environment: a review. *Environmental Chemistry Letters*, 18, 1451-1476.

Crossland, B.W., Rigby, B.R., Duplanty, A.A., King, G.A., Juma, S., Levine, N.A., Clark, C.E., Ramirez, K.P. and Varone, N.L. (2022) Acute Supplementation with Cannabidiol Does Not Attenuate Inflammation or Improve Measures of Performance following Strenuous Exercise. *Healthcare* [online], 10 (6), 1133
Available at: [Accessed:

Crowley, L.C., Scott, A.P., Marfell, B.J., Boughaba, J.A., Chojnowski, G. and Waterhouse, N.J. (2016) Measuring cell death by propidium iodide uptake and flow cytometry. *Cold Spring Harbor Protocols*, 2016 (7), pdb. prot087163.

Cuttler, C., Stueber, A., Cooper, Z.D. and Russo, E. (2024) Acute effects of cannabigerol on anxiety, stress, and mood: a double-blind, placebo-controlled, crossover, field trial. *Scientific Reports*, 14 (1), 16163.

Dahlgren, M.K., Sagar, K.A., Lambros, A.M., Smith, R.T. and Gruber, S.A. (2021) Urinary tetrahydrocannabinol after 4 weeks of a full-spectrum, high-cannabidiol treatment in an open-label clinical trial. *JAMA psychiatry*, 78 (3), 335-337.

Dalle, S. and Koppo, K. (2021) Cannabinoid receptor 1 expression is higher in muscle of old vs. young males, and increases upon resistance exercise in older adults. *Scientific Reports*, 11 (1), 18349.

Dalle, S., Schouten, M., Meeus, G., Slagmolen, L. and Koppo, K. (2022) Molecular networks underlying cannabinoid signaling in skeletal muscle plasticity. *Journal of Cellular Physiology*, 237 (9), 3517-3540.

de Almeida, D.L. and Devi, L.A. (2020) Diversity of molecular targets and signaling pathways for CBD. *Pharmacology research & perspectives*, 8 (6), e00682.

De Vita, M.J., Maisto, S.A., Gilmour, C.E., McGuire, L., Tarvin, E. and Moskal, D. (2021) The effects of cannabidiol and analgesic expectancies on experimental pain reactivity in healthy adults: A balanced placebo design trial. *Experimental and Clinical Psychopharmacology*.

Deiana, S., Watanabe, A., Yamasaki, Y., Amada, N., Arthur, M., Fleming, S., Woodcock, H., Dorward, P., Pigliacampo, B. and Close, S. (2012) Plasma and brain pharmacokinetic profile of cannabidiol (CBD), cannabidivarine (CBDV), Δ 9-tetrahydrocannabivarin (THCV) and cannabigerol (CBG) in rats and mice following oral and intraperitoneal administration and CBD action on obsessive–compulsive behaviour. *Psychopharmacology*, 219, 859-873.

Denes, L.T., Riley, L.A., Mijares, J.R., Arboleda, J.D., McKee, K., Esser, K.A. and Wang, E.T. (2019) Culturing C2C12 myotubes on micromolded gelatin hydrogels accelerates myotube maturation. *Skeletal muscle*, 9 (1), 1-10.

Devane, W.A., Dysarz, F.r., Johnson, M.R., Melvin, L.S. and Howlett, A.C. (1988) Determination and characterization of a cannabinoid receptor in rat brain. *Molecular pharmacology*, 34 (5), 605-613.

Devane, W.A., Hanus, L., Breuer, A., Pertwee, R.G., Stevenson, L.A., Griffin, G., Gibson, D., Mandelbaum, A., Etinger, A. and Mechoulam, R. (1992) Isolation and structure of a brain constituent that binds to the cannabinoid receptor. *Science*, 258 (5090), 1946-1949.

Devinsky, O., Patel, A.D., Thiele, E.A., Wong, M.H., Appleton, R., Harden, C.L., Greenwood, S., Morrison, G., Sommerville, K. and Group, G.P.A.S. (2018) Randomized, dose-ranging safety trial of cannabidiol in Dravet syndrome. *Neurology*, 90 (14), e1204-e1211.

Di Marzo, V. and De Petrocellis, L. (2012) Why do cannabinoid receptors have more than one endogenous ligand? *Philosophical Transactions of the Royal Society B: Biological Sciences*, 367 (1607), 3216-3228.

Di Marzo, V. and Piscitelli, F. (2015) The endocannabinoid system and its modulation by phytocannabinoids. *Neurotherapeutics*, 12 (4), 692-698.

Docter, S., Khan, M., Gohal, C., Ravi, B., Bhandari, M., Gandhi, R. and Leroux, T. (2020) Cannabis Use and Sport: A Systematic Review. *Sports health*, 12 (2), 189-199.

Driver, B., Marks, D.C. and van der Wal, D.E. (2020) Not all (N) SAID and done: Effects of nonsteroidal anti-inflammatory drugs and paracetamol intake on platelets. *Research and practice in thrombosis and haemostasis*, 4 (1), 36-45.

Dyar, K.A., Hubert, M.J., Mir, A.A., Ciciliot, S., Lutter, D., Greulich, F., Quagliarini, F., Kleinert, M., Fischer, K. and Eichmann, T.O. (2018) Transcriptional programming of lipid and amino acid metabolism by the skeletal muscle circadian clock. *PLoS biology*, 16 (8), e2005886.

ElSohly, M.A., Radwan, M.M., Gul, W., Chandra, S. and Galal, A. (2017) Phytochemistry of Cannabis sativa L. *Phytocannabinoids*, 1-36.

Emerson, D.M., Chen, S.C., Kelly, M.R., Parnell, B. and Torres-McGehee, T.M. (2021) Non-steroidal anti-inflammatory drugs on core body temperature during exercise: A systematic review. *Journal of Exercise Science & Fitness*.

Felig, P. (1975) Amino acid metabolism in man. *Annual review of biochemistry*, 44 (1), 933-955.

Filipiuc, L.E., Ababei, D.C., Alexa-Stratulat, T., Pricope, C.V., Bild, V., Stefanescu, R., Stanciu, G.D. and Tamba, B.-I. (2021) Major phytocannabinoids and their related compounds: should we only search for drugs that act on cannabinoid receptors? *Pharmaceutics*, 13 (11), 1823.

Franco, V., Gershkovich, P., Perucca, E. and Bialer, M. (2020) The Interplay Between Liver First-Pass Effect and Lymphatic Absorption of Cannabidiol and Its Implications for Cannabidiol Oral Formulations. *Clinical pharmacokinetics*, 59 (12), 1493-1500.

Franco, V. and Perucca, E. (2019) Pharmacological and therapeutic properties of cannabidiol for epilepsy. *Drugs*, 79, 1435-1454.

Freeman, A.M., Petrilli, K., Lees, R., Hindocha, C., Mokrysz, C., Curran, H.V., Saunders, R. and Freeman, T.P. (2019) How does cannabidiol (CBD) influence the acute effects of delta-9-tetrahydrocannabinol (THC) in humans? A systematic review. *Neuroscience & Biobehavioral Reviews*, 107, 696-712.

Frontera, W.R. and Ochala, J. (2015) Skeletal muscle: a brief review of structure and function. *Calcified tissue international*, 96 (3), 183-195.

Gaffal, E., Cron, M., Glodde, N. and Tüting, T. (2013) Anti-inflammatory activity of topical THC in DNFB-mediated mouse allergic contact dermatitis independent of CB 1 and CB 2 receptors. *Allergy*, 68 (8), 994-1000.

Gamelin, F.-X., Cuvelier, G., Mendes, A., Aucouturier, J., Berthoin, S., Di Marzo, V. and Heyman, E. (2020) Cannabidiol in sport: Ergogenic or else? *Pharmacological research*, 156, 104764.

Gaoni, Y. and Mechoulam, R. (1964) Isolation, structure, and partial synthesis of an active constituent of hashish. *Journal of the American Chemical Society*, 86 (8), 1646-1647.

García-Gutiérrez, M.S., Navarrete, F., Gasparyan, A., Austrich-Olivares, A., Sala, F. and Manzanares, J. (2020) Cannabidiol: a potential new alternative for the treatment of anxiety, depression, and psychotic disorders. *Biomolecules*, 10 (11), 1575.

Garthe, I. and Ramsbottom, R. (2020) Elite athletes, a rationale for the use of dietary supplements: A practical approach. *PharmaNutrition*, 14, 100234.

Ghasemi, M., Liang, S., Luu, Q.M. and Kempson, I. (2023) The MTT Assay: A Method for Error Minimization and Interpretation in Measuring Cytotoxicity and Estimating Cell Viability. In: (ed.) *Cell Viability Assays: Methods and Protocols.* Springer. pp. 15-33.

Gibson, L.P., Giordano, G.R., Bidwell, L.C., Hutchison, K.E. and Bryan, A.D. (2024) Acute Effects of Ad Libitum Use of Commercially Available Cannabis Products on the Subjective Experience of Aerobic Exercise: A Crossover Study. *Sports Medicine*, 54 (4), 1051-1066.

Goldstein, J.L. and Cryer, B. (2015) Gastrointestinal injury associated with NSAID use: a case study and review of risk factors and preventative strategies. *Drug, healthcare and patient safety*, 7, 31.

Gorelick, D.A., Goodwin, R.S., Schwilke, E., Schwope, D.M., Darwin, W.D., Kelly, D.L., McMahon, R.P., Liu, F., Ortemann-Renon, C. and Bonnet, D. (2013) Tolerance to effects of high-dose oral Δ9-tetrahydrocannabinol and plasma cannabinoid concentrations in male daily cannabis smokers. *Journal of analytical toxicology*, 37 (1), 11-16.

Gornall, J. (2020) Big cannabis in the UK: is industry support for wider patient access motivated by promises of recreational market worth billions? *BMJ*, 368.

Gries, K.J., Raue, U., Perkins, R.K., Lavin, K.M., Overstreet, B.S., D'Acquisto, L.J., Graham, B., Finch, W.H., Kaminsky, L.A. and Trappe, T.A. (2018) Cardiovascular and skeletal muscle health with lifelong exercise. *Journal of applied physiology*, 125 (5), 1636-1645.

Grotenhermen, F. (2003) Pharmacokinetics and pharmacodynamics of cannabinoids. *Clinical pharmacokinetics*, 42, 327-360.

Gugliandolo, A., Pollastro, F., Grassi, G., Bramanti, P. and Mazzon, E. (2018) In vitro model of neuroinflammation: efficacy of cannabigerol, a non-psychoactive cannabinoid. *International journal of molecular sciences*, 19 (7), 1992.

Gülck, T. and Møller, B.L. (2020) Phytocannabinoids: origins and biosynthesis. *Trends in Plant Science*, 25 (10), 985-1004.

Gunasekaran, N., Long, L., Dawson, B., Hansen, G., Richardson, D., Li, K., Arnold, J. and McGregor, I. (2009) Reintoxication: the release of fat-stored Δ9-tetrahydrocannabinol (THC) into blood is enhanced by food deprivation or ACTH exposure. *British journal of pharmacology*, 158 (5), 1330-1337.

Gurley, B.J., Murphy, T.P., Gul, W., Walker, L.A. and ElSohly, M. (2020) Content versus label claims in cannabidiol (CBD)-containing products obtained from commercial outlets in the state of Mississippi. *Journal of dietary supplements*, 17 (5), 599-607.

Haddad, M. (2021a) The impact of CB1 receptor on inflammation in skeletal muscle cells. *Journal of Inflammation Research*, 14, 3959.

Haddad, M. (2021b) The Impact of CB1 Receptor on Nuclear Receptors in Skeletal Muscle Cells. *Pathophysiology*, 28 (4), 457-470.

Hampson, A., Grimaldi, M., Axelrod, J. and Wink, D. (1998) Cannabidiol and (−) Δ9-tetrahydrocannabinol are neuroprotective antioxidants. *Proceedings of the National Academy of Sciences*, 95 (14), 8268-8273.

Haney, M. (2020) Perspectives on cannabis research—Barriers and recommendations. *JAMA psychiatry*, 77 (10), 994-995.

Hanuš, L.O., Meyer, S.M., Muñoz, E., Taglialatela-Scafati, O. and Appendino, G. (2016) Phytocannabinoids: a unified critical inventory. *Natural product reports*, 33 (12), 1357-1392.

Hatchett, A., Armstrong, K., Hughes, B. and Parr, B. (2020) The influence cannabidiol on delayed onset of muscle soreness.

Heinz, S., Benner, C., Spann, N., Bertolino, E., Lin, Y.C., Laslo, P., Cheng, J.X., Murre, C., Singh, H. and Glass, C.K. (2010) Simple combinations of lineage-determining transcription factors prime cis-regulatory elements required for macrophage and B cell identities. *Mol Cell*, 38 (4), 576-589.

Henry, C. (2010) Functional foods. *European Journal of Clinical Nutrition*, 64 (7), 657-659.

Hermann, A., Kaczocha, M. and Deutsch, D.G. (2006) 2-Arachidonoylglycerol (2-AG) membrane transport: history and outlook. *The AAPS journal*, 8, E409-E412.

Hernández-Hernández, J.M., García-González, E.G., Brun, C.E. and Rudnicki, M.A. (2017) The myogenic regulatory factors, determinants of muscle development, cell identity and regeneration. *Seminars in cell & developmental biology* [online], 72 10-18
Available at: [Accessed:

Hesketh, S.J., Stansfield, B.N., Stead, C.A. and Burniston, J.G. (2020) The application of proteomics in muscle exercise physiology. *Expert Review of Proteomics*, 17 (11-12), 813-825.

Holgado, D., Hopker, J., Sanabria, D. and Zabala, M. (2018a) Analgesics and sport performance: beyond the pain-modulating effects. *PM&R*, 10 (1), 72-82.

Holgado, D., Zandonai, T., Zabala, M., Hopker, J., Perakakis, P., Luque-Casado, A., Ciria, L., Guerra-Hernandez, E. and Sanabria, D. (2018b) Tramadol effects on physical performance and sustained attention during a 20-min indoor cycling time-trial: A randomised controlled trial. *Journal of science and medicine in sport*, 21 (7), 654-660.

Huestis, M.A. (2007) Human cannabinoid pharmacokinetics. *Chemistry & biodiversity*, 4 (8), 1770.

Hurley, E.N., Ellaway, C.J., Johnson, A.M., Truong, L., Gordon, R., Galettis, P., Martin, J.H. and Lawson, J.A. (2022) Efficacy and safety of cannabidivarin treatment of epilepsy in girls with Rett syndrome: A phase 1 clinical trial. *Epilepsia*, 63 (7), 1736-1747.

Hurley, E.T., Alaia, M.J., Vasavada, K., Markus, D.H., Britton, B., Gonzalez-Lomas, G., Rokito, A.S. and Jazrawi, L.M. (2023) Effects Of Cannabidiol On Post-Operative Pain Following Arthroscopic Rotator Cuff Repair. *Journal of Shoulder and Elbow Surgery*, 32 (5), e248.

Iannotti, F.A., Hill, C.L., Leo, A., Alhusaini, A., Soubrane, C., Mazzarella, E., Russo, E., Whalley, B.J., Di Marzo, V. and Stephens, G.J. (2014) Nonpsychotropic plant cannabinoids, cannabidivarin (CBDV) and cannabidiol (CBD), activate and desensitize transient receptor potential vanilloid 1 (TRPV1) channels in vitro: potential for the treatment of neuronal hyperexcitability. *ACS chemical neuroscience*, 5 (11), 1131-1141.

Iannotti, F.A., Pagano, E., Moriello, A.S., Alvino, F.G., Sorrentino, N.C., D'Orsi, L., Gazzerro, E., Capasso, R., De Leonibus, E. and De Petrocellis, L. (2019a) Effects of non-euphoric plant cannabinoids on muscle quality and performance of dystrophic mdx mice. *British journal of pharmacology*, 176 (10), 1568-1584.

Iannotti, F.A., Pagano, E., Moriello, A.S., Alvino, F.G., Sorrentino, N.C., D'Orsi, L., Gazzerro, E., Capasso, R., De Leonibus, E., De Petrocellis, L. and Di Marzo, V. (2019b) Effects of non-euphoric plant cannabinoids on muscle quality and performance of dystrophic mdx mice. *Br J Pharmacol*, 176 (10), 1568-1584.

Iffland, K. and Grotenhermen, F. (2017) An update on safety and side effects of cannabidiol: a review of clinical data and relevant animal studies. *Cannabis and Cannabinoid Research*, 2 (1), 139-154.

Irrcher, I., Ljubicic, V., Kirwan, A.F. and Hood, D.A. (2008) AMP-activated protein kinase-regulated activation of the PGC-1α promoter in skeletal muscle cells. *PLoS One*, 3 (10), e3614.

Isenmann, E., Veit, S. and Diel, P. (2020) Effects Of Cannabidiol Supplementation On The Skeletal Muscle Regeneration After Intensive Resistance Training: 2769 Board# 230 May 29 9: 30 AM-11: 00 AM. *Medicine & Science in Sports & Exercise*, 52 (7S), 766.

Isenmann, E., Veit, S., Flenker, U., Lesch, A., Lachenmeier, D.W. and Diel, P. (2024) Influence of short-term chronic oral cannabidiol application on muscle recovery and performance after an intensive training protocol-a randomized double-blind crossover study. *Journal of the International Society of Sports Nutrition*, 21 (1), 2337252.

Izzo, A.A., Borrelli, F., Capasso, R., Di Marzo, V. and Mechoulam, R. (2009) Non-psychotropic plant cannabinoids: new therapeutic opportunities from an ancient herb. *Trends in pharmacological sciences*, 30 (10), 515-527.

Jakowiecki, J., Abel, R., Orzeł, U., Pasznik, P., Preissner, R. and Filipek, S. (2021) Allosteric modulation of the CB1 cannabinoid receptor by cannabidiol—A molecular modeling study of the N-terminal domain and the allosteric-orthosteric coupling. *Molecules*, 26 (9), 2456.

Jastrząb, A., Gęgotek, A. and Skrzydlewska, E. (2019) Cannabidiol regulates the expression of keratinocyte proteins involved in the inflammation process through transcriptional regulation. *Cells*, 8 (8), 827.

Jeong, S., Jo, M.J., Yun, H.K., Kim, D.Y., Kim, B.R., Kim, J.L., Park, S.H., Na, Y.J., Jeong, Y.A. and Kim, B.G. (2019) Cannabidiol promotes apoptosis via regulation of XIAP/Smac in gastric cancer. *Cell death & disease*, 10 (11), 846.

Jiang, P., Wang, L., Zhang, M., Zhang, M., Wang, C., Zhao, R. and Guan, D. (2020) Cannabinoid type 2 receptor manipulates skeletal muscle regeneration partly by regulating macrophage M1/M2 polarization in IR injury in mice. *Life sciences*, 256, 117989.

Jiang, R., Yamaori, S., Takeda, S., Yamamoto, I. and Watanabe, K. (2011) Identification of cytochrome P450 enzymes responsible for metabolism of cannabidiol by human liver microsomes. *Life sciences*, 89 (5-6), 165-170.

Jin, D., Henry, P., Shan, J. and Chen, J. (2021) Identification of phenotypic characteristics in three chemotype categories in the genus Cannabis. *HortScience*, 56 (4), 481-490.

Johansson, E., Norén, K., Sjövall, J. and Halldin, M.M. (1989) Determination of Δ1-tetrahydrocannabinol in human fat biopsies from marihuana users by gas chromatography–mass spectrometry. *Biomedical Chromatography*, 3 (1), 35-38.

Johnson, D.A., Cable, T.G., Funnell, M.P., Peden, D.L., Thorley, J., Cunha, M.F.D., Reynolds, K.M., Harris, L., Wood, M. and Chavez-O'Reilly, T. (2025) Effects of Cannabidiol Ingestion on Thermoregulatory and Inflammatory Responses to Treadmill Exercise in the Heat in Recreationally Active Males. [online]

Available at:

Johnson, D.A., Hogan, M., Marriot, R., Heaney, L.M., Bailey, S.J., Clifford, T. and James, L.J. (2023) A comparison of advertised versus actual cannabidiol (CBD) content of oils, aqueous tinctures, e-liquids and drinks purchased in the UK. *Journal of Cannabis Research*, 5 (1), 28.

Johnson, E., Kilgore, M. and Babalonis, S. (2022) Label accuracy of unregulated cannabidiol (CBD) products: measured concentration vs. label claim. *Journal of Cannabis Research*, 4 (1), 1-7.

Judkins, C. and Prock, P. (2012) Supplements and inadvertent doping–how big is the risk to athletes. *Acute topics in sport nutrition*, 59, 143-152.

Kalkan, H., Panza, E., Pagano, E., Ercolano, G., Moriello, C., Piscitelli, F., Sztretye, M., Capasso, R., Di Marzo, V. and Iannotti, F.A. (2023a) Dysfunctional endocannabinoid CB1 receptor expression and signaling contribute to skeletal muscle cell toxicity induced by simvastatin. *Cell Death Dis*, 14 (8), 544.

Kalkan, H., Panza, E., Pagano, E., Ercolano, G., Moriello, C., Piscitelli, F., Sztretye, M., Capasso, R., Di Marzo, V. and Iannotti, F.A. (2023b) Dysfunctional endocannabinoid CB1 receptor expression and signaling contribute to skeletal muscle cell toxicity induced by simvastatin. *Cell death & disease*, 14 (8), 544.

Kasper, A.M., Sparks, S.A., Hooks, M., Skeer, M., Webb, B., Nia, H., Morton, J.P. and Close, G.L. (2020a) High Prevalence of Cannabidiol Use Within Male Professional Rugby Union and League Players: A Quest for Pain Relief and Enhanced Recovery. *Int J Sport Nutr Exerc Metab*, 30 (5), 315-322.

Kasper, A.M., Sparks, S.A., Hooks, M., Skeer, M., Webb, B., Nia, H., Morton, J.P. and Close, G.L. (2020b) High prevalence of cannabidiol use within male professional Rugby union and league players: a quest for pain relief and enhanced recovery. *International journal of sport nutrition and exercise metabolism*, 30 (5), 315-322.

Kevin, R.C., Allsop, D.J., Lintzeris, N., Dunlop, A.J., Booth, J. and McGregor, I.S. (2017) Urinary cannabinoid levels during nabiximols (Sativex®)-medicated inpatient cannabis withdrawal. *Forensic Toxicology*, 35, 33-44.

Khosropoor, S., Alavi, M.S., Etemad, L. and Roohbakhsh, A. (2023) Cannabidiol goes nuclear: The role of PPARγ. *Phytomedicine*, 114, 154771.

Kilaru, A. and Chapman, K.D. (2020) The endocannabinoid system. *Essays in Biochemistry*, 64 (3), 485-499.

King, S. (2014) Beyond the war on drugs? Notes on prescription opioids and the NFL. *Journal of Sport and Social Issues*, 38 (2), 184-193.

Klumpers, L.E. and Thacker, D.L. (2019) A brief background on cannabis: From plant to medical indications. *Journal of AOAC International*, 102 (2), 412-420.

Kolli, A.R. and Hoeng, J. (2025) Cannabidiol bioavailability is nonmonotonic with a long terminal elimination half-life: a pharmacokinetic modeling-based analysis. *Cannabis and Cannabinoid Research*, 10 (1), 81-91.

Koves, T.R., Ussher, J.R., Noland, R.C., Slentz, D., Mosedale, M., Ilkayeva, O., Bain, J., Stevens, R., Dyck, J.R. and Newgard, C.B. (2008) Mitochondrial overload and incomplete fatty acid oxidation contribute to skeletal muscle insulin resistance. *Cell metabolism*, 7 (1), 45-56.

Krentz, J.R., Quest, B., Farthing, J.P., Quest, D.W. and Chilibeck, P.D. (2008) The effects of ibuprofen on muscle hypertrophy, strength, and soreness during resistance training. *Applied Physiology, Nutrition, and Metabolism*, 33 (3), 470-475.

Kreuz, D.S. and Axelrod, J. (1973) Delta-9-tetrahydrocannabinol: localization in body fat. *Science*, 179 (4071), 391-393.

Kumar, K.K., Shalev-Benami, M., Robertson, M.J., Hu, H., Banister, S.D., Hollingsworth, S.A., Latorraca, N.R., Kato, H.E., Hilger, D. and Maeda, S. (2019) Structure of a signaling cannabinoid receptor 1-G protein complex. *Cell*, 176 (3), 448-458. e412.

Lakens, D. (2022) Sample size justification. *Collabra: Psychology*, 8 (1), 33267.

Lange, B.M. and Zager, J.J. (2022) Comprehensive inventory of cannabinoids in Cannabis sativa L.: can we connect genotype and chemotype? *Phytochemistry Reviews*, 21 (4), 1273-1313.

Langer, H.T., Avey, A. and Baar, K. (2021) Cannabidiol does not impact acute anabolic or inflammatory signaling in skeletal muscle in vitro. *Cannabis and Cannabinoid Research*.

Langer, H.T., Avey, A. and Baar, K. (2022) Cannabidiol Does Not Impact Acute Anabolic or Inflammatory Signaling in Skeletal Muscle In Vitro. *Cannabis Cannabinoid Res*, 7 (5), 628-636.

Langer, H.T., Mossakowski, A.A., Pathak, S., Mascal, M. and Baar, K. (2021) Cannabidiol Does Not Impair Anabolic Signaling Following Eccentric Contractions in Rats. *Int J Sport Nutr Exerc Metab*, 31 (2), 93-100.

Laprairie, R., Bagher, A., Kelly, M. and Denovan-Wright, E. (2015) Cannabidiol is a negative allosteric modulator of the cannabinoid CB1 receptor. *British journal of pharmacology*, 172 (20), 4790-4805.

Laun, A.S., Shrader, S.H., Brown, K.J. and Song, Z.-H. (2019) GPR3, GPR6, and GPR12 as novel molecular targets: their biological functions and interaction with cannabidiol. *Acta Pharmacologica Sinica*, 40 (3), 300-308.

Le Bacquer, O., Salles, J., Piscitelli, F., Sanchez, P., Martin, V., Montaurier, C., Di Marzo, V. and Walrand, S. (2022) Alterations of the endocannabinoid system and circulating and peripheral tissue levels of endocannabinoids in sarcopenic rats. *Journal of cachexia, sarcopenia and muscle*, 13 (1), 662-676.

Le Meur, Y. and Torres-Ronda, L. (2019) 10 Challenges facing today's applied sport scientist. *Science Performance and Science Reports*, 57, 1-7.

Le, N., Hufford, T.M., Park, J.S. and Brewster, R.M. (2021) Differential expression and hypoxia-mediated regulation of the N-myc downstream regulated gene family. *The FASEB Journal*, 35 (11), e21961.

Lecoeur, H. (2002) Nuclear apoptosis detection by flow cytometry: influence of endogenous endonucleases. *Experimental cell research*, 277 (1), 1-14.

Li, D., Ilnytskyy, Y., Ghasemi Gojani, E., Kovalchuk, O. and Kovalchuk, I. (2022) Analysis of anti-cancer and anti-inflammatory properties of 25 high-THC cannabis extracts. *Molecules*, 27 (18), 6057.

Li, H.-L. (1974) An archaeological and historical account of cannabis in China. *Economic Botany*, 28 (4), 437-448.

Li, J., Carvajal, R., Bruner, L. and Kaminski, N.E. (2021) The current understanding of the benefits, safety, and regulation of cannabidiol in consumer products. *Food and Chemical Toxicology*, 157, 112600.

Li, N., Alam, J., Venkatesan, M.I., Eiguren-Fernandez, A., Schmitz, D., Di Stefano, E., Slaughter, N., Killeen, E., Wang, X. and Huang, A. (2004) Nrf2 is a key transcription factor that regulates antioxidant defense in macrophages and epithelial cells: protecting against the proinflammatory and oxidizing effects of diesel exhaust chemicals. *The Journal of Immunology*, 173 (5), 3467-3481.

Liebling, J.P., Clarkson, N.J., Gibbs, B.W., Yates, A.S. and O'Sullivan, S.E. (2020) An analysis of over-the-counter cannabidiol products in the United Kingdom. *Cannabis and Cannabinoid Research*.

Lim, S.Y., Sharan, S. and Woo, S. (2020) Model-based analysis of cannabidiol dose-exposure relationship and bioavailability. *Pharmacotherapy: The Journal of Human Pharmacology and Drug Therapy*, 40 (4), 291-300.

Linher-Melville, K., Zhu, Y.F., Sidhu, J., Parzei, N., Shahid, A., Seesankar, G., Ma, D., Wang, Z., Zacal, N. and Sharma, M. (2020) Evaluation of the preclinical analgesic efficacy of

naturally derived, orally administered oil forms of Δ9-tetrahydrocannabinol (THC), cannabidiol (CBD), and their 1: 1 combination. *PLoS One*, 15 (6), e0234176.

Lins, B.R., Anyaegbu, C.C., Hellewell, S.C., Papini, M., McGonigle, T., De Prato, L., Shales, M. and Fitzgerald, M. (2023) Cannabinoids in traumatic brain injury and related neuropathologies: preclinical and clinical research on endogenous, plant-derived, and synthetic compounds. *Journal of neuroinflammation*, 20 (1), 77.

Louis-Gray, K., Tupal, S. and Premkumar, L.S. (2022) TRPV1: a common denominator mediating antinociceptive and antiemetic effects of cannabinoids. *International journal of molecular sciences*, 23 (17), 10016.

Love, M.I., Huber, W. and Anders, S. (2014) Moderated estimation of fold change and dispersion for RNA-seq data with DESeq2. *Genome Biol*, 15 (12), 550.

Lu, H.-C. and Mackie, K. (2020) Review of the endocannabinoid system. *Biological Psychiatry: Cognitive Neuroscience and Neuroimaging*.

Lundberg, T.R. and Howatson, G. (2018) Analgesic and anti-inflammatory drugs in sports: Implications for exercise performance and training adaptations. *Scandinavian journal of medicine & science in sports*, 28 (11), 2252-2262.

Luo, W., Wu, H., Ye, Y., Li, Z., Hao, S., Kong, L., Zheng, X., Lin, S., Nie, Q. and Zhang, X. (2014) The transient expression of miR-203 and its inhibiting effects on skeletal muscle cell proliferation and differentiation. *Cell death & disease*, 5 (7), e1347-e1347.

Maccarrone, M. (2020) Phytocannabinoids and endocannabinoids: Different in nature. *Rendiconti Lincei. Scienze Fisiche e Naturali*, 31, 931-938.

Mackie, K. (2005) Distribution of cannabinoid receptors in the central and peripheral nervous system. *Cannabinoids*, 299-325.

Malhotra, J.D. and Kaufman, R.J. (2007) Endoplasmic reticulum stress and oxidative stress: a vicious cycle or a double-edged sword? *Antioxidants & redox signaling*, 9 (12), 2277-2294.

Manzanares, J., Julian, M. and Carrascosa, A. (2006) Role of the cannabinoid system in pain control and therapeutic implications for the management of acute and chronic pain episodes. *Current neuropharmacology*, 4 (3), 239-257.

Mareck, U., Fusshöller, G., Geyer, H., Huestis, M.A., Scheiff, A.B. and Thevis, M. (2021) Preliminary data on the potential for unintentional antidoping rule violations by permitted cannabidiol (CBD) use. *Drug Testing and Analysis*, 13 (3), 539-549.

Marinotti, O. and Sarill, M. (2020) Differentiating full-spectrum hemp extracts from CBD isolates: implications for policy, safety and science. *Journal of dietary supplements*, 17 (5), 517-526.

Martin, J.H., Hill, C., Walsh, A., Efron, D., Taylor, K., Kennedy, M., Galettis, R., Lightfoot, P., Hanson, J. and Irving, H. (2020) Clinical trials with cannabis medicines—guidance for ethics committees, governance officers and researchers to streamline ethics applications and ensuring patient safety: considerations from the Australian experience. *Trials*, 21 (1), 1-7.

Masiero, E., Agatea, L., Mammucari, C., Blaauw, B., Loro, E., Komatsu, M., Metzger, D., Reggiani, C., Schiaffino, S. and Sandri, M. (2009) Autophagy is required to maintain muscle mass. *Cell metabolism*, 10 (6), 507-515.

Mata, F., Valenzuela, P.L., Gimenez, J., Tur, C., Ferreria, D., Domínguez, R., Sanchez-Oliver, A.J. and Martínez Sanz, J.M. (2019) Carbohydrate availability and physical performance: physiological overview and practical recommendations. *Nutrients*, 11 (5), 1084.

Matava, M.J. (2018) Injectable nonsteroidal anti-inflammatory drugs in sport. *Clinical Journal of Sport Medicine*, 28 (5), 443-450.

Mauger, A.R., Thomas, T., Smith, S.A. and Fennell, C.R. (2023) Tramadol is a performance-enhancing drug in highly trained cyclists: a randomized controlled trial. *Journal of applied physiology*, 135 (2), 467-474.

Maughan, R.J., Burke, L.M., Dvorak, J., Larson-Meyer, D.E., Peeling, P., Phillips, S.M., Rawson, E.S., Walsh, N.P., Garthe, I. and Geyer, H. (2018) IOC consensus statement: dietary supplements and the high-performance athlete. *International journal of sport nutrition and exercise metabolism*, 28 (2), 104-125.

McCartney, D., Benson, M.J., Desbrow, B., Irwin, C., Suraev, A. and McGregor, I.S. (2020) Cannabidiol and sports performance: a narrative review of relevant evidence and recommendations for future research. *Sports Medicine-Open*, 6 (1), 1-18.

McCartney, D., Irwin, C., Bawa, Z., Palmer, B., Sahinovic, A., Delang, N., Cox, G.R., Desbrow, B., Lau, N.S. and McGregor, I.S. (2024) The Effect of Cannabidiol on Subjective Responses to Endurance Exercise: A Randomised Controlled Trial. *Sports Medicine-Open*, 10 (1), 61.

McGregor, I.S., Cairns, E.A., Abelev, S., Cohen, R., Henderson, M., Couch, D., Arnold, J.C. and Gauld, N. (2020) Access to cannabidiol without a prescription: a cross-country comparison and analysis. *International Journal of Drug Policy*, 85, 102935.

McKinnon, K.M. (2018) Flow cytometry: an overview. *Current protocols in immunology*, 120 (1), 5.1. 1-5.1. 11.

McLeod, M., Breen, L., Hamilton, D.L. and Philp, A. (2016) Live strong and prosper: the importance of skeletal muscle strength for healthy ageing. *Biogerontology*, 17 (3), 497-510.

McPartland, J.M. (2017) Cannabis sativa and Cannabis indica versus “Sativa” and “Indica”. In: (ed.) *Cannabis sativa L.-botany and biotechnology.* Springer. pp. 101-121.

McPartland, J.M. (2018) Cannabis systematics at the levels of family, genus, and species. *Cannabis and Cannabinoid Research*, 3 (1), 203-212.

McPartland, J.M. and Small, E. (2020) A classification of endangered high-THC cannabis (Cannabis sativa subsp. indica) domesticates and their wild relatives. *PhytoKeys*, 144, 81.

Mechoulam, R. and Shvo, Y. (1963) Hashish—I: the structure of cannabidiol. *Tetrahedron*, 19 (12), 2073-2078.

Mendizabal-Zubiaga, J., Melser, S., Bénard, G., Ramos, A., Reguero, L., Arrabal, S., Elezgarai, I., Gerrikagoitia, I., Suarez, J., Rodríguez De Fonseca, F., Puente, N., Marsicano, G. and Grandes, P. (2016) Cannabinoid CB(1) Receptors Are Localized in Striated Muscle Mitochondria and Regulate Mitochondrial Respiration. *Front Physiol*, 7, 476.

Micalizzi, G., Vento, F., Alibrando, F., Donnarumma, D., Dugo, P. and Mondello, L. (2021) Cannabis Sativa L.: A comprehensive review on the analytical methodologies for cannabinoids and terpenes characterization. *Journal of Chromatography A*, 1637, 461864.

Migliaccio, G.M., Padulo, J. and Russo, L. (2024) The impact of wearable technologies on marginal gains in sports performance: An integrative overview on advances in sports, exercise, and health. *Applied sciences*, 14 (15), 6649.

Millar, S.A., Stone, N.L., Yates, A.S. and O'Sullivan, S.E. (2018) A systematic review on the pharmacokinetics of cannabidiol in humans. *Frontiers in pharmacology*, 9, 425858.

Miller, H.P., Bonawitz, S.C. and Ostrovsky, O. (2020) The effects of delta-9-tetrahydrocannabinol (THC) on inflammation: A review. *Cellular immunology*, 352, 104111.

Miller, O.S., Elder Jr, E.J., Jones, K.J. and Gidal, B.E. (2022) Analysis of cannabidiol (CBD) and THC in nonprescription consumer products: implications for patients and practitioners. *Epilepsy & Behavior*, 127, 108514.

Miyazaki, K., Kawamoto, T., Tanimoto, K., Nishiyama, M., Honda, H. and Kato, Y. (2002) Identification of functional hypoxia response elements in the promoter region of the DEC1 and DEC2 genes. *Journal of Biological Chemistry*, 277 (49), 47014-47021.

Mizushima, N., Noda, T., Yoshimori, T., Tanaka, Y., Ishii, T., George, M.D., Klionsky, D.J., Ohsumi, M. and Ohsumi, Y. (1998) A protein conjugation system essential for autophagy. *Nature*, 395 (6700), 395-398.

Morales, P., Reggio, P.H. and Jagerovic, N. (2017) An overview on medicinal chemistry of synthetic and natural derivatives of cannabidiol. *Frontiers in pharmacology*, 8, 422.

Morano, A., Fanella, M., Albini, M., Cifelli, P., Palma, E., Giallonardo, A.T. and Di Bonaventura, C. (2020) Cannabinoids in the treatment of epilepsy: current status and future prospects. *Neuropsychiatric Disease and Treatment*, 381-396.

Motohashi, H. and Yamamoto, M. (2004) Nrf2–Keap1 defines a physiologically important stress response mechanism. *Trends in molecular medicine*, 10 (11), 549-557.

Mukund, K. and Subramaniam, S. (2020) Skeletal muscle: A review of molecular structure and function, in health and disease. *Wiley Interdisciplinary Reviews: Systems Biology and Medicine*, 12 (1), e1462.

Munro, S., Thomas, K.L. and Abu-Shaar, M. (1993) Molecular characterization of a peripheral receptor for cannabinoids. *Nature*, 365 (6441), 61-65.

Murakami, K., Yumoto, F., Ohki, S.-y., Yasunaga, T., Tanokura, M. and Wakabayashi, T. (2005) Structural basis for Ca2+-regulated muscle relaxation at interaction sites of troponin with actin and tropomyosin. *Journal of molecular biology*, 352 (1), 178-201.

Muta, T., Khetan, R., Song, Y. and Garg, S. (2025) Optimising Cannabidiol Delivery: Improving Water Solubility and Permeability Through Phospholipid Complexation. *International journal of molecular sciences*, 26 (6), 2647.

Nachnani, R., Raup-Konsavage, W.M. and Vrana, K.E. (2021) The pharmacological case for cannabigerol. *Journal of Pharmacology and Experimental Therapeutics*, 376 (2), 204-212.

Naderi, A., Rothschild, J.A., Santos, H.O., Hamidvand, A., Koozehchian, M.S., Ghazzagh, A., Berjisian, E. and Podlogar, T. (2025) Nutritional Strategies to Improve Post-exercise Recovery and Subsequent Exercise Performance: A Narrative Review. *Sports Medicine*, 1-19.

Naughton, M., Miller, J. and Slater, G.J. (2018) Impact-induced muscle damage and contact sports: etiology, effects on neuromuscular function and recovery, and the modulating effects of adaptation and recovery strategies. *International Journal of Sports Physiology and Performance*, 13 (8), 962-969.

Navarro, G., Morales, P., Rodríguez-Cueto, C., Fernández-Ruiz, J., Jagerovic, N. and Franco, R. (2016) Targeting cannabinoid CB2 receptors in the central nervous system. Medicinal chemistry approaches with focus on neurodegenerative disorders. *Frontiers in Neuroscience*, 10, 406.

Nguyen, T., Li, J.X., Thomas, B.F., Wiley, J.L., Kenakin, T.P. and Zhang, Y. (2017) Allosteric modulation: an alternate approach targeting the cannabinoid CB1 receptor. *Medicinal research reviews*, 37 (3), 441-474.

Nutt, D. (2019) Why medical cannabis is still out of patients' reach—an essay by David Nutt. *BMJ*, 365.

Odell, M.S., Frei, M.Y., Gerostamoulos, D., Chu, M. and Lubman, D.I. (2015) Residual cannabis levels in blood, urine and oral fluid following heavy cannabis use. *Forensic science international*, 249, 173-180.

Oláh, A., Tóth, B.I., Borbíró, I., Sugawara, K., Szöllõsi, A.G., Czifra, G., Pál, B., Ambrus, L., Kloepper, J. and Camera, E. (2014) Cannabidiol exerts sebostatic and antiinflammatory effects on human sebocytes. *The Journal of clinical investigation*, 124 (9), 3713-3724.

Olejar, K.J. and Kinney, C.A. (2021) Evaluation of thermo-chemical conversion temperatures of cannabinoid acids in hemp (Cannabis sativa L.) biomass by pressurized liquid extraction. *Journal of Cannabis Research*, 3, 1-6.

Oomah, B.D., Busson, M., Godfrey, D.V. and Drover, J.C. (2002) Characteristics of hemp (Cannabis sativa L.) seed oil. *Food chemistry*, 76 (1), 33-43.

Owens, D.J., Twist, C., Cobley, J.N., Howatson, G. and Close, G.L. (2019) Exercise-induced muscle damage: What is it, what causes it and what are the nutritional solutions? *European Journal of Sport Science*, 19 (1), 71-85.

Pagano, S., Coniglio, M., Valenti, C., Federici, M.I., Lombardo, G., Cianetti, S. and Marinucci, L. (2020) Biological effects of Cannabidiol on normal human healthy cell populations: Systematic review of the literature. *Biomedicine & Pharmacotherapy*, 132, 110728.

Park, J.S., Gabel, A.M., Kassir, P., Kang, L., Chowdhary, P.K., Osei-Ntansah, A., Tran, N.D., Viswanathan, S., Canales, B. and Ding, P. (2022) N-myc downstream regulated gene 1 (ndrg1) functions as a molecular switch for cellular adaptation to hypoxia. *Elife*, 11, e74031.

Peng, J., Fan, M., An, C., Ni, F., Huang, W. and Luo, J. (2022) A narrative review of molecular mechanism and therapeutic effect of cannabidiol (CBD). *Basic & Clinical Pharmacology & Toxicology*, 130 (4), 439-456.

Periasamy, M., Herrera, J.L. and Reis, F.C. (2017) Skeletal muscle thermogenesis and its role in whole body energy metabolism. *Diabetes & metabolism journal*, 41 (5), 327.

Pertwee, R.G. (2006) Cannabinoid pharmacology: the first 66 years. *British journal of pharmacology*, 147 (S1), S163-S171.

Pertwee, R.G. (2014) *Handbook of cannabis*. Oxford University Press, USA.

Perucca, E. and Bialer, M. (2020) Critical aspects affecting cannabidiol oral bioavailability and metabolic elimination, and related clinical implications. *CNS drugs*, 34, 795-800.

Peters, E.N., Yardley, H., Harrison, A., Eglit, G.M., Antonio, J., Turcotte, C. and Bonn-Miller, M.O. (2023) A randomized, double-blind, placebo-controlled, repeated-dose pilot study of the safety, tolerability, and preliminary effects of a cannabidiol (CBD)-and cannabigerol (CBG)-based beverage powder to support recovery from delayed onset muscle soreness (DOMS). *Journal of the International Society of Sports Nutrition*, 20 (1), 2280113.

Phillips, S.M., Glover, E.I. and Rennie, M.J. (2009) Alterations of protein turnover underlying disuse atrophy in human skeletal muscle. *Journal of Applied Physiology*, 107 (3), 645-654.

Pillon, N.J., Gabriel, B.M., Dollet, L., Smith, J.A., Sardón Puig, L., Botella, J., Bishop, D.J., Krook, A. and Zierath, J.R. (2020) Transcriptomic profiling of skeletal muscle adaptations to exercise and inactivity. *Nature communications*, 11 (1), 470.

Piomelli, D. and Russo, E.B. (2016) The Cannabis sativa versus Cannabis indica debate: an interview with Ethan Russo, MD. *Cannabis and Cannabinoid Research*, 1 (1), 44-46.

Pisanello, D. and Caruso, G. (2018) *Novel foods in the European Union*. Springer.

Pressman, P., Hayes, A.W., Hoeng, J., Latino, D.A., Mazurov, A., Schlage, W.K. and Rana, A. (2024) Δ9-Tetrahydrocannabinol (THC): a critical overview of recent clinical trials and suggested guidelines for future research. *Journal of clinical medicine*, 13 (6), 1540.

Proudfoot, C.J., Garry, E.M., Cottrell, D.F., Rosie, R., Anderson, H., Robertson, D.C., Fleetwood-Walker, S.M. and Mitchell, R. (2006) Analgesia mediated by the TRPM8 cold receptor in chronic neuropathic pain. *Current Biology*, 16 (16), 1591-1605.

Puntel, L.A., Sawyer, J.E., Barker, D.W., Dietzel, R., Poffenbarger, H., Castellano, M.J., Moore, K.J., Thorburn, P. and Archontoulis, S.V. (2016) Modeling long-term corn yield response to nitrogen rate and crop rotation. *Frontiers in plant science*, 7, 1630.

Reimúndez, A., Fernández-Peña, C., García, G., Fernández, R., Ordás, P., Gallego, R., Pardo-Vazquez, J.L., Arce, V., Viana, F. and Señarís, R. (2018) Deletion of the cold thermoreceptor TRPM8 increases heat loss and food intake leading to reduced body temperature and obesity in mice. *Journal of Neuroscience*, 38 (15), 3643-3656.

Rickards, L., Lynn, A., Harrop, D., Barker, M.E., Russell, M. and Ranchordas, M.K. (2021) Effect of Polyphenol-Rich Foods, Juices, and Concentrates on Recovery from Exercise Induced Muscle Damage: A Systematic Review and Meta-Analysis. *Nutrients*, 13 (9).

Rohlfs, I.C.P.d.M., Rotta, T.M., Luft, C.D.B., Andrade, A., Krebs, R.J. and Carvalho, T.d. (2008) Brunel Mood Scale (BRUMS): an instrument for early detection of overtraining syndrome. *Revista Brasileira de Medicina Do Esporte*, 14, 176-181.

Rosenbaum, T., Morales-Lázaro, S.L. and Islas, L.D. (2022) TRP channels: a journey towards a molecular understanding of pain. *Nature Reviews Neuroscience*, 23 (10), 596-610.

Russo, E.B. (2019) The case for the entourage effect and conventional breeding of clinical cannabis: no "strain," no gain. *Frontiers in plant science*, 1969.

Sahinovic, A., Irwin, C., Doohan, P.T., Kevin, R.C., Cox, A.J., Lau, N.S., Desbrow, B., Johnson, N.A., Sabag, A. and Hislop, M. (2022) Effects of Cannabidiol on Exercise Physiology and Bioenergetics: A Randomised Controlled Pilot Trial. *Sports Medicine-Open*, 8 (1), 1-18.

Sainz-Cort, A., Müller-Sánchez, C. and Espel, E. (2020) Anti-proliferative and cytotoxic effect of cannabidiol on human cancer cell lines in presence of serum. *BMC research notes*, 13, 1-6.

Sakal, C., Lynskey, M., Schlag, A. and Nutt, D. (2021) Developing a real-world evidence base for prescribed cannabis in the United Kingdom: preliminary findings from Project Twenty21. *Psychopharmacology*, 1-9.

Salehi, A., Puchalski, K., Shokoohinia, Y., Zolfaghari, B. and Asgary, S. (2022) Differentiating cannabis products: Drugs, food, and supplements. *Frontiers in pharmacology*, 13, 906038.

Saltin, B. (1973) Metabolic fundamentals in exercise. *Medicine and science in sports*, 5 (3), 137-146.

Sams, L., Langdown, B.L., Simons, J. and Vseteckova, J. (2023) The effect of percussive therapy on musculoskeletal performance and experiences of pain: a systematic literature review. *International journal of sports physical therapy*, 18 (2), 309.

Schlag, A.K. (2020) An evaluation of regulatory regimes of medical cannabis: what lessons can be learned for the UK? *Medical Cannabis and Cannabinoids*, 3 (1), 76-83.

Schneider, T., Zurbriggen, L., Dieterle, M., Mauermann, E., Frei, P., Mercer-Chalmers-Bender, K. and Ruppen, W. (2022) Pain response to cannabidiol in induced acute nociceptive pain, allodynia, and hyperalgesia by using a model mimicking acute pain in healthy adults in a randomized trial (CANAB I). *Pain*, 163 (1), e62-e71.

Schoenfeld, B.J. (2012) The Use of Nonsteroidal anti-inflammatory drugs for exercise-induced muscle damage. *Sports Medicine*, 42 (12), 1017-1028.

Schönke, M., Martinez-Tellez, B. and Rensen, P.C. (2020) Role of the endocannabinoid system in the regulation of the skeletal muscle response to exercise. *Current opinion in pharmacology*, 52, 52-60.

Seçkin, A.Ç., Ateş, B. and Seçkin, M. (2023) Review on Wearable Technology in sports: Concepts, Challenges and opportunities. *Applied sciences*, 13 (18), 10399.

Sekar, K. and Pack, A. (2019) Epidiolex as adjunct therapy for treatment of refractory epilepsy: a comprehensive review with a focus on adverse effects. *F1000Research*, 8.

Sharples, A.P. and Stewart, C.E. (2011) Myoblast models of skeletal muscle hypertrophy and atrophy. *Current Opinion in Clinical Nutrition & Metabolic Care*, 14 (3), 230-236.

Shepard, E.M. and Blackley, P.R. (2016) Medical marijuana and crime: Further evidence from the western states. *Journal of Drug Issues*, 46 (2), 122-134.

Singh, J. and Neary, J.P. (2020) Neuroprotection following concussion: the potential role for cannabidiol. *Canadian Journal of Neurological Sciences*, 47 (3), 289-300.

Singh, K., Bhushan, B., Chanchal, D.K., Sharma, S.K., Rani, K., Yadav, M.K., Porwal, P., Kumar, S., Sharma, A. and Virmani, T. (2023) Emerging therapeutic potential of cannabidiol (CBD) in neurological disorders: a comprehensive review. *Behavioural neurology*, 2023 (1), 8825358.

Singlár, Z., Ganbat, N., Szentesi, P., Osgonsandag, N., Szabó, L., Telek, A., Fodor, J., Dienes, B., Gönczi, M. and Csernoch, L. (2022) Genetic manipulation of CB1 cannabinoid receptors reveals a role in maintaining proper skeletal muscle morphology and function in mice. *International journal of molecular sciences*, 23 (24), 15653.

Skelley, J.W., Deas, C.M., Curren, Z. and Ennis, J. (2020) Use of cannabidiol in anxiety and anxiety-related disorders. *Journal of the American Pharmacists Association*, 60 (1), 253-261.

Stiefel, P., Schmidt-Emrich, S., Maniura-Weber, K. and Ren, Q. (2015) Critical aspects of using bacterial cell viability assays with the fluorophores SYTO9 and propidium iodide. *BMC microbiology*, 15 (1), 1-9.

Storozhuk, M.V. (2023) Cannabidiol: potential in treatment of neurological diseases, flax as a possible natural source of cannabidiol. *Frontiers in Cellular Neuroscience*, 17, 1131653.

Stump, C.S., Henriksen, E.J., Wei, Y. and Sowers, J.R. (2006) The metabolic syndrome: role of skeletal muscle metabolism. *Annals of medicine*, 38 (6), 389-402.

Sugiura, T., Kondo, S., Sukagawa, A., Nakane, S., Shinoda, A., Itoh, K., Yamashita, A. and Waku, K. (1995) 2-Arachidonoylgylcerol: a possible endogenous cannabinoid receptor ligand in brain. *Biochemical and biophysical research communications*, 215 (1), 89-97.

Tahir, M.N., Shahbazi, F., Rondeau-Gagné, S. and Trant, J.F. (2021) The biosynthesis of the cannabinoids. *Journal of Cannabis Research*, 3, 1-12.

Taylor, B.N., Mueller, M. and Sauls, R.S. (2018) Cannaboinoid antiemetic therapy.

Taylor, L., Gidal, B., Blakey, G., Tayo, B. and Morrison, G. (2018) A phase I, randomized, double-blind, placebo-controlled, single ascending dose, multiple dose, and food effect trial of the safety, tolerability and pharmacokinetics of highly purified cannabidiol in healthy subjects. *CNS drugs*, 32 (11), 1053-1067.

Tedesco, L., Valerio, A., Dossena, M., Cardile, A., Ragni, M., Pagano, C., Pagotto, U., Carruba, M.O., Vettor, R. and Nisoli, E. (2010) Cannabinoid receptor stimulation impairs mitochondrial biogenesis in mouse white adipose tissue, muscle, and liver: the role of eNOS, p38 MAPK, and AMPK pathways. *Diabetes*, 59 (11), 2826-2836.

Ten Haaf, D.S., Bongers, C.C., Hulshof, H.G., Eijsvogels, T.M. and Hopman, M.T. (2020) The Impact of Protein Supplementation on Exercise-Induced Muscle Damage, Soreness and Fatigue Following Prolonged Walking Exercise in Vital Older Adults: A Randomized Double-Blind Placebo-Controlled Trial. *Nutrients*, 12 (6), 1806.

Terman, A., Gustafsson, B. and Brunk, U. (2007) Autophagy, organelles and ageing. *The Journal of Pathology: A Journal of the Pathological Society of Great Britain and Ireland*, 211 (2), 134-143.

Thevis, M., Kuuranne, T. and Geyer, H. (2024) Annual banned-substance review 16th edition—Analytical approaches in human sports drug testing 2022/2023. *Drug Testing and Analysis*, 16 (1), 5-29.

Thomas, K.C., Sabnis, A.S., Johansen, M.E., Lanza, D.L., Moos, P.J., Yost, G.S. and Reilly, C.A. (2007) Transient receptor potential vanilloid 1 agonists cause endoplasmic reticulum stress and cell death in human lung cells. *The Journal of pharmacology and experimental therapeutics*, 321 (3), 830-838.

Tian, J., Geiss, C., Zarse, K., Madreiter-Sokolowski, C.T. and Ristow, M. (2021) Green tea catechins EGCG and ECG enhance the fitness and lifespan of Caenorhabditis elegans by complex I inhibition. *Aging (Albany NY)*, 13 (19), 22629.

Toczek, M. and Malinowska, B. (2018) Enhanced endocannabinoid tone as a potential target of pharmacotherapy. *Life sciences*, 204, 20-45.

Tran, T. and Kavuluru, R. (2020) Social media surveillance for perceived therapeutic effects of cannabidiol (CBD) products. *International Journal of Drug Policy*, 77, 102688.

Trappe, T.A., White, F., Lambert, C.P., Cesar, D., Hellerstein, M. and Evans, W.J. (2002) Effect of ibuprofen and acetaminophen on postexercise muscle protein synthesis. *American Journal of Physiology-Endocrinology and Metabolism*, 282 (3), E551-E556.

Tsitsimpikou, C., Jamurtas, A., Fitch, K., Papalexis, P. and Tsarouhas, K. (2009) Medication use by athletes during the Athens 2004 Paralympic Games. *British Journal of Sports Medicine*, 43 (13), 1062-1066.

Tsuboi, K., Uyama, T., Okamoto, Y. and Ueda, N. (2018) Endocannabinoids and related N-acylethanolamines: biological activities and metabolism. *Inflammation and Regeneration*, 38, 1-10.

Turkoglu, S.A. and Kockar, F. (2016) SP1 and USF differentially regulate ADAMTS1 gene expression under normoxic and hypoxic conditions in hepatoma cells. *Gene*, 575 (1), 48-57.

Ujváry, I. and Hanuš, L. (2016) Human metabolites of cannabidiol: a review on their formation, biological activity, and relevance in therapy. *Cannabis and Cannabinoid Research*, 1 (1), 90-101.

Urits, I., Gress, K., Charipova, K., Habib, K., Lee, D., Lee, C., Jung, J.W., Kassem, H., Cornett, E. and Paladini, A. (2020) Use of cannabidiol (CBD) for the treatment of chronic pain. *Best Practice & Research Clinical Anaesthesiology*, 34 (3), 463-477.

Valdeolivas, S., Navarrete, C., Cantarero, I., Bellido, M.L., Muñoz, E. and Sagredo, O. (2015) Neuroprotective properties of cannabigerol in Huntington's disease: studies in R6/2 mice and 3-nitropropionate-lesioned mice. *Neurotherapeutics*, 12 (1), 185-199.

Vercherat, C., Chung, T.-K., Yalcin, S., Gulbagci, N., Gopinadhan, S., Ghaffari, S. and Taneja, R. (2009) Stra13 regulates oxidative stress mediated skeletal muscle degeneration. *Human molecular genetics*, 18 (22), 4304-4316.

Vernec, A., Pipe, A. and Slack, A. (2017) A painful dilemma? Analgesic use in sport and the role of anti-doping. [online]
Available at:

Vieira, A.F., Costa, R.R., Macedo, R.C.O., Coconcelli, L. and Kruel, L.F.M. (2016) Effects of aerobic exercise performed in fasted v. fed state on fat and carbohydrate metabolism in adults: a systematic review and meta-analysis. *British Journal of Nutrition*, 116 (7), 1153-1164.

Vogel, C. and Marcotte, E.M. (2012) Insights into the regulation of protein abundance from proteomic and transcriptomic analyses. *Nature reviews genetics*, 13 (4), 227-232.

Vollner, L., Bieniek, D. and Korte, F. (1969) Hashish. XX. Cannabidivarin, a new hashish constituent. *Tetrahedron letters* (3), 145-147.

Vučković, S., Srebro, D., Vujović, K.S., Vučetić, Č. and Prostran, M. (2018) Cannabinoids and pain: new insights from old molecules. *Frontiers in pharmacology*, 9, 416167.

WADA (2025) *Prohibited List 2025* [online]
Available at: https://www.wada-ama.org/en/news/wadas-2025-prohibited-list-now-force
[Accessed:

Waddington, I. and Møller, V. (2019) WADA at twenty: old problems and old thinking? *International Journal of Sport Policy and Politics*, 11 (2), 219-231.

Wagoner, K.G., Lazard, A.J., Romero-Sandoval, E.A. and Reboussin, B.A. (2021) Health claims about cannabidiol products: a retrospective analysis of US Food and Drug Administration warning letters from 2015 to 2019. *Cannabis and cannabinoid research*, 6 (6), 559-563.

Walder, R.Y., Radhakrishnan, R., Loo, L., Rasmussen, L.A., Mohapatra, D.P., Wilson, S.P. and Sluka, K.A. (2012) TRPV1 is important for mechanical and heat sensitivity in uninjured animals and development of heat hypersensitivity after muscle inflammation. *Pain®*, 153 (8), 1664-1672.

Waldron, M. and Highton, J. (2014) Fatigue and pacing in high-intensity intermittent team sport: an update. *Sports Medicine*, 44 (12), 1645-1658.

Wheeler, M., Merten, J.W., Gordon, B.T. and Hamadi, H. (2020) CBD (cannabidiol) product attitudes, knowledge, and use among young adults. *Substance use & misuse*, 55 (7), 1138-1145.

Wiewelhove, T., Döweling, A., Schneider, C., Hottenrott, L., Meyer, T., Kellmann, M., Pfeiffer, M. and Ferrauti, A. (2019) A meta-analysis of the effects of foam rolling on performance and recovery. *Frontiers in physiology*, 10, 449926.

Wiley, J.L. and Martin, B.R. (2002) Cannabinoid pharmacology: implications for additional cannabinoid receptor subtypes. *Chemistry and physics of lipids*, 121 (1-2), 57-63.

Williams, N.N.B., Ewell, T.R., Abbotts, K.S.S., Harms, K.J., Woelfel, K.A., Dooley, G.P., Weir, T.L. and Bell, C. (2021) Comparison of five oral cannabidiol preparations in adult humans: pharmacokinetics, body composition, and heart rate variability. *Pharmaceuticals*, 14 (1), 35.

Wishart, D.S., Hiebert-Giesbrecht, M., Inchehborouni, G., Cao, X., Guo, A.C., LeVatte, M.A., Torres-Calzada, C., Gautam, V., Johnson, M., Liigand, J., Wang, F., Zahrei, S., Bhumireddy, S., Wang, Y., Zheng, J., Mandal, R. and Dyck, J.R.B. (2024) Chemical Composition of Commercial Cannabis. *J Agric Food Chem*.

Wong, A., Keats, K., Rooney, K., Hicks, C., Allsop, D.J., Arnold, J.C. and McGregor, I.S. (2014) Fasting and exercise increase plasma cannabinoid levels in THC pre-treated rats: an examination of behavioural consequences. *Psychopharmacology*, 231, 3987-3996.

Wong, A., Montebello, M.E., Norberg, M.M., Rooney, K., Lintzeris, N., Bruno, R., Booth, J., Arnold, J.C. and McGregor, I.S. (2013) Exercise increases plasma THC concentrations in regular cannabis users. *Drug and alcohol dependence*, 133 (2), 763-767.

Wright, M., Di Ciano, P. and Brands, B. (2020) Use of cannabidiol for the treatment of anxiety: a short synthesis of pre-clinical and clinical evidence. *Cannabis and Cannabinoid Research*, 5 (3), 191-196.

Wu, H., Kanatous, S.B., Thurmond, F.A., Gallardo, T., Isotani, E., Bassel-Duby, R. and Williams, R.S. (2002) Regulation of mitochondrial biogenesis in skeletal muscle by CaMK. *Science*, 296 (5566), 349-352.

Yaffe, D. and Saxel, O. (1977) A myogenic cell line with altered serum requirements for differentiation. *Differentiation*, 7 (1-3), 159-166.

Yang, J. (2014) Enhanced skeletal muscle for effective glucose homeostasis. *Progress in molecular biology and translational science*, 121, 133-163.

Yu, T.-S., Cheng, Z.-H., Li, L.-Q., Zhao, R., Fan, Y.-Y., Du, Y., Ma, W.-X. and Guan, D.-W. (2010) The cannabinoid receptor type 2 is time-dependently expressed during skeletal muscle wound healing in rats. *International journal of legal medicine*, 124, 397-404.

Zandonai, T., Holgado, D., Ciria, L.F., Zabala, M., Hopker, J., Bekinschtein, T. and Sanabria, D. (2021) Novel evidence on the effect of tramadol on self-paced high-intensity cycling. *Journal of sports sciences*, 39 (13), 1452-1460.

Zhai, K., Liskova, A., Kubatka, P. and Büsselberg, D. (2020) Calcium entry through TRPV1: a potential target for the regulation of proliferation and apoptosis in cancerous and healthy cells. *International journal of molecular sciences*, 21 (11), 4177.

Zou, S. and Kumar, U. (2018) Cannabinoid receptors and the endocannabinoid system: signaling and function in the central nervous system. *International journal of molecular sciences*, 19 (3), 833.

Zurlo, F., Larson, K., Bogardus, C. and Ravussin, E. (1990) Skeletal muscle metabolism is a major determinant of resting energy expenditure. *The Journal of clinical investigation*, 86 (5), 1423-1427.

10 Appendices

10.1 Appendix 1: Next-Generation RNAseq Supplementary Material

Supplementary Table 1. RNA-seq analysis report for all samples.

Sample Name	Total Reads	Total Alignments	Aligned	Unique singleton	Unique Paired	Non unique paired	Non unique singleton	Coverage	Average Coverage Depth	Average Length	Average Quality	% GC
Control 1	64,126,659	148,292,088	96.86%	0%	86.29%	10.57%	0%	2.90%	119.88	64.46	33.41	50.52%
Control 2	22,713,571	52,619,782	97.00%	0%	86.45%	10.55%	0%	2.34%	52.69	64.46	33.42	50.59%
Control 3	23,564,379	55,805,953	97.51%	0%	85.94%	11.56%	0%	2.46%	53.24	64.46	33.41	50.20%
Control 4	19,886,054	46,270,354	97.19%	0%	86.44%	10.75%	0%	2.18%	49.73	64.46	33.43	50.39%
Control 5	15,546,529	36,181,618	97.27%	0%	86.66%	10.62%	0%	2.11%	40.19	64.46	33.43	50.73%
Control 6	24,091,894	56,408,542	97.02%	0%	85.84%	11.18%	0%	2.30%	57.53	64.46	33.42	50.47%
CBD 1	21,174,045	49,396,243	96.97%	0%	86.13%	10.84%	0%	2.14%	54.31	64.46	33.42	50.92%
CBD 2	18,267,709	42,158,999	97.62%	0%	87.82%	9.79%	0%	2.36%	42.02	64.46	33.42	50.87%
CBD 3	25,160,078	58,288,151	97.69%	0%	87.59%	10.09%	0%	2.58%	53.05	64.46	33.42	50.99%
CBD 4	21,655,022	50,251,580	97.51%	0%	87.17%	10.34%	0%	2.42%	48.74	64.46	33.42	50.65%
CBD 5	25,092,971	58,369,189	97.55%	0%	87.18%	10.38%	0%	2.57%	53.4	64.46	33.42	51.14%
CBD 6	16,656,862	39,195,786	97.24%	0%	85.89%	11.35%	0%	2.21%	41.7	64.46	33.41	50.67%
sCBD 1	18,354,631	42,798,242	97.51%	0%	86.93%	10.58%	0%	2.32%	43.32	64.46	33.43	50.36%
sCBD 2	25,542,692	60,510,362	97.35%	0%	85.70%	11.65%	0%	2.50%	56.83	64.47	33.42	50.05%
sCBD 3	21,107,615	49,347,107	97.28%	0%	86.45%	10.83%	0%	2.41%	48.17	64.46	33.42	50.81%
sCBD 4	19,061,367	44,379,116	96.63%	0%	85.80%	10.83%	0%	2.25%	46.24	64.46	33.45	50.93%
sCBD 5	22,163,696	51,559,992	97.30%	0%	86.76%	10.54%	0%	2.52%	47.96	64.46	33.42	50.75%
sCBD 6	20,816,663	48,730,997	97.35%	0%	86.56%	10.79%	0%	2.15%	53.24	64.46	33.42	50.98%

Supplementary Table 2. Details of genes included in Markov clusters for commonly up-regulated genes presented in figure 5.

Cluster number	Cluster colour	Gene count	Protein name	Protein identifier	Protein description
1	Red	38	Atf4	10090.ENSMUSP00000105234	Cyclic AMP-dependent transcription factor ATF-4; Transcriptional activator.
1	Red	38	Atf6	10090.ENSMUSP00000027974	Processed cyclic AMP-dependent transcription factor ATF-6 alpha; Transmembrane glycoprotein of the endoplasmic reticulum that functions as a transcription activator and initiates the unfolded protein response (UPR) during endoplasmic reticulum stress.
1	Red	38	Atf6b	10090.ENSMUSP00000015605	Processed cyclic AMP-dependent transcription factor ATF-6 beta; Transcriptional factor that acts in the unfolded protein response (UPR) pathway by activating UPR target genes induced during ER stress.
1	Red	38	Atp2a2	10090.ENSMUSP00000031423	Sarcoplasmic/endoplasmic reticulum calcium ATPase 2; This magnesium-dependent enzyme catalyzes the hydrolysis of ATP coupled with the translocation of calcium from the cytosol to the sarcoplasmic reticulum lumen.
1	Red	38	Calr	10090.ENSMUSP00000003912	Calreticulin; Calcium-binding chaperone that promotes folding, oligomeric assembly and quality control in the endoplasmic reticulum (ER) via the calreticulin/calnexin cycle.
1	Red	38	Canx	10090.ENSMUSP00000137440	Calnexin; Calcium-binding protein that interacts with newly synthesized glycoproteins in the endoplasmic reticulum.
1	Red	38	Cd14	10090.ENSMUSP00000056669	Monocyte differentiation antigen CD14; Coreceptor for bacterial lipopolysaccharide.
1	Red	38	Cebpa	10090.ENSMUSP00000096129	CCAAT/enhancer-binding protein alpha; Transcription factor that coordinates proliferation arrest and the differentiation of myeloid progenitors, adipocytes, hepatocytes, and cells of the lung and the placenta.
1	Red	38	Cebpb	10090.ENSMUSP00000069850	CCAAT/enhancer-binding protein beta; Important transcription factor regulating the expression of genes involved in immune and inflammatory responses.
1	Red	38	Cebpd	10090.ENSMUSP00000148145	CCAAT/enhancer-binding protein delta; Transcription activator that recognizes two different DNA motifs: the CCAAT homology common to many promoters and the enhanced core homology common to many enhancers.
1	Red	38	Cebpg	10090.ENSMUSP00000118588	CCAAT/enhancer-binding protein gamma; Transcription factor that binds to the promoter and the enhancer regions of target genes.
1	Red	38	Dnajc1	10090.ENSMUSP00000126321	DnaJ homolog subfamily C member 1; May modulate protein synthesis.
1	Red	38	Hsp90b1	10090.ENSMUSP00000020238	Endoplasmin; Molecular chaperone that functions in the processing and transport of secreted proteins.
1	Red	38	Hspa1b	10090.ENSMUSP00000133815	Heat shock 70 kDa protein 1B; Molecular chaperone implicated in a wide variety of cellular processes, including protection of the proteome from stress, folding and transport of newly synthesized polypeptides, activation of proteolysis of misfolded proteins and the formation and dissociation of protein complexes.
1	Red	38	Hspa4l	10090.ENSMUSP00000145468	Heat shock 70 kDa protein 4L; Possesses chaperone activity in vitro where it inhibits aggregation of citrate synthase.
1	Red	38	Hspa5	10090.ENSMUSP00000028222	Endoplasmic reticulum chaperone BiP; Endoplasmic reticulum chaperone that plays a key role in protein folding and quality control in the endoplasmic reticulum lumen.
1	Red	38	Hspa8	10090.ENSMUSP00000015800	Heat shock cognate 71 kDa protein; Molecular chaperone implicated in a wide variety of cellular processes, including protection of the proteome from stress, folding and transport of newly synthesized polypeptides, activation of proteolysis of misfolded proteins and the formation and dissociation of protein complexes.
1	Red	38	Hspa9	10090.ENSMUSP00000025217	Stress-70 protein, mitochondrial; Chaperone protein which plays an important role in mitochondrial iron-sulfur cluster (ISC) biogenesis.

1	Red	38	Hspd1	10090.ENSMUSP00000027123	60 kDa heat shock protein, mitochondrial; Chaperonin implicated in mitochondrial protein import and macromolecular assembly.
1	Red	38	Hsph1	10090.ENSMUSP00000144413	Heat shock protein 105 kDa; Acts as a nucleotide-exchange factor (NEF) for chaperone proteins HSPA1A and HSPA1B, promoting the release of ADP from HSPA1A/B thereby triggering client/substrate protein release. Prevents the aggregation of denatured proteins in cells under severe stress, on which the ATP levels decrease markedly. Inhibits HSPA8/HSC70 ATPase and chaperone activities.
1	Red	38	Hyou1	10090.ENSMUSP00000123700	Hypoxia up-regulated protein 1; Has a pivotal role in cytoprotective cellular mechanisms triggered by oxygen deprivation.
1	Red	38	Il1rap	10090.ENSMUSP00000093843	Interleukin-1 receptor accessory protein; Coreceptor for IL1RL2 in the IL-36 signaling system. Coreceptor with IL1R1 in the IL-1 signaling system.
1	Red	38	Il33	10090.ENSMUSP00000025724	Interleukin-33(102-266); Cytokine that binds to and signals through the IL1RL1/ST2 receptor which in turn activates NF-kappa-B and MAPK signaling pathways in target cells. Involved in the maturation of Th2 cells inducing the secretion of T-helper type 2-associated cytokines. Also involved in activation of mast cells, basophils, eosinophils and natural killer cells. Acts as a chemoattractant for Th2 cells, and may function as an 'alarmin', that amplifies immune responses during tissue injury; Belongs to the IL-1 family. Highly divergent.
1	Red	38	Itpr3	10090.ENSMUSP00000038150	Inositol 1,4,5-trisphosphate receptor type 3; Receptor for inositol 1,4,5-trisphosphate, a second messenger that mediates the release of intracellular calcium.
1	Red	38	Lamp2	10090.ENSMUSP00000074448	Lysosome-associated membrane glycoprotein 2; Plays an important role in chaperone-mediated autophagy. Functions by binding target proteins, such as GAPDH and MLLT11, and targeting them for lysosomal degradation. Required for the fusion of autophagosomes with lysosomes during autophagy.
1	Red	38	Manf	10090.ENSMUSP00000124562	Mesencephalic astrocyte-derived neurotrophic factor; Selectively promotes the survival of dopaminergic neurons of the ventral mid-brain.
1	Red	38	Myd88	10090.ENSMUSP00000035092	Myeloid differentiation primary response protein MyD88; Adapter protein involved in the Toll-like receptor and IL-1 receptor signaling pathway in the innate immune response.
1	Red	38	P4ha2	10090.ENSMUSP00000019050	Prolyl 4-hydroxylase subunit alpha-2; Catalyzes the post-translational formation of 4- hydroxyproline in -Xaa-Pro-Gly- sequences in collagens and other proteins.
1	Red	38	P4hb	10090.ENSMUSP00000026122	Protein disulfide-isomerase; This multifunctional protein catalyzes the formation, breakage and rearrangement of disulfide bonds.
1	Red	38	Pdia3	10090.ENSMUSP00000028683	Protein disulfide-isomerase A3.
1	Red	38	Pdia4	10090.ENSMUSP00000076521	Protein disulfide-isomerase A4.
1	Red	38	Plin2	10090.ENSMUSP00000000466	Perilipin-2; May be involved in development and maintenance of adipose tissue.
1	Red	38	Plin3	10090.ENSMUSP00000019726	Perilipin-3; Required for the transport of mannose 6-phosphate receptors (MPR) from endosomes to the trans-Golgi network; Belongs to the perilipin family.
1	Red	38	Sdf2l1	10090.ENSMUSP00000023453	Stromal cell-derived factor 2-like protein 1.
1	Red	38	Sigmar1	10090.ENSMUSP00000056027	Sigma non-opioid intracellular receptor 1; Functions in lipid transport from the endoplasmic reticulum and is involved in a wide array of cellular functions probably through regulation of the biogenesis of lipid microdomains at the plasma membrane.
1	Red	38	St13	10090.ENSMUSP00000130195	Hsc70-interacting protein; One HIP oligomer binds the ATPase domains of at least two HSC70 molecules dependent on activation of the HSC70 ATPase by HSP40.

1	Red	38	Tirap	10090.ENSMUSP00000135435	Toll/interleukin-1 receptor domain-containing adapter protein; Adapter involved in the TLR2 and TLR4 signaling pathways in the innate immune response. Acts via IRAK2 and TRAF-6, leading to the activation of NF-kappa-B, MAPK1, MAPK3 and JNK, and resulting in cytokine secretion and the inflammatory response. Positively regulates the production of TNF-alpha and interleukin-6.
1	Red	38	Tlr4	10090.ENSMUSP00000045770	Toll-like receptor 4; Cooperates with LY96 and CD14 to mediate the innate immune response to bacterial lipopolysaccharide (LPS). Acts via MYD88, TIRAP and TRAF6, leading to NF-kappa-B activation, cytokine secretion and the inflammatory response. Also involved in LPS- independent inflammatory responses triggered by free fatty acids, such as palmitate.
2	Salmon	6	Atp6ap1	10090.ENSMUSP00000019231	V-type proton ATPase subunit S1; Accessory subunit of the proton-transporting vacuolar (V)- ATPase protein pump, which is required for luminal acidification of secretory vesicles. Guides the V-type ATPase into specialized subcellular compartments, such as neuroendocrine regulated secretory vesicles or the ruffled border of the osteoclast, thereby regulating its activity. Involved in membrane trafficking and Ca^{2+}-dependent membrane fusion.
2	Salmon	6	Atp6v0b	10090.ENSMUSP00000047682	V-type proton ATPase 21 kDa proteolipid subunit; Proton-conducting pore forming subunit of the membrane integral V0 complex of vacuolar ATPase. V-ATPase is responsible for acidifying a variety of intracellular compartments in eukaryotic cells.
2	Salmon	6	Atp6v0c	10090.ENSMUSP00000024932	V-type proton ATPase 16 kDa proteolipid subunit; Proton-conducting pore forming subunit of the membrane integral V0 complex of vacuolar ATPase. V-ATPase is responsible for acidifying a variety of intracellular compartments in eukaryotic cells.
2	Salmon	6	Atp6v1a	10090.ENSMUSP00000110314	V-type proton ATPase catalytic subunit A; Catalytic subunit of the peripheral V1 complex of vacuolar ATPase. V-ATPase vacuolar ATPase is responsible for acidifying a variety of intracellular compartments in eukaryotic cells. In aerobic conditions, involved in intracellular iron homeostasis, thus triggering the activity of Fe(2+) prolyl hydroxylase (PHD) enzymes, and leading to HIF1A hydroxylation and subsequent proteasomal degradation.
2	Salmon	6	Atp6v1b2	10090.ENSMUSP00000006435	V-type proton ATPase subunit B, brain isoform; Non-catalytic subunit of the peripheral V1 complex of vacuolar ATPase. V-ATPase is responsible for acidifying a variety of intracellular compartments in eukaryotic cells.
2	Salmon	6	Atp6v1c1	10090.ENSMUSP00000022904	V-type proton ATPase subunit C 1; Subunit of the peripheral V1 complex of vacuolar ATPase. Subunit C is necessary for the assembly of the catalytic sector of the enzyme and is likely to have a specific function in its catalytic activity. V-ATPase is responsible for acidifying a variety of intracellular compartments in eukaryotic cells.
3	Fire Brick	4	Maff	10090.ENSMUSP00000094076	Transcription factor MafF; Since they lack a putative transactivation domain, the small Mafs behave as transcriptional repressors when they dimerize among themselves. However, they seem to serve as transcriptional activators by dimerizing with other (usually larger) basic-zipper proteins, such as NFE2L1/NRF1, and recruiting them to specific DNA-binding sites. Interacts with the upstream promoter region of the oxytocin receptor gene. May be a transcriptional enhancer in the up-regulation of the oxytocin receptor gene at parturition.
3	Fire Brick	4	Mafg	10090.ENSMUSP00000053899	Transcription factor MafG; Since they lack a putative transactivation domain, the small Mafs behave as transcriptional repressors when they dimerize among themselves. However, they seem to serve as transcriptional activators by dimerizing with other (usually larger) basic-zipper proteins, such as NFE2, NFE2L1 and NFE2L2, and recruiting them to specific DNA-binding sites.
3	Fire Brick	4	Mafk	10090.ENSMUSP00000106460	Transcription factor MafK; Since they lack a putative transactivation domain, the small Mafs behave as transcriptional repressors when they dimerize among themselves (By similarity). However, they act as transcriptional activators by dimerizing with other (usually larger) basic-zipper proteins, such as NFE2, NFE2L1/NRF1, NFE2L2/NRF2 and NFE2L3/NRF3, and recruiting them to specific DNA-binding sites. Small Maf proteins heterodimerize with Fos and may act as competitive repressors of the NF-E2 transcription factor.

3	Fire Brick	4	Nfe2l2	10090.ENSMUSP00000099733	Nuclear factor erythroid 2-related factor 2; Transcription factor that plays a key role in the response to oxidative stress: binds to antioxidant response (ARE) elements present in the promoter region of many cytoprotective genes, such as phase 2 detoxifying enzymes, and promotes their expression, thereby neutralizing reactive electrophiles.
4	Sandy Brown	3	Plpp2	10090.ENSMUSP00000069670	Phospholipid phosphatase 2; Magnesium-independent phospholipid phosphatase that catalyzes the dephosphorylation of a variety of glycerolipid and sphingolipid phosphate esters including phosphatidate/PA, lysophosphatidate/LPA, sphingosine 1-phosphate/S1P and ceramide 1-phosphate/C1P.
4	Sandy Brown	3	Sgpp1	10090.ENSMUSP00000021450	Sphingosine-1-phosphate phosphatase 1; Specifically dephosphorylates sphingosine 1-phosphate (S1P), dihydro-S1P, and phyto-S1P. Does not act on ceramide 1-phosphate, lysophosphatidic acid or phosphatidic acid.
4	Sandy Brown	3	Sphk1	10090.ENSMUSP00000131010	Sphingosine kinase 1; Catalyzes the phosphorylation of sphingosine to form sphingosine 1-phosphate (SPP), a lipid mediator with both intra- and extracellular functions.
5	Saddle Brown	3	Il13ra1	10090.ENSMUSP00000033418	Interleukin-13 receptor subunit alpha-1; Binds with low affinity to interleukin-13 (IL13). Together with IL4RA can form a functional receptor for IL13.
5	Saddle Brown	3	Il13ra2	10090.ENSMUSP00000033646	Interleukin-13 receptor subunit alpha-2; Binds as a monomer with high affinity to interleukin-13 (IL13); Belongs to the type I cytokine receptor family. Type 5 subfamily.
5	Saddle Brown	3	Il4ra	10090.ENSMUSP00000033004	Soluble interleukin-4 receptor subunit alpha; Receptor for both interleukin 4 and interleukin 13.
6	Sandy Brown 2	3	Rpn1	10090.ENSMUSP00000032143	Dolichyl-diphosphooligosaccharide--protein glycosyltransferase subunit 1; Subunit of the oligosaccharyl transferase (OST) complex that catalyzes the initial transfer of a defined glycan (Glc(3)Man(9)GlcNAc(2) in eukaryotes) from the lipid carrier dolichol- pyrophosphate to an asparagine residue within an Asn-X-Ser/Thr consensus motif in nascent polypeptide chains, the first step in protein N-glycosylation.
6	Sandy Brown 2	3	Stt3a	10090.ENSMUSP00000113116	Dolichyl-diphosphooligosaccharide--protein glycosyltransferase subunit STT3A; Catalytic subunit of the oligosaccharyl transferase (OST) complex that catalyzes the initial transfer of a defined glycan (Glc(3)Man(9)GlcNAc(2) in eukaryotes) from the lipid carrier dolichol- pyrophosphate to an asparagine residue within an Asn-X-Ser/Thr consensus motif in nascent polypeptide chains, the first step in protein N-glycosylation.
6	Sandy Brown 2	3	Stt3b	10090.ENSMUSP00000035010	Dolichyl-diphosphooligosaccharide--protein glycosyltransferase subunit STT3B; Catalytic subunit of the oligosaccharyl transferase (OST) complex that catalyzes the initial transfer of a defined glycan (Glc(3)Man(9)GlcNAc(2) in eukaryotes) from the lipid carrier dolichol- pyrophosphate to an asparagine residue within an Asn-X-Ser/Thr consensus motif in nascent polypeptide chains, the first step in protein N-glycosylation.
7	Dark Golden Rod	3	Utp15	10090.ENSMUSP00000048204	U3 small nucleolar RNA-associated protein 15 homolog; Ribosome biogenesis factor. Involved in nucleolar processing of pre-18S ribosomal RNA. Required for optimal pre-ribosomal RNA transcription by RNA polymerase I.
7	Dark Golden Rod	3	Utp4	10090.ENSMUSP00000048377	U3 small nucleolar RNA-associated protein 4 homolog; Ribosome biogenesis factor. Involved in nucleolar processing of pre-18S ribosomal RNA. Involved in small subunit (SSU) pre-rRNA processing at sites A', A0, 1 and 2b. Required for optimal pre-ribosomal RNA transcription by RNA polymerase. May be a transcriptional regulator. Acts as a positive regulator of HIVEP1.
7	Dark Golden Rod	3	Wdr75	10090.ENSMUSP00000027139	WD repeat-containing protein 75; Ribosome biogenesis factor. Involved in nucleolar processing of pre-18S ribosomal RNA. Required for optimal pre-ribosomal RNA transcription by RNA polymerase I.
8	Sandy Brown 3	3	Amfr	10090.ENSMUSP00000052258	E3 ubiquitin-protein ligase AMFR; E3 ubiquitin-protein ligase that mediates the polyubiquitination of a number of proteins such as CD3D, CYP3A4, CFTR and APOB for proteasomal degradation.
8	Sandy Brown 3	3	Insig1	10090.ENSMUSP00000061877	Insulin-induced gene 1 protein; Mediates feedback control of cholesterol synthesis by controlling SCAP and HMGCR. Functions by blocking the processing of sterol regulatory element-binding proteins (SREBPs).

8	Sandy Brown 3	3	Scap	10090.ENSMUSP00000095953	Sterol regulatory element-binding protein cleavage-activating protein; Escort protein required for cholesterol as well as lipid homeostasis. Regulates export of the SCAP/SREBF complex from the ER upon low cholesterol.
9	Brown	3	Dab2	10090.ENSMUSP00000079689	Disabled homolog 2; Adapter protein that functions as clathrin-associated sorting protein (CLASP) required for clathrin-mediated endocytosis of selected cargo proteins.
9	Brown	3	Dab2ip	10090.ENSMUSP00000088532	Disabled homolog 2-interacting protein; Functions as a scaffold protein implicated in the regulation of a large spectrum of both general and specialized signaling pathways. Involved in several processes such as innate immune response, inflammation and cell growth inhibition, apoptosis, cell survival, angiogenesis, cell migration and maturation.
9	Brown	3	Ldlr	10090.ENSMUSP00000034713	Low-density lipoprotein receptor; Binds LDL, the major cholesterol-carrying lipoprotein of plasma, and transports it into cells by endocytosis. In order to be internalized, the receptor-ligand complexes must first cluster into clathrin-coated pits; Belongs to the LDLR family.
10	Yellow	3	Atic	10090.ENSMUSP00000027384	Phosphoribosylaminoimidazolecarboxamide formyltransferase; Bifunctional enzyme that catalyzes 2 steps in purine biosynthesis; Belongs to the PurH family.
10	Yellow	3	Mthfd1	10090.ENSMUSP00000021443	C-1-tetrahydrofolate synthase, cytoplasmic, N-terminally processed; In the N-terminal section; belongs to the tetrahydrofolate dehydrogenase/cyclohydrolase family.
10	Yellow	3	Mthfd1l	10090.ENSMUSP00000112897	Monofunctional C1-tetrahydrofolate synthase, mitochondrial; May provide the missing metabolic reaction required to link the mitochondria and the cytoplasm in the mammalian model of one-carbon folate metabolism in embryonic an transformed cells complementing thus the enzymatic activities of MTHFD2; In the N-terminal section; belongs to the tetrahydrofolate dehydrogenase/cyclohydrolase family.
11	Green	2	Arhgdia	10090.ENSMUSP00000063714	Rho GDP-dissociation inhibitor 1; Controls Rho proteins homeostasis. Regulates the GDP/GTP exchange reaction of the Rho proteins by inhibiting the dissociation of GDP from them, and the subsequent binding of GTP to them.
11	Green	2	Ngfr	10090.ENSMUSP00000000122	Tumor necrosis factor receptor superfamily member 16; Low affinity neurotrophin receptor which can bind to mature NGF, BDNF, NTF3, and NTF4.
12	Light Green	2	Map3k3	10090.ENSMUSP00000002044	Mitogen-activated protein kinase kinase kinase 3; Component of a protein kinase signal transduction cascade. Mediates activation of the NF-kappa-B, AP1 and DDIT3 transcriptional regulators.
12	Light Green	2	Sqstm1	10090.ENSMUSP00000099835	Sequestosome-1; Autophagy receptor required for selective macroautophagy (aggrephagy). Functions as a bridge between polyubiquitinated cargo and autophagosomes. Interacts directly with both the cargo to become degraded and an autophagy modifier of the MAP1 LC3 family.
13	Medium Aqua Marine	2	Plaur	10090.ENSMUSP00000002284	Urokinase plasminogen activator surface receptor; Acts as a receptor for urokinase plasminogen activator. Plays a role in localizing and promoting plasmin formation. Mediates the proteolysis-independent signal transduction activation effects of U-PA.
13	Medium Aqua Marine	2	Serpine1	10090.ENSMUSP00000039586	Plasminogen activator inhibitor 1; Serine protease inhibitor. Inhibits TMPRSS7. Is a primary inhibitor of tissue-type plasminogen activator (PLAT) and urokinase- type plasminogen activator (PLAU).
14	Aquamarine 4	2	Lamc1	10090.ENSMUSP00000027752	Laminin subunit gamma-1; Binding to cells via a high affinity receptor, laminin is thought to mediate the attachment, migration and organization of cells into tissues during embryonic development by interacting with other extracellular matrix components.
14	Aquamarine 4	2	Nid1	10090.ENSMUSP00000005532	Nidogen-1; Sulfated glycoprotein widely distributed in basement membranes and tightly associated with laminin. Also binds to collagen IV and perlecan. It probably has a role in cell-extracellular matrix interactions.
15	Aquamarine 2	2	Hmox1	10090.ENSMUSP00000005548	Heme oxygenase 1; Heme oxygenase cleaves the heme ring at the alpha methene bridge to form biliverdin. Biliverdin is subsequently converted to bilirubin by biliverdin reductase. Under physiological conditions, the activity of heme oxygenase

					is highest in the spleen, where senescent erythrocytes are sequestrated and destroyed. Exhibits cytoprotective effects since excess of free heme sensitizes cells to undergo apoptosis.
15	Aquamarine 2	2	Por	10090.ENSMUSP00000005651	NADPH--cytochrome P450 reductase; This enzyme is required for electron transfer from NADP to cytochrome P450 in microsomes. It can also provide electron transfer to heme oxygenase and cytochrome B5; In the N-terminal section; belongs to the flavodoxin family.
16	Cyan	2	Acat2	10090.ENSMUSP00000007005	Acetyl-CoA acetyltransferase, cytosolic; Involved in the biosynthetic pathway of cholesterol.
16	Cyan	2	Acat3	10090.ENSMUSP00000125454	Acetyl-Coenzyme A acetyltransferase 3; Belongs to the thiolase-like superfamily. Thiolase family.
17	Aquamarine	2	Fads1	10090.ENSMUSP00000010807	Acyl-CoA (8-3)-desaturase; Acts as a front-end fatty acyl-coenzyme A (CoA) desaturase that introduces a cis double bond at carbon 5 located between a preexisting double bond and the carboxyl end of the fatty acyl chain.
17	Aquamarine	2	Hsd17b12	10090.ENSMUSP00000028619	Very-long-chain 3-oxoacyl-CoA reductase; Catalyzes the second of the four reactions of the long-chain fatty acids elongation cycle.
18	Aquamarine 3	2	Cd68	10090.ENSMUSP00000018918	Macrosialin; Could play a role in phagocytic activities of tissue macrophages, both in intracellular lysosomal metabolism and extracellular cell-cell and cell-pathogen interactions.
18	Aquamarine 3	2	Lamp1	10090.ENSMUSP00000033824	Lysosome-associated membrane glycoprotein 1; Presents carbohydrate ligands to selectins. Also implicated in tumor cell metastasis.
19	Sky Blue 5	2	Eprs	10090.ENSMUSP00000045841	Bifunctional glutamate/proline--tRNA ligase; Multifunctional protein which is primarily part of the aminoacyl-tRNA synthetase multienzyme complex, also know as multisynthetase complex, that catalyzes the attachment of the cognate amino acid to the corresponding tRNA in a two-step reaction: the amino acid is first activated by ATP to form a covalent intermediate with AMP and is then transferred to the acceptor end of the cognate tRNA (By similarity).
19	Sky Blue 5	2	Rars	10090.ENSMUSP00000018992	Arginine--tRNA ligase, cytoplasmic; Forms part of a macromolecular complex that catalyzes the attachment of specific amino acids to cognate tRNAs during protein synthesis. Modulates the secretion of AIMP1 and may be involved in generation of the inflammatory cytokine EMAP2 from AIMP1.
20	Sky Blue 3	2	Galc	10090.ENSMUSP00000021390	Galactocerebrosidase; Hydrolyzes the galactose ester bonds of galactosylceramide, galactosylsphingosine, lactosylceramide, and monogalactosyldiglyceride. Enzyme with very low activity responsible for the lysosomal catabolism of galactosylceramide, a major lipid in myelin, kidney and epithelial cells of small intestine and colon.
20	Sky Blue 3	2	Psap	10090.ENSMUSP00000137476	Saposin-B-Val; [Prosaposin]: Behaves as a myelinotrophic and neurotrophic factor, these effects are mediated by its G-protein-coupled receptors, GPR37 and GPR37L1, undergoing ligand-mediated internalization followed by ERK phosphorylation signaling.
21	Sky Blue	2	Fgf10	10090.ENSMUSP00000022246	Fibroblast growth factor 10; Plays an important role in the regulation of embryonic development, cell proliferation and cell differentiation. Required for normal branching morphogenesis. May play a role in wound healing; Belongs to the heparin-binding growth factors family.
21	Sky Blue	2	Fgfr1	10090.ENSMUSP00000081041	Fibroblast growth factor receptor 1; Tyrosine-protein kinase that acts as cell-surface receptor for fibroblast growth factors and plays an essential role in the regulation of embryonic development, cell proliferation, differentiation and migration.
22	Sky Blue 2	2	Bnip3l	10090.ENSMUSP00000022634	BCL2/adenovirus E1B 19 kDa protein-interacting protein 3-like; Induces apoptosis. Interacts with viral and cellular anti-apoptosis proteins.
22	Sky Blue 2	2	Steap3	10090.ENSMUSP00000108260	Metalloreductase STEAP3; Endosomal ferrireductase required for efficient transferrin- dependent iron uptake in erythroid cells. Participates in erythroid iron homeostasis by reducing Fe(3+) to Fe(2+). Also mediates reduction of Cu(2+) to Cu(1+), suggesting that it participates in copper homeostasis.

23	Sky Blue 4	2	Washc2	10090.ENSMUSP00000038983	WASH complex subunit 2; Acts at least in part as component of the WASH core complex whose assembly at the surface of endosomes inhibits WASH nucleation- promoting factor (NPF) activity in recruiting and activating the Arp2/3 complex to induce actin polymerization and is involved in the fission of tubules that serve as transport intermediates during endosome sorting.
23	Sky Blue 4	2	Washc5	10090.ENSMUSP00000022976	WASH complex subunit 5; Acts at least in part as component of the WASH core complex whose assembly at the surface of endosomes seems to inhibit WASH nucleation-promoting factor (NPF) activity in recruiting and activating the Arp2/3 complex to induce actin polymerization, and which is involved in regulation of the fission of tubules that serve as transport intermediates during endosome sorting.
24	Cornflower Blue 3	2	Got1	10090.ENSMUSP00000026196	Aspartate aminotransferase, cytoplasmic; Biosynthesis of L-glutamate from L-aspartate or L-cysteine. Important regulator of levels of glutamate, the major excitatory neurotransmitter of the vertebrate central nervous system. Acts as a scavenger of glutamate in brain neuroprotection.
24	Cornflower Blue 3	2	Got2	10090.ENSMUSP00000034097	Aspartate aminotransferase, mitochondrial; Catalyzes the irreversible transamination of the L-tryptophan metabolite L-kynurenine to form kynurenic acid (KA). Plays a key role in amino acid metabolism. Important for metabolite exchange between mitochondria and cytosol. Facilitates cellular uptake of long-chain free fatty acids.
25	Cornflower Blue	2	Il6	10090.ENSMUSP00000026845	Interleukin-6; Cytokine with a wide variety of biological functions. It is a potent inducer of the acute phase response.
25	Cornflower Blue	2	Tnfrsf1a	10090.ENSMUSP00000032491	Tumor necrosis factor receptor superfamily member 1A; Receptor for TNFSF2/TNF-alpha and homotrimeric TNFSF1/lymphotoxin-alpha.
26	Blue	2	Ssr1	10090.ENSMUSP00000021864	Translocon-associated protein subunit alpha; TRAP proteins are part of a complex whose function is to bind calcium to the ER membrane and thereby regulate the retention of ER resident proteins.
26	Blue	2	Ssr3	10090.ENSMUSP00000029414	Translocon-associated protein subunit gamma; TRAP proteins are part of a complex whose function is to bind calcium to the ER membrane and thereby regulate the retention of ER resident proteins; Belongs to the TRAP-gamma family.
27	Cornflower Blue 2	2	Gclc	10090.ENSMUSP00000034905	Glutamate--cysteine ligase catalytic subunit; Belongs to the glutamate--cysteine ligase type 3 family.
27	Cornflower Blue 2	2	Gclm	10090.ENSMUSP00000029769	Glutamate--cysteine ligase regulatory subunit; Belongs to the aldo/keto reductase family. Glutamate-- cysteine ligase light chain subfamily.
28	Medium Slate Blue	2	Pi4k2a	10090.ENSMUSP00000069284	Phosphatidylinositol 4-kinase type 2-alpha; Membrane-bound phosphatidylinositol-4 kinase (PI4-kinase) that catalyzes the phosphorylation of phosphatidylinositol (PI) to phosphatidylinositol 4-phosphate (PI4P), a lipid that plays important roles in endocytosis, Golgi function, protein sorting and membrane trafficking and is required for prolonged survival of neurons.
28	Medium Slate Blue	2	Pi4k2b	10090.ENSMUSP00000031081	Phosphatidylinositol 4-kinase type 2-beta; Together with PI4K2A and the type III PI4Ks (PIK4CA and PIK4CB) it contributes to the overall PI4-kinase activity of the cell.
29	Purple	2	Antxr1	10090.ENSMUSP00000045634	Anthrax toxin receptor 1; Plays a role in cell attachment and migration. Interacts with extracellular matrix proteins and with the actin cytoskeleton. Mediates adhesion of cells to type 1 collagen and gelatin, reorganization of the actin cytoskeleton and promotes cell spreading.
29	Purple	2	Antxr2	10090.ENSMUSP00000031281	Anthrax toxin receptor 2; Necessary for cellular interactions with laminin and the extracellular matrix; Belongs to the ATR family.
30	Medium Slate Blue 2	2	Sec61a1	10090.ENSMUSP00000032168	Protein transport protein Sec61 subunit alpha isoform 1; Component of SEC61 channel-forming translocon complex that mediates transport of signal peptide-containing precursor polypeptides across endoplasmic reticulum (ER).

30	Medium Slate Blue 2	2	Sec61b	10090.ENSMUSP00000067681	Protein transport protein Sec61 subunit beta; Component of SEC61 channel-forming translocon complex that mediates transport of signal peptide-containing precursor polypeptides across endoplasmic reticulum (ER).
31	Medium Purple	2	Adm	10090.ENSMUSP00000033054	Proadrenomedullin N-20 terminal peptide; AM and PAMP are potent hypotensive and vasodilatator agents; Belongs to the adrenomedullin family.
31	Medium Purple	2	Ramp3	10090.ENSMUSP00000047518	Receptor activity-modifying protein 3; Plays a role in cardioprotection by reducing cardiac hypertrophy and perivascular fibrosis in a GPER1-dependent manner. Transports the calcitonin gene-related peptide type 1 receptor (CALCRL) to the plasma membrane. Acts as a receptor for adrenomedullin (AM) together with CALCRL; Belongs to the RAMP family.
32	Medium Purple 2	2	Mt1	10090.ENSMUSP00000034215	Metallothionein-1; Metallothioneins have a high content of cysteine residues that bind various heavy metals; these proteins are transcriptionally regulated by both heavy metals and glucocorticoids; Belongs to the metallothionein superfamily. Type 1 family.
32	Medium Purple 2	2	Mt2	10090.ENSMUSP00000034214	Metallothionein-2; Metallothioneins have a high content of cysteine residues that bind various heavy metals; these proteins are transcriptionally regulated by both heavy metals and glucocorticoids; Belongs to the metallothionein superfamily. Type 1 family.
33	Medium Purple 3	2	Anpep	10090.ENSMUSP00000103015	Aminopeptidase N; Broad specificity aminopeptidase which plays a role in the final digestion of peptides generated from hydrolysis of proteins by gastric and pancreatic proteases. Also involved in the processing of various peptides including peptide hormones, such as angiotensin III and IV, neuropeptides, and chemokines.
33	Medium Purple 3	2	Lap3	10090.ENSMUSP00000040222	Cytosol aminopeptidase; Presumably involved in the processing and regular turnover of intracellular proteins. Catalyses the removal of unsubstituted N- terminal amino acids from various peptides.
34	Orchid 5	2	Grem1	10090.ENSMUSP00000097170	Gremlin-1; Cytokine that may play an important role during carcinogenesis and metanephric kidney organogenesis, as BMP a antagonist required for early limb outgrowth and patterning in maintaining the FGF4-SHH feedback loop. Down-regulates the BMP4 signalling in a dose-dependent manner.
34	Orchid 5	2	Grem2	10090.ENSMUSP00000049640	Gremlin-2; Cytokine that inhibits the activity of BMP2 and BMP4 in a dose-dependent manner, and thereby modulates signalling by BMP family members.
35	Orchid 4	2	Eps8	10090.ENSMUSP00000052776	Epidermal growth factor receptor kinase substrate 8; Signalling adapter that controls various cellular protrusions by regulating actin cytoskeleton dynamics and architecture.
35	Orchid 4	2	Nrn1	10090.ENSMUSP00000040900	Neuritin; Promotes neurite outgrowth and especially branching of neuritic processes in primary hippocampal and cortical cells.
36	Orchid 2	2	Chka	10090.ENSMUSP00000025760	Choline kinase alpha; Has a key role in phospholipid biosynthesis and may contribute to tumour cell growth. Catalyses the first step in phosphatidylcholine biosynthesis. Contributes to phosphatidylethanolamine biosynthesis. Phosphorylates choline and ethanolamine. Has higher activity with choline. Belongs to the choline/ethanolamine kinase family.
36	Orchid 2	2	Phospho1	10090.ENSMUSP00000057858	Phosphoethanolamine/phosphocholine phosphatase; Phosphatase that has a high activity toward phosphoethanolamine (PEA) and phosphocholine (PCho). Involved in the generation of inorganic phosphate for bone mineralization.
37	Violet 3	2	Fosl1	10090.ENSMUSP00000025850	Fos-related antigen 1; Belongs to the bZIP family. Fos subfamily.
37	Violet 3	2	Junb	10090.ENSMUSP00000064680	Transcription factor jun-B; Transcription factor involved in regulating gene activity following the primary growth factor response. Binds to the DNA sequence 5'-TGA[CG]TCA-3'; Belongs to the bZIP family. Jun subfamily.
38	Violet	2	Nectin1	10090.ENSMUSP00000034510	Nectin-1; Involved in cell adhesion and synaptogegesis. Has some neurite outgrowth-promoting activity. Receptor for alphaherpesvirus (HSV-1, HSV-2 and pseudorabies virus) entry into cells. Belongs to the nectin family.

38	Violet	2	Nectin2	10090.ENSMUSP00000074898	Nectin-2; Modulator of T-cell signaling. Can be either a costimulator of T-cell function, or a coinhibitor, depending on the receptor it binds to.
39	Violet 2	2	Ampd2	10090.ENSMUSP00000077946	AMP deaminase 2; AMP deaminase plays a critical role in energy metabolism. Catalyzes the deamination of AMP to IMP and plays an important role in the purine nucleotide cycle (By similarity); Belongs to the metallo-dependent hydrolases superfamily. Adenosine and AMP deaminases family.
39	Violet 2	2	Ampd3	10090.ENSMUSP00000005829	AMP deaminase 3; AMP deaminase plays a critical role in energy metabolism; Belongs to the metallo-dependent hydrolases superfamily. Adenosine and AMP deaminases family.
40	Orchid	2	Pdxk	10090.ENSMUSP00000038540	Pyridoxal kinase; Required for synthesis of pyridoxal-5-phosphate from vitamin B6.
40	Orchid	2	Pdxp	10090.ENSMUSP00000086796	Pyridoxal phosphate phosphatase; Protein serine phosphatase that dephosphorylates 'Ser-3' in cofilin and probably also dephosphorylates phospho-serine residues in DSTN. Regulates cofilin-dependent actin cytoskeleton reorganization.
41	Orchid 3	2	Lrrc8a	10090.ENSMUSP00000092690	Volume-regulated anion channel subunit LRRC8A; Essential component of the volume-regulated anion channel (VRAC, also named VSOAC channel), an anion channel required to maintain a constant cell volume in response to extracellular or intracellular osmotic changes.
41	Orchid 3	2	Lrrc8d	10090.ENSMUSP00000113603	Volume-regulated anion channel subunit LRRC8D; Non-essential component of the volume-regulated anion channel (VRAC, also named VSOAC channel), an anion channel required to maintain a constant cell volume in response to extracellular or intracellular osmotic changes.
42	Hot Pink	2	Hmga2	10090.ENSMUSP00000123998	High mobility group protein HMGI-C; Functions as a transcriptional regulator. Functions in cell cycle regulation through CCNA2. Plays an important role in chromosome condensation during the meiotic G2/M transition of spermatocytes. Plays a role in postnatal myogenesis, is involved in satellite cell activation.
42	Hot Pink	2	Igf2bp2	10090.ENSMUSP00000097629	Insulin-like growth factor 2 mRNA-binding protein 2; RNA-binding factor that recruits target transcripts to cytoplasmic protein-RNA complexes (mRNPs). This transcript 'caging' into mRNPs allows mRNA transport and transient storage.
43	Pink	2	Ctsa	10090.ENSMUSP00000099381	Lysosomal protective protein 20 kDa chain; Protective protein appears to be essential for both the activity of beta-galactosidase and neuraminidase, it associates with these enzymes and exerts a protective function necessary for their stability and activity. This protein is also a carboxypeptidase and can deamidate tachykinins.
43	Pink	2	Neu1	10090.ENSMUSP00000007253	Sialidase-1; Catalyzes the removal of sialic acid (N-acetylneuraminic acid) moieties from glycoproteins and glycolipids. To be active, it is strictly dependent on its presence in the multienzyme complex. Appears to have a preference for alpha 2-3 and alpha 2-6 sialyl linkage. Belongs to the glycosyl hydrolase 33 family.
44	Hot Pink 2	2	Atg7	10090.ENSMUSP00000133215	Ubiquitin-like modifier-activating enzyme ATG7; E1-like activating enzyme involved in the 2 ubiquitin-like systems required for cytoplasm to vacuole transport (Cvt) and autophagy. Activates ATG12 for its conjugation with ATG5 as well as the ATG8 family proteins for their conjugation with phosphatidylethanolamine. Both systems are needed for the ATG8 association to Cvt vesicles and autophagosomes membranes. Required for autophagic death induced by caspase-8 inhibition. Required for mitophagy.
44	Hot Pink 2	2	Sirt1	10090.ENSMUSP00000112595	NAD-dependent protein deacetylase sirtuin-1; NAD-dependent protein deacetylase that links transcriptional regulation directly to intracellular energetics and participates in the coordination of several separated cellular functions such as cell cycle, response to DNA damage, metabolism, apoptosis and autophagy. Can modulate chromatin function through deacetylation of histones and can promote alterations in the methylation of histones and DNA, leading to transcriptional repression.
45	Pale Violet Red	2	Nqo1	10090.ENSMUSP00000003947	NAD(P)H dehydrogenase [quinone] 1; The enzyme apparently serves as a quinone reductase in connection with conjugation reactions of hydroquinons involved in detoxification pathways as well as in biosynthetic processes such as the vitamin K-dependent gamma-carboxylation of glutamate residues in prothrombin synthesis.

45	Pale Violet Red	2	Odc1	10090.ENSMUSP00000128661	Ornithine decarboxylase; Catalyzes the first and rate-limiting step of polyamine biosynthesis that converts ornithine into putrescine, which is the precursor for the polyamines, spermidine and spermine. Polyamines are essential for cell proliferation and are implicated in cellular processes, ranging from DNA replication to apoptosis.
46	Light Coral 2	2	Pfkfb2	10090.ENSMUSP00000066426	6-phosphofructo-2-kinase/fructose-2,6-bisphosphatase 2; Synthesis and degradation of fructose 2,6-bisphosphate.
46	Light Coral 2	2	Pfkfb3	10090.ENSMUSP00000142079	6-phosphofructo-2-kinase/fructose-2, 6-biphosphatase 3 splice variant 2.
47	Light Coral	2	Nedd4l	10090.ENSMUSP00000158026	E3 ubiquitin-protein ligase NEDD4-like; E3 ubiquitin-protein ligase which accepts ubiquitin from an E2 ubiquitin-conjugating enzyme in the form of a thioester and then directly transfers the ubiquitin to targeted substrates. Inhibits TGF- beta signalling by triggering SMAD2 and TGFBR1 ubiquitination and proteasome-dependent degradation.
47	Light Coral	2	Sgk1	10090.ENSMUSP00000114074	Serine/threonine-protein kinase Sgk1; Serine/threonine-protein kinase which is involved in the regulation of a wide variety of ion channels, membrane transporters, cellular enzymes, transcription factors, neuronal excitability, cell growth, proliferation, survival, migration and apoptosis. Plays an important role in cellular stress response.

Supplementary Table 3. Details of genes included in Markov clusters for commonly down-regulated genes presented in figure 6.

Cluster number	Cluster colour	Gene count	Protein name	Protein identifier	Protein description
1	Red	10	Acta1	10090.ENSMUSP00000034453	Actin, alpha skeletal muscle, intermediate form; Actins are highly conserved proteins that are involved in various types of cell motility and are ubiquitously expressed in all eukaryotic cells.
1	Red	10	Actc1	10090.ENSMUSP00000087736	Actin, alpha cardiac muscle 1, intermediate form; Actins are highly conserved proteins that are involved in various types of cell motility and are ubiquitously expressed in all eukaryotic cells; Belongs to the actin family.
1	Red	10	Baiap2	10090.ENSMUSP00000026436	Brain-specific angiogenesis inhibitor 1-associated protein 2; Adapter protein that links membrane-bound small G-proteins to cytoplasmic effector proteins. Necessary for CDC42-mediated reorganization of the actin cytoskeleton and for RAC1-mediated membrane ruffling.
1	Red	10	Myh4	10090.ENSMUSP00000018632	Myosin-4; Muscle contraction.
1	Red	10	Myl1	10090.ENSMUSP00000027151	Myosin light chain 1/3, skeletal muscle isoform; Non-regulatory myosin light chain required for proper formation and/or maintenance of myofibers, and thus appropriate muscle function.
1	Red	10	Myl4	10090.ENSMUSP00000102570	Myosin light chain 4; Regulatory light chain of myosin. Does not bind calcium.

1	Red	10	Mylpf	10090.ENSMUSP00000032910	Myosin regulatory light chain 2, skeletal muscle isoform.
1	Red	10	Tpm1	10090.ENSMUSP00000109337	Tropomyosin alpha-1 chain; Binds to actin filaments in muscle and non-muscle cells. Plays a central role, in association with the troponin complex, in the calcium dependent regulation of vertebrate striated muscle contraction. Smooth muscle contraction is regulated by interaction with caldesmon. In non-muscle cells is implicated in stabilizing cytoskeleton actin filaments.
1	Red	10	Tpm2	10090.ENSMUSP00000103546	Tropomyosin beta chain; Binds to actin filaments in muscle and non-muscle cells. Plays a central role, in association with the troponin complex, in the calcium dependent regulation of vertebrate striated muscle contraction. Smooth muscle contraction is regulated by interaction with caldesmon. In non-muscle cells is implicated in stabilizing cytoskeleton actin filaments. The non-muscle isoform may have a role in agonist-mediated receptor internalization. Belongs to the tropomyosin family.
1	Red	10	Vasp	10090.ENSMUSP00000032561	Vasodilator-stimulated phosphoprotein; Ena/VASP proteins are actin-associated proteins involved in a range of processes dependent on cytoskeleton remodelling and cell polarity such as axon guidance, lamellipodial and filopodial dynamics, platelet activation and cell migration.
2	Salmon	5	Acta2	10090.ENSMUSP00000048218	Actin, aortic smooth muscle, intermediate form; Actins are highly conserved proteins that are involved in various types of cell motility and are ubiquitously expressed in all eukaryotic cells.
2	Salmon	5	Actg2	10090.ENSMUSP00000074658	Actin, gamma-enteric smooth muscle, intermediate form; Actins are highly conserved proteins that are involved in various types of cell motility and are ubiquitously expressed in all eukaryotic cells; Belongs to the actin family.
2	Salmon	5	Myl12a	10090.ENSMUSP00000123412	Myosin, light chain 12A, regulatory, non-sarcomeric.
2	Salmon	5	Myl6	10090.ENSMUSP00000128803	Myosin light polypeptide 6; Regulatory light chain of myosin. Does not bind calcium.
2	Salmon	5	Myl9	10090.ENSMUSP00000085913	Myosin regulatory light polypeptide 9; Myosin regulatory subunit that plays an important role in regulation of both smooth muscle and non-musical cell contractile activity via its phosphorylation. Implicated in cytokinesis, receptor capping, and cell locomotion.
3	Saddle Brown	5	Dag1	10090.ENSMUSP00000142109	Alpha-dystroglycan; The dystroglycan complex is involved in a number of processes including laminin and basement membrane assembly, sacrolemmal stability, cell survival, peripheral nerve myelination, nodal structure, cell migration, and epithelial polarization.
3	Saddle Brown	5	Nrxn3	10090.ENSMUSP00000129678	Neurexin-3; Neuronal cell surface protein that may be involved in cell recognition and cell adhesion. May mediate intracellular signaling (By similarity).
3	Saddle Brown	5	Pgm5	10090.ENSMUSP00000036025	Phosphoglucomutase-like protein 5; Component of adherens-type cell-cell and cell-matrix junctions. Lacks phosphoglucomutase activity (By similarity). Belongs to the phosphohexose mutase family.
3	Saddle Brown	5	Sgcg	10090.ENSMUSP00000077106	Gamma-sarcoglycan; Component of the sarcoglycan complex, a subcomplex of the dystrophin-glycoprotein complex which forms a link between the F-actin cytoskeleton and the extracellular matrix.
3	Saddle Brown	5	Sspn	10090.ENSMUSP00000032383	Sarcospan; Component of the dystrophin-glycoprotein complex (DGC), a complex that spans the muscle plasma membrane and forms a link between the F-actin cytoskeleton and the extracellular matrix. Preferentially associates with the sarcoglycan subcomplex of the DGC (By similarity).
4	Sandy Brown	4	Tnnc1	10090.ENSMUSP00000131991	Troponin C, slow skeletal and cardiac muscles; Troponin is the central regulatory protein of striated muscle contraction. Tn consists of three components: Tn-I which is the inhibitor of actomyosin ATPase, Tn-T which contains the binding site for tropomyosin and Tn-C. The binding of calcium to Tn-C abolishes the inhibitory action of Tn on actin filaments.
4	Sandy Brown	4	Tnnc2	10090.ENSMUSP00000099384	Troponin C, skeletal muscle; Troponin is the central regulatory protein of striated muscle contraction. Tn consists of three components: Tn-I which is the inhibitor of actomyosin ATPase, Tn-T which contains the binding site for tropomyosin and Tn-C. The binding of calcium to Tn-C abolishes the inhibitory action of Tn on actin filaments.

4	Sandy Brown	4	Tnni2	10090.ENSMUSP00000122733	Troponin I, fast skeletal muscle; Troponin I is the inhibitory subunit of troponin, the thin filament regulatory complex which confers calcium-sensitivity to striated muscle actomyosin ATPase activity.
4	Sandy Brown	4	Tnnt2	10090.ENSMUSP00000140941	Troponin T, cardiac muscle; Troponin T is the tropomyosin-binding subunit of troponin, the thin filament regulatory complex which confers calcium-sensitivity to striated muscle actomyosin ATPase activity.
5	Brown	3	Tgfb2	10090.ENSMUSP00000142149	Transforming growth factor beta-2 proprotein; Transforming growth factor beta-2 proprotein: Precursor of the Latency-associated peptide (LAP) and Transforming growth factor beta-2 (TGF-beta-2) chains, which constitute the regulatory and active subunit of TGF-beta-2, respectively. Transforming growth factor beta-2: Multifunctional protein that regulates various processes such as angiogenesis and heart development.
5	Brown	3	Tgfb3	10090.ENSMUSP00000003687	Transforming growth factor beta-3 proprotein; Transforming growth factor beta-3 proprotein: Precursor of the Latency-associated peptide (LAP) and Transforming growth factor beta-3 (TGF-beta-3) chains, which constitute the regulatory and active subunit of TGF-beta-3, respectively. Transforming growth factor beta-3: Multifunctional protein that regulates embryogenesis and cell differentiation and is required in various processes such as secondary palate development.
5	Brown	3	Tgfbr2	10090.ENSMUSP00000062333	TGF-beta receptor type-2; Transmembrane serine/threonine kinase forming with the TGF- beta type I serine/threonine kinase receptor, TGFBR1, the non- promiscuous receptor for the TGF-beta cytokines TGFB1, TGFB2 and TGFB3. Transduces the TGFB1, TGFB2 and TGFB3 signal from the cell surface to the cytoplasm and is thus regulating a plethora of physiological and pathological processes.
6	Yellow	3	Chrna1	10090.ENSMUSP00000028515	Acetylcholine receptor subunit alpha; After binding acetylcholine, the AChR responds by an extensive change in conformation that affects all subunits and leads to opening of an ion-conducting channel across the plasma membrane.
6	Yellow	3	Chrnb1	10090.ENSMUSP00000047270	Acetylcholine receptor subunit beta; After binding acetylcholine, the AChR responds by an extensive change in conformation that affects all subunits and leads to opening of an ion-conducting channel across the plasma membrane.
6	Yellow	3	Chrng	10090.ENSMUSP00000027470	Acetylcholine receptor subunit gamma; After binding acetylcholine, the AChR responds by an extensive change in conformation that affects all subunits and leads to opening of an ion-conducting channel across the plasma membrane; Belongs to the ligand-gated ion channel (TC 1.A.9) family. Acetylcholine receptor (TC 1.A.9.1) subfamily. Gamma/CHRNG sub- subfamily.
7	Olive	3	Casq2	10090.ENSMUSP00000029454	Calsequestrin-2; Calsequestrin is a high-capacity, moderate affinity, calcium- binding protein and thus acts as an internal calcium store in muscle. Calcium ions are bound by clusters of acidic residues at the protein surface, especially at the interface between subunits.
7	Olive	3	Jph1	10090.ENSMUSP00000039072	Junctophilin-1; Junctophilins contribute to the formation of junctional membrane complexes (JMCs) which link the plasma membrane with the endoplasmic or sarcoplasmic reticulum in excitable cells. Provides a structural foundation for functional cross-talk between the cell surface and intracellular calcium release channels. JPH1 contributes to the construction of the skeletal muscle triad by linking the t-tubule (transverse-tubule) and SR (sarcoplasmic reticulum) membranes.
7	Olive	3	Ryr3	10090.ENSMUSP00000147250	Ryanodine receptor 3; Calcium channel that mediates the release of Ca(2+) from the sarcoplasmic reticulum into the cytoplasm in muscle and thereby plays a role in triggering muscle contraction. May regulate Ca(2+) release by other calcium channels. Calcium channel that mediates Ca(2+)-induced Ca(2+) release from the endoplasmic reticulum in non-muscle cells. Plays a role in cellular calcium signaling. Contributes to cellular calcium ion homeostasis.
8	Green	3	Myod1	10090.ENSMUSP00000072330	Myoblast determination protein 1; Acts as a transcriptional activator that promotes transcription of muscle-specific target genes and plays a role in muscle differentiation. Together with MYF5 and MYOG, co-occupies muscle-specific gene promoter core region during myogenesis.
8	Green	3	Smarcd3	10090.ENSMUSP00000030791	SWI/SNF-related matrix-associated actin-dependent regulator of chromatin subfamily D member 3; Involved in transcriptional activation and repression of select genes by chromatin remodeling (alteration of DNA-nucleosome topology).

8	Green	3	Tcf4	10090.ENSMUSP00000110636	Transcription factor 4; Transcription factor that binds to the immunoglobulin enhancer Mu-E5/KE5-motif. Involved in the initiation of neuronal differentiation. Activates transcription by binding to the E box (5'- CANNTG-3'). Isoform 2 inhibits MYOD1 activation of the cardiac alpha- actin promoter.
9	Lime Green	3	Igf1	10090.ENSMUSP00000100937	Insulin-like growth factor I; The insulin-like growth factors, isolated from plasma, are structurally and functionally related to insulin but have a much higher growth-promoting activity.
9	Lime Green	3	Igfbp5	10090.ENSMUSP00000027377	Insulin-like growth factor-binding protein 5; IGF-binding proteins prolong the half-life of the IGFs and have been shown to either inhibit or stimulate the growth promoting effects of the IGFs on cell culture. They alter the interaction of IGFs with their cell surface receptors.
9	Lime Green	3	Irs1	10090.ENSMUSP00000063795	Insulin receptor substrate 1; May mediate the control of various cellular processes by insulin. When phosphorylated by the insulin receptor binds specifically to various cellular proteins containing SH2 domains such as phosphatidylinositol 3-kinase p85 subunit or GRB2. Activates phosphatidylinositol 3-kinase when bound to the regulatory p85 subunit (By similarity).
10	Light Green	2	Col6a1	10090.ENSMUSP00000001147	Collagen alpha-1(VI) chain; Collagen VI acts as a cell-binding protein; Belongs to the type VI collagen family.
10	Light Green	2	Col6a2	10090.ENSMUSP00000001181	Collagen alpha-2(VI) chain; Collagen VI acts as a cell-binding protein.
11	Sky Blue	2	Col3a1	10090.ENSMUSP00000085192	Collagen alpha-1(III) chain; Collagen type III occurs in most soft connective tissues along with type I collagen. Involved in regulation of cortical development.
11	Sky Blue	2	Col5a3	10090.ENSMUSP00000004201	Collagen type V alpha 3 chain.
12	Cornflower Blue	2	Cav1	10090.ENSMUSP00000007799	Caveolin-1; May act as a scaffolding protein within caveolar membranes (By similarity). Forms a stable heterooligomeric complex with CAV2 that targets to lipid rafts and drives caveolae formation. Mediates the recruitment of CAVIN proteins (CAVIN1/2/3/4) to the caveolae. Interacts directly with G-protein alpha subunits and can functionally regulate their activity.
12	Cornflower Blue	2	Cavin1	10090.ENSMUSP00000058321	Caveolae-associated protein 1; Plays an important role in caveolae formation and organization. Essential for the formation of caveolae in all tissues. Core component of the CAVIN complex which is essential for recruitment of the complex to the caveolae in presence of calveolin-1 (CAV1).
13	Blue	2	Cd82	10090.ENSMUSP00000028644	CD82 antigen; Associates with CD4 or CD8 and delivers costimulatory signals for the TCR/CD3 pathway; Belongs to the tetraspanin (TM4SF) family.
13	Blue	2	Cyb5d2	10090.ENSMUSP00000078623	Neuferricin; Heme-binding protein which promotes neuronal but not astrocyte differentiation.
14	Purple	2	Kcnj12	10090.ENSMUSP00000041696	ATP-sensitive inward rectifier potassium channel 12; Inward rectifying potassium channel that is activated by phosphatidylinositol 4,5-bisphosphate and that probably participates in controlling the resting membrane potential in electrically excitable cells.
14	Purple	2	Kcnq4	10090.ENSMUSP00000030376	Potassium voltage-gated channel subfamily KQT member 4; Probably important in the regulation of neuronal excitability.
15	Medium Purple	2	Atp2a1	10090.ENSMUSP00000032974	Sarcoplasmic/endoplasmic reticulum calcium ATPase 1; Key regulator of striated muscle performance by acting as the major Ca(2+) ATPase responsible for the reuptake of cytosolic Ca(2+) into the sarcoplasmic reticulum.
15	Medium Purple	2	Hrc	10090.ENSMUSP00000082459	Histidine-rich calcium-binding protein.
16	Medium Purple 2	2	Lpar3	10090.ENSMUSP00000037712	Lysophosphatidic acid receptor 3; Receptor for lysophosphatidic acid (LPA), a mediator of diverse cellular activities. Seems to be coupled to the G(i)/G(o) and G(q) families of heteromeric G proteins.
16	Medium Purple 2	2	Lpar4	10090.ENSMUSP00000053986	Lysophosphatidic acid receptor 4; Receptor for lysophosphatidic acid (LPA), a mediator of diverse cellular activities.

17	Orchid 2	2	Fyn	10090.ENSMUSP00000097547	Tyrosine-protein kinase Fyn; Non-receptor tyrosine-protein kinase that plays a role in many biological processes including regulation of cell growth and survival, cell adhesion, integrin-mediated signaling, cytoskeletal remodeling, cell motility, immune response and axon guidance.
17	Orchid 2	2	Ncam1	10090.ENSMUSP00000130668	Neural cell adhesion molecule 1; This protein is a cell adhesion molecule involved in neuron- neuron adhesion, neurite fasciculation, outgrowth of neurites, etc.
18	Violet	2	Ndufa13	10090.ENSMUSP00000105796	NADH dehydrogenase [ubiquinone] 1 alpha subcomplex subunit 13; Accessory subunit of the mitochondrial membrane respiratory chain NADH dehydrogenase (Complex I), that is believed not to be involved in catalysis. Complex I functions in the transfer of electrons from NADH to the respiratory chain.
18	Violet	2	Ndufb4	10090.ENSMUSP00000023514	NADH dehydrogenase [ubiquinone] 1 beta subcomplex subunit 4; Accessory subunit of the mitochondrial membrane respiratory chain NADH dehydrogenase (Complex I), that is believed not to be involved in catalysis. Complex I functions in the transfer of electrons from NADH to the respiratory chain. The immediate electron acceptor for the enzyme is believed to be ubiquinone.
19	Violet 2	2	Cacna1s	10090.ENSMUSP00000107695	Voltage-dependent L-type calcium channel subunit alpha-1S; Pore-forming, alpha-1S subunit of the voltage-gated calcium channel that gives rise to L-type calcium currents in skeletal muscle.
19	Violet 2	2	Cacng1	10090.ENSMUSP00000021065	Voltage-dependent calcium channel gamma-1 subunit; Regulatory subunit of the voltage-gated calcium channel that gives rise to L-type calcium currents in skeletal muscle. Regulates channel inactivation kinetics; Belongs to the PMP-22/EMP/MP20 family. CACNG subfamily.
20	Orchid	2	Cdon	10090.ENSMUSP00000113977	Cell adhesion molecule-related/down-regulated by oncogenes; Component of a cell-surface receptor complex that mediates cell-cell interactions between muscle precursor cells. Promotes differentiation of myogenic cells. Required for response to NTN3 and activation of NFATC3.
20	Orchid	2	Gas1	10090.ENSMUSP00000153311	Growth arrest-specific protein 1; Specific growth arrest protein involved in growth suppression. Blocks entry to S phase. Prevents cycling of normal and transformed cells.
21	Hot Pink	2	Mef2a	10090.ENSMUSP00000117496	Myocyte-specific enhancer factor 2A; Transcriptional activator which binds specifically to the MEF2 element, 5'-YTA[AT](4)TAR-3', found in numerous muscle-specific genes. Also involved in the activation of numerous growth factor- and stress-induced genes. Mediates cellular functions not only in skeletal and cardiac muscle development, but also in neuronal differentiation and survival.
21	Hot Pink	2	Mef2c	10090.ENSMUSP00000143401	Myocyte-specific enhancer factor 2C; Transcription activator which binds specifically to the MEF2 element present in the regulatory regions of many muscle-specific genes. Controls cardiac morphogenesis and myogenesis, and is also involved in vascular development. Enhances transcriptional activation mediated by SOX18.
22	Pink	2	Ckb	10090.ENSMUSP00000001304	Creatine kinase B-type; Reversibly catalyzes the transfer of phosphate between ATP and various phosphogens (e.g. creatine phosphate). Creatine kinase isoenzymes play a central role in energy transduction in tissues with large, fluctuating energy demands, such as skeletal muscle, heart, brain and spermatozoa; Belongs to the ATP:guanido phosphotransferase family.
22	Pink	2	Ckm	10090.ENSMUSP00000146972	Creatine kinase M-type; Reversibly catalyzes the transfer of phosphate between ATP and various phosphogens (e.g. creatine phosphate). Creatine kinase isoenzymes play a central role in energy transduction in tissues with large, fluctuating energy demands, such as skeletal muscle, heart, brain and spermatozoa; Belongs to the ATP:guanido phosphotransferase family.

Supplementary Table 4. Details of putative transcription factor binding motifs for common up-regulated genes.

Motif Name	Consensus	P-value	Log P-value	q-value (Benjamini)	# of Target Sequences with Motif(of 724)	% of Target Sequences with Motif	# of Background Sequences with Motif(of 27615)	% of Background Sequences with Motif

USF1(bHLH)/GM12878-Usf1-ChIP-Seq(GSE32465)/Homer	SGTCACGTGR	1.00E-08	-1.93E+01	0	265	36.60%	7351.2	26.62%
bHLHE40(bHLH)/HepG2-BHLHE40-ChIP-Seq(GSE31477)/Homer	KCACGTGMCN	1.00E-05	-1.38E+01	0.0001	192	26.52%	5281.8	19.13%
CLOCK(bHLH)/Liver-Clock-ChIP-Seq(GSE39860)/Homer	GHCACGTG	1.00E-05	-1.28E+01	0.0003	285	39.36%	8620.7	31.22%
Sp1(Zf)/Promoter/Homer	GGCCCCGCCCCC	1.00E-05	-1.25E+01	0.0003	356	49.17%	11253.1	40.75%
n-Myc(bHLH)/mES-nMyc-ChIP-Seq(GSE11431)/Homer	VRCCACGTGG	1.00E-05	-1.22E+01	0.0003	321	44.34%	9983.1	36.15%
c-Myc(bHLH)/LNCAP-cMyc-ChIP-Seq(Unpublished)/Homer	VCCACGTG	1.00E-05	-1.22E+01	0.0003	270	37.29%	8143	29.49%
Max(bHLH)/K562-Max-ChIP-Seq(GSE31477)/Homer	RCCACGTGGYYN	1.00E-05	-1.22E+01	0.0003	304	41.99%	9371.6	33.94%
c-Myc(bHLH)/mES-cMyc-ChIP-Seq(GSE11431)/Homer	VVCCACGTGG	1.00E-04	-1.05E+01	0.0009	238	32.87%	7177.6	25.99%
E-box(bHLH)/Promoter/Homer	SSGGTCACGTGA	1.00E-04	-9.55E+00	0.0021	76	10.50%	1823.7	6.60%
Usf2(bHLH)/C2C12-Usf2-ChIP-Seq(GSE36030)/Homer	GTCACGTGGT	1.00E-03	-8.91E+00	0.0036	174	24.03%	5098.2	18.46%
HIF-1b(HLH)/T47D-HIF1b-ChIP-Seq(GSE59937)/Homer	RTACGTGC	1.00E-03	-8.34E+00	0.0057	454	62.71%	15505	56.15%
BMAL1(bHLH)/Liver-Bmal1-ChIP-Seq(GSE39860)/Homer	GNCACGTG	1.00E-03	-7.73E+00	0.0097	543	75.00%	19122.7	69.25%
NPAS2(bHLH)/Liver-NPAS2-ChIP-	KCCACGTGAC	1.00E-03	-7.51E+00	0.0111	409	56.49%	13885	50.29%

Seq(GSE39860)/Homer								
SpiB(ETS)/OCILY3-SPIB-ChIP-Seq(GSE56857)/Homer	AAAGRGGAAGTG	1.00E-02	-6.63E+00	0.025	148	20.44%	4442.5	16.09%
Atf3(bZIP)/GBM-ATF3-ChIP-Seq(GSE33912)/Homer	DATGASTCATHN	1.00E-02	-6.30E+00	0.0324	256	35.36%	8339.4	30.20%
PU.1(ETS)/ThioMac-PU.1-ChIP-Seq(GSE21512)/Homer	AGAGGAAGTG	1.00E-02	-6.12E+00	0.0362	265	36.60%	8695.6	31.49%
AP-1(bZIP)/ThioMac-PU.1-ChIP-Seq(GSE21512)/Homer	VTGACTCATC	1.00E-02	-6.01E+00	0.0381	280	38.67%	9264.9	33.55%
Olig2(bHLH)/Neuron-Olig2-ChIP-Seq(GSE30882)/Homer	RCCATMTGTT	1.00E-02	-5.93E+00	0.0391	564	77.90%	20231.9	73.27%
KLF5(Zf)/LoVo-KLF5-ChIP-Seq(GSE49402)/Homer	DGGGYGKGGC	1.00E-02	-5.88E+00	0.0391	593	81.91%	21421.2	77.58%
Klf4(Zf)/mES-Klf4-ChIP-Seq(GSE11431)/Homer	GCCACACCCA	1.00E-02	-5.50E+00	0.0539	283	39.09%	9457.6	34.25%
AMYB(HTH)/Testes-AMYB-ChIP-Seq(GSE44588)/Homer	TGGCAGTTGG	1.00E-02	-4.98E+00	0.0861	543	75.00%	19539.2	70.76%
CRX(Homeobox)/Retina-Crx-ChIP-Seq(GSE20012)/Homer	GCTAATCC	1.00E-02	-4.96E+00	0.0861	634	87.57%	23255	84.22%
Fra1(bZIP)/BT549-Fra1-ChIP-Seq(GSE46166)/Homer	NNATGASTCATH	1.00E-02	-4.92E+00	0.0861	218	30.11%	7167	25.96%
ELF5(ETS)/T47D-ELF5-ChIP-Seq(GSE30407)/Homer	ACVAGGAAGT	1.00E-02	-4.79E+00	0.0914	357	49.31%	12355.6	44.75%
NFkB-p65-Rel(RHD)/ThioMac-LPS-	GGAAATTCCC	1.00E-02	-4.76E+00	0.0914	40	5.52%	1012.6	3.67%

Expression(GSE23622)/Homer								
Nkx6.1(Homeobox)/Islet-Nkx6.1-ChIP-Seq(GSE40975)/Homer	GKTAATGR	1.00E-01	-4.44E+00	0.1197	630	87.02%	23162.4	83.88%
Isl1(Homeobox)/Neuron-Isl1-ChIP-Seq(GSE31456)/Homer	CTAATKGV	1.00E-01	-4.39E+00	0.1208	589	81.35%	21490.4	77.83%
Fosl2(bZIP)/3T3L1-Fosl2-ChIP-Seq(GSE56872)/Homer	NATGASTCABNN	1.00E-01	-4.28E+00	0.131	136	18.78%	4319.9	15.64%
BATF(bZIP)/Th17-BATF-ChIP-Seq(GSE39756)/Homer	DATGASTCAT	1.00E-01	-4.11E+00	0.1497	249	34.39%	8446.1	30.59%
ETS:RUNX(ETS,Runt)/Jurkat-RUNX1-ChIP-Seq(GSE17954)/Homer	RCAGGATGTGGT	1.00E-01	-4.04E+00	0.1544	63	8.70%	1820.6	6.59%
EWS:ERG-fusion(ETS)/CADO_ES1-EWS:ERG-ChIP-Seq(SRA014231)/Homer	ATTTCCTGTN	1.00E-01	-3.90E+00	0.1732	329	45.44%	11476.6	41.56%
Srebp1a(bHLH)/HepG2-Srebp1a-ChIP-Seq(GSE31477)/Homer	RTCACSCCAY	1.00E-01	-3.90E+00	0.1732	111	15.33%	3491.1	12.64%
PPARE(NR),DR1/3T3L1-Pparg-ChIP-Seq(GSE13511)/Homer	TGACCTTTGCCCCA	1.00E-01	-3.71E+00	0.1951	397	54.83%	14098.7	51.06%
SCL(bHLH)/HPC7-Scl-ChIP-Seq(GSE13511)/Homer	AVCAGCTG	1.00E-01	-3.66E+00	0.1992	704	97.24%	26440.5	95.76%
RXR(NR),DR1/3T3L1-RXR-ChIP-Seq(GSE13511)/Homer	TAGGGCAAAGGTCA	1.00E-01	-3.61E+00	0.2034	439	60.64%	15734.8	56.98%
Ascl1(bHLH)/NeuralTubes-Ascl1-ChIP-Seq(GSE55840)/Homer	NNVVCAGCTGBN	1.00E-01	-3.55E+00	0.2098	494	68.23%	17882.9	64.76%

HRE(HSF)/Striatum-HSF1-ChIP-Seq(GSE38000)/Homer	TTCTAGAABNTTCTA	1.00E-01	-3.47E+00	0.2211	127	17.54%	4121.6	14.93%
MafK(bZIP)/C2C12-MafK-ChIP-Seq(GSE36030)/Homer	GCTGASTCAGCA	1.00E-01	-3.43E+00	0.2255	99	13.67%	3135.5	11.36%
HOXD13(Homeobox)/Chicken-Hoxd13-ChIP-Seq(GSE38910)/Homer	NCYAATAAAA	1.00E-01	-3.36E+00	0.2343	416	57.46%	14906.9	53.99%
HIF-1a(bHLH)/MCF7-HIF1a-ChIP-Seq(GSE28352)/Homer	TACGTGCV	1.00E-01	-3.20E+00	0.2693	134	18.51%	4418.5	16.00%
Ets1-distal(ETS)/CD4+-PolII-ChIP-Seq(Barski et al.)/Homer	MACAGGAAGT	1.00E-01	-3.04E+00	0.3084	160	22.10%	5389.7	19.52%
p53(p53)/mES-cMyc-ChIP-Seq(GSE11431)/Homer	ACATGCCCGGGCAT	1.00E-01	-3.00E+00	0.3142	11	1.52%	233	0.84%
CTCF(Zf)/CD4+-CTCF-ChIP-Seq(Barski et al.)/Homer	AYAGTGCCMYCTRGTGGCCA	1.00E-01	-2.94E+00	0.3258	87	12.02%	2784.3	10.08%
CRE(bZIP)/Promoter/Homer	CSGTGACGTCAC	1.00E-01	-2.89E+00	0.3335	140	19.34%	4692	16.99%
Stat3(Stat)/mES-Stat3-ChIP-Seq(GSE11431)/Homer	CTTCCGGGAA	1.00E-01	-2.89E+00	0.3335	264	36.46%	9264.9	33.55%
Tcfcp2l1(CP2)/mES-Tcfcp2l1-ChIP-Seq(GSE11431)/Homer	NRAACCRGTTYRAACCRGYT	1.00E-01	-2.88E+00	0.3335	86	11.88%	2757.9	9.99%
BORIS(Zf)/K562-CTCFL-ChIP-Seq(GSE32465)/Homer	CNNBRGCGCCCCCTGSTGGC	1.00E-01	-2.72E+00	0.3718	134	18.51%	4507.3	16.32%
CEBP:AP1(bZIP)/ThioMac-CEBPb-ChIP-Seq(GSE21512)/Homer	DRTGTTGCAA	1.00E-01	-2.70E+00	0.3718	294	40.61%	10436.6	37.80%

Znf263(Zf)/K562-Znf263-ChIP-Seq(GSE31477)/Homer	CVGTSCTCCC	1.00E-01	-2.70E+00	0.3718	566	78.18%	20904.9	75.71%
NF1:FOXA1(CTF,Forkhead)/LNCAP-FOXA1-ChIP-Seq(GSE27824)/Homer	WNTGTTTRYTTTGGCA	1.00E-01	-2.69E+00	0.3718	30	4.14%	849.2	3.08%
MYB(HTH)/ERMYB-Myb-ChIPSeq(GSE22095)/Homer	GGCVGTTR	1.00E-01	-2.66E+00	0.3718	573	79.14%	21189	76.74%
MITF(bHLH)/MastCells-MITF-ChIP-Seq(GSE48085)/Homer	RTCATGTGAC	1.00E-01	-2.63E+00	0.3718	357	49.31%	12837.8	46.49%
Rbpj1(?)/Panc1-Rbpj1-ChIP-Seq(GSE47459)/Homer	HTTTCCCASG	1.00E-01	-2.62E+00	0.3718	520	71.82%	19118.9	69.24%
HNF4a(NR),DR1/HepG2-HNF4a-ChIP-Seq(GSE25021)/Homer	CARRGKBCAAAGTYCA	1.00E-01	-2.59E+00	0.3718	222	30.66%	7771.5	28.15%
RORgt(NR)/EL4-RORgt.Flag-ChIP-Seq(GSE56019)/Homer	AAYTAGGTCA	1.00E-01	-2.57E+00	0.3718	64	8.84%	2028.9	7.35%
STAT1(Stat)/HelaS3-STAT1-ChIP-Seq(GSE12782)/Homer	NATTTCCNGGAAAT	1.00E-01	-2.57E+00	0.3718	162	22.38%	5560.7	20.14%
NeuroD1(bHLH)/Islet-NeuroD1-ChIP-Seq(GSE30298)/Homer	GCCATCTGTT	1.00E-01	-2.55E+00	0.3718	309	42.68%	11042.2	39.99%
Maz(Zf)/HepG2-Maz-ChIP-Seq(GSE31477)/Homer	GGGGGGGG	1.00E-01	-2.54E+00	0.3718	586	80.94%	21732.2	78.70%
GATA(Zf),IR3/iTreg-Gata3-ChIP-Seq(GSE20898)/Homer	NNNNNBAGATAWYATCTVHN	1.00E-01	-2.52E+00	0.3718	67	9.25%	2140.8	7.75%
Foxo1(Forkhead)/RAW-Foxo1-ChIP-Seq(Fan et al.)/Homer	CTGTTTAC	1.00E-01	-2.52E+00	0.3718	566	78.18%	20948.8	75.87%

EHF(ETS)/LoVo-EHF-ChIP-Seq(GSE49402)/Homer	AVCAGGAAGT	1.00E-01	-2.47E+00	0.3718	493	68.09%	18106.4	65.57%
Srebp2(bHLH)/HepG2-Srebp2-ChIP-Seq(GSE31477)/Homer	CGGTCACSCCAC	1.00E-01	-2.45E+00	0.3718	71	9.81%	2292.2	8.30%
Sox4(HMG)/proB-Sox4-ChIP-Seq(GSE50066)/Homer	YCTTTGTTCC	1.00E-01	-2.39E+00	0.3823	345	47.65%	12448.6	45.08%
IRF1(IRF)/PBMC-IRF1-ChIP-Seq(GSE43036)/Homer	GAAAGTGAAAGT	1.00E-01	-2.38E+00	0.383	74	10.22%	2410.5	8.73%
EWS:FLI1-fusion(ETS)/SK_N_MC-EWS:FLI1-ChIP-Seq(SRA014231)/Homer	VACAGGAAAT	1.00E-01	-2.34E+00	0.3922	293	40.47%	10497.1	38.02%
Bcl6(Zf)/Liver-Bcl6-ChIP-Seq(GSE31578)/Homer	NNNCTTTCCAGGAAA	1.00E-01	-2.32E+00	0.3922	493	68.09%	18146.1	65.72%
GABPA(ETS)/Jurkat-GABPa-ChIP-Seq(GSE17954)/Homer	RACCGGAAGT	1.00E-01	-2.32E+00	0.3922	424	58.56%	15485.3	56.08%
ETV1(ETS)/GIST48-ETV1-ChIP-Seq(GSE22441)/Homer	AACCGGAAGT	1.00E+00	-2.26E+00	0.4073	526	72.65%	19448.3	70.43%
Arnt:Ahr(bHLH)/MCF7-Arnt-ChIP-Seq(Lo et al.)/Homer	TBGCACGCAA	1.00E+00	-2.22E+00	0.4161	294	40.61%	10569.3	38.28%
Chop(bZIP)/MEF-Chop-ChIP-Seq(GSE35681)/Homer	ATTGCATCAT	1.00E+00	-2.19E+00	0.4208	88	12.15%	2943.7	10.66%
Cdx2(Homeobox)/mES-Cdx2-ChIP-Seq(GSE14586)/Homer	GYMATAAAAH	1.00E+00	-2.18E+00	0.4208	291	40.19%	10466.7	37.91%
Tcf3(HMG)/mES-Tcf3-ChIP-Seq(GSE11724)/Homer	ASWTCAAAGG	1.00E+00	-2.16E+00	0.4235	128	17.68%	4404.9	15.95%

Smad2(MAD)/ES-SMAD2-ChIP-Seq(GSE29422)/Homer	CTGTCTGG	1.00E+00	-2.15E+00	0.4235	516	71.27%	19089.3	69.13%
Reverb(NR),DR2/RAW-Reverba.biotin-ChIP-Seq(GSE45914)/Homer	GTRGGTCASTGGGTCA	1.00E+00	-2.13E+00	0.4254	65	8.98%	2130.3	7.72%
Ap4(bHLH)/AML-Tfap4-ChIP-Seq(GSE45738)/Homer	NAHCAGCTGD	1.00E+00	-2.09E+00	0.4336	406	56.08%	14864.1	53.83%
RUNX(Runt)/HPC7-Runx1-ChIP-Seq(GSE22178)/Homer	SAAACCACAG	1.00E+00	-2.09E+00	0.4336	291	40.19%	10494.9	38.01%
Tcf4(HMG)/Hct116-Tcf4-ChIP-Seq(SRA012054)/Homer	ASATCAAAGGVA	1.00E+00	-2.09E+00	0.4336	211	29.14%	7493.8	27.14%
Stat3+il21(Stat)/CD4-Stat3-ChIP-Seq(GSE19198)/Homer	SVYTTCCNGGAARB	1.00E+00	-2.08E+00	0.4336	321	44.34%	11633.9	42.13%
NF1(CTF)/LNCAP-NF1-ChIP-Seq(Unpublished)/Homer	CYTGGCABNSTGCCAR	1.00E+00	-2.04E+00	0.4336	177	24.45%	6239.4	22.60%
HRE(HSF)/HepG2-HSF1-ChIP-Seq(GSE31477)/Homer	BSTTCTRGAABVTTCYAGAA	1.00E+00	-2.02E+00	0.4388	86	11.88%	2904.8	10.52%
HIF2a(bHLH)/785_O-HIF2a-ChIP-Seq(GSE34871)/Homer	GCACGTACCC	1.00E+00	-1.99E+00	0.4458	173	23.90%	6105.6	22.11%
Esrrb(NR)/mES-Esrrb-ChIP-Seq(GSE11431)/Homer	KTGACCTTGA	1.00E+00	-1.94E+00	0.4648	274	37.85%	9901.8	35.86%
Ptf1a(bHLH)/Panc1-Ptf1a-ChIP-Seq(GSE47459)/Homer	ACAGCTGTTN	1.00E+00	-1.93E+00	0.4648	622	85.91%	23304.2	84.40%
TCFL2(HMG)/K562-TCF7L2-ChIP-Seq(GSE29196)/Homer	ACWTCAAAGG	1.00E+00	-1.92E+00	0.4648	46	6.35%	1488	5.39%
Atf4(bZIP)/MEF-Atf4-ChIP-	MTGATGCAAT	1.00E+00	-1.86E+00	0.4824	112	15.47%	3885.6	14.07%

Seq(GSE35681)/Homer								
Atoh1(bHLH)/Cerebellum-Atoh1-ChIP-Seq(GSE22111)/Homer	VNRVCAGCTGGY	1.00E+00	-1.85E+00	0.4839	380	52.49%	13951.7	50.53%
Foxh1(Forkhead)/hESC-FOXH1-ChIP-Seq(GSE29422)/Homer	NNTGTGGATTSS	1.00E+00	-1.77E+00	0.5164	258	35.64%	9351.8	33.87%
Jun-AP1(bZIP)/K562-cJun-ChIP-Seq(GSE31477)/Homer	GATGASTCATCN	1.00E+00	-1.73E+00	0.5295	88	12.15%	3035.7	10.99%
Bach2(bZIP)/OCILy7-Bach2-ChIP-Seq(GSE44420)/Homer	TGCTGAGTCA	1.00E+00	-1.72E+00	0.5316	77	10.64%	2637.9	9.55%
RUNX1(Runt)/Jurkat-RUNX1-ChIP-Seq(GSE29180)/Homer	AAACCACARM	1.00E+00	-1.69E+00	0.5435	383	52.90%	14122.3	51.14%
AR-halfsite(NR)/LNCaP-AR-ChIP-Seq(GSE27824)/Homer	CCAGGAACAG	1.00E+00	-1.69E+00	0.5435	692	95.58%	26164.1	94.76%
Smad4(MAD)/ESC-SMAD4-ChIP-Seq(GSE29422)/Homer	VBSYGTCTGG	1.00E+00	-1.68E+00	0.5435	523	72.24%	19503.3	70.63%
NFkB-p50,p52(RHD)/Monocyte-p50-ChIP-Chip(Schreiber et al.)/Homer	GGGGGAATCCCC	1.00E+00	-1.67E+00	0.5435	65	8.98%	2210.5	8.01%
Fli1(ETS)/CD8-FLI-ChIP-Seq(GSE20898)/Homer	NRYTTCCGGH	1.00E+00	-1.63E+00	0.5525	485	66.99%	18055.7	65.39%
Tcf12(bHLH)/GM12878-Tcf12-ChIP-Seq(GSE32465)/Homer	VCAGCTGYTG	1.00E+00	-1.61E+00	0.5555	347	47.93%	12778.9	46.28%
GRHL2(CP2)/HBE-GRHL2-ChIP-Seq(GSE46194)/Homer	AAACYKGTTWDACMRGTTTB	1.00E+00	-1.60E+00	0.5565	169	23.34%	6068.4	21.98%

AP-2gamma(AP2)/MCF7-TFAP2C-ChIP-Seq(GSE21234)/Homer	SCCTSAGGSCAW	1.00E+00	-1.60E+00	0.5565	425	58.70%	15761.2	57.08%
Lhx3(Homeobox)/Neuron-Lhx3-ChIP-Seq(GSE31456)/Homer	ADBTAATTAR	1.00E+00	-1.60E+00	0.5565	514	70.99%	19185.7	69.48%
Nur77(NR)/K562-NR4A1-ChIP-Seq(GSE31363)/Homer	TGACCTTTNCNT	1.00E+00	-1.57E+00	0.5575	94	12.98%	3294.7	11.93%
Unknown(Homeobox)/Limb-p300-ChIP-Seq/Homer	SSCMATWAAA	1.00E+00	-1.54E+00	0.5674	280	38.67%	10263.5	37.17%
Nrf2(bZIP)/Lymphoblast-Nrf2-ChIP-Seq(GSE37589)/Homer	HTGCTGAGTCAT	1.00E+00	-1.49E+00	0.5891	18	2.49%	559.9	2.03%
Smad3(MAD)/NPC-Smad3-ChIP-Seq(GSE36673)/Homer	TWGTCTGV	1.00E+00	-1.43E+00	0.6171	661	91.30%	24970.1	90.43%
NFY(CCAAT)/Promoter/Homer	RGCCAATSRG	1.00E+00	-1.38E+00	0.6439	378	52.21%	14049	50.88%
Egr2(Zf)/Thymocytes-Egr2-ChIP-Seq(GSE34254)/Homer	NGCGTGGGCGGR	1.00E+00	-1.36E+00	0.6543	124	17.13%	4463.4	16.16%
MyoG(bHLH)/C2C12-MyoG-ChIP-Seq(GSE36024)/Homer	AACAGCTG	1.00E+00	-1.31E+00	0.6792	376	51.93%	14002.9	50.71%
TR4(NR),DR1/Hela-TR4-ChIP-Seq(GSE24685)/Homer	GAGGTCAAAGGTCA	1.00E+00	-1.30E+00	0.6794	61	8.43%	2142.1	7.76%
ERE(NR),IR3/MCF7-ERa-ChIP-Seq(Unpublished)/Homer	VAGGTCACNSTGACC	1.00E+00	-1.30E+00	0.6794	113	15.61%	4070	14.74%
ETS1(ETS)/Jurkat-ETS1-ChIP-Seq(GSE17954)/Homer	ACAGGAAGTG	1.00E+00	-1.29E+00	0.6794	436	60.22%	16305.2	59.05%
ISRE(IRF)/ThioMac-LPS-Expression(GSE23622)/Homer	AGTTTCASTTTC	1.00E+00	-1.28E+00	0.6794	30	4.14%	1013.8	3.67%

STAT4(Stat)/CD4-Stat4-ChIP-Seq(GSE22104)/Homer	NYTTCCWGGAAR	1.00E+00	-1.28E+00	0.6794	388	53.59%	14473	52.42%
Otx2(Homeobox)/EpiLC-Otx2-ChIP-Seq(GSE56098)/Homer	NYTAATCCYB	1.00E+00	-1.27E+00	0.6794	310	42.82%	11507.3	41.67%
Pax7(Paired,Homeobox),long/Myoblast-Pax7-ChIP-Seq(GSE25064)/Homer	TAATCHGATTAC	1.00E+00	-1.25E+00	0.6794	12	1.66%	375.1	1.36%
RBPJ:Ebox(?,bHLH)/Panc1-Rbpj1-ChIP-Seq(GSE47459)/Homer	GGGRAARRGRMCAGMTG	1.00E+00	-1.22E+00	0.6899	147	20.30%	5368.2	19.44%
Pax7(Paired,Homeobox)/Myoblast-Pax7-ChIP-Seq(GSE25064)/Homer	TAATCAATTA	1.00E+00	-1.22E+00	0.6899	41	5.66%	1425.8	5.16%
Sox2(HMG)/mES-Sox2-ChIP-Seq(GSE11431)/Homer	BCCATTGTTC	1.00E+00	-1.20E+00	0.69	341	47.10%	12715.6	46.05%
EBF(EBF)/proBcell-EBF-ChIP-Seq(GSE21978)/Homer	DGTCCCYRGGGA	1.00E+00	-1.16E+00	0.717	113	15.61%	4115	14.90%
NF-E2(bZIP)/K562-NFE2-ChIP-Seq(GSE31477)/Homer	GATGACTCAGCA	1.00E+00	-1.14E+00	0.7229	20	2.76%	673.8	2.44%
Pitx1(Homeobox)/Chicken-Pitx1-ChIP-Seq(GSE38910)/Homer	TAATCCCN	1.00E+00	-1.14E+00	0.7229	706	97.51%	26821.8	97.14%
GFY-Staf(?,Zf)/Promoter/Homer	RACTACAATTCCCAGAAKGC	1.00E+00	-1.13E+00	0.7229	48	6.63%	1700.1	6.16%
HNF6(Homeobox)/Liver-Hnf6-ChIP-Seq(ERP000394)/Homer	NTATYGATCH	1.00E+00	-1.13E+00	0.7229	217	29.97%	8041.5	29.12%
Pax8(Paired,Homeobox)/Thyroid-Pax8-ChIP-Seq(GSE26938)/Homer	GTCATGCHTGRCTGS	1.00E+00	-1.11E+00	0.7229	138	19.06%	5068.6	18.36%

IRF2(IRF)/Erythroblas-IRF2-ChIP-Seq(GSE36985)/Homer	GAAASYGAAASY	1.00E+00	-1.11E+00	0.7229	53	7.32%	1891.4	6.85%
Nkx2.1(Homeobox)/LungAC-Nkx2.1-ChIP-Seq(GSE43252)/Homer	RSCACTYRAG	1.00E+00	-1.11E+00	0.7229	658	90.88%	24937.2	90.31%
Sox6(HMG)/Myotubes-Sox6-ChIP-Seq(GSE32627)/Homer	CCATTGTTNY	1.00E+00	-1.10E+00	0.7229	505	69.75%	19030	68.92%
GFY(?)/Promoter/Homer	ACTACAATTCCC	1.00E+00	-1.10E+00	0.7229	57	7.87%	2042.4	7.40%
MafF(bZIP)/HepG2-MafF-ChIP-Seq(GSE31477)/Homer	HWWGTCAGCAWWTTT	1.00E+00	-1.10E+00	0.7229	103	14.23%	3760.2	13.62%
RUNX2(Runt)/PCa-RUNX2-ChIP-Seq(GSE33889)/Homer	NWAACCACADNN	1.00E+00	-1.09E+00	0.7229	312	43.09%	11664.5	42.24%
PR(NR)/T47D-PR-ChIP-Seq(GSE31130)/Homer	VAGRACAKNCTGTBC	1.00E+00	-1.09E+00	0.7229	591	81.63%	22346.8	80.93%
BMYB(HTH)/Hela-BMYB-ChIP-Seq(GSE27030)/Homer	NHAACBGYYV	1.00E+00	-1.09E+00	0.7229	520	71.82%	19613.7	71.03%
PAX5(Paired,Homeobox)/GM12878-PAX5-ChIP-Seq(GSE32465)/Homer	GCAGCCAAGCRTGACH	1.00E+00	-1.06E+00	0.7229	165	22.79%	6104.9	22.11%
p63(p53)/Keratinocyte-p63-ChIP-Seq(GSE17611)/Homer	NNDRCATGYCYNRRCATGYH	1.00E+00	-1.06E+00	0.7229	143	19.75%	5276.4	19.11%
RUNX-AML(Runt)/CD4+-PolII-ChIP-Seq(Barski et al.)/Homer	GCTGTGGTTW	1.00E+00	-1.05E+00	0.7229	277	38.26%	10351.5	37.49%
Nkx3.1(Homeobox)/LNCaP-Nkx3.1-ChIP-Seq(GSE28264)/Homer	AAGCACTTAA	1.00E+00	-1.03E+00	0.7229	612	84.53%	23178.4	83.94%

Nkx2.5(Homeobox)/HL1-Nkx2.5.biotin-ChIP-Seq(GSE21529)/Homer	RRSCACTYAA	1.00E+00	-1.02E+00	0.7229	608	83.98%	23026.9	83.39%
STAT5(Stat)/mCD4+-Stat5-ChIP-Seq(GSE12346)/Homer	RTTTCTNAGAAA	1.00E+00	-9.96E-01	0.7229	171	23.62%	6359.5	23.03%
Foxa2(Forkhead)/Liver-Foxa2-ChIP-Seq(GSE25694)/Homer	CYTGTTTACWYW	1.00E+00	-9.65E-01	0.7395	318	43.92%	11953.9	43.29%
EBF1(EBF)/Near-E2A-ChIP-Seq(GSE21512)/Homer	GTCCCCWGGGGA	1.00E+00	-9.47E-01	0.7476	407	56.22%	15355.5	55.61%
E2A(bHLH)/proBcell-E2A-ChIP-Seq(GSE21978)/Homer	DNRCAGCTGY	1.00E+00	-9.45E-01	0.7476	457	63.12%	17266.2	62.53%
Oct4(POU,Homeobox)/mES-Oct4-ChIP-Seq(GSE11431)/Homer	ATTTGCATAW	1.00E+00	-9.44E-01	0.7476	183	25.28%	6836.6	24.76%
PU.1-IRF(ETS:IRF)/Bcell-PU.1-ChIP-Seq(GSE21512)/Homer	MGGAAGTGAAAC	1.00E+00	-9.40E-01	0.7476	476	65.75%	17995.9	65.17%
Mef2c(MADS)/GM12878-Mef2c-ChIP-Seq(GSE32465)/Homer	DCYAAAAATAGM	1.00E+00	-9.34E-01	0.7476	181	25.00%	6765.7	24.50%
TEAD4(TEA)/Tropoblast-Tead4-ChIP-Seq(GSE37350)/Homer	CCWGGAATGY	1.00E+00	-9.03E-01	0.7537	333	45.99%	12557.5	45.48%
GRE(NR),IR3/A549-GR-ChIP-Seq(GSE32465)/Homer	NRGVACABNVTGTYCY	1.00E+00	-8.94E-01	0.7553	57	7.87%	2096.2	7.59%
GATA:SCL(Zf,bHLH)/Ter119-SCL-ChIP-Seq(GSE18720)/Homer	CRGCTGBNGNSNNSAGATAA	1.00E+00	-8.88E-01	0.7553	56	7.73%	2060.9	7.46%
Erra(NR)/HepG2-Erra-ChIP-	CAAAGGTCAG	1.00E+00	-8.86E-01	0.7553	582	80.39%	22081.3	79.97%

Seq(GSE31477)/Homer								
ELF1(ETS)/Jurkat-ELF1-ChIP-Seq(SRA014231)/Homer	AVCCGGAAGT	1.00E+00	-8.82E-01	0.7553	303	41.85%	11426.4	41.38%
Nanog(Homeobox)/mES-Nanog-ChIP-Seq(GSE11724)/Homer	RGCCATTAAC	1.00E+00	-8.60E-01	0.7602	703	97.10%	26751.7	96.88%
p53(p53)/Saos-p53-ChIP-Seq(GSE15780)/Homer	RRCATGYCYRGRCATGYYYN	1.00E+00	-8.54E-01	0.7602	39	5.39%	1430.9	5.18%
p53(p53)/Saos-p53-ChIP-Seq/Homer	RRCATGYCYRGRCATGYYYN	1.00E+00	-8.54E-01	0.7602	39	5.39%	1430.9	5.18%
ZNF143|STAF(Zf)/CUTLL-ZNF143-ChIP-Seq(GSE29600)/Homer	ATTTCCCAGVAKSCY	1.00E+00	-8.52E-01	0.7602	175	24.17%	6576.3	23.82%
EKLF(Zf)/Erythrocyte-Klf1-ChIP-Seq(GSE20478)/Homer	NWGGGTGTGGCY	1.00E+00	-8.33E-01	0.7602	118	16.30%	4422.6	16.02%
MafA(bZIP)/Islet-MafA-ChIP-Seq(GSE30298)/Homer	TGCTGACTCA	1.00E+00	-8.30E-01	0.7602	289	39.92%	10922.7	39.56%
TEAD(TEA)/Fibroblast-PU.1-ChIP-Seq(Unpublished)/Homer	YCWGGAATGY	1.00E+00	-8.09E-01	0.7684	265	36.60%	10021	36.29%
Tbx20(T-box)/Heart-Tbx20-ChIP-Seq(GSE29636)/Homer	GGTGYTGACAGS	1.00E+00	-8.08E-01	0.7684	99	13.67%	3712.1	13.44%
ZFX(Zf)/mES-Zfx-ChIP-Seq(GSE11431)/Homer	AGGCCTRG	1.00E+00	-7.92E-01	0.7714	435	60.08%	16509.4	59.79%
TEAD2(TEA)/Py2T-Tead2-ChIP-Seq(GSE55709)/Homer	CCWGGAATGY	1.00E+00	-7.84E-01	0.7724	219	30.25%	8283.3	30.00%
Tbx5(T-box)/HL1-Tbx5.biotin-ChIP-Seq(GSE21529)/Homer	AGGTGTCA	1.00E+00	-7.78E-01	0.7727	668	92.27%	25423.6	92.07%

GATA(Zf),IR4/iTreg-Gata3-ChIP-Seq(GSE20898)/Homer	NAGATWNBNATCTNN	1.00E+00	-7.67E-01	0.7763	37	5.11%	1377	4.99%
Sox3(HMG)/NPC-Sox3-ChIP-Seq(GSE33059)/Homer	CCWTTGTY	1.00E+00	-7.39E-01	0.7932	530	73.20%	20165.7	73.03%
Tbet(T-box)/CD8-Tbet-ChIP-Seq(GSE33802)/Homer	AGGTGTGAAM	1.00E+00	-7.35E-01	0.7932	387	53.45%	14713.3	53.29%
Nr5a2(NR)/Pancreas-LRH1-ChIP-Seq(GSE34295)/Homer	BTCAAGGTCA	1.00E+00	-7.17E-01	0.8007	283	39.09%	10760.1	38.97%
THRa(NR)/C17.2-THRa-ChIP-Seq(GSE38347)/Homer	GGTCANYTGAGGWCA	1.00E+00	-7.17E-01	0.8007	177	24.45%	6721.4	24.34%
Tlx?(NR)/NPC-H3K4me1-ChIP-Seq(GSE16256)/Homer	CTGGCAGSCTGCCA	1.00E+00	-7.16E-01	0.8007	174	24.03%	6607.6	23.93%
FOXA1:AR(Forkhead,NR)/LNCAP-AR-ChIP-Seq(GSE27824)/Homer	AGTAAACAAAAAAGAACAND	1.00E+00	-7.02E-01	0.8007	30	4.14%	1128.7	4.09%
ARE(NR)/LNCAP-AR-ChIP-Seq(GSE27824)/Homer	RGRACASNSTGTYCYB	1.00E+00	-7.02E-01	0.8007	102	14.09%	3872	14.02%
MyoD(bHLH)/Myotube-MyoD-ChIP-Seq(GSE21614)/Homer	RRCAGCTGYTSY	1.00E+00	-6.92E-01	0.8007	279	38.54%	10623.2	38.47%
CEBP(bZIP)/ThioMac-CEBPb-ChIP-Seq(GSE21512)/Homer	ATTGCGCAAC	1.00E+00	-6.87E-01	0.8007	262	36.19%	9978.9	36.14%
AP-2alpha(AP2)/Hela-AP2alpha-ChIP-Seq(GSE31477)/Homer	ATGCCCTGAGGC	1.00E+00	-6.85E-01	0.8007	341	47.10%	12991.8	47.05%
Egr1(Zf)/K562-Egr1-ChIP-Seq(GSE32465)/Homer	TGCGTGGGYG	1.00E+00	-6.78E-01	0.8007	350	48.34%	13339.7	48.31%

Tbox:Smad(T-box,MAD)/ESCd5-Smad2_3-ChIP-Seq(GSE29422)/Homer	AGGTGHCAGACA	1.00E+00	-6.71E-01	0.8007	83	11.46%	3160.1	11.44%
NRF(NRF)/Promoter/Homer	STGCGCATGCGC	1.00E+00	-6.61E-01	0.8007	132	18.23%	5035.2	18.24%
Bach1(bZIP)/K562-Bach1-ChIP-Seq(GSE31477)/Homer	AWWNTGCTGAGTCAT	1.00E+00	-6.35E-01	0.8136	18	2.49%	685.3	2.48%
Pbx3(Homeobox)/GM12878-PBX3-ChIP-Seq(GSE32465)/Homer	SCTGTCAMTCAN	1.00E+00	-6.27E-01	0.8153	114	15.75%	4365.9	15.81%
FOXP1(Forkhead)/H9-FOXP1-ChIP-Seq(GSE31006)/Homer	NYYTGTTTACHN	1.00E+00	-6.22E-01	0.8153	190	26.24%	7272.7	26.34%
PAX5(Paired,Homeobox),condensed/GM12878-PAX5-ChIP-Seq(GSE32465)/Homer	GTCACGCTCSCTGM	1.00E+00	-6.16E-01	0.8153	44	6.08%	1689.4	6.12%
TATA-Box(TBP)/Promoter/Homer	CCTTTTAWAGSC	1.00E+00	-6.02E-01	0.8213	491	67.82%	18762.3	67.95%
Lhx2(Homeobox)/HFSC-Lhx2-ChIP-Seq(GSE48068)/Homer	TAATTAGN	1.00E+00	-5.97E-01	0.8213	370	51.10%	14157.3	51.27%
GSC(Homeobox)/FrogEmbryos-GSC-ChIP-Seq(DRA000576)/Homer	RGGATTAR	1.00E+00	-5.94E-01	0.8213	403	55.66%	15417.8	55.84%
Gata2(Zf)/K562-GATA2-ChIP-Seq(GSE18829)/Homer	BBCTTATCTS	1.00E+00	-5.89E-01	0.8213	261	36.05%	10005.8	36.24%
Elk1(ETS)/Hela-Elk1-ChIP-Seq(GSE31477)/Homer	HACTTCCGGY	1.00E+00	-5.85E-01	0.8213	322	44.48%	12336.7	44.68%
ETS(ETS)/Promoter/Homer	AACCGGAAGT	1.00E+00	-5.82E-01	0.8213	207	28.59%	7947.9	28.78%
Myf5(bHLH)/GM-Myf5-ChIP-	BAACAGCTGT	1.00E+00	-5.68E-01	0.8217	262	36.19%	10058.1	36.43%

Seq(GSE24852)/Homer								
NF1-halfsite(CTF)/LNCaP-NF1-ChIP-Seq(Unpublished)/Homer	YTGCCAAG	1.00E+00	-5.59E-01	0.8248	517	71.41%	19780.9	71.64%
PRDM14(Zf)/H1-PRDM14-ChIP-Seq(GSE22767)/Homer	RGGTCTCTAACY	1.00E+00	-5.56E-01	0.8248	156	21.55%	6013.3	21.78%
Oct2(POU,Homeobox)/Bcell-Oct2-ChIP-Seq(GSE21512)/Homer	ATATGCAAAT	1.00E+00	-5.49E-01	0.8248	117	16.16%	4522.3	16.38%
ETS:E-box(ETS,bHLH)/HPC7-Scl-ChIP-Seq(GSE22178)/Homer	AGGAARCAGCTG	1.00E+00	-5.08E-01	0.854	41	5.66%	1612.6	5.84%
Nr5a2(NR)/mES-Nr5a2-ChIP-Seq(GSE19019)/Homer	BTCAAGGTCA	1.00E+00	-4.93E-01	0.8622	220	30.39%	8508.5	30.81%
Elk4(ETS)/Hela-Elk4-ChIP-Seq(GSE31477)/Homer	NRYTTCCGGY	1.00E+00	-4.88E-01	0.8624	325	44.89%	12526.3	45.37%
Oct4:Sox17(POU,Homeobox,HMG)/F9-Sox17-ChIP-Seq(GSE44553)/Homer	CCATTGTATGCAAAT	1.00E+00	-4.82E-01	0.8624	56	7.73%	2205.1	7.99%
ERG(ETS)/VCaP-ERG-ChIP-Seq(GSE14097)/Homer	ACAGGAAGTG	1.00E+00	-4.73E-01	0.8662	538	74.31%	20638.2	74.74%
RARg(NR)/ES-RARg-ChIP-Seq(GSE30538)/Homer	AGGTCAAGGTCA	1.00E+00	-4.60E-01	0.8723	14	1.93%	569.5	2.06%
Hoxc9(Homeobox)/Ainv15-Hoxc9-ChIP-Seq(GSE21812)/Homer	GGCCATAAATCA	1.00E+00	-4.42E-01	0.8834	197	27.21%	7666.6	27.77%
REST-NRSF(Zf)/Jurkat-NRSF-ChIP-Seq/Homer	GGMGCTGTCCATGGTGCTGA	1.00E+00	-4.41E-01	0.8834	4	0.55%	168	0.61%

T1ISRE(IRF)/ThioMac-Ifnb-Expression/Homer	ACTTTCGTTTCT	1.00E+00	-4.38E-01	0.8834	5	0.69%	210.1	0.76%
E2F(E2F)/Hela-CellCycle-Expression/Homer	TTSGCGCGAAAA	1.00E+00	-4.26E-01	0.8843	35	4.83%	1410	5.11%
Atf1(bZIP)/K562-ATF1-ChIP-Seq(GSE31477)/Homer	GATGACGTCA	1.00E+00	-4.20E-01	0.8846	257	35.50%	9985.4	36.16%
Phox2a(Homeobox)/Neuron-Phox2a-ChIP-Seq(GSE31456)/Homer	YTAATYNRATTA	1.00E+00	-4.02E-01	0.8962	152	20.99%	5967.6	21.61%
Gata4(Zf)/Heart-Gata4-ChIP-Seq(GSE35151)/Homer	NBWGATAAGR	1.00E+00	-3.97E-01	0.8967	365	50.41%	14133.6	51.19%
IRF4(IRF)/GM12878-IRF4-ChIP-Seq(GSE32465)/Homer	ACTGAAACCA	1.00E+00	-3.89E-01	0.8993	178	24.59%	6981	25.28%
EBNA1(EBV virus)/Raji-EBNA1-ChIP-Seq(GSE30709)/Homer	GGYAGCAYDTGCTDCCCNNN	1.00E+00	-3.85E-01	0.8993	6	0.83%	261.3	0.95%
HOXA9(Homeobox)/HSC-Hoxa9-ChIP-Seq(GSE33509)/Homer	GGCCATAAATCA	1.00E+00	-3.75E-01	0.9031	249	34.39%	9721.6	35.21%
Fox:Ebox(Forkhead,bHLH)/Panc1-Foxa2-ChIP-Seq(GSE47459)/Homer	NNNVCTGWGYAAACASN	1.00E+00	-3.74E-01	0.9031	363	50.14%	14080	50.99%
CEBP:CEBP(bZIP)/MEF-Chop-ChIP-Seq(GSE35681)/Homer	NTNATGCAAYMNNHTGMAAY	1.00E+00	-3.70E-01	0.9031	53	7.32%	2144.6	7.77%
Mef2a(MADS)/HL1-Mef2a.biotin-ChIP-Seq(GSE21529)/Homer	CYAAAAATAG	1.00E+00	-3.68E-01	0.9031	169	23.34%	6651.1	24.09%
FXR(NR),IR1/Liver-FXR-ChIP-Seq(Chong et al.)/Homer	AGGTCANTGACCTB	1.00E+00	-3.68E-01	0.9031	162	22.38%	6381.8	23.11%

Mouse_Recombination_Hotspot(Zf)/Testis-DMC1-ChIP-Seq(GSE24438)/Homer	ACTYKNATTCGTGNTACTTC	1.00E+00	-3.54E-01	0.9031	27	3.73%	1123.9	4.07%
HOXA2(Homeobox)/mES-Hoxa2-ChIP-Seq(Donaldson et al.)/Homer	GYCATCMATCAT	1.00E+00	-3.51E-01	0.9031	36	4.97%	1483.7	5.37%
LXRE(NR),DR4/RAW-LXRb.biotin-ChIP-Seq(GSE21512)/Homer	RGGTTACTANAGGTCA	1.00E+00	-3.50E-01	0.9031	19	2.62%	804	2.91%
NFkB-p65(RHD)/GM12787-p65-ChIP-Seq(GSE19485)/Homer	WGGGGATTTCCC	1.00E+00	-3.42E-01	0.9031	216	29.83%	8486.6	30.73%
c-Jun-CRE(bZIP)/K562-cJun-ChIP-Seq(GSE31477)/Homer	ATGACGTCATCY	1.00E+00	-3.41E-01	0.9031	123	16.99%	4895.8	17.73%
STAT6(Stat)/Macrophage-Stat6-ChIP-Seq(GSE38377)/Homer	TTCCKNAGAA	1.00E+00	-3.40E-01	0.9031	231	31.91%	9064.6	32.83%
Gata1(Zf)/K562-GATA1-ChIP-Seq(GSE18829)/Homer	SAGATAAGRV	1.00E+00	-3.40E-01	0.9031	232	32.04%	9103.5	32.97%
CArG(MADS)/PUER-Srf-ChIP-Seq(Sullivan et al.)/Homer	CCATATATGGNM	1.00E+00	-3.30E-01	0.9031	140	19.34%	5564.7	20.15%
GATA3(Zf),DR4/iTreg-Gata3-ChIP-Seq(GSE20898)/Homer	AGATGKDGAGATAAG	1.00E+00	-3.21E-01	0.9031	31	4.28%	1298.2	4.70%
VDR(NR),DR3/GM10855-VDR+vitD-ChIP-Seq(GSE22484)/Homer	ARAGGTCANWGAGTTCANNN	1.00E+00	-3.15E-01	0.9031	87	12.02%	3513.4	12.72%
FOXA1(Forkhead)/LNCAP-FOXA1-ChIP-Seq(GSE27824)/Homer	WAAGTAAACA	1.00E+00	-3.05E-01	0.9031	419	57.87%	16284.3	58.97%

Sox10(HMG)/SciaticNerve-Sox3-ChIP-Seq(GSE35132)/Homer	CCWTTGTYYB	1.00E+00	-3.02E-01	0.9031	494	68.23%	19127.4	69.27%
Meis1(Homeobox)/MastCells-Meis1-ChIP-Seq(GSE48085)/Homer	VGCTGWCAVB	1.00E+00	-2.93E-01	0.9033	510	70.44%	19741	71.49%
Pit1+1bp(Homeobox)/GCrat-Pit1-ChIP-Seq(GSE58009)/Homer	ATGCATAATTCA	1.00E+00	-2.88E-01	0.9035	131	18.09%	5253.6	19.03%
GRE(NR),IR3/RAW264.7-GRE-ChIP-Seq(Unpublished)/Homer	VAGRACAKWCTGTYC	1.00E+00	-2.88E-01	0.9035	93	12.85%	3770.4	13.65%
ZNF711(Zf)/SHSY5Y-ZNF711-ChIP-Seq(GSE20673)/Homer	AGGCCTAG	1.00E+00	-2.87E-01	0.9035	526	72.65%	20349.2	73.70%
E2A(bHLH),near_PU.1/Bcell-PU.1-ChIP-Seq(GSE21512)/Homer	NVCACCTGBN	1.00E+00	-2.75E-01	0.9035	454	62.71%	17646.8	63.91%
Six1(Homeobox)/Myoblast-Six1-ChIP-Chip(GSE20150)/Homer	GKVTCADRTTWC	1.00E+00	-2.67E-01	0.9063	101	13.95%	4102.1	14.86%
Pit1(Homeobox)/GCrat-Pit1-ChIP-Seq(GSE58009)/Homer	ATGMATATDC	1.00E+00	-2.40E-01	0.9271	338	46.69%	13284.7	48.11%
X-box(HTH)/NPC-H3K4me1-ChIP-Seq(GSE16256)/Homer	GGTTGCCATGGCAA	1.00E+00	-2.33E-01	0.9296	52	7.18%	2194.9	7.95%
Eomes(T-box)/H9-Eomes-ChIP-Seq(GSE26097)/Homer	ATTAACACCT	1.00E+00	-2.29E-01	0.9296	571	78.87%	22099.7	80.04%
NFAT(RHD)/Jurkat-NFATC1-ChIP-Seq(Jolma et al.)/Homer	ATTTTCCATT	1.00E+00	-2.24E-01	0.9297	331	45.72%	13040.2	47.23%
Hnf1(Homeobox)/Liver-Foxa2-Chip-Seq(GSE25694)/Homer	GGTTAAWCATTAA	1.00E+00	-2.21E-01	0.9297	60	8.29%	2524.5	9.14%

Atf2(bZIP)/3T3L1-Atf2-ChIP-Seq(GSE56872)/Homer	NRRTGACGTCAT	1.00E+00	-2.20E-01	0.9297	135	18.65%	5483.4	19.86%
PAX3:FKHR-fusion(Paired,Homeobox)/Rh4-PAX3:FKHR-ChIP-Seq(GSE19063)/Homer	ACCRTGACTAATTNN	1.00E+00	-2.13E-01	0.9297	76	10.50%	3168.9	11.48%
YY1(Zf)/Promoter/Homer	CAAGATGGCGGC	1.00E+00	-2.07E-01	0.9297	31	4.28%	1364.5	4.94%
NFAT:AP1(RHD,bZIP)/Jurkat-NFATC1-ChIP-Seq(Jolma et al.)/Homer	SARTGGAAAAWRTGAGTCAB	1.00E+00	-1.97E-01	0.9346	67	9.25%	2826.6	10.24%
GATA3(Zf)/iTreg-Gata3-ChIP-Seq(GSE20898)/Homer	AGATAASR	1.00E+00	-1.84E-01	0.9426	473	65.33%	18490.2	66.96%
CHR(?)/Hela-CellCycle-Expression/Homer	SRGTTTCAAA	1.00E+00	-1.80E-01	0.9428	268	37.02%	10696.6	38.74%
Hoxb4(Homeobox)/ES-Hoxb4-ChIP-Seq(GSE34014)/Homer	TGATTRATGGCY	1.00E+00	-1.73E-01	0.9448	66	9.12%	2811.9	10.18%
GATA3(Zf),DR8/iTreg-Gata3-ChIP-Seq(GSE20898)/Homer	AGATSTNDNNDSAGATAASN	1.00E+00	-1.69E-01	0.9448	24	3.31%	1101.5	3.99%
bZIP:IRF(bZIP,IRF)/Th17-BatF-ChIP-Seq(GSE39756)/Homer	NAGTTTCABTHTGACTNW	1.00E+00	-1.67E-01	0.9448	168	23.20%	6846.4	24.79%
FOXA1(Forkhead)/MCF7-FOXA1-ChIP-Seq(GSE26831)/Homer	WAAGTAAACA	1.00E+00	-1.45E-01	0.96	357	49.31%	14170.3	51.32%
E2F1(E2F)/Hela-E2F1-ChIP-Seq(GSE22478)/Homer	CWGGCGGGAA	1.00E+00	-1.42E-01	0.96	131	18.09%	5437.4	19.69%
PBX1(Homeobox)/MCF7-PBX1-ChIP-Seq(GSE28007)/Homer	GSCTGTCACTCA	1.00E+00	-1.34E-01	0.9626	36	4.97%	1633.7	5.92%
GLI3(Zf)/Limb-GLI3-ChIP-	CGTGGGTGGTCC	1.00E+00	-1.32E-01	0.9626	51	7.04%	2252.8	8.16%

Chip(GSE11077)/Homer								
Pax7(Paired,Homeobox),longest/Myoblast-Pax7-ChIP-Seq(GSE25064)/Homer	NTAATTDGCYAATTANNWWD	1.00E+00	-1.26E-01	0.9626	8	1.10%	435.8	1.58%
JunD(bZIP)/K562-JunD-ChIP-Seq/Homer	ATGACGTCATCN	1.00E+00	-1.22E-01	0.9626	43	5.94%	1936.4	7.01%
Gfi1b(Zf)/HPC7-Gfi1b-ChIP-Seq(GSE22178)/Homer	MAATCACTGC	1.00E+00	-1.18E-01	0.9626	233	32.18%	9468	34.29%
Atf7(bZIP)/3T3L1-Atf7-ChIP-Seq(GSE56872)/Homer	NGRTGACGTCAY	1.00E+00	-1.14E-01	0.9626	179	24.72%	7375.1	26.71%
CTCF-SatelliteElement(Zf?)/CD4+-CTCF-ChIP-Seq(Barski et al.)/Homer	TGCAGTTCCMVNWRTGGCCA	1.00E+00	-1.04E-01	0.9676	4	0.55%	256.2	0.93%
Pdx1(Homeobox)/Islet-Pdx1-ChIP-Seq(SRA008281)/Homer	YCATYAATCA	1.00E+00	-9.85E-02	0.9686	315	43.51%	12676.2	45.91%
NRF1(NRF)/MCF7-NRF1-ChIP-Seq(Unpublished)/Homer	CTGCGCATGCGC	1.00E+00	-8.96E-02	0.9733	105	14.50%	4506.5	16.32%
OCT4-SOX2-TCF-NANOG(POU,Homeobox,HMG)/mES-Oct4-ChIP-Seq(GSE11431)/Homer	ATTTGCATAACAATG	1.00E+00	-8.52E-02	0.9737	64	8.84%	2857.7	10.35%
Unknown-ESC-element(?)/mES-Nanog-ChIP-Seq(GSE11724)/Homer	CACAGCAGGGGG	1.00E+00	-8.19E-02	0.9737	208	28.73%	8591.1	31.11%
E2F7(E2F)/Hela-E2F7-ChIP-Seq(GSE32673)/Homer	VDTTTCCCGCCA	1.00E+00	-8.05E-02	0.9737	70	9.67%	3112	11.27%
Rfx1(HTH)/NPC-H3K4me1-ChIP-Seq(GSE16256)/Homer	KGTTGCCATGGCAA	1.00E+00	-7.89E-02	0.9737	86	11.88%	3766.1	13.64%

SPDEF(ETS)/VCaP-SPDEF-ChIP-Seq(SRA014231)/Homer	ASWTCCTGBT	1.00E+00	-7.24E-02	0.9737	393	54.28%	15730.1	56.97%
STAT6(Stat)/CD4-Stat6-ChIP-Seq(GSE22104)/Homer	ABTTCYYRRGAA	1.00E+00	-4.71E-02	0.9915	213	29.42%	8918	32.30%
Rfx5(HTH)/GM12878-Rfx5-ChIP-Seq(GSE31477)/Homer	SCCTAGCAACAG	1.00E+00	-3.97E-02	0.995	129	17.82%	5630.6	20.39%
E2F6(E2F)/Hela-E2F6-ChIP-Seq(GSE31477)/Homer	GGCGGGAARN	1.00E+00	-3.03E-02	1	250	34.53%	10460.6	37.88%
PRDM9(Zf)/Testis-DMC1-ChIP-Seq(GSE35498)/Homer	ADGGYAGYAGCATCT	1.00E+00	-3.03E-02	1	140	19.34%	6123.9	22.18%
Brachyury(T-box)/Mesoendoderm-Brachyury-ChIP-exo(GSE54963)/Homer	ANTTMRCASBNNNGTGYKAAN	1.00E+00	-2.57E-02	1	95	13.12%	4328.5	15.68%
PRDM1(Zf)/Hela-PRDM1-ChIP-Seq(GSE31477)/Homer	ACTTTCACTTTC	1.00E+00	-1.07E-02	1	212	29.28%	9184.6	33.26%
ZBTB33(Zf)/GM12878-ZBTB33-ChIP-Seq(GSE32465)/Homer	GGVTCTCGCGAGAAC	1.00E+00	-4.98E-03	1	20	2.76%	1267.6	4.59%
GFX(?)/Promoter/Homer	ATTCTCGCGAGA	1.00E+00	-3.68E-03	1	6	0.83%	557	2.02%
RFX(HTH)/K562-RFX3-ChIP-Seq(SRA012198)/Homer	CGGTTGCCATGGCAAC	1.00E+00	-2.60E-03	1	32	4.42%	1893.8	6.86%
Rfx2(HTH)/LoVo-RFX2-ChIP-Seq(GSE49402)/Homer	GTTGCCATGGCAACM	1.00E+00	-1.58E-03	1	35	4.83%	2078.3	7.53%
E2F4(E2F)/K562-E2F4-ChIP-Seq(GSE31477)/Homer	GGCGGGAAAH	1.00E+00	-1.11E-03	1	214	29.56%	9640	34.91%

Supplementary Table 5. Details of putative transcription factor binding motifs for common down-regulated genes.

Motif Name	Consensus	P-value	Log P-value	q-value (Benjamini)	# of Target Sequences with Motif(of 515)	% of Target Sequences with Motif	# of Background Sequences with Motif(of 27925)	% of Background Sequences with Motif
Myf5(bHLH)/GM-Myf5-ChIP-Seq(GSE24852)/Homer	BAACAGCTGT	1.00E-04	-1.12E+01	0.0036	238	46.21%	10329.6	36.99%
Nkx2.1(Homeobox)/LungAC-Nkx2.1-ChIP-Seq(GSE43252)/Homer	RSCACTYRAG	1.00E-04	-1.01E+01	0.0054	489	94.95%	25139.5	90.03%
MyoD(bHLH)/Myotube-MyoD-ChIP-Seq(GSE21614)/Homer	RRCAGCTGYTSY	1.00E-03	-9.08E+00	0.01	242	46.99%	10841.1	38.82%
Otx2(Homeobox)/EpiLC-Otx2-ChIP-Seq(GSE56098)/Homer	NYTAATCCYB	1.00E-03	-8.24E+00	0.0175	255	49.51%	11663.3	41.77%
Ap4(bHLH)/AML-Tfap4-ChIP-Seq(GSE45738)/Homer	NAHCAGCTGD	1.00E-03	-7.33E+00	0.0346	320	62.14%	15349.3	54.97%
Tcf12(bHLH)/GM12878-Tcf12-ChIP-Seq(GSE32465)/Homer	VCAGCTGYTG	1.00E-03	-7.30E+00	0.0346	280	54.37%	13165.9	47.15%
p53(p53)/mES-cMyc-ChIP-Seq(GSE11431)/Homer	ACATGCCCGGGCAT	1.00E-03	-7.20E+00	0.0346	13	2.52%	239	0.86%
TEAD4(TEA)/Tropoblast-Tead4-ChIP-Seq(GSE37350)/Homer	CCWGGAATGY	1.00E-02	-6.73E+00	0.0394	272	52.82%	12837.7	45.98%
Maz(Zf)/HepG2-Maz-ChIP-Seq(GSE31477)/Homer	GGGGGGGG	1.00E-02	-6.35E+00	0.0511	413	80.19%	20823.6	74.57%
AMYB(HTH)/Testes-AMYB-ChIP-Seq(GSE44588)/Homer	TGGCAGTTGG	1.00E-02	-6.29E+00	0.0511	391	75.92%	19552.7	70.02%
ZFX(Zf)/mES-Zfx-ChIP-Seq(GSE11431)/Homer	AGGCCTRG	1.00E-02	-5.95E+00	0.0623	334	64.85%	16386.2	58.68%
Nkx2.5(Homeobox)/HL1-Nkx2.5.biotin-ChIP-	RRSCACTYAA	1.00E-02	-5.90E+00	0.0623	453	87.96%	23296.9	83.43%

Seq(GSE21529)/Homer								
TEAD(TEA)/Fibroblast-PU.1-ChIP-Seq(Unpublished)/Homer	YCWGGAATGY	1.00E-02	-5.79E+00	0.0623	222	43.11%	10350.6	37.07%
Egr1(Zf)/K562-Egr1-ChIP-Seq(GSE32465)/Homer	TGCGTGGGYG	1.00E-02	-5.72E+00	0.0623	261	50.68%	12442.6	44.56%
TATA-Box(TBP)/Promoter/Homer	CCTTTTAWAGSC	1.00E-02	-5.29E+00	0.0885	375	72.82%	18827.3	67.43%
CArG(MADS)/PUER-Srf-ChIP-Seq(Sullivan et al.)/Homer	CCATATATGGNM	1.00E-02	-5.26E+00	0.0885	130	25.24%	5708.7	20.44%
Rbpj1(?)/Panc1-Rbpj1-ChIP-Seq(GSE47459)/Homer	HTTTCCCASG	1.00E-02	-5.22E+00	0.0885	389	75.53%	19641.6	70.34%
Tcf4(HMG)/Hct116-Tcf4-ChIP-Seq(SRA012054)/Homer	ASATCAAAGGVA	1.00E-02	-5.20E+00	0.0885	170	33.01%	7754.6	27.77%
Tcf3(HMG)/mES-Tcf3-ChIP-Seq(GSE11724)/Homer	ASWTCAAAGG	1.00E-02	-5.18E+00	0.0885	106	20.58%	4527.4	16.21%
Sox10(HMG)/SciaticNerve-Sox3-ChIP-Seq(GSE35132)/Homer	CCWTTGTYYB	1.00E-02	-4.88E+00	0.1	388	75.34%	19653.5	70.38%
NF1-halfsite(CTF)/LNCaP-NF1-ChIP-Seq(Unpublished)/Homer	YTGCCAAG	1.00E-02	-4.79E+00	0.1049	395	76.70%	20074.3	71.89%
HOXD13(Homeobox)/Chicken-Hoxd13-ChIP-Seq(GSE38910)/Homer	NCYAATAAAA	1.00E-02	-4.62E+00	0.1188	303	58.83%	14963	53.59%
RBPJ:Ebox(?,bHLH)/Panc1-Rbpj1-ChIP-Seq(GSE47459)/Homer	GGGRAARRGRMCAGMTG	1.00E-01	-4.59E+00	0.1188	126	24.47%	5625.8	20.15%
AR-halfsite(NR)/LNCaP-AR-ChIP-	CCAGGAACAG	1.00E-01	-4.58E+00	0.1188	500	97.09%	26487.2	94.86%

Seq(GSE27824)/Homer								
NFkB-p65-Rel(RHD)/ThioMac-LPS-Expression(GSE23622)/Homer	GGAAATTCCC	1.00E-01	-4.56E+00	0.1188	32	6.21%	1111.8	3.98%
Meis1(Homeobox)/MastCells-Meis1-ChIP-Seq(GSE48085)/Homer	VGCTGWCAVB	1.00E-01	-4.29E+00	0.139	393	76.31%	20067	71.87%
Stat3(Stat)/mES-Stat3-ChIP-Seq(GSE11431)/Homer	CTTCCGGGAA	1.00E-01	-4.28E+00	0.139	194	37.67%	9194.6	32.93%
CHR(?)/Hela-CellCycle-Expression/Homer	SRGTTTCAAA	1.00E-01	-4.22E+00	0.1393	220	42.72%	10582.8	37.90%
Sox2(HMG)/mES-Sox2-ChIP-Seq(GSE11431)/Homer	BCCATTGTTC	1.00E-01	-4.05E+00	0.1586	267	51.84%	13140.1	47.06%
AP-1(bZIP)/ThioMac-PU.1-ChIP-Seq(GSE21512)/Homer	VTGACTCATC	1.00E-01	-4.02E+00	0.1586	204	39.61%	9782.8	35.03%
NeuroD1(bHLH)/Islet-NeuroD1-ChIP-Seq(GSE30298)/Homer	GCCATCTGTT	1.00E-01	-4.00E+00	0.1586	238	46.21%	11594	41.52%
MyoG(bHLH)/C2C12-MyoG-ChIP-Seq(GSE36024)/Homer	AACAGCTG	1.00E-01	-3.95E+00	0.1586	289	56.12%	14358.1	51.42%
HNF4a(NR),DR1/HepG2-HNF4a-ChIP-Seq(GSE25021)/Homer	CARRGKBCAAAGTYCA	1.00E-01	-3.90E+00	0.1623	173	33.59%	8183.3	29.31%
CEBP:CEBP(bZIP)/MEF-Chop-ChIP-Seq(GSE35681)/Homer	NTNATGCAAYMNNHTGMAAY	1.00E-01	-3.75E+00	0.1832	55	10.68%	2260.1	8.09%
Atf3(bZIP)/GBM-ATF3-ChIP-Seq(GSE33912)/Homer	DATGASTCATHN	1.00E-01	-3.74E+00	0.1832	184	35.73%	8795	31.50%
Atoh1(bHLH)/Cerebellum-Atoh1-	VNRVCAGCTGGY	1.00E-01	-3.74E+00	0.1832	291	56.50%	14522.7	52.01%

ChIP-Seq(GSE22111)/Homer								
GATA:SCL(Zf,bHLH)/Ter119-SCL-ChIP-Seq(GSE18720)/Homer	CRGCTGBNGNSNNSAGATAA	1.00E-01	-3.58E+00	0.1984	53	10.29%	2187.6	7.83%
FOXA1(Forkhead)/MCF7-FOXA1-ChIP-Seq(GSE26831)/Homer	WAAGTAAACA	1.00E-01	-3.52E+00	0.2062	286	55.53%	14310.4	51.25%
Sox6(HMG)/Myotubes-Sox6-ChIP-Seq(GSE32627)/Homer	CCATTGTTNY	1.00E-01	-3.41E+00	0.2245	379	73.59%	19484.1	69.78%
Olig2(bHLH)/Neuron-Olig2-ChIP-Seq(GSE30882)/Homer	RCCATMTGTT	1.00E-01	-3.41E+00	0.2245	403	78.25%	20843.9	74.65%
RUNX1(Runt)/Jurkat-RUNX1-ChIP-Seq(GSE29180)/Homer	AAACCACARM	1.00E-01	-3.33E+00	0.2297	288	55.92%	14470.9	51.82%
KLF5(Zf)/LoVo-KLF5-ChIP-Seq(GSE49402)/Homer	DGGGYGKGGC	1.00E-01	-3.31E+00	0.2297	395	76.70%	20412	73.10%
FOXA1(Forkhead)/LNCAP-FOXA1-ChIP-Seq(GSE27824)/Homer	WAAGTAAACA	1.00E-01	-3.31E+00	0.2297	325	63.11%	16505.4	59.11%
Isl1(Homeobox)/Neuron-Isl1-ChIP-Seq(GSE31456)/Homer	CTAATKGV	1.00E-01	-3.23E+00	0.2386	418	81.17%	21744.5	77.87%
Ascl1(bHLH)/NeuralTubes-Ascl1-ChIP-Seq(GSE55840)/Homer	NNVVCAGCTGBN	1.00E-01	-3.22E+00	0.2386	356	69.13%	18245.5	65.34%
Arnt:Ahr(bHLH)/MCF7-Arnt-ChIP-Seq(Lo et al.)/Homer	TBGCACGCAA	1.00E-01	-3.17E+00	0.24	199	38.64%	9733.4	34.86%
Smad3(MAD)/NPC-Smad3-ChIP-Seq(GSE36673)/Homer	TWGTCTGV	1.00E-01	-3.16E+00	0.24	479	93.01%	25340.2	90.75%

Fra1(bZIP)/BT549-Fra1-ChIP-Seq(GSE46166)/Homer	NNATGASTCATH	1.00E-01	-3.13E+00	0.2414	158	30.68%	7588.4	27.18%
AP-2alpha(AP2)/Hela-AP2alpha-ChIP-Seq(GSE31477)/Homer	ATGCCCTGAGGC	1.00E-01	-3.09E+00	0.2453	253	49.13%	12644.7	45.28%
NFAT(RHD)/Jurkat-NFATC1-ChIP-Seq(Jolma et al.)/Homer	ATTTTCCATT	1.00E-01	-3.09E+00	0.2453	265	51.46%	13293.9	47.61%
GSC(Homeobox)/FrogEmbryos-GSC-ChIP-Seq(DRA000576)/Homer	RGGATTAR	1.00E-01	-3.08E+00	0.2453	307	59.61%	15582.6	55.81%
ZNF711(Zf)/SHSY5Y-ZNF711-ChIP-Seq(GSE20673)/Homer	AGGCCTAG	1.00E-01	-3.04E+00	0.2453	383	74.37%	19806.9	70.93%
Foxa2(Forkhead)/Liver-Foxa2-ChIP-Seq(GSE25694)/Homer	CYTGTTTACWYW	1.00E-01	-3.04E+00	0.2453	245	47.57%	12229.2	43.80%
E2A(bHLH)/proBcell-E2A-ChIP-Seq(GSE21978)/Homer	DNRCAGCTGY	1.00E-01	-3.02E+00	0.2453	342	66.41%	17526.2	62.77%
BORIS(Zf)/K562-CTCFL-ChIP-Seq(GSE32465)/Homer	CNNBRGCGCCCCCTGSTGGC	1.00E-01	-3.01E+00	0.2453	90	17.48%	4115.1	14.74%
Smad2(MAD)/ES-SMAD2-ChIP-Seq(GSE29422)/Homer	CTGTCTGG	1.00E-01	-2.96E+00	0.2453	373	72.43%	19269.9	69.01%
Cdx2(Homeobox)/mES-Cdx2-ChIP-Seq(GSE14586)/Homer	GYMATAAAAH	1.00E-01	-2.95E+00	0.2453	215	41.75%	10647.4	38.13%
p63(p53)/Keratinocyte-p63-ChIP-Seq(GSE17611)/Homer	NNDRCATGYCYNRRCATGYH	1.00E-01	-2.89E+00	0.2522	115	22.33%	5416.3	19.40%
BMYB(HTH)/Hela-BMYB-ChIP-Seq(GSE27030)/Homer	NHAACBGYYV	1.00E-01	-2.82E+00	0.2677	377	73.20%	19533.8	69.96%

Egr2(Zf)/Thymocytes-Egr2-ChIP-Seq(GSE34254)/Homer	NGCGTGGGCGGR	1.00E-01	-2.81E+00	0.2677	84	16.31%	3854	13.80%
Jun-AP1(bZIP)/K562-cJun-ChIP-Seq(GSE31477)/Homer	GATGASTCATCN	1.00E-01	-2.80E+00	0.2677	72	13.98%	3249.1	11.64%
EBF1(EBF)/Near-E2A-ChIP-Seq(GSE21512)/Homer	GTCCCCWGGGGA	1.00E-01	-2.79E+00	0.2677	305	59.22%	15561	55.73%
TEAD2(TEA)/Py2T-Tead2-ChIP-Seq(GSE55709)/Homer	CCWGGAATGY	1.00E-01	-2.76E+00	0.2677	175	33.98%	8580.3	30.73%
Erra(NR)/HepG2-Erra-ChIP-Seq(GSE31477)/Homer	CAAAGGTCAG	1.00E-01	-2.75E+00	0.2677	427	82.91%	22379.8	80.15%
PRDM9(Zf)/Testis-DMC1-ChIP-Seq(GSE35498)/Homer	ADGGYAGYAGCATCT	1.00E-01	-2.64E+00	0.2897	131	25.44%	6308.4	22.59%
VDR(NR),DR3/GM10855-VDR+vitD-ChIP-Seq(GSE22484)/Homer	ARAGGTCANWGAGTTCANNN	1.00E-01	-2.64E+00	0.2897	79	15.34%	3636.4	13.02%
EBF(EBF)/proBcell-EBF-ChIP-Seq(GSE21978)/Homer	DGTCCCYRGGGA	1.00E-01	-2.63E+00	0.2897	91	17.67%	4247.4	15.21%
Nanog(Homeobox)/mES-Nanog-ChIP-Seq(GSE11724)/Homer	RGCCATTAAC	1.00E-01	-2.62E+00	0.2897	505	98.06%	27050.5	96.88%
SPDEF(ETS)/VCaP-SPDEF-ChIP-Seq(SRA014231)/Homer	ASWTCCTGBT	1.00E-01	-2.53E+00	0.3039	309	60.00%	15861.9	56.81%
Unknown(Homeobox)/Limb-p300-ChIP-Seq/Homer	SSCMATWAAA	1.00E-01	-2.52E+00	0.3039	204	39.61%	10193.6	36.51%
RUNX-AML(Runt)/CD4+-PolII-ChIP-Seq(Barski et al.)/Homer	GCTGTGGTTW	1.00E-01	-2.44E+00	0.3234	214	41.55%	10752.4	38.51%

GLI3(Zf)/Limb-GLI3-ChIP-Chip(GSE11077)/Homer	CGTGGGTGGTCC	1.00E-01	-2.40E+00	0.3322	51	9.90%	2278	8.16%
Smad4(MAD)/ESC-SMAD4-ChIP-Seq(GSE29422)/Homer	VBSYGTCTGG	1.00E-01	-2.37E+00	0.3392	376	73.01%	19614.2	70.24%
Bcl6(Zf)/Liver-Bcl6-ChIP-Seq(GSE31578)/Homer	NNNCTTTCCAGGAAA	1.00E-01	-2.33E+00	0.3489	358	69.51%	18628.6	66.71%
FXR(NR),IR1/Liver-FXR-ChIP-Seq(Chong et al.)/Homer	AGGTCANTGACCTB	1.00E+00	-2.26E+00	0.3676	132	25.63%	6468.5	23.17%
Sox4(HMG)/proB-Sox4-ChIP-Seq(GSE50066)/Homer	YCTTTGTTCC	1.00E+00	-2.24E+00	0.3684	253	49.13%	12917.5	46.26%
Tcfcp2l1(CP2)/mES-Tcfcp2l1-ChIP-Seq(GSE11431)/Homer	NRAACCRGTTYRAACCRGYT	1.00E+00	-2.23E+00	0.3684	60	11.65%	2761	9.89%
Esrrb(NR)/mES-Esrrb-ChIP-Seq(GSE11431)/Homer	KTGACCTTGA	1.00E+00	-2.22E+00	0.3684	202	39.22%	10185.5	36.48%
Fosl2(bZIP)/3T3L1-Fosl2-ChIP-Seq(GSE56872)/Homer	NATGASTCABNN	1.00E+00	-2.20E+00	0.3721	96	18.64%	4612.3	16.52%
NFkB-p65(RHD)/GM12787-p65-ChIP-Seq(GSE19485)/Homer	WGGGGATTTCCC	1.00E+00	-2.10E+00	0.4029	176	34.17%	8842	31.67%
Foxh1(Forkhead)/hESC-FOXH1-ChIP-Seq(GSE29422)/Homer	NNTGTGGATTSS	1.00E+00	-2.10E+00	0.4029	189	36.70%	9534.4	34.15%
GATA(Zf),IR3/iTreg-Gata3-ChIP-Seq(GSE20898)/Homer	NNNNNBAGATAWYATCTVHN	1.00E+00	-2.10E+00	0.4029	50	9.71%	2285.8	8.19%
CEBP(bZIP)/ThioMac-CEBPb-ChIP-Seq(GSE21512)/Homer	ATTGCGCAAC	1.00E+00	-2.10E+00	0.4029	198	38.45%	10015.1	35.87%
STAT4(Stat)/CD4-Stat4-ChIP-	NYTTCCWGGAAR	1.00E+00	-2.09E+00	0.4029	287	55.73%	14818	53.07%

Seq(GSE22104)/Homer								
ERE(NR),IR3/MCF7-ERa-ChIP-Seq(Unpublished)/Homer	VAGGTCACNSTGACC	1.00E+00	-2.08E+00	0.4029	88	17.09%	4228.5	15.14%
NFY(CCAAT)/Promoter/Homer	RGCCAATSRG	1.00E+00	-2.06E+00	0.4029	269	52.23%	13850.9	49.60%
AP-2gamma(AP2)/MCF7-TFAP2C-ChIP-Seq(GSE21234)/Homer	SCCTSAGGSCAW	1.00E+00	-2.05E+00	0.4029	297	57.67%	15375.4	55.06%
Mef2c(MADS)/GM12878-Mef2c-ChIP-Seq(GSE32465)/Homer	DCYAAAAATAGM	1.00E+00	-2.00E+00	0.4069	139	26.99%	6918.5	24.78%
SCL(bHLH)/HPC7-Scl-ChIP-Seq(GSE13511)/Homer	AVCAGCTG	1.00E+00	-1.95E+00	0.4242	499	96.89%	26766.9	95.86%
p53(p53)/Saos-p53-ChIP-Seq(GSE15780)/Homer	RRCATGYCYRGRCATGYYYN	1.00E+00	-1.89E+00	0.4405	34	6.60%	1525.6	5.46%
p53(p53)/Saos-p53-ChIP-Seq/Homer	RRCATGYCYRGRCATGYYYN	1.00E+00	-1.89E+00	0.4405	34	6.60%	1525.6	5.46%
RXR(NR),DR1/3T3L1-RXR-ChIP-Seq(GSE13511)/Homer	TAGGGCAAAGGTCA	1.00E+00	-1.84E+00	0.4575	311	60.39%	16224.9	58.11%
NFkB-p50,p52(RHD)/Monocyte-p50-ChIP-Chip(Schreiber et al.)/Homer	GGGGGAATCCCC	1.00E+00	-1.83E+00	0.4575	47	9.13%	2190.6	7.84%
Stat3+il21(Stat)/CD4-Stat3-ChIP-Seq(GSE19198)/Homer	SVYTTCCNGGAARB	1.00E+00	-1.81E+00	0.4611	230	44.66%	11843	42.41%
Mef2a(MADS)/HL1-Mef2a.biotin-ChIP-Seq(GSE21529)/Homer	CYAAAAATAG	1.00E+00	-1.80E+00	0.4611	135	26.21%	6773.5	24.26%
BATF(bZIP)/Th17-BATF-ChIP-Seq(GSE39756)/Homer	DATGASTCAT	1.00E+00	-1.77E+00	0.4703	175	33.98%	8911	31.91%
HIF-1b(HLH)/T47D-	RTACGTGC	1.00E+00	-1.76E+00	0.4703	278	53.98%	14458.9	51.78%

HIF1b-ChIP-Seq(GSE59937)/Homer								
PR(NR)/T47D-PR-ChIP-Seq(GSE31130)/Homer	VAGRACAKNCTGTBC	1.00E+00	-1.76E+00	0.4703	430	83.50%	22833.7	81.77%
CRX(Homeobox)/Retina-Crx-ChIP-Seq(GSE20012)/Homer	GCTAATCC	1.00E+00	-1.76E+00	0.4703	444	86.21%	23623.5	84.60%
PPARE(NR),DR1/3T3L1-Pparg-ChIP-Seq(GSE13511)/Homer	TGACCTTTGCCCCA	1.00E+00	-1.75E+00	0.4703	282	54.76%	14678.9	52.57%
Nur77(NR)/K562-NR4A1-ChIP-Seq(GSE31363)/Homer	TGACCTTTNCNT	1.00E+00	-1.75E+00	0.4703	70	13.59%	3387.5	12.13%
Nkx6.1(Homeobox)/Islet-Nkx6.1-ChIP-Seq(GSE40975)/Homer	GKTAATGR	1.00E+00	-1.74E+00	0.4703	440	85.44%	23403.2	83.81%
Nkx3.1(Homeobox)/LNCaP-Nkx3.1-ChIP-Seq(GSE28264)/Homer	AAGCACTTAA	1.00E+00	-1.71E+00	0.4703	440	85.44%	23413.3	83.85%
Klf4(Zf)/mES-Klf4-ChIP-Seq(GSE11431)/Homer	GCCACACCCA	1.00E+00	-1.69E+00	0.4703	175	33.98%	8941	32.02%
Lhx2(Homeobox)/HFSC-Lhx2-ChIP-Seq(GSE48068)/Homer	TAATTAGN	1.00E+00	-1.68E+00	0.4703	275	53.40%	14328.1	51.31%
CTCF-SatelliteElement(Zf?)/CD4+-CTCF-ChIP-Seq(Barski et al.)/Homer	TGCAGTTCCMVNWRTGGCCA	1.00E+00	-1.64E+00	0.4834	7	1.36%	253.5	0.91%
Fox:Ebox(Forkhead,bHLH)/Panc1-Foxa2-ChIP-Seq(GSE47459)/Homer	NNNVCTGWGYAAACASN	1.00E+00	-1.59E+00	0.5011	278	53.98%	14530.5	52.04%
PAX3:FKHR-fusion(Paired,Homeobox)/Rh4-PAX3:FKHR-ChIP-	ACCRTGACTAATTNN	1.00E+00	-1.58E+00	0.5013	66	12.82%	3226.8	11.56%

Seq(GSE19063)/Homer								
Sp1(Zf)/Promoter/Homer	GGCCCCGCCCCC	1.00E+00	-1.57E+00	0.5062	185	35.92%	9528	34.12%
Znf263(Zf)/K562-Znf263-ChIP-Seq(GSE31477)/Homer	CVGTSCTCCC	1.00E+00	-1.55E+00	0.5091	394	76.50%	20904	74.86%
CTCF(Zf)/CD4+-CTCF-ChIP-Seq(Barski et al.)/Homer	AYAGTGCCMYCTRGTGGCCA	1.00E+00	-1.54E+00	0.5091	55	10.68%	2667.4	9.55%
E2F6(E2F)/Hela-E2F6-ChIP-Seq(GSE31477)/Homer	GGCGGGAARN	1.00E+00	-1.53E+00	0.5124	178	34.56%	9169.7	32.84%
Hoxc9(Homeobox)/Ainv15-Hoxc9-ChIP-Seq(GSE21812)/Homer	GGCCATAAATCA	1.00E+00	-1.51E+00	0.5142	154	29.90%	7892.1	28.26%
MYB(HTH)/ERMYB-Myb-ChIPSeq(GSE22095)/Homer	GGCVGTTR	1.00E+00	-1.51E+00	0.5142	397	77.09%	21087.6	75.52%
EKLF(Zf)/Erythrocyte-Klf1-ChIP-Seq(GSE20478)/Homer	NWGGGTGTGGCY	1.00E+00	-1.47E+00	0.5291	89	17.28%	4465.1	15.99%
Hoxb4(Homeobox)/ES-Hoxb4-ChIP-Seq(GSE34014)/Homer	TGATTRATGGCY	1.00E+00	-1.39E+00	0.5674	59	11.46%	2918	10.45%
Hnf1(Homeobox)/Liver-Foxa2-Chip-Seq(GSE25694)/Homer	GGTTAAWCATTAA	1.00E+00	-1.36E+00	0.58	52	10.10%	2562.6	9.18%
PRDM14(Zf)/H1-PRDM14-ChIP-Seq(GSE22767)/Homer	RGGTCTCTAACY	1.00E+00	-1.35E+00	0.58	121	23.50%	6202.8	22.21%
Ptf1a(bHLH)/Panc1-Ptf1a-ChIP-Seq(GSE47459)/Homer	ACAGCTGTTN	1.00E+00	-1.34E+00	0.5839	441	85.63%	23596	84.50%
RUNX(Runt)/HPC7-Runx1-ChIP-Seq(GSE22178)/Homer	SAAACCACAG	1.00E+00	-1.32E+00	0.5877	207	40.19%	10821.9	38.76%
FOXA1:AR(Forkhead,NR)/LNCAP-	AGTAAACAAAAAAGAACAND	1.00E+00	-1.31E+00	0.5894	24	4.66%	1129.6	4.05%

AR-ChIP-Seq(GSE27824)/Homer								
NFAT:AP1(RHD,bZIP)/Jurkat-NFATC1-ChIP-Seq(Jolma et al.)/Homer	SARTGGAAAAWRTGAGTCAB	1.00E+00	-1.30E+00	0.5911	60	11.65%	2998.2	10.74%
Phox2a(Homeobox)/Neuron-Phox2a-ChIP-Seq(GSE31456)/Homer	YTAATYNRATTA	1.00E+00	-1.26E+00	0.6101	117	22.72%	6029	21.59%
Gata4(Zf)/Heart-Gata4-ChIP-Seq(GSE35151)/Homer	NBWGATAAGR	1.00E+00	-1.25E+00	0.6101	275	53.40%	14532.1	52.04%
HIF-1a(bHLH)/MCF7-HIF1a-ChIP-Seq(GSE28352)/Homer	TACGTGCV	1.00E+00	-1.23E+00	0.6159	78	15.15%	3968.7	14.21%
HNF6(Homeobox)/Liver-Hnf6-ChIP-Seq(ERP000394)/Homer	NTATYGATCH	1.00E+00	-1.21E+00	0.6278	158	30.68%	8244.8	29.53%
Tbx5(T-box)/HL1-Tbx5.biotin-ChIP-Seq(GSE21529)/Homer	AGGTGTCA	1.00E+00	-1.20E+00	0.6278	478	92.82%	25710.1	92.07%
RUNX2(Runt)/PCa-RUNX2-ChIP-Seq(GSE33889)/Homer	NWAACCACADNN	1.00E+00	-1.19E+00	0.6278	230	44.66%	12128.4	43.43%
Tbx20(T-box)/Heart-Tbx20-ChIP-Seq(GSE29636)/Homer	GGTGYTGACAGS	1.00E+00	-1.16E+00	0.6416	74	14.37%	3783.9	13.55%
Oct4(POU,Homeobox)/mES-Oct4-ChIP-Seq(GSE11431)/Homer	ATTTGCATAW	1.00E+00	-1.14E+00	0.6523	135	26.21%	7045.8	25.23%
YY1(Zf)/Promoter/Homer	CAAGATGGCGGC	1.00E+00	-1.13E+00	0.6523	24	4.66%	1166.9	4.18%
Oct4:Sox17(POU,Homeobox,HMG)/F9-Sox17-ChIP-Seq(GSE44553)/Homer	CCATTGTATGCAAAT	1.00E+00	-1.13E+00	0.6523	46	8.93%	2316.7	8.30%

Reverb(NR),DR2/RAW-Reverba.biotin-ChIP-Seq(GSE45914)/Homer	GTRGGTCASTGGGTCA	1.00E+00	-1.10E+00	0.6615	45	8.74%	2272.8	8.14%
T1ISRE(IRF)/ThioMac-Ifnb-Expression/Homer	ACTTTCGTTTCT	1.00E+00	-1.09E+00	0.6616	5	0.97%	206.5	0.74%
Pdx1(Homeobox)/Islet-Pdx1-ChIP-Seq(SRA008281)/Homer	YCATYAATCA	1.00E+00	-1.08E+00	0.6616	245	47.57%	12998.7	46.55%
Tlx?(NR)/NPC-H3K4me1-ChIP-Seq(GSE16256)/Homer	CTGGCAGSCTGCCA	1.00E+00	-1.06E+00	0.6725	133	25.83%	6975.1	24.98%
Tbet(T-box)/CD8-Tbet-ChIP-Seq(GSE33802)/Homer	AGGTGTGAAM	1.00E+00	-1.06E+00	0.6725	284	55.15%	15127.2	54.17%
NF1(CTF)/LNCAP-NF1-ChIP-Seq(Unpublished)/Homer	CYTGGCABNSTGCCAR	1.00E+00	-1.06E+00	0.6725	124	24.08%	6495.6	23.26%
Pitx1(Homeobox)/Chicken-Pitx1-ChIP-Seq(GSE38910)/Homer	TAATCCCN	1.00E+00	-1.04E+00	0.6725	502	97.48%	27105.2	97.07%
Ets1-distal(ETS)/CD4+-PolII-ChIP-Seq(Barski et al.)/Homer	MACAGGAAGT	1.00E+00	-1.03E+00	0.6748	110	21.36%	5758.3	20.62%
Unknown-ESC-element(?)/mES-Nanog-ChIP-Seq(GSE11724)/Homer	CACAGCAGGGGG	1.00E+00	-1.03E+00	0.6748	171	33.20%	9035.3	32.36%
Srebp2(bHLH)/HepG2-Srebp2-ChIP-Seq(GSE31477)/Homer	CGGTCACSCCAC	1.00E+00	-9.96E-01	0.687	46	8.93%	2358.8	8.45%
HRE(HSF)/Striatum-HSF1-ChIP-Seq(GSE38000)/Homer	TTCTAGAABNTTCTA	1.00E+00	-9.90E-01	0.687	84	16.31%	4384.2	15.70%
Rfx5(HTH)/GM12878-Rfx5-ChIP-Seq(GSE31477)/Homer	SCCTAGCAACAG	1.00E+00	-9.88E-01	0.687	108	20.97%	5670.9	20.31%

RARg(NR)/ES-RARg-ChIP-Seq(GSE30538)/Homer	AGGTCAAGGTCA	1.00E+00	-9.61E-01	0.6962	12	2.33%	578.9	2.07%
GATA3(Zf),DR4/iTreg-Gata3-ChIP-Seq(GSE20898)/Homer	AGATGKDGAGATAAG	1.00E+00	-9.59E-01	0.6962	28	5.44%	1417.7	5.08%
E2F(E2F)/Hela-CellCycle-Expression/Homer	TTSGCGCGAAAA	1.00E+00	-9.41E-01	0.7008	23	4.47%	1158.2	4.15%
STAT1(Stat)/HelaS3-STAT1-ChIP-Seq(GSE12782)/Homer	NATTTCCNGGAAAT	1.00E+00	-9.39E-01	0.7008	109	21.17%	5748.8	20.59%
Rfx1(HTH)/NPC-H3K4me1-ChIP-Seq(GSE16256)/Homer	KGTTGCCATGGCAA	1.00E+00	-9.27E-01	0.7012	72	13.98%	3770.5	13.50%
MafF(bZIP)/HepG2-MafF-ChIP-Seq(GSE31477)/Homer	HWWGTCAGCAWWTTT	1.00E+00	-9.26E-01	0.7012	75	14.56%	3931.8	14.08%
NF1:FOXA1(CTF,Forkhead)/LNCAP-FOXA1-ChIP-Seq(GSE27824)/Homer	WNTGTTTRYTTTGGCA	1.00E+00	-9.19E-01	0.7012	18	3.50%	901	3.23%
Bach2(bZIP)/OCILy7-Bach2-ChIP-Seq(GSE44420)/Homer	TGCTGAGTCA	1.00E+00	-8.89E-01	0.7143	54	10.49%	2824	10.11%
GATA3(Zf)/iTreg-Gata3-ChIP-Seq(GSE20898)/Homer	AGATAASR	1.00E+00	-8.53E-01	0.7351	351	68.16%	18892.1	67.66%
Lhx3(Homeobox)/Neuron-Lhx3-ChIP-Seq(GSE31456)/Homer	ADBTAATTAR	1.00E+00	-8.45E-01	0.7362	359	69.71%	19332.5	69.23%
IRF1(IRF)/PBMC-IRF1-ChIP-Seq(GSE43036)/Homer	GAAAGTGAAAGT	1.00E+00	-8.45E-01	0.7362	48	9.32%	2519.8	9.02%
Six1(Homeobox)/Myoblast-Six1-ChIP-Chip(GSE20150)/Homer	GKVTCADRTTWC	1.00E+00	-8.39E-01	0.7362	80	15.53%	4240.6	15.19%
GRE(NR),IR3/A549-GR-ChIP-	NRGVACABNVTGTYCY	1.00E+00	-8.38E-01	0.7362	42	8.16%	2200.6	7.88%

Seq(GSE32465)/Homer								
HIF2a(bHLH)/785_O-HIF2a-ChIP-Seq(GSE34871)/Homer	GCACGTACCC	1.00E+00	-8.26E-01	0.7362	105	20.39%	5593.1	20.03%
Nr5a2(NR)/Pancreas-LRH1-ChIP-Seq(GSE34295)/Homer	BTCAAGGTCA	1.00E+00	-8.12E-01	0.7372	207	40.19%	11112.8	39.80%
Nrf2(bZIP)/Lymphoblast-Nrf2-ChIP-Seq(GSE37589)/Homer	HTGCTGAGTCAT	1.00E+00	-8.12E-01	0.7372	12	2.33%	607	2.17%
EWS:FLI1-fusion(ETS)/SK_N_MC-EWS:FLI1-ChIP-Seq(SRA014231)/Homer	VACAGGAAAT	1.00E+00	-7.97E-01	0.7392	195	37.86%	10473.4	37.51%
ZNF143|STAF(Zf)/CUTLL-ZNF143-ChIP-Seq(GSE29600)/Homer	ATTTCCCAGVAKSCY	1.00E+00	-7.90E-01	0.7397	126	24.47%	6747.2	24.16%
Brachyury(T-box)/Mesoendoderm-Brachyury-ChIP-exo(GSE54963)/Homer	ANTTMRCASBNNNGTGYKAAN	1.00E+00	-7.69E-01	0.7507	83	16.12%	4437.6	15.89%
EWS:ERG-fusion(ETS)/CADO_ES1-EWS:ERG-ChIP-Seq(SRA014231)/Homer	ATTTCCTGTN	1.00E+00	-7.61E-01	0.7523	222	43.11%	11960.6	42.83%
LXRE(NR),DR4/RAW-LXRb.biotin-ChIP-Seq(GSE21512)/Homer	RGGTTACTANAGGTCA	1.00E+00	-7.57E-01	0.7523	16	3.11%	832.1	2.98%
ERG(ETS)/VCaP-ERG-ChIP-Seq(GSE14097)/Homer	ACAGGAAGTG	1.00E+00	-7.51E-01	0.7523	387	75.15%	20913.6	74.90%
TCFL2(HMG)/K562-TCF7L2-ChIP-Seq(GSE29196)/Homer	ACWTCAAAGG	1.00E+00	-7.41E-01	0.7533	29	5.63%	1536.7	5.50%
Pax7(Paired,Homeobox)/Myoblast-	TAATCAATTA	1.00E+00	-7.36E-01	0.7533	28	5.44%	1484.6	5.32%

Pax7-ChIP-Seq(GSE25064)/Homer								
RORgt(NR)/EL4-RORgt.Flag-ChIP-Seq(GSE56019)/Homer	AAYTAGGTCA	1.00E+00	-7.27E-01	0.7552	41	7.96%	2189.5	7.84%
Sox3(HMG)/NPC-Sox3-ChIP-Seq(GSE33059)/Homer	CCWTTGTY	1.00E+00	-7.25E-01	0.7552	383	74.37%	20713.4	74.18%
STAT6(Stat)/Macrophage-Stat6-ChIP-Seq(GSE38377)/Homer	TTCCKNAGAA	1.00E+00	-7.16E-01	0.7552	175	33.98%	9448	33.84%
X-box(HTH)/NPC-H3K4me1-ChIP-Seq(GSE16256)/Homer	GGTTGCCATGGCAA	1.00E+00	-7.12E-01	0.7552	41	7.96%	2195.4	7.86%
Pax7(Paired,Homeobox),long/Myoblast-Pax7-ChIP-Seq(GSE25064)/Homer	TAATCHGATTAC	1.00E+00	-7.09E-01	0.7552	7	1.36%	358.8	1.28%
Pax8(Paired,Homeobox)/Thyroid-Pax8-ChIP-Seq(GSE26938)/Homer	GTCATGCHTGRCTGS	1.00E+00	-7.05E-01	0.7552	96	18.64%	5176.7	18.54%
THRa(NR)/C17.2-THRa-ChIP-Seq(GSE38347)/Homer	GGTCANYTGAGGWCA	1.00E+00	-6.99E-01	0.7552	129	25.05%	6967.6	24.95%
OCT4-SOX2-TCF-NANOG(POU,Homeobox,HMG)/mES-Oct4-ChIP-Seq(GSE11431)/Homer	ATTTGCATAACAATG	1.00E+00	-6.94E-01	0.7552	55	10.68%	2961.3	10.61%
Usf2(bHLH)/C2C12-Usf2-ChIP-Seq(GSE36030)/Homer	GTCACGTGGT	1.00E+00	-6.87E-01	0.7552	93	18.06%	5024.7	17.99%
STAT6(Stat)/CD4-Stat6-ChIP-Seq(GSE22104)/Homer	ABTTCYYRRGAA	1.00E+00	-6.78E-01	0.7552	171	33.20%	9258.1	33.16%
MafK(bZIP)/C2C12-MafK-ChIP-Seq(GSE36030)/Homer	GCTGASTCAGCA	1.00E+00	-6.65E-01	0.7582	62	12.04%	3355.7	12.02%

MafA(bZIP)/Islet-MafA-ChIP-Seq(GSE30298)/Homer	TGCTGACTCA	1.00E+00	-6.65E-01	0.7582	210	40.78%	11382.1	40.76%
IRF2(IRF)/Erythroblas-IRF2-ChIP-Seq(GSE36985)/Homer	GAAASYGAAASY	1.00E+00	-6.49E-01	0.7625	36	6.99%	1950.5	6.99%
Gata1(Zf)/K562-GATA1-ChIP-Seq(GSE18829)/Homer	SAGATAAGRV	1.00E+00	-6.28E-01	0.7738	175	33.98%	9513.2	34.07%
NPAS2(bHLH)/Liver-NPAS2-ChIP-Seq(GSE39860)/Homer	KCCACGTGAC	1.00E+00	-6.27E-01	0.7738	258	50.10%	14014.9	50.19%
CLOCK(bHLH)/Liver-Clock-ChIP-Seq(GSE39860)/Homer	GHCACGTG	1.00E+00	-6.24E-01	0.7738	154	29.90%	8377.1	30.00%
Nr5a2(NR)/mES-Nr5a2-ChIP-Seq(GSE19019)/Homer	BTCAAGGTCA	1.00E+00	-6.01E-01	0.7825	161	31.26%	8775.4	31.43%
CEBP:AP1(bZIP)/ThioMac-CEBPb-ChIP-Seq(GSE21512)/Homer	DRTGTTGCAA	1.00E+00	-5.98E-01	0.7825	198	38.45%	10786.5	38.63%
bHLHE40(bHLH)/HepG2-BHLHE40-ChIP-Seq(GSE31477)/Homer	KCACGTGMCN	1.00E+00	-5.71E-01	0.798	89	17.28%	4881.3	17.48%
HOXA9(Homeobox)/HSC-Hoxa9-ChIP-Seq(GSE33509)/Homer	GGCCATAAATCA	1.00E+00	-5.64E-01	0.7992	184	35.73%	10055.8	36.01%
Foxo1(Forkhead)/RAW-Foxo1-ChIP-Seq(Fan et al.)/Homer	CTGTTTAC	1.00E+00	-5.27E-01	0.8244	393	76.31%	21396.2	76.63%
ETS:E-box(ETS,bHLH)/HPC7-Scl-ChIP-Seq(GSE22178)/Homer	AGGAARCAGCTG	1.00E+00	-5.24E-01	0.8244	30	5.83%	1675.8	6.00%
TR4(NR),DR1/Hela-TR4-ChIP-	GAGGTCAAAGGTCA	1.00E+00	-5.21E-01	0.8244	40	7.77%	2228.3	7.98%

Seq(GSE24685)/Homer								
GRE(NR),IR3/RAW264.7-GRE-ChIP-Seq(Unpublished)/Homer	VAGRACAKWCTGTYC	1.00E+00	-5.17E-01	0.8244	71	13.79%	3933.1	14.09%
Gata2(Zf)/K562-GATA2-ChIP-Seq(GSE18829)/Homer	BBCTTATCTS	1.00E+00	-5.07E-01	0.8244	190	36.89%	10432.6	37.36%
PRDM1(Zf)/Hela-PRDM1-ChIP-Seq(GSE31477)/Homer	ACTTTCACTTTC	1.00E+00	-4.92E-01	0.8323	171	33.20%	9413.9	33.71%
n-Myc(bHLH)/mES-nMyc-ChIP-Seq(GSE11431)/Homer	VRCCACGTGG	1.00E+00	-4.81E-01	0.8367	176	34.17%	9695.7	34.72%
c-Myc(bHLH)/LNCAP-cMyc-ChIP-Seq(Unpublished)/Homer	VCCACGTG	1.00E+00	-4.73E-01	0.8395	131	25.44%	7250.4	25.97%
Tbox:Smad(T-box,MAD)/ESCd5-Smad2_3-ChIP-Seq(GSE29422)/Homer	AGGTGHCAGACA	1.00E+00	-4.63E-01	0.8436	59	11.46%	3310.9	11.86%
Max(bHLH)/K562-Max-ChIP-Seq(GSE31477)/Homer	RCCACGTGGYYN	1.00E+00	-4.56E-01	0.8451	168	32.62%	9284.3	33.25%
Rfx2(HTH)/LoVo-RFX2-ChIP-Seq(GSE49402)/Homer	GTTGCCATGGCAACM	1.00E+00	-4.45E-01	0.8503	35	6.80%	1992.3	7.14%
EHF(ETS)/LoVo-EHF-ChIP-Seq(GSE49402)/Homer	AVCAGGAAGT	1.00E+00	-4.42E-01	0.8503	337	65.44%	18457.3	66.10%
E-box(bHLH)/Promoter/Homer	SSGGTCACGTGA	1.00E+00	-4.36E-01	0.8503	28	5.44%	1606.6	5.75%
Pit1+1bp(Homeobox)/GCrat-Pit1-ChIP-Seq(GSE58009)/Homer	ATGCATAATTCA	1.00E+00	-4.35E-01	0.8503	96	18.64%	5367.5	19.22%
PU.1-IRF(ETS:IRF)/Bcell-PU.1-ChIP-	MGGAAGTGAAAC	1.00E+00	-4.03E-01	0.8693	336	65.24%	18444.4	66.05%

Seq(GSE21512)/Homer								
Mouse_Recombination_Hotspot(Zf)/Testis-DMC1-ChIP-Seq(GSE24438)/Homer	ACTYKNATTCGTGNTACTTC	1.00E+00	-3.96E-01	0.8712	20	3.88%	1175.4	4.21%
FOXP1(Forkhead)/H9-FOXP1-ChIP-Seq(GSE31006)/Homer	NYYTGTTTACHN	1.00E+00	-3.84E-01	0.8776	132	25.63%	7391.4	26.47%
Atf1(bZIP)/K562-ATF1-ChIP-Seq(GSE31477)/Homer	GATGACGTCA	1.00E+00	-3.77E-01	0.8792	181	35.15%	10077.8	36.09%
GFY(?)/Promoter/Homer	ACTACAATTCCC	1.00E+00	-3.77E-01	0.8792	34	6.60%	1976.1	7.08%
USF1(bHLH)/GM12878-Usf1-ChIP-Seq(GSE32465)/Homer	SGTCACGTGR	1.00E+00	-3.40E-01	0.9033	127	24.66%	7164.9	25.66%
PAX5(Paired,Homeobox)/GM12878-PAX5-ChIP-Seq(GSE32465)/Homer	GCAGCCAAGCRTGACH	1.00E+00	-3.40E-01	0.9033	105	20.39%	5953.5	21.32%
bZIP:IRF(bZIP,IRF)/Th17-BatF-ChIP-Seq(GSE39756)/Homer	NAGTTTCABTHTGACTNW	1.00E+00	-3.38E-01	0.9033	126	24.47%	7111.6	25.47%
E2A(bHLH),near_PU.1/Bcell-PU.1-ChIP-Seq(GSE21512)/Homer	NVCACCTGBN	1.00E+00	-3.30E-01	0.9033	323	62.72%	17830	63.85%
E2F1(E2F)/Hela-E2F1-ChIP-Seq(GSE22478)/Homer	CWGGCGGGAA	1.00E+00	-3.28E-01	0.9033	77	14.95%	4416	15.82%
c-Jun-CRE(bZIP)/K562-cJun-ChIP-Seq(GSE31477)/Homer	ATGACGTCATCY	1.00E+00	-2.96E-01	0.9218	88	17.09%	5060.1	18.12%
EBNA1(EBV virus)/Raji-EBNA1-ChIP-Seq(GSE30709)/Homer	GGYAGCAYDTGCTDCCCNNN	1.00E+00	-2.83E-01	0.9297	4	0.78%	278.1	1.00%
BMAL1(bHLH)/Liver-Bmal1-ChIP-	GNCACGTG	1.00E+00	-2.70E-01	0.9375	351	68.16%	19412.8	69.52%

Seq(GSE39860)/Homer								
Chop(bZIP)/MEF-Chop-ChIP-Seq(GSE35681)/Homer	ATTGCATCAT	1.00E+00	-2.67E-01	0.9375	53	10.29%	3133.9	11.22%
c-Myc(bHLH)/mES-cMyc-ChIP-Seq(GSE11431)/Homer	VVCCACGTGG	1.00E+00	-2.65E-01	0.9375	124	24.08%	7092.1	25.40%
GFY-Staf(?,Zf)/Promoter/Homer	RACTACAATTCCCAGAAKGC	1.00E+00	-2.59E-01	0.9375	26	5.05%	1600.6	5.73%
MITF(bHLH)/MastCells-MITF-ChIP-Seq(GSE48085)/Homer	RTCATGTGAC	1.00E+00	-2.53E-01	0.9375	232	45.05%	13023	46.64%
CRE(bZIP)/Promoter/Homer	CSGTGACGTCAC	1.00E+00	-2.35E-01	0.949	74	14.37%	4351.8	15.59%
Eomes(T-box)/H9-Eomes-ChIP-Seq(GSE26097)/Homer	ATTAACACCT	1.00E+00	-2.17E-01	0.9611	410	79.61%	22619	81.00%
Pbx3(Homeobox)/GM12878-PBX3-ChIP-Seq(GSE32465)/Homer	SCTGTCAMTCAN	1.00E+00	-2.17E-01	0.9611	76	14.76%	4486.1	16.07%
RFX(HTH)/K562-RFX3-ChIP-Seq(SRA012198)/Homer	CGGTTGCCATGGCAAC	1.00E+00	-2.16E-01	0.9611	29	5.63%	1810.4	6.48%
E2F4(E2F)/K562-E2F4-ChIP-Seq(GSE31477)/Homer	GGCGGGAAAH	1.00E+00	-2.15E-01	0.9611	139	26.99%	7995.8	28.64%
ARE(NR)/LNCAP-AR-ChIP-Seq(GSE27824)/Homer	RGRACASNSTGTYCYB	1.00E+00	-2.14E-01	0.9611	69	13.40%	4096.3	14.67%
ELF5(ETS)/T47D-ELF5-ChIP-Seq(GSE30407)/Homer	ACVAGGAAGT	1.00E+00	-2.12E-01	0.9611	224	43.50%	12658.4	45.33%
PU.1(ETS)/ThioMac-PU.1-ChIP-Seq(GSE21512)/Homer	AGAGGAAGTG	1.00E+00	-1.95E-01	0.9611	158	30.68%	9079.4	32.52%
Pit1(Homeobox)/GCrat-Pit1-ChIP-	ATGMATATDC	1.00E+00	-1.88E-01	0.9611	240	46.60%	13573.7	48.61%

Seq(GSE58009)/Homer								
GRHL2(CP2)/HBE-GRHL2-ChIP-Seq(GSE46194)/Homer	AAACYKGTTWDACMRGTTTB	1.00E+00	-1.88E-01	0.9611	107	20.78%	6267	22.44%
GATA3(Zf),DR8/iTreg-Gata3-ChIP-Seq(GSE20898)/Homer	AGATSTNDNNDSAGATAASN	1.00E+00	-1.86E-01	0.9611	18	3.50%	1188.4	4.26%
Srebp1a(bHLH)/HepG2-Srebp1a-ChIP-Seq(GSE31477)/Homer	RTCACSCCAY	1.00E+00	-1.83E-01	0.9611	60	11.65%	3629.3	13.00%
Atf2(bZIP)/3T3L1-Atf2-ChIP-Seq(GSE56872)/Homer	NRRTGACGTCAT	1.00E+00	-1.76E-01	0.9611	95	18.45%	5615.7	20.11%
STAT5(Stat)/mCD4+-Stat5-ChIP-Seq(GSE12346)/Homer	RTTTCTNAGAAA	1.00E+00	-1.48E-01	0.9776	112	21.75%	6621.4	23.71%
E2F7(E2F)/Hela-E2F7-ChIP-Seq(GSE32673)/Homer	VDTTTCCCGCCA	1.00E+00	-1.47E-01	0.9776	40	7.77%	2529.8	9.06%
IRF4(IRF)/GM12878-IRF4-ChIP-Seq(GSE32465)/Homer	ACTGAAACCA	1.00E+00	-1.37E-01	0.98	120	23.30%	7092.5	25.40%
NF-E2(bZIP)/K562-NFE2-ChIP-Seq(GSE31477)/Homer	GATGACTCAGCA	1.00E+00	-1.30E-01	0.982	10	1.94%	743.6	2.66%
ETS:RUNX(ETS,Runt)/Jurkat-RUNX1-ChIP-Seq(GSE17954)/Homer	RCAGGATGTGGT	1.00E+00	-1.25E-01	0.9834	28	5.44%	1854.3	6.64%
GATA(Zf),IR4/iTreg-Gata3-ChIP-Seq(GSE20898)/Homer	NAGATWNBNATCTNN	1.00E+00	-1.19E-01	0.985	21	4.08%	1440.2	5.16%
Atf7(bZIP)/3T3L1-Atf7-ChIP-Seq(GSE56872)/Homer	NGRTGACGTCAY	1.00E+00	-1.16E-01	0.985	126	24.47%	7477.8	26.78%
JunD(bZIP)/K562-JunD-ChIP-Seq/Homer	ATGACGTCATCN	1.00E+00	-9.52E-02	1	28	5.44%	1901.2	6.81%

HRE(HSF)/HepG2-HSF1-ChIP-Seq(GSE31477)/Homer	BSTTCTRGAABVTTCYAGAA	1.00E+00	-8.20E-02	1	47	9.13%	3061.3	10.96%
HOXA2(Homeobox)/mES-Hoxa2-ChIP-Seq(Donaldson et al.)/Homer	GYCATCMATCAT	1.00E+00	-4.85E-02	1	21	4.08%	1573	5.63%
ZBTB33(Zf)/GM12878-ZBTB33-ChIP-Seq(GSE32465)/Homer	GGVTCTCGCGAGAAC	1.00E+00	-4.36E-02	1	11	2.14%	934	3.34%
Atf4(bZIP)/MEF-Atf4-ChIP-Seq(GSE35681)/Homer	MTGATGCAAT	1.00E+00	-4.08E-02	1	62	12.04%	4088.3	14.64%
ISRE(IRF)/ThioMac-LPS-Expression(GSE23622)/Homer	AGTTTCASTTTC	1.00E+00	-3.03E-02	1	13	2.52%	1110.4	3.98%
PBX1(Homeobox)/MCF7-PBX1-ChIP-Seq(GSE28007)/Homer	GSCTGTCACTCA	1.00E+00	-2.60E-02	1	21	4.08%	1658.6	5.94%
Gfi1b(Zf)/HPC7-Gfi1b-ChIP-Seq(GSE22178)/Homer	MAATCACTGC	1.00E+00	-2.36E-02	1	160	31.07%	9818.6	35.16%
Fli1(ETS)/CD8-FLI-ChIP-Seq(GSE20898)/Homer	NRYTTCCGGH	1.00E+00	-2.11E-02	1	304	59.03%	17681.8	63.32%
Bach1(bZIP)/K562-Bach1-ChIP-Seq(GSE31477)/Homer	AWWNTGCTGAGTCAT	1.00E+00	-1.87E-02	1	7	1.36%	733.8	2.63%
PAX5(Paired,Homeobox),condensed/GM12878-PAX5-ChIP-Seq(GSE32465)/Homer	GTCACGCTCSCTGM	1.00E+00	-1.85E-02	1	20	3.88%	1636.4	5.86%
ETV1(ETS)/GIST48-ETV1-ChIP-Seq(GSE22441)/Homer	AACCGGAAGT	1.00E+00	-1.59E-02	1	338	65.63%	19536	69.96%
Oct2(POU,Homeobox)/Bcell-Oct2-ChIP-	ATATGCAAAT	1.00E+00	-1.53E-02	1	70	13.59%	4754.1	17.03%

Seq(GSE21512)/Homer								
Pax7(Paired,Homeobox),longest/Myoblast-Pax7-ChIP-Seq(GSE25064)/Homer	NTAATTDGCYAATTANNWWD	1.00E+00	-1.52E-02	1	3	0.58%	427.4	1.53%
NRF1(NRF)/MCF7-NRF1-ChIP-Seq(Unpublished)/Homer	CTGCGCATGCGC	1.00E+00	-1.26E-02	1	47	9.13%	3400.3	12.18%
Elk4(ETS)/Hela-Elk4-ChIP-Seq(GSE31477)/Homer	NRYTTCCGGY	1.00E+00	-9.68E-03	1	185	35.92%	11424	40.91%
SpiB(ETS)/OCILY3-SPIB-ChIP-Seq(GSE56857)/Homer	AAAGRGGAAGTG	1.00E+00	-8.93E-03	1	66	12.82%	4613.6	16.52%
GFX(?)/Promoter/Homer	ATTCTCGCGAGA	1.00E+00	-4.29E-03	1	2	0.39%	412.9	1.48%
ETS1(ETS)/Jurkat-ETS1-ChIP-Seq(GSE17954)/Homer	ACAGGAAGTG	1.00E+00	-3.79E-03	1	272	52.82%	16362.7	58.60%
ELF1(ETS)/Jurkat-ELF1-ChIP-Seq(SRA014231)/Homer	AVCCGGAAGT	1.00E+00	-1.31E-03	1	164	31.84%	10659.2	38.17%
NRF(NRF)/Promoter/Homer	STGCGCATGCGC	1.00E+00	-1.11E-03	1	52	10.10%	4073.5	14.59%
Elk1(ETS)/Hela-Elk1-ChIP-Seq(GSE31477)/Homer	HACTTCCGGY	1.00E+00	-9.62E-04	1	176	34.17%	11390.4	40.79%
GABPA(ETS)/Jurkat-GABPa-ChIP-Seq(GSE17954)/Homer	RACCGGAAGT	1.00E+00	-3.63E-04	1	245	47.57%	15350.4	54.97%
ETS(ETS)/Promoter/Homer	AACCGGAAGT	1.00E+00	-8.00E-06	1	95	18.45%	7399.8	26.50%
REST-NRSF(Zf)/Jurkat-NRSF-ChIP-Seq/Homer	GGMGCTGTCCATGGTGCTGA	1.00E+00	0.00E+00	1	0	0.00%	172.5	0.62%

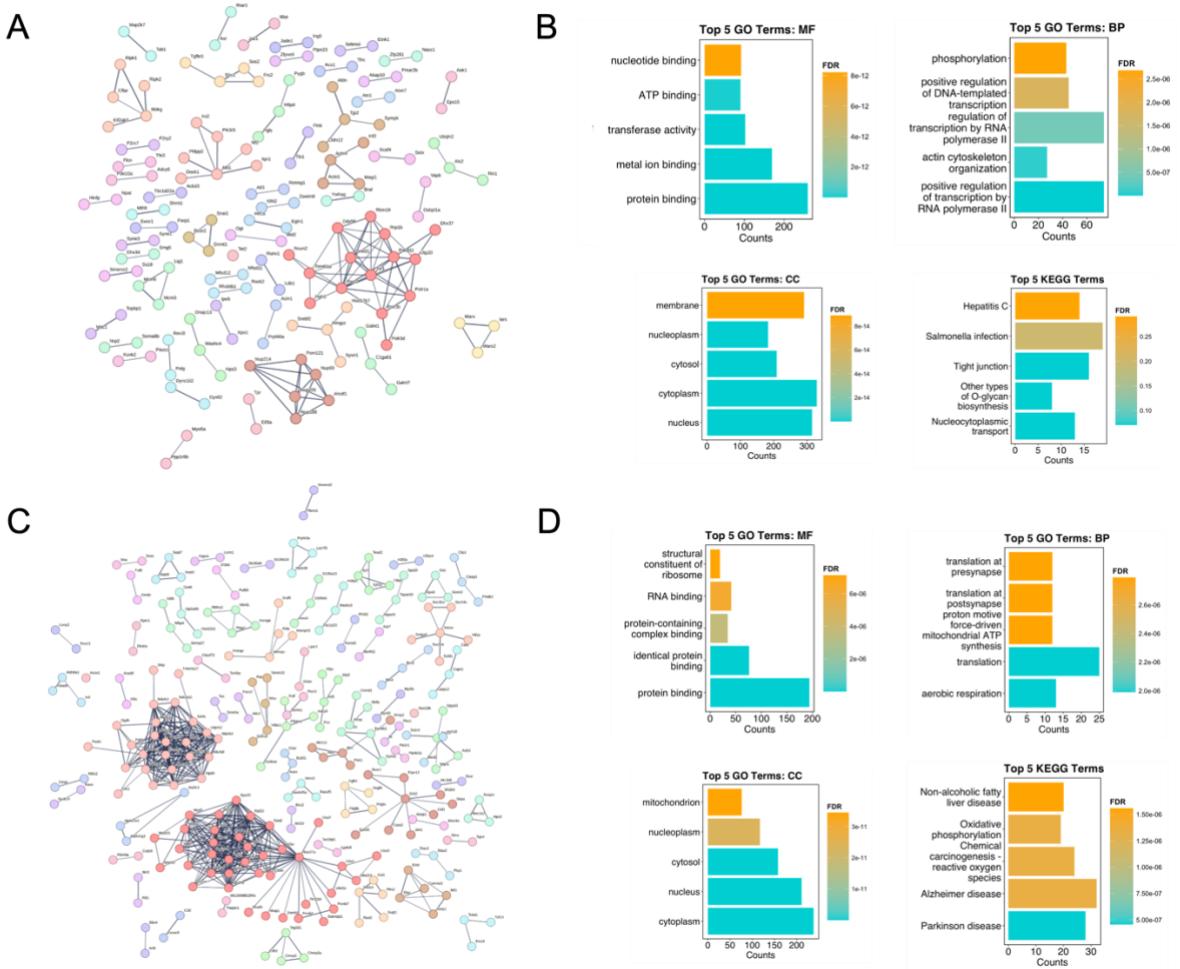

Supplementary figure 1. Summary of uniquely up- and downregulated DEGs by CBD. Unique upregulated (A) and downregulated (C) genes and their known protein-protein interactions, single nodes are not shown, highest confidence (0.9), clusters are coloured individually using K-means clustering. The top 5 Enriched KEGG pathways and GO terms for common upregulated (B) and downregulated genes (D). BP = biological process; CC = cellular compartment; MF = molecular function.

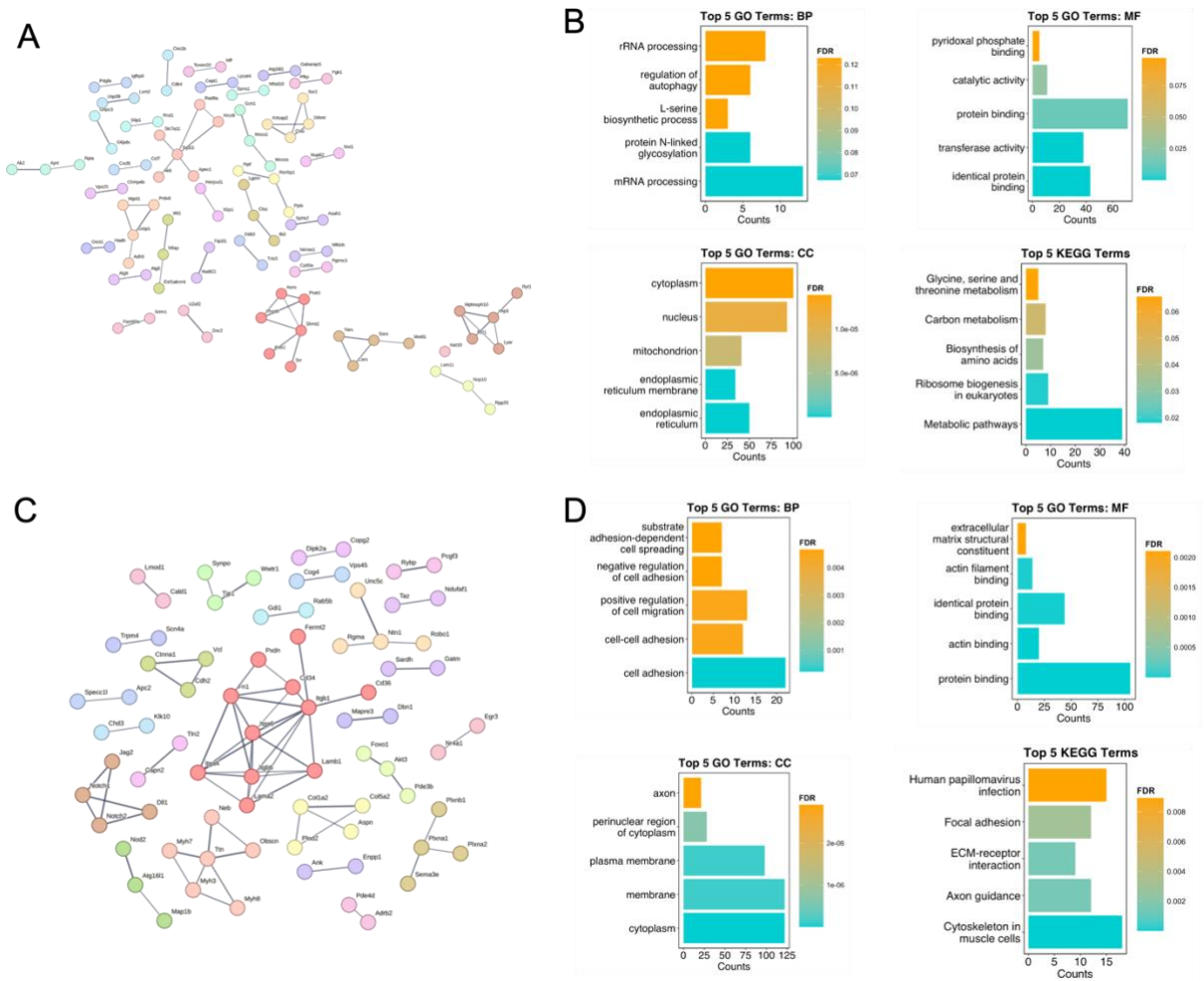

Supplementary figure 2. Summary of uniquely up- and downregulated DEGs by synthetic CBD. Unique upregulated (A) and downregulated (C) genes and their known protein-protein interactions, single nodes are not shown, highest confidence (0.9), clusters are coloured individually using K-means clustering. The top 5 Enriched KEGG pathways and GO terms for common upregulated (B) and downregulated genes (D). BP = biological process; CC = cellular compartment; MF = molecular function.

10.2 Appendix 2: Certificate of Analysis: 40% Broad-Spectrum CBD Oil.

Certificate of Analysis

Powered by Confident Cannabis
1 of 5

Spring Creek Labs
7 South 1550 West Suite 100
Lindon, UT 84042
glugo2008@gmail.com
(503) 884-8056
Lic. #

Sample: 2010TSF0214.10383
Strain: 40% - 4000mg, CBD, BS, MCT, NF, Tincture, 10ml
Batch #: 2010059; Lot #: 2010059;
Sample Received: 10/26/2020; Report Generated: 10/30/2020

40% - 4000mg, CBD, BS, MCT, NF, Tincture, 10ml

Ingestible, Tincture, Other
Harvest Process Lot: ; METRC Batch: ; METRC Sample:

The photo on this report is of a sample collected by the lab and may vary from the final packaging

<LOD
Total Potential THC

4,148.87 mg/unit
Total Potential CBD

Cannabinoids

Analyte	LOD	LOQ	Result	Result
	mg/unit	mg/unit	mg/unit	mg/g
THCa	1.05	1.05	ND	ND
Δ9-THC	1.05	1.05	ND	ND
Δ8-THC	1.05	1.05	ND	ND
CBD	1.05	1.05	4148.87	395.13
CBDa	1.05	1.05	ND	ND
CBC	1.05	1.05	ND	ND
CBG	1.05	1.05	92.72	8.83
CBN	1.05	1.05	ND	ND
THCV	1.05	1.05	ND	ND
CBGa	1.05	1.05	ND	ND
Total			**4241.58**	**403.96**

1 Unit = , 10.5g

Test performed via HPLC-UV. Total Potential THC and CBD: Liquid chromatography occurs at room temperature and does not decarboxylate any cannabinoids, thereby yielding separate values for THCa, THC, CBDa and CBD, which are then combined to derive the Total Potential THC and Total Potential CBD result using the following formulae:
Total Potential THC = THCa * 0.877 + Δ9-THC+ Δ8-THC
Total Potential CBD = CBDa * 0.877 + CBD
LOQ = Limit of Quantitation; Cannabinoids for flower and trim reported as received. LOQ has been set to the Limit of Detection (LOD) / Method Detection Limit (MDL) for all endpoints.

10 Greg St
Sparks, NV
(844) 374-5227
www.374labs.com

Dr. Jeff Angermann
Scientific Director

All pass limits are as specified in NAC 453.A and DPBH Policies. Unless otherwise stated all quality control samples performed within specifications established by the Laboratory. This product has been tested by 374 Labs, LLC (MME# 03754325902079441647) using valid testing methodologies and a quality system as required by Nevada state law. Values reported relate only to the product tested. 374 Labs makes no claims as to the efficacy, safety or other risks associated with any detected or non-detected levels of any compounds reported herein. This Certificate shall not be reproduced except in full, without the written approval of 374 Labs. Uncertainty information is available upon request. 374 Labs complies with ISO/IEC 17025 standards. Potency performed per SOP-000001, Terpenes performed per SOP-000002, Metals performed per SOP-000003, Microbial testing performed per SOP-000004, Pesticides performed per SOP-000005. Moisture per SOP-000006. Photo is of sample collected by the lab and may vary from final packaging. LOQ has been set to the Limit of Detection (LOD) / Method Detection Limit (MDL) for all endpoints.